

From polymers to plastics

From polymers to plastics

A.K. van der Vegt

© VSSD 2002

DUP Blue Print is an imprint of:

Delft University Press

P.O. Box 98, 2600 MG Delft, The Netherlands

tel. +31 15 27 85678, telefax +31 15 27 85706, e-mail info@library.tudelft.nl

internet: <http://www.library.tudelft.nl/dup>

Published on behalf of:

Vereniging voor Studie- en Studentenbelangen te Delft

Poortlandplein 6, 2628 BM Delft, The Netherlands

tel. +31 15 27 82124, telefax +31 15 27 87585, e-mail: hlf@vssd.nl

internet: <http://www.vssd.nl/hlf>

URL on this book: **<http://www.vssd.nl/hlf/m008.htm>**

A collection of digital pictures, printed in the book, can be made available for lecturers who adopt this book. Please send an e-mail to hlf@vssd.nl.

All rights reserved. No part of this publication may be reproduced, stored in a retrieval system, or transmitted, in any form or by any means, electronic, mechanical, photo-copying, recording, or otherwise, without the prior written permission of the publisher.

Printed in The Netherlands.

Internet edition

NUGI 831

Key word: polymers

Preface

The two words in the title of this book, “polymers” and “plastics”, could be considered as referring to two different worlds.

In the world of polymers, the properties of chain molecules are in the focus of attention, and are subject of thorough theoretical studies.

In the world of plastics, the end-use performance of the technically used materials counts, as well as their behaviour in the various processing operations in which they are transformed into finished articles.

Nevertheless, these two worlds are closely related to each other. The typical behaviour of plastics materials, strongly deviating from other materials, can only be understood on the basis of the chain properties.

In this book an attempt has been made to give a survey of polymer properties, and of the way these are, on the one hand, governed by their molecular structure, and are, on the other hand, responsible for the technological behaviour of plastics materials.

As a result of this intention, cross-references are given throughout the whole book: every aspect of polymer science and of plastics technology is closely related to practically every other aspect!

This book originates from several series of lectures at the Delft University of Technology during the years 1978 - 1988, later on integrated into a number of post-graduate and other courses. Since only a first introduction is given, more detailed treatment and more scientific depth have been sacrificed to the striving for survey and integration.

Delft, May 1999
A.K. van der Vegt

Contents

| | |
|--|----|
| PREFACE | 5 |
| 1. INTRODUCTION | 11 |
| 1.1. Origin of plastics / polymers | 11 |
| 1.2. Main categories | 14 |
| 1.3. The most important plastics | 15 |
| 1.3.1. Thermoplastics | 15 |
| 1.3.2. Thermosets | 18 |
| 1.3.3. Synthetic elastomers | 19 |
| 1.3.4. Composite plastics | 20 |
| 2. MOLECULAR COMPOSITION | 22 |
| 2.1. Chain structure | 22 |
| 2.1.1. Main chain | 22 |
| 2.1.2. Side groups | 25 |
| 2.1.3. Copolymers | 26 |
| 2.2. Chain length and distribution | 26 |
| 2.2.1. Averages | 26 |
| 2.2.2. Example of a chain length distribution | 31 |
| 2.2.3. Measuring methods | 33 |
| 2.3. Chain regularity | 38 |
| 2.4. Chain conformations | 41 |
| 2.5. Chain flexibility | 47 |
| 2.6. Chain interactions | 48 |
| 2.7. Cross-linking | 49 |
| 3. GLASSY STATE AND GLASS-RUBBER TRANSITION | 52 |
| 3.1. Glassy state | 52 |
| 3.2. Molecular picture | 54 |
| 3.3. Thermodynamics of the glass-rubber transition | 56 |
| 3.4. Factors governing T_g | 59 |
| 3.4.1. Chain flexibility | 60 |
| 3.4.2. Chain interactions | 61 |
| 3.4.3. Chain length | 62 |
| 3.4.4. Effect of time scale | 62 |
| 3.5. Glass-rubber transition of blends | 63 |
| 3.6. Methods of measuring T_g | 64 |

| | | |
|--------|--------------------------------------|-----|
| 4. | CRYSTALLINE POLYMERS | 65 |
| 4.1. | Conditions for crystallization | 65 |
| 4.2. | The melting point | 67 |
| 4.3. | The crystallization process | 72 |
| 4.3.1. | Nucleus formation and crystal growth | 72 |
| 4.3.2. | Isothermal crystallization | 75 |
| 4.4. | Crystalline structure | 78 |
| 4.4.1. | Crystalline fraction | 78 |
| 4.4.2. | Crystal morphology | 79 |
| 4.5. | Effect on properties | 81 |
| 4.6. | Liquid-crystalline polymers | 84 |
| 5. | RUBBERY AND LIQUID PHASES | 86 |
| 5.1. | Rubbery phase | 86 |
| 5.2. | Transition of rubber to fluid | 91 |
| 5.3. | Fluid condition | 92 |
| 5.3.1. | Viscosity | 92 |
| 5.3.2. | Non-Newtonian behaviour | 93 |
| 5.3.3. | Melt elasticity | 97 |
| 5.4. | Some consequences for processing | 97 |
| 6. | VISCO-ELASTICITY | 102 |
| 6.1. | Models | 102 |
| 6.2. | Dynamic mechanical behaviour | 110 |
| 6.3. | Integration | 112 |
| 7. | MECHANICAL PROPERTIES | 117 |
| 7.1. | Stress-strain diagram | 117 |
| 7.2. | Stiffness and creep | 118 |
| 7.2.1. | Modulus of elasticity | 118 |
| 7.2.2. | Creep | 120 |
| 7.2.3. | Non-linearity | 122 |
| 7.2.4. | Physical ageing | 124 |
| 7.3. | Damping | 126 |
| 7.4. | Strength | 130 |
| 7.4.1. | Tensile strength | 130 |
| 7.4.2. | Long term strength | 131 |
| 7.4.3. | Impact strength | 136 |
| 7.5. | Surface properties | 138 |
| 7.5.1. | Hardness | 138 |
| 7.5.2. | Friction | 139 |
| 7.5.3. | Abrasion | 142 |

| | | |
|---------|------------------------------------|-----|
| 8. | FURTHER PROPERTIES | 144 |
| 8.1. | Thermal properties | 144 |
| 8.1.1. | Brittleness temperature | 144 |
| 8.1.2. | Softening | 145 |
| 8.1.3. | Thermal expansion | 147 |
| 8.1.4. | Thermal conduction | 148 |
| 8.1.5. | Maximum temperature of use | 150 |
| 8.1.6. | Burning behaviour | 150 |
| 8.2. | Electrical properties | 151 |
| 8.2.1. | Electric resistance | 151 |
| 8.2.2. | Dielectric properties | 154 |
| 8.2.3. | Electric strength | 155 |
| 8.3. | Optical properties | 155 |
| 8.4. | Effects of environment | 156 |
| 8.5. | Stress corrosion | 158 |
| 8.6. | Diffusion and permeability | 159 |
| 9. | POLYMERIC COMPOUNDS AND COMPOSITES | 161 |
| 9.1. | Polymer blends | 161 |
| 9.1.1. | General | 161 |
| 9.1.2. | Miscibility of polymers | 161 |
| 9.1.3. | Detection of miscibility | 164 |
| 9.1.4. | Block copolymers | 165 |
| 9.1.5. | The formation of dispersions | 168 |
| 9.1.6. | Properties of blends | 171 |
| 9.2. | Reinforcement by particles | 176 |
| 9.3. | Short fibres | 177 |
| 9.4. | Long fibres | 181 |
| 10. | DATA ON MATERIALS | 184 |
| 10.1. | Thermoplastics | 185 |
| 10.2. | Thermosets | 189 |
| 10.3. | Elastomers | 190 |
| 11. | PROCESSING TECHNIQUES | 193 |
| 11.1. | Principles of processing | 193 |
| 11.1.1. | General | 193 |
| 11.1.2. | Production cost | 195 |
| 11.1.3. | Compounding | 197 |
| 11.2. | Casting and compression moulding | 198 |
| 11.2.1. | Casting | 198 |
| 11.2.2. | Rotational moulding | 199 |

| | |
|---------------------------------|-----|
| 11.2.3. Compression moulding | 201 |
| 11.3. Injection moulding | 205 |
| 11.3.1. General | 205 |
| 11.3.2. Limitations | 208 |
| 11.3.3. Defects | 209 |
| 11.3.4. Foam | 213 |
| 11.4. Calendering and extrusion | 213 |
| 11.4.1. Calendering | 213 |
| 11.4.2. Extrusion | 215 |
| 11.4.3. Film blowing | 219 |
| 11.4.3. Bottle blowing | 220 |
| 11.5. Secondary shaping | 222 |
| 11.5.1. Thermoforming | 222 |
| 11.5.2. Cold sheet forming | 224 |
| 11.5.3. Forging | 224 |
| 11.5.4. Bending | 225 |
| 11.5.5. Machining | 226 |
| 11.5.6. Welding | 226 |
| 11.5.7. Gluing | 228 |
| 11.5.8. Surface coating | 229 |
| 11.6. Processing of composites | 230 |
| 11.6.1. General | 230 |
| 11.6.2. Impregnating | 230 |
| 11.6.3. Foaming | 232 |
| LITERATURE | 236 |
| INDEX | 237 |

1

Introduction

1.1. Origin of plastics / polymers

The main characteristic of polymers is, that they are composed of extremely large molecules; their molecular mass ranges from 10.000 to more than 1.000.000 g/mol, in contradiction to “normal” low-molecular substances, which in general are in the order of 100 g/mol (water 18, sugar 342). Polymer molecules are often long, *thread-like chains*, which are sometimes branched, sometimes chemically cross-linked with each other so that they form a network.

Polymers are abundantly present in nature, in vegetable and animal tissues (mainly as cellulose and proteins). Several technically used polymers have a natural origin; they are being used as technical materials as they are harvested from natural materials (“*natural polymers*”).

Other polymers are partly from a natural origin; the chain molecule has grown in a living tissue, but has been chemically modified into a “*half-synthetic polymer*”.

A growing number of polymers is wholly *synthetic*; the chain molecule or the network is being built up from small molecules (monomers) in a chemical process.

Some examples of these categories are given below:

Natural polymers:

- vegetable: timber, cotton, jute, sisal, hemp, cork, etc.
- animal : wool, silk, fur, etc.

Half-synthetic polymers:

- from wood: celluloid, cellophane, viscose-rayon, cellulose plastics,
- from milk: casein, from which casein plastics,
- from hides, via a tanning process: leather,
- from rubber latex, via i.a. vulcanization: technical rubber.

Synthetic polymers:

These are synthesized from low-molecular components, mostly organic monomers. Most of the monomers are prepared from fossil fuels; here we can distinguish between two main categories:

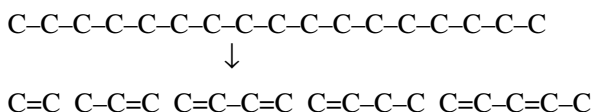
- *carbochemistry* (from coal)
- *petrochemistry* (from petroleum or natural gas).

Carbochemistry

- Coal can be pyrolysed above 800 °C into coke, tar and a series of hydrocarbons.
- Gasification of coal with steam and air results in, a.o., a series of hydrocarbons.

Petrochemistry

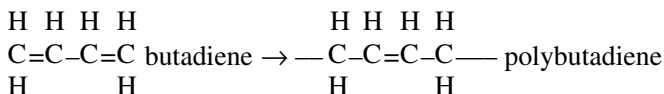
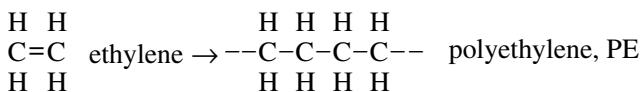
From distillation of crude oil a number of fuels are obtained (kerosine, petrol, gasoline, etc.) and a residue. The latter can be transformed into a series of lighter components by vacuum distillation and thermal cracking. Also lighter fuels (“naphtha”) can be converted to a series of various hydrocarbons by thermal cracking and fractionation. Natural gas can supply a range of other components by steam conversion or partial oxidation. It is important that thermal cracking of saturated hydrocarbons results in unsaturated ones, containing one or more double bonds between the C-atoms. This renders these molecules very suitable to be used as *monomers* in polymerisation reactions. A long saturated chain is, for instance, split up into a number of shorter molecules which are *unsaturated* due to a shortage of H-atoms; they contain, therefore, one or more double bonds:



Some of these molecules, such as the first and the second (ethylene and propylene) can be used to build saturated chains (PE and PP). Other ones, such as the third one (butadiene) form unsaturated chains, which can react with sulphur to form vulcanized rubbers. (See Qu. 1.3, 1.4 and 1.5).

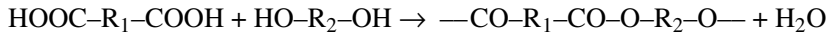
Polymer synthesis

From the monomers obtained from carbochemical or petrochemical sources polymers can be built up. As mentioned above, *double bonds* can thereby play an important role. Some simple examples:



Polymers can also be synthesized from saturated monomers, e.g. by *condensation* of an organic acid with an alcohol into an ester with the formation of water. Simple alcohols and fatty acids, such as ethyl alcohol (C₂H₅OH) and acetic acid (C₂H₅COOH) result in a low-molecular ester, ethyl acetate, but when bifunctional

molecules are used, a polymer chain (a *polyester*) is formed:



When the alcohol is trifunctional (a triol), the result is a *network*:

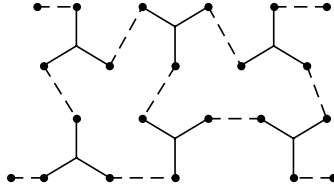


Figure 1.1.

Plastics

Plastics as technical materials are based on polymers (or macromolecular substances), but in most cases they contain a number of added components. Such an added material may be another polymer; in this case we have a polymer *blend*. Moreover, there is a large variety of *additives* and *fillers*, compounded into the polymer for various purposes, which are roughly categorized below:

- in behalf of *processing*:
 - lubricants for the transportation in the processing machine,
 - antioxydants for protection of the polymer against oxydative degradation during processing,
 - sulphur, for the vulcanization of rubbers,
 - accelerators, for speeding up the network forming reaction with rubbers and thermosets,
 - blowing agents, for producing foams,
 - etc.
- in behalf of *mechanical properties*:
 - plasticizers, e.g. in PVC, to obtain flexibility,
 - quartz powder, mica, talcum etc. to improve the stiffness.
 - short glass fibres, to improve stiffness and strength,
 - rubber particles, to improve impact strength,
 - etc.
- in behalf of *other properties*:
 - ultraviolet stabilizers, to protect the polymer against degradation in sunlight,
 - antioxydants, for protection against degradation during use at elevated temperatures,
 - antistatic agents, to reduce electrostatic charging,
 - pigments,
 - cheap fillers such as wood flour, for price reduction,
 - flame retarding additives, etc

1.2. Main categories

Taking the chain structure as a criterion, polymers can be subdivided into two main categories, viz. single chains and networks.

Single chains are linear macromolecules, though the chains may be branched. An average scale model for such a polymer chain is a human hair with a length of a metre. Normally, chains are not present in this extended shape, but rather as *diluted coils*, which may, in the scale model, have a diameter of a few cm.

The coils are mutually *entangled*; this fact is largely responsible for the special behaviour of polymers! Between chain segments relatively *weak interaction* forces are present; chain segments can move with respect to each other under the influence of relatively small external stresses. Consequently, the *stiffness* of polymers is rather low.

Flow, on the contrary, is strongly hindered by the entanglements between the coils; this is why fluid polymers show excessively *high viscosities*, which necessitate the use of heavy processing machines.

In *networks* the molecular chains are connected by strong primary chemical links; in fact a network is a single gigantic molecule. Networks can be formed in two different ways:

- a. by forming *bridges* between single chains; this is the case with the vulcanization of rubbers, mostly by sulphur bridges. But also curing of unsaturated polyester resins is a matter of forming bridges between chains, in this case with the aid of (poly)styrene.
- b. by reacting *bivalent* with *tri-(or more)-valent* molecules, e.g. in synthesizing formaldehyde resins.

In networks chain entanglements and local movements of chain segments with respect to each other also occur, but flow is not possible.

From the foregoing we can divide the field of macromolecular materials into three main categories:

Thermoplastics are non-crosslinked systems, which flow at elevated temperatures and which, upon cooling, return to the solid state.

Synthetic elastomers are analogous to thermoplastics, but they are in a softened condition. As such they show flow, but after the formation of a network (by cross-linking) they are no longer fluid but retain their shape.

Thermosets owe their name to the fact that the formation of a network, the curing reaction, in many (but not in all) cases occurs at elevated temperature. The network is considerably tighter than in vulcanized rubbers. A formed thermoset does not increase in hardness or stiffness upon temperature increase, but, on the contrary, shows softening, but no flow.

Within each of these three categories a large number of main types exists, each characterized by a specific structure of the macromolecule. Within each main type several variations occur, e.g. concerning chain length, chain regularity, copolymerisation (presence of more than one monomer in the chain), etc.

In the assortment of technically used materials we also meet a broad variability of additives and fillers, added by the manufacturer.

In the next section an (incomplete) survey is given of a number of polymers, as a first orientation in the field of plastics materials.

1.3. The most important plastics

(See Qu. 1.14 – 1.20).

1.3.1. Thermoplastics

Polyethylene (PE) is a rather soft and tough, crystalline polymer, which is being manufactured in three main types: *LDPE* (low-density PE $\approx 0.92 \text{ g/cm}^3$), *HDPE* (high-density PE $\approx 0.95 \text{ g/cm}^3$), and, more recently, *LLDPE* (linear-low-density PE, $\approx 0.92 - 0.95 \text{ g/cm}^3$). The stiffness of PE increases strongly with increasing density. All types gradually lose their properties upon temperature increase, and they melt at 105 to 130 °C, respectively. Principal applications are: packaging film, bags, pipes, crates, pails, bottles, etc. Special grades are made in smaller quantities, such as *UHMPE* (ultra-high-molecular), which is extremely tough and abrasion resistant, and which is, moreover, used for making super-strong PE-fibres. A new development is a series of PE with very low density (.86 to .90 g/cm^3), a series which extends into the region of rubbers.

Polypropylene (PP) resembles PE, but is somewhat harder and stiffer than HDPE. It is crystalline as well, and melts at $\approx 165 \text{ °C}$. Its impact strength at lower temperatures is quite poor; therefore PP is often modified with a certain amount of rubber (mostly built-in as a copolymer). Main applications are: film for packaging, fibres, crates, pipes, automotive parts (often with reinforcing fillers). A special feature of PP is its ability to form integral hinges with a practically unlimited resistance against repeated bending.

Polyvinylchloride (PVC) is a hard, amorphous polymer which softens at about 85 °C. Also in PVC rubbers are sometimes added in order to improve the impact strength. The main applications of PVC are: pipes, gutters, front panels of buildings, cables, bottles, floor tiles. A much softer and more flexible material is obtained by blending with plasticizers: soft or plasticized PVC is being used in artificial leather, tubes and hoses, footwear, films, etc.

Polystyrene (PS) is an amorphous, very brittle, hard polymer with a softening temperature of about 90 °C. Improvement of its impact strength is again obtained by

blending with rubber (in most cases butadiene rubber), which goes at the cost of stiffness. Unmodified PS is being largely applied as foam for packaging and thermal insulation. High-impact PS (TPS or HIPS) is used for coffee cups, household ware etc.

Styrene-Acrylonitrile (SAN) is somewhat stiffer than TPS, and has a better resistance against impact and temperature. It is mainly used in parts of household- and electrical appliances, battery houses etc.

Acrylonitrile-Butadiene-Styrene (ABS) is sometimes a terpolymer of three monomers, but in most cases a blend of two copolymers. ABS has an excellent impact strength and a relatively high softening temperature (about 110 °C). Its stiffness is only marginally lower than that of PS. It finds large-scale applications in the automotive industry, in toys, telephones, TV-housings, etc.

Polymethylmethacrylate (PMMA), carrying trade names such as Perspex and Plexiglass, is an amorphous, relatively hard and transparent polymer. Its stiffness is retained until near its softening temperature (110 °C). Most applications are based on its superior optical qualities: safety glass, decoration material, traffic signs, etc.

Polyamide (PA) is generally known as “nylon”. This is a collection of polymers, which differ in chain structure, and which are, according to the numbers of consecutive C-atoms in the chain, designated as (a.o.) PA-6, PA-6,6, PA-11, PA-4,6 and PA-12. Initially PA’s were only used as fibre materials, but later on they found a position under the engineering plastics. Polyamides are crystalline polymers with relatively high melting points (between about 200 and 300 °C). They possess a good impact strength, due to the fact that they absorb several percents of water from the atmosphere. Moreover, a good abrasion resistance and a low friction make them suitable for technical use, such as in bearings and gear wheels. Quite often polyamides are reinforced with short glass fibres to improve their stiffness.

Polyoxymethylene (POM) is, again, a crystalline polymer, with a melting point of about 180 °C. Its mechanical properties enable it to gradually replace metals in a number of applications. Many technical parts are being made from POM, such as gear wheels, bars, automotive accessories, parts of several apparatuses and machines. The polymer is used as such (e.g. “Delrin”), but also as a copolymer with a small amount of ethylene oxide (e.g. “Celcon” and “Hostaform”).

Polycarbonate (PC) is, up to about 140 °C, an amorphous glassy transparent polymer with excellent mechanical properties, in particular as regards its impact strength. This renders it very suitable for substitution of glass, but also for a series of technical applications in which it replaces metals. For the latter, reinforcement with short glass fibres opens further possibilities. A weak point of PC is its poor resistance against environmental stress cracking in contact with a number of organic liquids.

Polyethylene terephthalate (PETP) is a (saturated) polyester and is, like nylon, known for its large-scale use as a textile fibre. Moreover it is being applied at an increasing scale as a plastic, viz. in films, bottles (the “PET-bottle”) and injection-mouldings. Though its stiffness decreases significantly above 70 °C, it remains a solid up to its melting point (255 °C).

Polybutylene terephthalate (PBTP) differs in its chemical structure only slightly from PETP; its melting point is somewhat lower and its processability is better. The applications in injection moulded articles are similar to those for PETP.

Polyphenylene oxide (PPO) or *Polyphenylene ether* (PPE) is an amorphous polymer with a softening temperature of about 210 °C. To improve its processability it is mostly blended with PS (modified PPE, e.g. “Noryl”), which is at the cost of its heat distortion temperature. The properties are excellent; the applications are mainly in fine-mechanical construction, in automotive parts, in household equipment etc.

Polysulphone (PSU) is a high-performance polymer with superior mechanical, electrical and thermal properties in a temperature region from –100 up to 180 °C. It is mainly used in exacting mechanical and electrical applications.

Polyphenylene sulphide (PPS) (e.g. “Ryton”) is a highly crystalline polymer with a melting point of 290 °C. It combines good mechanical properties with very high thermal and chemical resistance; it is, moreover, self-extinguishing. It is, i.a., used as protective coating on metal surfaces.

Polyimide (PI) caps all other polymers in its temperature range of use (–200 to 260 °C in air; short-time even up to 500 °C). Because of its high price, it is used in special cases only, such as space vehicles, nuclear reactors and some electronic parts. Newer developments, related to polyimide, are the polyether imides (e.g. “Ultem”), polyester imides and polyamide imides (e.g. “Torlon”), all with very good mechanical, thermal and electrical properties and self-extinguishing.

Polytetrafluoroethylene (PTFE), mostly known as “Teflon”, has as special properties its high melting point (327 °C), its very good resistance against chemicals and its extremely low friction. though the polymer is mechanically weak and shows a strong tendency to creep, though processing is very difficult (only possible via a sintering process) and though it is very expensive, it is being used in a number of applications such as bearings, pipes, sealing rings, electrical insulation and coatings on kitchen pans. Often the polymer is reinforced with fillers.

Tetrafluoroethylene-perfluoropropylene (FEP) resembles PTFE in its properties, but can be processed as a thermoplastic polymer.

Polyvinylidene fluoride (PVDF) and *Ethylene tetrafluoroethylene copolymer* (ETFE) can be considered as “diluted” PTFE’s, which in their structure and their properties

are in between PTFE and the polyolefins PE and PP. They are processable with the normal techniques and find similar applications as PTFE.

Cellulose acetate (CA) and *Cellulose acetate butyrate* (CAB) are, contrary to the polymers mentioned so far, not fully synthetic, but derivatives of vegetable cellulose. They are strong, tough and well processable materials, used in many household- and technical applications, such as hammer heads, magnetic tape, toys etc. CAB has a higher form stability than CA, and is used in automotive accessories and in pipes.

Polybutylene (PB) belongs to the family of polyolefins (PE and PP), but is much less used because of its higher price. Though it does not differ very much from PE in stiffness and melting point, it has a better resistance against creep and environmental stress cracking than PE and PP and a higher toughness and tear resistance. Its applications are mainly in film for heavy-duty bags and in hot water transport pipes.

Polymethylene pentylene (PMP) is, again, a polyolefin, but with a much higher melting point than the other ones (240 °C). Despite its crystalline nature PMP can be well transparent. It is used a.o. in laboratory bottles. One of its trade names is “TPX”.

Polyether ether ketone (PEEK) and *Polyether sulphone* (PES) belong to the most recent developments in the field of technical high-performance polymers. Both possess very good thermal and mechanical properties, which can be further improved by reinforcing fibres. Their application is mainly in aircraft and space vehicles.

Polyketone (PK) (“CARILON”) is a new polymer with an attractive combination of properties (very tough, high abrasion resistance, high temperature resistance, easy to process, good chemical resistance and barrier properties). It is trying to find its way in various potential applications.

1.3.2. Thermosets

Phenol-formaldehyde (PF) was the first fully synthetic macromolecular material (“Bakelite”, 1907). In a slightly precured condition and provided with fillers, it is, as a moulding powder, available for processing into end-use articles such as bulb fittings, switch housings, coils, laminated wood and foam for thermal insulation.

Ureum-formaldehyde (UF) is comparable to PF, but is somewhat stiffer and has, because of its colourlessness and gloss, a more attractive appearance. The applications are in the same fields as PF.

Melamine-formaldehyde (MF) is qualitatively better than UF. It is, therefore, used in more demanding applications such as crockery, various electrotechnical articles and decorative panels.

Unsaturated polyesters (UP) can, with a second component, e.g. styrene, and with

initiators and accelerators be cured into a network structure. The reaction can take place at room temperature. UP is, in most cases, used in combination with glass fibres, and finds its applications in pipes, vessels, boat building etc.

Epoxy resin (EP) has to be mixed with a second component, the curing agent, to undergo the curing reaction, which, as with UP, can take place at ambient temperatures. Epoxy/fibre composites (with glass, carbon or aramid fibres) find similar applications as UP/glass, but are being applied more selectively because of their higher price and better properties. Besides, epoxies are used in lacquers and adhesives and as casting resins in electrotechnical applications.

Polyurethanes (PU). The thermosetting type of this large family of polymers is mainly used as foam. A mixture of two components with a foaming agent forms a light, hard foam, which is a superior thermal insulator.

1.3.3. Synthetic elastomers

Styrene butadiene rubber (SBR) is, quantitatively, the most important synthetic rubber. It is a copolymer of styrene and butadiene in such a ratio that its rubbery nature predominates. vulcanization is carried out with sulphur, reinforcement with carbon black. It is used at a very large scale in tyres for passenger cars, thanks to its excellent combination of abrasion resistance and friction on the road. In large tyres it can not replace natural rubber because of its heat development (hysteresis losses).

Butadiene rubber (BR) or Polybutadiene has an excellent abrasion resistance and a very low damping, but is, undiluted, too “jumpy” for use in tyres. In blends with SBR or natural rubber a good compromise of properties can be obtained.

Isoprene rubber (IR) or Polyisoprene is a synthetic copy of natural rubber (NR) and approaches NR in its properties. Besides for tyres, IR is, because of its good flow properties, suitable for injection moulding.

Butyl rubber (IIR) is derived from polyisobutylene, a polymer which is not further mentioned in this chapter, which has a rubbery nature, but which can not be vulcanised in the conventional way with sulphur. This objection is taken away by copolymerisation with a small amount of isoprene. Butyl rubber has a very low resilience, but outrivals all other rubbers in resistance to gas permeation; for that reason it is generally used for tyre inner tubes.

Chloroprene rubber (CR) is a synthetic rubber with very high chemical resistance, and is, therefore, applied in cable protection, oil transport tubes etc.

Nitrile rubber (NBR), a copolymer of butadiene and acrylonitrile, is characterized by its high resistance against light and oxygen, thus against ageing. Moreover it is not attacked by oil and several organic solvents. For these reasons, it finds its place in demanding applications.

Ethylene-propylene rubber (EPR or EPDM) is, basically, a copolymer of ethylene and propylene. Because of the random arrangement of the monomers in the chain, crystallization does not occur, and the material behaves as a rubber. Just as with polyisobutylene, vulcanization with sulphur is impossible (the chain is saturated). Also here, a small amount of another monomer is incorporated, which enables the vulcanization and thus the use as a technical elastomer. EPR has a high resistance against ageing and chemical attack, and is, compared with other “specialty” rubbers, relatively cheap.

Silicone rubbers have, contrary to all other polymers, no carbon atoms in their main chain, but silicon and oxygen atoms only. They can be used up to very high temperatures (250 °C) and are highly resistant against ageing, so that, despite of their high price, they are frequently used in demanding applications.

Thermoplastic elastomers (TPE’s) are characterized by the exceptional property that, without vulcanization, they behave as cross-linked rubbers. They are block-copolymers, in which blocks of the same nature assemble in hard domains, acting as cross-links between the rubbery parts of the chain. These hard domains lose their function when they reach their softening temperature, so that the material can then be processed as a thermoplast. One of the oldest member of the family of TPE’s is SBS (styrene-butadiene-styrene block copolymer), but several other TPE’s have been developed, i.a. on the basis of polyesters, polyurethanes and polyolefins. In their properties these polymers cover a broad range between conventional rubbers and soft thermoplastics.

Polyurethane rubber (PUR). Not only in the thermosets (and the thermoplastics), but also in the field of synthetic elastomers polyurethanes have found a position, namely as a softer type. It is, again, formed from two components and is, with a blowing agent, processed into a foam. Polyether mattresses belong to this category, but also microcellular structural foams, used in bumpers, head- and arm-rests in motorcars, etc.

1.3.4. *Composite plastics*

Blends of polymers are manufactured and applied at an increasing scale. Only in exceptional cases are polymers soluble in each other and can form a homogeneous blend (an example: PPE + PS, a blend known as “Noryl”). In most cases blends are, therefore, dispersions. Rubber particles are dispersed in brittle polymers to improve their impact strength (toughened PS and PP, ABS etc.), but also hard polymers are combined to reach a favourable compromise between properties (and price).

Reinforcement with particles such as chalk, quartz, mica and glass spheres, is frequently carried out with thermoplastics and thermosets to obtain a higher stiffness (and sometimes a higher strength). There is a gradual transition from high-quality to

cheap fillers, the latter being mainly used as price reducing agents, but also for. e.g. reducing shrinkage in processing. Rubber vulcanisates gain considerably in strength and abrasion resistance by the incorporation of carbon black (up to 40 weight %)

Reinforcement with short fibres is important for thermoplasts and thermosets. With the former, very short fibres (glass or other) are blended into the polymer; the latter allow the use of longer fibres. The effect is a 3- to 5-fold increase of the stiffness and a 1.5 to 3-fold increase in strength.

Foams can be made from thermoplastics, thermosets and rubbers. Densities can be obtained from nearly solid down to 200 times diluted. Structural (or integral) foams have a solid skin. The best known foam materials are polystyrene foam, polyurethane foam and polyether foam.

Reinforcement with continuous fibres. In this case the fibres, as strands or cloth, are largely responsible for the mechanical properties. Traditionally, thermosetting resins are used in this case, because of the ease of impregnating fibre bundles or cloth with the low-viscosity uncured resin. Recently however, techniques have been developed to also reinforce thermoplastics with long fibres. Conventional combinations are polyester/glass (GF-UP) and epoxy/glass (GF-EP), but also high-quality fibres as carbon and aramide, and thermoplastic matrices such as PEEK are being used for special applications.

2

Molecular composition

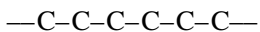
2.1. Chain structure

A linear chain consists of a “backbone”, the main chain, at which side groups are attached. In this section a simple classification of the various types of main chain will be given, followed by a survey of frequently occurring side groups.

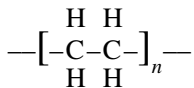
2.1.1. Main chain (Qu. 2.1 and 2.2)

Carbon atoms only:

- saturated:

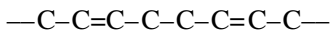


example: polyethylene (PE)

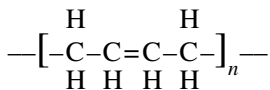


also PP, PS, PVC, PB, PMMA, PTFE, etc. (see § 2.1.2)

- unsaturated:

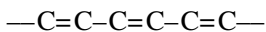


example: polybutadiene

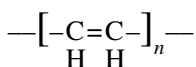


also IR, CR, etc. (see § 2.1.2)

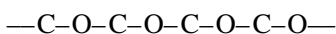
- more unsaturated:



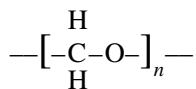
example: polyacetylene.



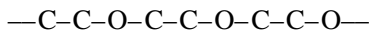
Carbon and oxygen atoms:



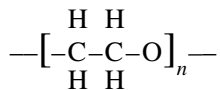
example: polyoxymethylene (POM) :



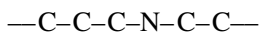
also



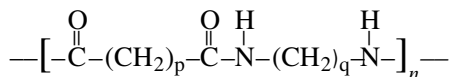
example polyethyleneoxyde (PEO)



Carbon and nitrogen atoms:



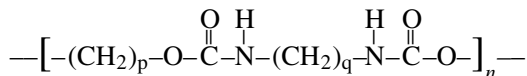
example: various types of PA (nylon):



Carbon, oxygen and nitrogen atoms:



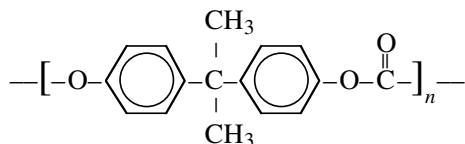
example: various types of polyurethanes:



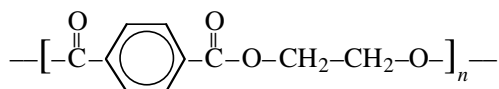
Carbon rings:



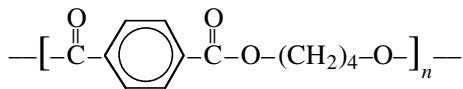
example: polycarbonate (PC):



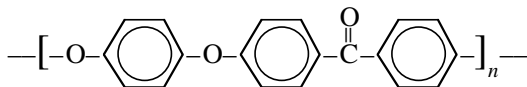
other example: polyethylene terephthalate (PETP):



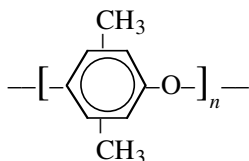
also PBTP, with four instead of two CH₂ groups,



polyetherether ketone, PEEK:



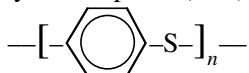
polyphenylene ether, PPE:



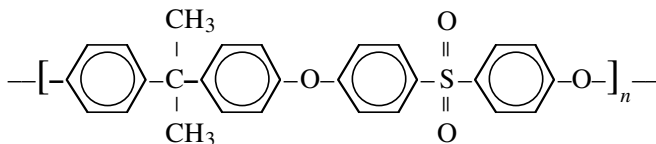
Combination with sulphur atoms:

examples:

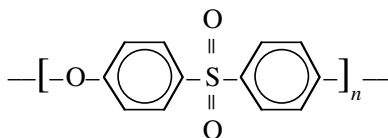
polyphenylene sulphide (PPS):



polysulphone (PSU)

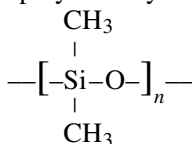


polyether sulphone, PES:



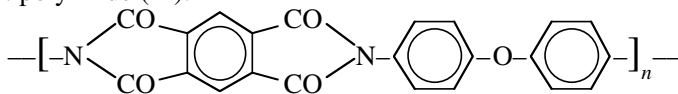
Silicium and oxygen atoms only:

example: polydimethylsiloxane (silicone rubber):

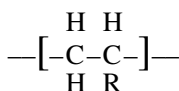


Multiple rings:

example: polyimide (PI):

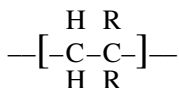
**2.1.2. Side groups**

- The most frequently occurring side group is the hydrogen atom; it is the only one with polyethylene, polybutadiene and polyoxymethylene.
- Other arrangements often met are:
- vinyl polymers



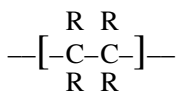
- with:
- | | |
|--------------------------------------|-------------------------|
| R = CH ₃ | polypropylene (PP) |
| R = Cl | polyvinylchloride (PVC) |
| R = C ₆ H ₅ = | polystyrene (PS) |
| R = CH ₂ -CH ₃ | polybutylene (PB) |
| R = CN | polyacrylonitrile (PAN) |

- vinylidene polymers



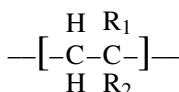
- with:
- | | |
|---------------------|--------------------------------|
| R = Cl | polyvinylidenechloride (PVDC) |
| R = F | polyvinylidene fluoride (PVDF) |
| R = CH ₃ | polyisobutene (PIB) |

- polytetrafluorethylene (PTFE)



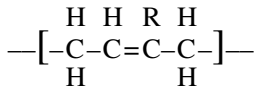
- with: R = F

- polymethylmethacrylate (PMMA)



- with: R₁ = CH₃ and R₂ = COOCH₃

– polydienes



with: (R = H polybutadiene (BR)
 R = CH₃ polyisoprene (IR)
 R = Cl polychloroprene (CR)

– etc. etc.

2.1.3. Copolymers

Copolymer chains are built up from more than one type of monomeric units. Some examples::

| | |
|--------------------------|------------------------|
| ethylene + propylene: | EPR |
| styrene + butadiene: | SBR or SBS (see § 2.3) |
| styrene + acrylonitrile: | SAN |
| isobutylene + isoprene: | IIR (butyl rubber) |
| etc. | |

Also terpolymers (with three monomers) are made:

| | |
|--|------------------------------|
| ethylene + propylene + a diene: | EPDM |
| acrylonitrile + styrene + acrylic ester: | ASA |
| ethylene + CO + propylene: | PK, poly ketone (“Carilon”). |
| (see further § 2.3) | |

2.2. Chain length and distribution

2.2.1. Averages

The chain length can be expressed as degree of polymerisation P (number of monomeric units in the chain), or, in most cases, as molar mass (or molecular weight) in g/mol. Sometimes the “better” unit, kg/mol is used; the difference is a factor of 1000. In this book the older unit, g/mol, will mostly be used.

An example: PE with a degree of polymerisation P of 5000 has a molar mass:

$$M = 5,000 \cdot (2C + 4H) = 5,000 \cdot (24 + 4) = 140,000$$

Of most polymers various types exist, which differ in molecular mass. The strongest example is PE, which is made at more than 10 different levels of M , the extremes differing by a factor of 20. But also within each type the chains may largely differ in length, namely by a factor of 100 or even 1000. Therefore every statement about a molar mass indicates an *average*.

Averages can be defined in several ways, for example after number or after weight. A simple example:

1 chain with mass 100 and
1 chain with mass 10

then the *number average* is:

$$\frac{1}{2} \cdot 100 + \frac{1}{2} \cdot 10 = 55$$

since the numbers are equal, and the number fractions n_1 and n_2 are both $\frac{1}{2}$.
Now consider a system with:

1 chain with mass 100 (total mass 100) and
10 chains with mass 10 (total mass 100)

then the *weight average* is:

$$\frac{1}{2} \cdot 100 + \frac{1}{2} \cdot 10 = 55$$

because now the weight fractions are equal (w_1 en w_2 both $\frac{1}{2}$).

Expressed in a formula:

$$\text{number average } \bar{M}_n = \sum n_i \cdot M_i$$

in which n_i is the number fraction of the chains with mass M_i , and $\sum n_i = 1$.

The weight fraction is $W_i = n_i \cdot M_i$; now however, $\sum W_i$ is not equal to 1; the fractions W_i must, consequently, be reduced (*normalized*) to w_i , so that $\sum w_i = 1$:

$$w_i = \frac{n_i \cdot M_i}{\sum n_i \cdot M_i} = \frac{W_i}{\sum W_i}$$

The weight average is now:

$$\bar{M}_w = \sum w_i \cdot M_i$$

Also valid is:

$$\bar{M}_w = \frac{\sum n_i \cdot M_i^2}{\sum n_i \cdot M_i} = \frac{\sum n_i \cdot M_i^2}{\bar{M}_n}$$

In most cases it is necessary to work backward from the weight fractions w_i :

$$N_i = \frac{w_i}{M_i}$$

but

$$\sum N_i \neq 1$$

so N_i has to be normalized to n_i with:

$$n_i = \frac{N_i}{\sum N_i} = \frac{w_i/M_i}{\sum (w_i/M_i)}$$

Now $\sum n_i = 1$, and \bar{M}_n follows from $\bar{M}_n = \sum n_i \cdot M_i$.

The calculation of \bar{M}_n is easier with:

$$\bar{M}_n = \sum n_i \cdot M_i = \frac{\sum w_i}{\sum (w_i/M_i)} = \frac{1}{\sum (w_i/M_i)}$$

Also “higher” averages are used:

$$\bar{M}_z = \sum z_i \cdot M_i$$

in which

$$z_i = \frac{w_i \cdot M_i}{\sum w_i \cdot M_i} \quad (\text{normalized})$$

so

$$\bar{M}_z = \frac{\sum w_i \cdot M_i^2}{\sum w_i \cdot M_i} = \frac{\sum n_i \cdot M_i^3}{\sum n_i \cdot M_i^2}$$

This is the so-called *z-average*. A further step in the same direction gives the $(z+1)$ -average:

$$\bar{M}_{z+1} = \frac{\sum n_i \cdot M_i^4}{\sum n_i \cdot M_i^3}$$

We apply the formulae for \bar{M}_n , \bar{M}_w and \bar{M}_z to the simple example given above:

| | | | | |
|---|-------------|--|---------|-----------------|
| A | 100 | 10 | | (100 + 10) |
| B | 100 | 10 | _____ | (100 + 10 × 10) |
| | | | A | B |
| | M_1 | = mass chain 1 | 100 | 100 |
| | M_2 | = mass chain 2 | 10 | 10 |
| | n_1 | = number fraction 1 | 1/2 | 1/11 |
| | n_2 | = number fraction 2 | 1/2 | 10/11 |
| | \bar{M}_n | = $\sum n_i \cdot M_i$ | 55 | 18.2 |
| | w_1 | = weight fraction 1 = $n_1 \cdot M_1 / \sum n_i \cdot M_i$ | 10/11 | 1/2 |
| | w_2 | = weight fraction 2 = $n_2 \cdot M_2 / \sum n_i \cdot M_i$ | 1/11 | 1/2 |
| | \bar{M}_w | = $\sum w_i \cdot M_i$ | 91.8 | 55 |
| | z_1 | = z-fraction 1 = $w_1 \cdot M_1 / \sum w_i \cdot M_i$ | 100/101 | 10/11 |
| | z_2 | = z-fraction 2 = $w_2 \cdot M_2 / \sum w_i \cdot M_i$ | 1/101 | 1/11 |

$$\bar{M}_z = \sum z_i \cdot M_i \qquad 99.1 \qquad 91.8$$

Another, more realistic example: A blend is made of three monodisperse fractions (i.e. in each fraction all chains have the same length), with masses of 20, 50 and 30 grammes and molar masses of 20,000, 100,000 and 300,000 g/mol, respectively. The mass fractions are now:

$$w_1 = \frac{20}{100} = 0.2$$

$$w_2 = \frac{50}{100} = 0.5$$

$$w_3 = \frac{30}{100} = 0.3 \quad (\sum w_i = 1)$$

This leads to:

$$\bar{M}_w = 0.2 \cdot 20000 + 0.5 \cdot 100000 + 0.3 \cdot 300000 = 144000$$

\bar{M}_n can be calculated with:

$$N_1 = \frac{0.2}{20000}, \quad N_2 = \frac{0.5}{100000}, \quad N_3 = \frac{0.3}{300000}, \quad \sum N_i = \frac{4.8}{300000}$$

After normalization we find: $n_1 = 10/16$, $n_2 = 5/16$, $n_3 = 1/16$.

$$\bar{M}_n = (10/16) \cdot 20000 + (5/16) \cdot 100000 + (1/16) \cdot 300000 = 62.500$$

(The calculation is simpler with $\bar{M}_n = 1/\sum(w_i/M_i)$).

The z -fractions are, unnormalized:

$$Z_1 = 0.2 \cdot 20000 \qquad Z_2 = 0.5 \cdot 100000 \qquad Z_3 = 0.3 \cdot 300000$$

and normalized:

$$z_1 = \frac{4}{144} \qquad z_2 = \frac{50}{144} \qquad z_3 = \frac{90}{144}$$

It simply follows now that:

$$\bar{M}_z = 222,778$$

The examples show clearly that in \bar{M}_n , \bar{M}_w and \bar{M}_z in this order of sequence, the longer chains play an increasingly dominant part.

In most cases \bar{M}_w is used for general characterization of the molar mass besides $D = \bar{M}_w/\bar{M}_n$, the heterogeneity index, is of importance as a simple measure for the spread in chain length. In the first example $D = 1.67$ for A and 3.03 for B. In the second example $D = 2.3$. For technical polymers D can have values from 1.1 up to 30.

An even more realistic question is, how the averages change when two polydisperse polymers of the same type are being blended. Suppose two batches, A and B, are available with weight average molar masses $(\bar{M}_w)_A$ and $(\bar{M}_w)_B$ and a blend is made of a weight fraction φ of A with a weight fraction $(1 - \varphi)$ of B. For the blend C the weight average is now:

$$(\bar{M}_w)_C = \varphi \cdot (\bar{M}_w)_A + (1 - \varphi) \cdot (\bar{M}_w)_B.$$

The number of chains in 1 gramme of polymer is N/\bar{M}_n (N is the Avogadro number). In 1 gramme of the blend C, φ grammes of A and $1 - \varphi$ grammes of B are present, so).

$$N/(\bar{M}_n)_C = \varphi N/(\bar{M}_n)_A + (1 - \varphi) N/(\bar{M}_n)_B,$$

or:

$$\varphi/(\bar{M}_n)_C = 1/(\bar{M}_n)_A + (1 - \varphi)/(\bar{M}_n)_B$$

How broad is now the distribution of the blend C? We find D_C by multiplying the expressions for $(\bar{M}_w)_C$ and $1/(\bar{M}_n)_C$. A much simpler expression is found when we consider a special case, viz. two components with the same degree of dispersion D , in which $(\bar{M}_w)_A = \alpha \cdot (\bar{M}_w)_B$ (and, therefore, $(\bar{M}_n)_A = \alpha \cdot (\bar{M}_n)_B$). Some calculation leads to

$$D_C = \frac{(\bar{M}_w)_C}{(\bar{M}_n)_C} = D[\varphi \cdot (1 - \varphi) \cdot \frac{(\alpha - 1)^2}{\alpha} + 1].$$

An example: $\alpha = 4$, \bar{M}_w of A (e.g. 60,000) is four times greater than \bar{M}_w of B (15,000). We choose $\varphi = \frac{1}{2}$, so we blend equal masses, and the blend has an \bar{M}_w of 37,500. When now, for instance, $D = 6$, so that the \bar{M}_n 's of both components are six times smaller than the \bar{M}_w 's (10,000 en 2,500, respectively), then

$$D_C = 6 \cdot [\frac{1}{2} \cdot \frac{1}{2} \cdot \frac{9}{4} + 1] = 6 \cdot \frac{25}{16} = 9.375 ;$$

the distribution width is increased by more than a factor 1.5. \bar{M}_n of the blend is now $37,500 / 9.375 = 4,000$.

This simple rule, though based on the assumption that the molar mass distributions are similar, has practical significance because polymers made in one and the same process, do in general not differ much in their heterogeneity index.

So far, we have considered the magnitudes of several types of average molar masses. The question may arise what the use is of these different averages; the attention paid to them might look a bit artificial. Well, it is easy to understand that various polymer properties are influenced by the molar mass. Moreover, it appears that different physical properties of polymers are controlled by different types of average molar mass. A few examples:

- The *number average*, \bar{M}_n , is proportional to the mass of one gramme of the polymer divided by the number of chains. It is, therefore, a function of the number of chains, and thus of the number of *chain ends* (apart from branching). Now suppose that a crack with a sharp tip propagates through a piece of the polymer, then this propagation is easier as less chains have to be broken, and it meets more chain ends on its way. This means that all properties in which crack propagation plays a role, such as impact strength, tear strength and environmental stress cracking are governed by \bar{M}_n .
- The *weight average*, \bar{M}_w , is the most practical one. If you blend, for instance, equal quantities (in kg) of two batches with molar masse M_1 and M_2 , then you would expect the average $(M_1 + M_2) / 2$. And this is, of course, a weight average, for nobody would consider to blend equal numbers of chains with each others! In addition, \bar{M}_w is specially responsible for the *viscosity* of the polymer in molten condition, and, therefore, for the processability. This holds, however, only as a first approximation, as we will see later in § 5.3.
- As a third example we look at the *z-average*, \bar{M}_z . In the foregoing we have seen that \bar{M}_z (and, in particular, \bar{M}_{z+1}), are governed by the longest cahains, while the sort chains have hardly any effect. A property in which the longest chains have a predominant effect, is the *melt elasticity*. This is a rather unexpected expression, because a fluid is, in general, not an elastic substance. Yes, but for polymers, it is! Let us consider a polymer, consisting for the larger part of short chains, with a single very long chain. When this polymer is deformed in a flow field, the long chain will, as a tracking-thread, keep the short chains together, and force them to return to the most probable conformation, so to return back. This is further treated in § 5.3.2. This “melt-elasticity” is of major importance for practical processing technology and for some other properties. It is clear that we cannot neglect higher averages, such as \bar{M}_z and \bar{M}_{z+1}

2.2.2. Example of a chain length distribution

In a polymerization process the chain length distribution or molar mass distribution (MMD) is influenced by a large number of factors and conditions; the kinetics of the reaction plays a very important role. The calculation of the resulting MMD is thus very complicated. For one of the simplest cases, a step reaction with polycondensation, a first-order approach is given here. As an example we take a hydroxy acid HO-R-COOH, which, upon condensation, forms the chain $[-O-R-CO-]_n$.

With each step a -COOH and an -OH group react with each other, forming an ester group and a water molecule. If we denote the numbers of -COOH and -OH groups both by U , then at the start of the reaction $U = U_0$ = the total number of hydroxy acid molecules.

After some time t , $U = U(t)$; the number of $-\text{COOH}$ and $-\text{OH}$ groups disappeared is $(U_0 - U)$, which also is the number of ester groups formed. We define the *conversion grade* p as the fraction of the number of groups which have reacted:

$$p = \frac{U_0 - U}{U_0} \quad \text{or} \quad U = (1 - p)U_0$$

Now there are U molecules, containing together U_0 basic units; the number of units per chain, the average *degree of polymerization* \bar{P} , is, therefore:

$$\bar{P} = \frac{U_0}{(1 - p) \cdot U_0} = \frac{1}{1 - p}$$

An example: With a conversion grade of 0,99 $\bar{P} = 100$. Evidently, this \bar{P} is a number average degree of polymerization, \bar{P}_n .

The question is now, how the distribution of P (and thus of M) looks like. We consider, during the reaction, when the conversion grade is p , a single $-\text{COOH}$ group. The chance that the $-\text{OH}$ group of this monomer has reacted with another $-\text{COOH}$ group, is p ; the chance that it has not reacted, is $(1 - p)$.

The chance of HOOC-R-OH thus is $(1 - p)$

The chance of HOOC-R-OOCR is p

The chance of HOOC-R-OOCR-OH is $p(1 - p)$

The chance of HOOC-R-OOC-R-OOCR is p^2

etc.

The chance of $(i - 1)$ times addition is p^{i-1}

the chance of not reacting with the i^{th} monomer is $(1 - p)$

the chance of both events, so the chance of the occurrence of a chain of i units, is the product $p^{i-1} (1 - p)$. This is, therefore the number fraction, n_i .

$$\frac{N_i}{N} = n_i = p^{i-1} (1 - p)$$

It follows easily that:

$$\sum_1^{\infty} n_i = 1$$

With this formula the value of the number average, found before, can be checked:

$$\bar{P}_n = \bar{i} = \frac{\sum n_i \cdot i}{\sum n_i} = \frac{1 - p}{1 - p} \cdot \frac{1 + 2p + 3p^2 + \dots}{1 + p + p^2 + \dots} = \frac{1}{1 - p}$$

The weight average degree of polymerization is:

$$\begin{aligned}\bar{P}_w &= \frac{\sum W_i \cdot i}{\sum W_i} = \frac{\sum n_i \cdot i^2}{\sum n_i \cdot i} = \frac{\sum p^{i-1} (1-p) i^2}{\sum p^{i-1} (1-p) i} = \frac{1 + 4p + 9p^2 + 16p^3 + \dots}{1 + 2p + 3p^2 + 4p^3 + \dots} \\ &= \frac{1+p}{(1-p)^3} = \frac{1+p}{(1-p)^2}\end{aligned}$$

The ratio $D = \bar{P}_w / \bar{P}_n$, the heterogeneity index, is $D = (1 + p)$. For the usually high conversion rates (e.g. $p = .995$), $D \approx 2$.

The chain length distribution can be represented graphically in several ways, e.g. as number fractions or as weight fractions. In Figure 2.1 both cases are given (together with the z -fractions) for a p -value of 0.99. From the graph of number fractions it appears that the monomer has, numerically, the highest fraction! The distribution of the weight fractions w_i has its maximum at the number average degree of polymerization, $\bar{P}_n = 100$, while $\bar{P}_w = 199$. Further calculation gives: $\bar{P}_z = 299$.

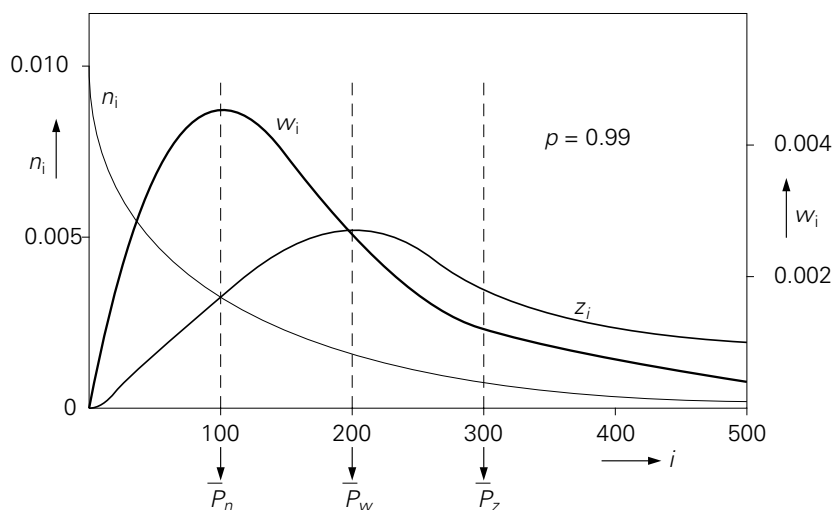


Figure 2.1. Chain length distribution of a polycondensate.

2.2.3. Measuring methods

The *number average* \bar{M}_n can, in principle, be determined by counting the molecules in a gramme of polymer. This is possible by measuring colligative properties of the polymer in solution; these are properties which are strictly dependent on the *number* of molecules per unit volume of the solution, and independent of their nature or size. Colligative properties are:

- vapour pressure reduction,
- freezing point reduction,
- boiling point increase,
- osmotic pressure

For polymers with normal, high molar masses the osmotic pressure is the only possibility; the other methods give a too small effect because of the relatively small number of molecules.

The *osmotic pressure*, Π , is the pressure difference between solution and pure solvent when these are separated by a semipermeable membrane (see Figure 2.2). For very dilute solutions the osmotic pressure is given by (see Qu. 2.35 and 2.36):

$$\Pi = kT \frac{N}{V}$$

in which N is the number of molecules in a volume V , k is Boltzmann's constant and T the absolute temperature. N can, via the molar fraction and the weight fraction, be expressed in the concentration c (g/dl) and the molar mass M ; the formula then reads:

$$\Pi = RT \frac{c}{\bar{M}_n}$$

However, Π/c does not automatically lead to the correct value of \bar{M}_n , since Π/c is still slightly dependent on c . Measurements are, therefore, carried out at a number of different concentrations and a plot of Π/c against c is extrapolated to $c = 0$.

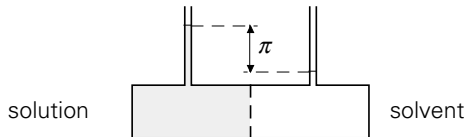


Figure 2.2. Principle of osmometry.

For the determination of the *weight average*, \bar{M}_w , about *light scattering* is the standard method. This is based on the fact that a density fluctuation in a solution, brought away by the presence of a coil molecule, causes a deviation of a ray of light. The amplitude of the scattered waves is proportional to the mass of the particle; the intensity is proportional to the square of the amplitude and thus to the square of the mass. From this simple reasoning it can be intuitively understood (though not proven), that the total amount of scattered light from all molecules present is related to the weight average molar mass.

A strict condition is, that the scattered waves do not interfere with each other so that the concentration must be very low. Light scattering is a very laborious and difficult method; minor contaminations are disastrous for the result. It is only used when

absolute determinations of \overline{M}_w are necessary.

Higher averages can be obtained by measuring the rate of sedimentation in solvents with the aid of an ultracentrifuge. This is based on the fact that the rate of sedimentation depends on the molar mass. The measurements supply \overline{M}_w and \overline{M}_z , sometimes \overline{M}_{z+1} .

The *viscosity average*, \overline{M}_v , does not belong to the series \overline{M}_n , \overline{M}_w , \overline{M}_z etc. The measurement does not supply an absolute value of the molar mass, but can, by contrast with the other methods mentioned so far, be carried out in an easy way. Its principle is, that a polymer, even at very low concentrations, brings about a significant viscosity increase of the solvent. This increase is not only dependent on the concentration but also on the molar mass. The measurement is carried out as follows (see also Qu. 2.14 - 2.18 and 2.31 - 2.34):

In a capillary viscometer the time is determined in which the liquid has dropped from the initial level h_1 to h_2 (see Figure 2.3); this time is proportional to the viscosity of the liquid. When we denote the viscosity of the solvent by η_0 and that of the solution by η , then the *specific viscosity* is defined as:

$$\eta_{\text{sp}} = \frac{\eta - \eta_0}{\eta_0}$$

This is the relative increase in viscosity, which, in a first approximation, appears to be proportional to the concentration c . A better measure is, therefore :

$$\frac{\eta_{\text{sp}}}{c} = \frac{\eta - \eta_0}{\eta_0 \cdot c} = \eta_{\text{red}},$$

the *reduced viscosity*.

This η_{red} is still somewhat dependent on the concentration. It is, therefore, measured at a number of (low) concentrations; the values found are extrapolated to $c = 0$, where the *intrinsic viscosity* is read off, which is denoted by $[\eta]$:

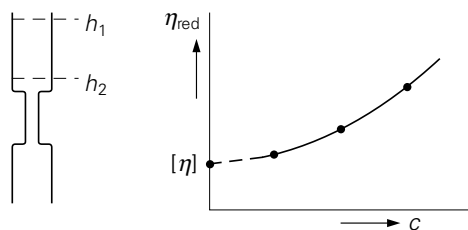


Figure 2.3. Principles of measuring intrinsic viscosity

$$[\eta] = \lim_{c \rightarrow 0} \eta_{\text{red}} = \lim_{c \rightarrow 0} \frac{\eta - \eta_0}{\eta_0 \cdot c}$$

$[\eta]$ does *not* have the dimension of a viscosity, but of c^{-1} ; in most cases it is given in dl/g.

A strongly schematized example: For a certain polymer in a certain solvent, times of flow through the capillary at several concentrations are found as indicated in the table. The specific viscosities $(\eta - \eta_0)/\eta_0$ can now be calculated as $(t - t_0)/t_0$; from these values the reduced viscosities follow, and extrapolation to $c = 0$ (in this case very simple, because the relation is linear) leads to:

$$[\eta] = 1.525 \text{ dl/g}$$

| c (g/dl) | t (sec) | η_{sp} (-) | η_{red} (dl/g) |
|------------|-----------|------------------------|----------------------------|
| 0 | 10 | | |
| 0.2 | 13.3 | 0.33 | 1.65 |
| 0.4 | 17.1 | 0.71 | 1.775 |
| 0.6 | 21.4 | 1.14 | 1.90 |

The intrinsic viscosity appears to depend on the molar mass according to the *Mark-Houwink relation*:

$$[\eta] = k \cdot M^a$$

in which k and a are constants for a given combination of polymer, solvent and temperature. k is in the order of magnitude of 10^{-3} when $[\eta]$ is expressed in dl/g; a is mostly in between 0.5 and 1. The measurement of the molar mass is not an absolute one; for each combination k and a have to be determined in an empirical way with the help of absolute characterization methods such as light scattering. Values of k and a are amply being supplied in handbooks.

The question is now, what kind of average molar mass is found from the intrinsic viscosity and the Mark-Houwink equation. To answer this question, we imagine the polymer to be split-up into a number of monodisperse fractions. Each of these fractions brings about a viscosity increase, which for the i^{th} fraction amounts to:

$$\eta_{\text{sp},i} = (\eta_i - \eta_0)/\eta_0.$$

We assume that the total increase in viscosity is, simply, the sum of the contribution of all fractions, while the concentration of the i^{th} fraction is c_i . Then

$$\eta_{\text{red}} = \frac{\sum \eta_{\text{sp},i}}{\sum c_i} = \frac{\sum (\eta_{\text{red},i} \cdot c_i)}{\sum c_i}$$

When the limit to $c \rightarrow 0$ is taken, this becomes:

$$[\eta] = \frac{\sum [\eta]_i \cdot c_i}{\sum c_i} = \sum \left\{ [\eta]_i \cdot \frac{c_i}{\sum c_i} \right\} = \sum w_i \cdot [\eta]_i$$

since

$$\frac{c_i}{\sum c_i} = w_i$$

$$[\eta] = \sum (w_i \cdot k \cdot M_i^a) = k \cdot \sum (w_i \cdot M_i^a) \equiv k \cdot \bar{M}_v^a$$

In this way the average \bar{M}_v is defined as

$$\bar{M}_v = [\sum w_i \cdot M_i^a]^{1/a}$$

So, for $a = 1$, $\bar{M}_v = \bar{M}_w$; for usual values of a , such as 0.8, \bar{M}_v is situated between \bar{M}_n and \bar{M}_w , but more closely to \bar{M}_w . In practice the full procedure of measuring at different concentrations and extrapolation to zero concentration, is often replaced by a simpler standard method; for a given polymer in a given solvent, only one concentration is taken. Optionally, a correction factor can be applied to obtain from η_{red} the best estimate of $[\eta]$.

Sometimes, from such a *single-point measurement* of the solution viscosity, an arbitrary measure has been defined, which for a given polymer supplies a useful measure for comparing levels of the molar mass. An example is the so-called k -value for PVC; k values of 55, 60, 65 and 70 denote grades of increasing M . (see Qu. 2.40 and 2.41).

The *melt index m.i.* (or melt flow index m.f.i.) is a rough empirical measure of the molar mass of some polymers. It is, again, based on a viscosity measurement, but now not of a solution, but of the molten polymer. Through a standard capillary the polymer moves under a standard pressure at a standard temperature. The number of grammes transported in 10 minutes is defined as the melt index (in dg/min). The method is frequently applied to e.g. PE and PP, and results in some measure for the molar mass. The m.i. values range from 0.1 (high M) to 80 (low M) dg/min. In fact a reciprocal melt viscosity is determined. In a first approximation this depends on \bar{M}_w , viz according to $\eta (\cdot) \bar{M}_w^{3,4}$ (see § 5.3). In a certain sense this characterization of the molar mass is functional, since the processability is one of the most important criteria for the selection from a number of grades of the same type of polymer (see § 5.4).

Molar mass distribution MMD

The oldest method to determine the whole molar mass distribution is *fractionation*. This method is based on the fact that in some solvents the short chains are better soluble than the long ones. The polymer is precipitated onto a column, e.g. on small

glass spheres, over which a mixture of solvent and non-solvent is passed while the concentration of the solvent increases with time. First the smaller molecules are taken away from the column, later on the bigger ones. The fractions are collected and characterized as to their concentration and molar mass (e.g. by a viscosity measurement). From this procedure the MMD can be derived in a number (e.g. 20) of different fractions. This Baker-Williams method is very time-consuming: fractionation and characterization of a sample takes, in total, about a week.

A more modern method to determine the MMD is *GPC*, *gel permeation chromatography*, also named size-exclusion chromatography, *SEC*. A polymer solution is passed over a column with a porous structure. The residence time of the chains on the column depends on the diameter of the coiled chain: smaller chains can migrate through more pores (they can also enter into the smaller ones), and it takes a longer time for them to pass along the column. The bigger ones cannot enter into any of the side-pores and pass in the shortest time.

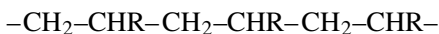
The concentration of the eluted solution is continuously measured as a function of time (or of eluted volume), e.g. via its refractive index, in comparison to that of the pure solvent.

This procedure results in a concentration - volume curve, from which, after previous calibration, the molar mass distribution can be derived. Calibration can be carried out with known monodisperse polymers, and is needed only once for a certain type of polymer on a certain column. The measurement takes only a few hours. From the measured MMD the various averages can be computed easily. It is also possible to characterise the eluted polymer solution not only on concentration, but also on molar mass, e.g. by laser light scattering. In this way the calibration can be avoided.

2.3. Chain regularity

Polymer chains are, in general, regularly built-up, but a few variations are possible. We shall, successively, consider: arrangement of monomers, situation of side groups, arrangement round a double bond, branching, and copolymer structure.

- *monomer arrangement* is, in principle, possible as “head-tail” or as a “head-head” (or “tail-tail”) i.e. for a vinyl polymer $-\text{CH}_2-\text{CHR}-$:

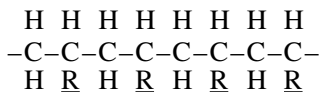


or:

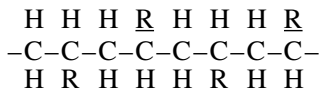


Practically always the head-tail connection is formed. One of the exceptions is polyvinylalcohol, in which between 1.5 and 2 % head-to-head sequences occur.

- *situation of side groups*; the chain $-\text{CH}_2-\text{CHR}-$ can be regular or irregular:



regular; all R's are at one side: *isotactic*.



regular; the position of the R's is alternating: *syndiotactic*.

irregular: *atactic*.

This can, more clearly, be seen in a three-dimensional representation, in view of the actual valency angles (tetrahedral, 109°); the $-\text{C}-\text{C}-$ main chain is situated in the plane of drawing (Figure 2.4), while the side groups protrude at the front side or the backside. (syndiotactic configuration)

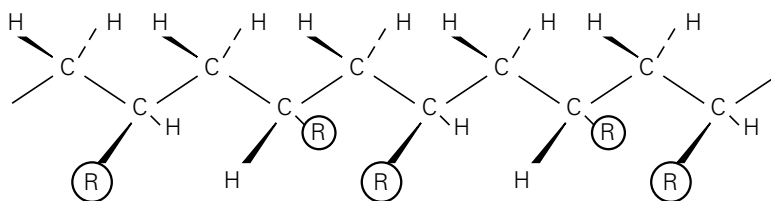


Figure 2.4. Syndiotactic chain.

With conventional polymerization processes, atactic chains are predominantly formed; for the formation of isotactic and syndiotactic chains a special catalyst system is required, e.g. Ziegler-Natta catalysts. Such a process is called: *stereospecific* polymerization. It enables the manufacture of, i.a., technically usable PP and also unbranched PE (see § 4.1). The newest development is the metallocene catalyst; it enables the building-up of “chains-to-measure” with very high degrees of chain regularity; also the manufacture of syndiotactic polystyrene is technically possible in this way (see Qu. 2.47).

- Round a *double bond* the main chain can show two different configurations, e.g. with polybutadiene and polyisoprene (Figure 2.5):

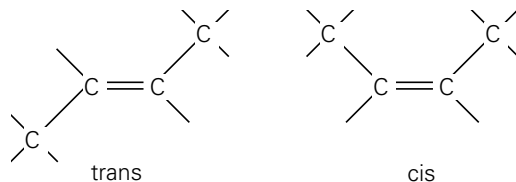


Figure 2.5. Cis- and trans-configuration. E.g. polybutadiene and polyisoprene

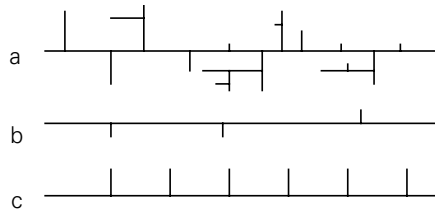
Cis-1,4 polyisoprene (natural rubber or synthetic isoprene rubber) and trans-1,4 polyisoprene (balata or guttapercha) show strongly different properties.

Within a single chain cis- and trans configuration can also both occur in a random sequence; the chain is than irregular (some kinds of polybutadiene). This has consequences for the occurrence of strain-induced crystallization (see Chapter 4).

- Branching disturbs the chain regularity if the branches are situated at random positions along the chain. In particular with PE a number of branching types are present (see Figure 2.6):

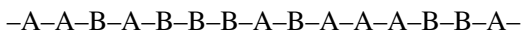
- a. strongly branched with irregular branches: low-density PE (LDPE)
- b. little branched: high-density PE, (HDPE)
- c. strongly branched, but more regularly: linear-low-density PE (LLDPE)

The names reflect the effect of the branches on the crystallinity and thus on the density and the stiffness.



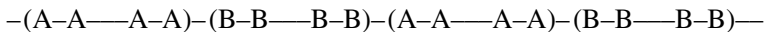
Figuur 2.6. Three types of branching for PE.

- With copolymerization irregular chains are formed when the sequence of the monomers is random::

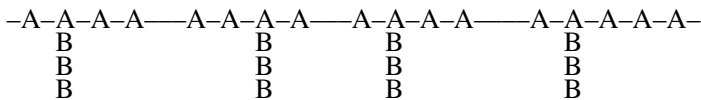


This is called a random-copolymer. An example is styrene - butadiene rubber, SBR.

A more regular chain structure is the block copolymer:



examples are the thermoplastic elastomer SBS (see § 9.1.4) and the graft copolymer:



and, in particular, the alternating copolymer:



Strictly speaking, condensation polymers such as polyesters could be considered to belong to this category. Also polyketone (“Carilon”) would be a strictly alternating copolymer, if the regularity would not have been disturbed by a third comonomer, propylene.

2.4. Chain conformations

Polymer chains are hardly ever met in a totally stretched condition, but are, because of their mobility and flexibility, present as coils. The coil can show all kinds of shape, as dictated by chance; as a first approximation we may assume a spherical shape. The diameter of this sphere is hard to define; the density in the coil decreases from the centre to the outer boundary. The easiest criterion is the *end-to-end distance*, r_0 ; this is a strongly fluctuating statistical quantity, of which we must, therefore, try to define some kind of average. This average has some relation with the effective coil diameter.

In order to estimate the end-to-end distance r_0 we assume, as a first approximation, that the chain segments can move freely with respect to each other in all directions. The chain contains n segments, each with a length b_0 . The next simplification is, that we consider the chain in two dimensions. We now have a simple “random walk” (“drunk man’s walk”) problem. We situate one chain end in the origin of an x - y coordinate system and we build the chain step by step with randomly chosen angles φ (see Figure 2.7). The position of the other end is then given by

$$x = b_0 \cdot \cos \varphi_1 + b_0 \cdot \cos \varphi_2 + \dots + b_0 \cdot \cos \varphi_n$$

$$y = b_0 \cdot \sin \varphi_1 + b_0 \cdot \sin \varphi_2 + \dots + b_0 \cdot \sin \varphi_n$$

or:

$$x = b_0 \cdot \sum_{i=1}^n \cos \varphi_i; \quad y = b_0 \cdot \sum_{i=1}^n \sin \varphi_i$$

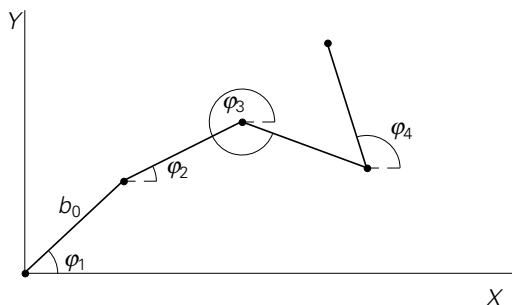


Figure 2.7. ‘Random walk’.

The end-to-end distance is $r_0 = \sqrt{x^2 + y^2}$.

$$r_0^2 = x^2 + y^2 = b_0^2 \cdot (\sum \cos \varphi_i)^2 + b_0^2 \cdot (\sum \sin \varphi_i)^2$$

$$\frac{r_0^2}{b_0^2} = \sum^i \cos^2 \varphi_i + \sum^i \sum^j \cos \varphi_i \cdot \cos \varphi_j + \sum^i \sin^2 \varphi_i + \sum^i \sum^j \sin \varphi_i \sin \varphi_j =$$

$$= \sum_1^n (\cos^2 \varphi_i + \sin^2 \varphi_i) + \sum^i \sum^j \cos(\varphi_i - \varphi_j) =$$

$$= n \cdot 1 + 0 = n$$

The second sum is 0 because $\varphi_i - \varphi_j$ is distributed at random.

The statistical value (the average) of the square of the end-to-end distance is given by:

$$\langle r_0^2 \rangle = n \cdot b_0^2 \quad \text{or} \quad \sqrt{\langle r_0^2 \rangle} = b_0 \cdot \sqrt{n}$$

Further calculation shows that for a three-dimensional random walk the same result is obtained.

In a second approximation we have to introduce a fixed value for the angle between two links of the chain; since, e.g., the angle between two valency bonds of the C-atom is always $\theta = 109.5^\circ$. (Figure 2.8). For the time being, we suppose *free rotation* around this angle. The approach is similar to the previous case (of course now three-dimensional), and results in:

$$\langle r_0^2 \rangle = n \cdot b_0^2 \cdot \frac{1 - \cos \theta}{1 + \cos \theta}$$

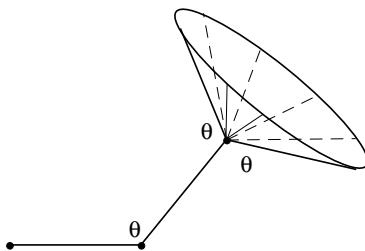


Figure 2.8. Free rotation with fixed valency angle.

This formula is not valid when θ is close to 0° or 180° . It appears that the correction factor

$$\begin{aligned}
 &= 1 \text{ for } \theta = 90^\circ \\
 &< 1 \text{ for } \theta < 90^\circ \\
 &> 1 \text{ for } \theta > 90^\circ \\
 &= 2 \text{ for } \theta = 109,5^\circ
 \end{aligned}$$

In a third approximation we also limit the *freedom of rotation*. This can be illustrated with ethane $\text{CH}_3\text{-CH}_3$; when this molecule is rotated around the C-C bond, potential barriers have to be overcome as a result of the interaction between the H-atoms (see Figure 2.9). For PE a similar potential curve can be calculated; this has a more complicated shape as also indicated in Figure 2.9.

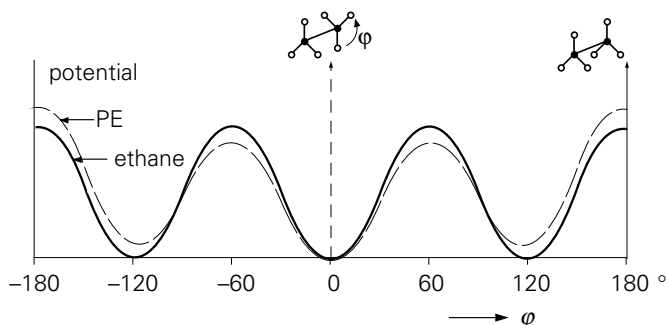


Figure 2.9. Potential curve for rotation

The hindering in rotation necessitates the introduction of an extra correction factor in the formula for $\langle r_0^2 \rangle$. This factor contains the quantity $\langle \cos \varphi \rangle$, which is the average cosine of the rotation angles. For free rotation $\langle \cos \varphi \rangle = 0$ (all values for φ are equally probable), but it differs from 0 when potential barriers are present. It can be calculated from the potential curves. The formula becomes now

$$\langle r_0^2 \rangle = n \cdot b_0^2 \frac{1 - \cos \theta}{1 + \cos \theta} \cdot \frac{1 + \langle \cos \varphi \rangle}{1 - \langle \cos \varphi \rangle}$$

A simplified formula is:

$$\langle r_0^2 \rangle = n \cdot b^2$$

in which b is the effective bond distance, i.e. the length of the fictitious link, which behaves without restrictions as a random walk. We maintain n as the number of primary links (sometimes n is taken as the number of fictitious links), and we define b/b_0 as the *characteristic chain stiffness*. This quantity is, therefore $= \sqrt{2}$ for a -C-C- chain with unrestricted rotation; $b/b_0 > \sqrt{2}$ with hindered rotation.

Still further approximations are required to account for the “*excluded volume*”: the

chain parts cannot coincide. An important complication is met when the side groups are big enough to hinder each other during chain rotations (see § 2.5). In all cases the formula $\langle r_0^2 \rangle = n \cdot b^2$ remains valid, though b/b_0 increases as a result of these effects. Some estimated values:

| | PE | PVC | PMMA | PVAc | PS |
|-----------|------|------|------|------|------|
| (b/b_0) | 2.50 | 2.61 | 2.97 | 3.00 | 3.29 |

We can now ask the question: What is the magnitude of the *coil density*? How far is the statistical coil, which we have considered so far, diluted? How many monomer units are present in a unit volume? It is possible to calculate how the density, ρ , depends on the distance to the centre of gravity and on the number of links n . It appears that the volume fraction in the centre equals $f_0 = 1/\sqrt{n}$, i.e.:

$$\begin{array}{ll} \text{for } n = 1,000 & f_0 = 0.03 \\ \text{for } n = 1,0000 & f_0 = 0.01 \end{array}$$

in other words: the coils are, even in their centre, *highly diluted*!

A rough estimate can also be made without much theory, namely from $\langle r_0^2 \rangle = n \cdot b^2$, for example for PE with $M = 140,000$. A chain contains 10,000 CH_2 links, so $n = 10,000$. The length of a link is $b_0 = 0.154$ nm, and we simply assume unrestricted rotation, so that $b = b_0 \cdot \sqrt{2} = 0.218$ nm. We then find:

$$\langle r_0^2 \rangle = 10,000 \cdot (0.218 \cdot 10^{-9})^2 \text{ m}^2$$

If we, loosely, think of a sphere with radius r_0 , then the volume of this sphere is:

$$V = \frac{4}{3} \pi \cdot \langle r_0^2 \rangle^{3/2} = 0.433 \cdot 10^{-22} \text{ m}^3$$

The mass is $m = 140.000 \text{ g} / 6 \cdot 10^{23} = 2.3 \cdot 10^{-22} \text{ kg}$. The specific mass of the coil is:

$$\rho = m/V = 5.3 \text{ kg/m}^3$$

When we compare this value with the density of amorphous PE ($\rho = 855 \text{ kg/m}^3$), then the polymer in the coil appears to be 160 times diluted. If we choose the value for b/b_0 as given above, then the result is a dilution factor of 890. Taking into account that the formula $f_0 = 1/\sqrt{n}$ holds for the tightest packed centre, then the results are in the same order of magnitude.

Coiled chains, are, therefore, strongly interwoven; in each volume element of the size of a coil, parts of hundreds of separate chains are present!

The reasoning followed so far is based on the assumption that chains, in finding their most probable coil dimensions, are not affected by their environment; in other words, that no special interactions, either attractive or repulsive, with neighbouring

molecules are present. This holds, therefore, for an undiluted polymer, in which a chain does not undergo interactions from the surrounding chains other than those from parts of the chain under consideration itself.

If we now look at polymer solutions, then there are three possibilities (see also Qu. 2.20–2.23):

- A very *good solvent*; this means that there is an extra interaction between parts of the chain and the molecules of the solvent, so that the chain segments prefer to be surrounded by more solvent molecules. The coil will then become more expanded.
- A *poor solvent*; parts of the chain feel better in an environment consisting of similar chain segments; the coil will become more compact.
- In between these cases we can define a so-called *theta-solvent*, which, as far as interactions are concerned, behaves, at a certain temperature, like the polymer.

Our calculation of $\langle r_0^2 \rangle$ is therefore, for polymer solutions, only valid for theta conditions. We shall consider this case in somewhat more detail. We have seen that for the determination of the viscosity average molar mass, the Mark-Houwink equation is valid

$$[\eta] = k \cdot M^a$$

in which, in general, a is in between 0.5 and 1. Moreover, it is known that under theta conditions $a = 0.5$.

We have also seen that we have to extrapolate to concentration zero to obtain the intrinsic viscosity $[\eta] = \lim \eta_{\text{red}}$.

Considering the calculation of coil density, this is not surprising. A concentration of 1% in a solution seems small, but when the coil is more than 100 times diluted, considerable mutual penetrations of the coils can be expected, and, therefore, strong deviations from the behaviour of single, separate coils.

Only at very low concentrations can the coils be considered as separate spheres. In that case *Einstein's relation* for the viscosity of suspensions can be applied:

$$\eta = \eta_0 \cdot (1 + 2.5 \cdot \varphi),$$

in which φ is the volume concentration and η_0 the viscosity of the liquid. Then:

$$\eta_{\text{sp}} = \frac{\eta - \eta_0}{\eta_0} = 2.5 \cdot \varphi \quad \text{en} \quad \eta_{\text{red}} = 2.5 \cdot \varphi / c = 2.5 / \rho$$

in which ρ is the specific mass of the coil, or:

$$\rho = \frac{M}{V}$$

with M the molar mass and V the volume of the coil.

This, combined with the Mark-Houwink equation, yields:

$$[\eta] (\cdot) M^a (\cdot) \frac{V}{M}$$

or

$$V (\cdot) M^{1+a}$$

If, as above, we express V as:

$$V (\cdot) \langle r_0^2 \rangle^{3/2}$$

and

$$\langle r_0^2 \rangle (\cdot) \text{number of links, so } (\cdot) M$$

then:

$$V (\cdot) M^{3/2} (\cdot) M^{1+a}$$

so: $a = 0.5$.

This (too) simple derivation confirms that for theta conditions: $a = 0.5$!

When another type of solvent is chosen, a higher value for a can be found, e.g. $a = 1$; in this case:

$$\langle r_0^2 \rangle (\cdot) M^{4/3} \text{ instead of } (\cdot) M$$

or a lower a , e.g. 0.35; then $\langle r_0^2 \rangle (\cdot) M^{0.9}$.

Deviations of $\langle r_0^2 \rangle (\cdot) M$ can also be brought about by other causes, for example by chain *branching*; as an extreme case we can think of a highly complex branched structure in which the many branches are again branched, so that it can hardly be defined as a chain. The conformation statistics is then no longer applicable, and for such polymers a value of a near to 0 has even been found; this means that $V (\cdot) M$, just as with small molecules. Viscosimetric determination of M is then no longer applicable, since $[\eta]$ is independent of M .

A deviation in the other direction occurs with super-stiff chains, in the extreme case with rigid rods. The end-to-end distance then equals the whole chain length, so:

$$\langle r_0^2 \rangle (\cdot) M^2$$

which means $a = 2$.

This value is, therefore, mentioned as the theoretical maximum of a ; it remains an open question what the significance of V is in such a case, thinking of our spheres! For liquid-crystalline polymers values round $a = 1.5$ are indeed being found.

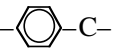
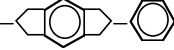
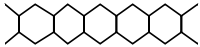
2.5. Chain flexibility

The flexibility of chains is governed by the freedom of rotation of the main chain, and also by the effect of side groups. First we consider the *main chain*. In the foregoing we have already seen that the possibilities for rotation of the main chain are restricted by potential barriers. Some examples for simple compounds are:

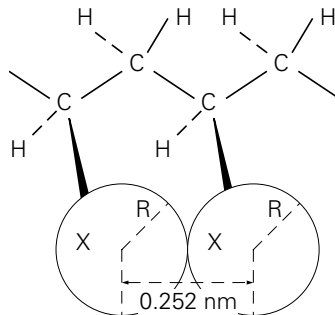
| | |
|--|--------------|
| $\text{CH}_3\text{--}(\text{CH}_3)$ | 2.8 kcal/mol |
| $\text{CH}_3\text{--}(\text{CH}_2\text{--CH}_3)$ | 3.3 |
| $\text{CH}_3\text{--}(\text{CH}\cdot\text{CH}_3\text{--CH}_3)$ | 3.9 |
| $\text{CH}_3\text{--}(\text{OH})$ | 1.0 |
| $\text{CH}_3\text{--}(\text{O--CH}_3)$ | 2.7 |
| $\text{CH}_3\text{--}(\text{COH})$ | 1.0 |
| $\text{CH}_3\text{--}(\text{C}\equiv\text{C})$ | 0.5 |

Double ($\text{C}=\text{C}$) and triple ($\text{C}\equiv\text{C}$) bonds cannot rotate; the ease of rotation of the neighbouring bonds is, however, increased.

The series shown below represents a number of types of main chains with decreasing flexibility:

| | |
|---|----------------------------|
| --C--O--C-- | e.g. POM, polyoxymethylene |
| --C--N--C-- | e.g. PA, polyamide, nylon |
| $\text{--C}=\text{C--C--}$ | e.g. BR, butadienerubber |
| --C--C--C-- | e.g. PE, polyethene |
|  | e.g. PC, polycarbonate |
|  | PI, polyimide |
|  | ladderpolymers |

Side groups mainly affect chain flexibility when the main chain is flexible. An example is *steric hindrance* with (see Figure 2.10)



Figuur 2.10. Steric hindrance.

| | | |
|---------------------|-------------------------|------------------------|
| $X = \text{H}$: | $R = 0.09 \text{ nm}$, | little hindrance |
| $X = \text{F}$: | $R = 0.14 \text{ nm}$, | some hindrance |
| $X = \text{Cl}$: | $R = 0.18 \text{ nm}$, | considerable hindrance |
| $X = \text{CH}_3$: | $R = 0.20 \text{ nm}$, | considerable hindrance |

The situation sketched above is not quite exact, since the substitution of a side group also causes a slight change of θ .

When the sterical hindrance is considerable, no zig-zag conformation of the chain is possible; the number of conformations is then drastically reduced.

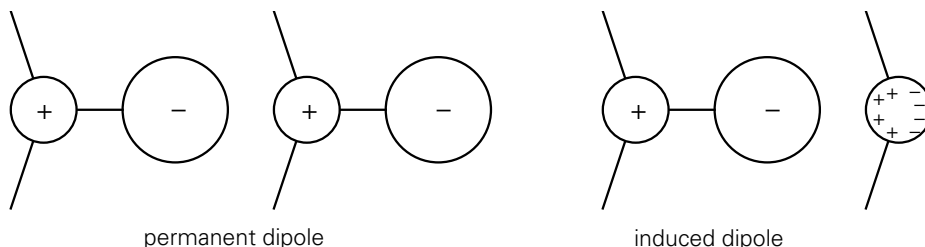
The effect of a restriction in rotation is an increase of b/b_0 , and, therefore, of the effective coil diameter $\sqrt{\langle r_0^2 \rangle}$.

The chain flexibility has, a.o., a large influence on the glass-rubber transition temperature, and (if applicable) on the melting point.

2.6. Chain interactions

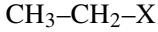
Between parts of the chains interaction forces are active, the *secondary binding forces*, which are much smaller than the primary chemical bonds by which the chains are held together. Several kinds of secondary binding forces exist:

- *dipole forces*; here the distribution of electrical charges within an atom or group of atoms is asymmetric with respect to the centre of gravity (see Figure 2.11). Polar groups form permanent dipoles, which align in the electric field of their neighbours; this results in an electrical attraction force. The interaction is proportional to $1/r^3$ (r = distance), and is slightly dependent on the temperature as a result of the thermal motion of the dipoles. A measure for the interaction force is the *dipole moment*, the value of which is, for a few groups, given in the table below.



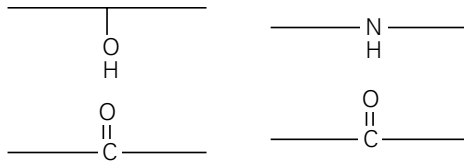
Figuur 2.11. Permanent and induced dipoles.

- *induced dipole*; this is formed when a neutral group is being polarized by induction from a neighbouring permanent dipole. The attraction force is proportional to $1/r^6$ and is slightly temperature dependent.



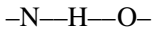
| X | dipolemoment | X | dipolemoment |
|--------------------|--------------|---------------------|--------------|
| -CH ₃ | 0 | -COOH | 1.73 |
| -O-CH ₃ | 1.2 | -COOCH ₃ | 1.76 |
| -NH ₂ | 1.2 | -COCH ₃ | 2.78 |
| -OH | 1.69 | -NO ₂ | 3.68 |
| -Cl | 2.05 | -CN | 4.0 |

- *dispersion forces* originate from random fluctuations in the charge distribution of an apolar group as a result of the revolution of electrons. A fluctuating dipole induces another one; the net result is an attraction force. Dispersion forces, also called London-Van der Waals forces, are independent of temperature and proportional to $1/r^6$. They form the most important class of interaction forces, as for instance in hydrocarbons.
- *hydrogen bridges* occur between chains in e.g. the following situations (Figure 2.12):



Figuur 2.12. Hydrogen bridges.

The H-valency is being shared with the neighbouring atom, e.g.:



This leads to relatively strong bonds, as in nylon and cellulose. The hydrogen bonds are also responsible for the strong link between water molecules; that is why water, as a very small molecule, has a high boiling point!

Consequences of chain interactions for the behaviour of a polymer are, just as with chain flexibility, mainly the height of the *glass-rubber transition* and the *melting point*.

2.7. Cross-linking

The most important characteristic of a network is the tightness, the spacing between cross-links. Some quantities frequently used will be elucidated in a simple schematic example:

Suppose that we have two chains, each of 20 links, which are, at equal distances, connected by cross-links, as illustrated in Figure 2.13.

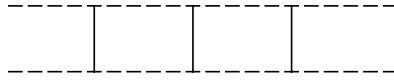


Figure 2.13. Cross-links.

The *cross-link density* is defined as:

$$\rho = \frac{\text{number of units connected}}{\text{total number of units}} = \frac{6}{40} = 0.15$$

The quantity ρ is between 0 and 1; ρ is low for vulcanized rubbers, namely 0.01 – 0.02, and much higher for thermosets.

We further define:

M_0 = molar mass of the monomer (here e.g. $M = 50$)

M_c = molar mass between cross-links (here $5 \times 50 = 250$)

M = molar mass of the whole chain (here $20 \times 50 = 1000$)

ν = a number of chain elements, separated by cross-links (here $\nu = 8$)

ν_e = effective number of chain parts, contributing to the coherence and the elasticity of the network (here $\nu_e = 4$).

ν_e is related to ν , M and M_c according to

$$\nu_e = \nu \cdot \left[1 - 2 \cdot \frac{M_c}{M} \right]$$

since the chain is divided into $n = M/M_c$ parts, two of which are always loose, so that the effective fraction is $(n - 2)/n = 1 - 2/n$.

In our case $\nu_e = 8(1 - 2 \times 250/1000) = 4$.

In this example only one half of the chain parts are effectively contributing to the network properties; the remaining part, the loose ends, are not being deformed when the material is strained.

The various parameters can be determined from measurements of the modulus of elasticity (see § 5.1) and from swelling in solvents.

In most cases, cross-linking is effected by the formation of *chemical bonds* between the chains; the network is then stable, such as with:

- sulphur bridges with rubbers,
- polystyrene chains with unsaturated polyesters,
- bivalent with three- (or more-)valent reacting components,
- cross-linking by irradiation; via radical formation a chemical link between chains is formed.
- other cross-linking agents such as peroxides.

Also *physical cross-linking* occurs with:

- crystallization (see § 4.5 and § 7.2.1),
- domain formation in block copolymers, “self-vulcanizing rubber” or “thermoplastic elastomer” (see § 9.1.4),
- temporary entanglements, causing rubbery behaviour in unvulcanized rubbers and in molten thermoplastics.

3

Glassy state and glass-rubber transition

3.1. Glassy state

In the usual schedule “solid - liquid” the solid is crystalline and passes into the liquid state at the melting point, T_m . This transition is, in nearly all cases, accompanied by an increase in volume (one of the exceptions is water!), and with an increase in the heat content (enthalpy), the heat of melting.

The jump in volume is illustrated in Figure 3.1; the slope of the line FC is the thermal expansion coefficient of the crystalline phase; at the melting point the volume jumps from C to B, and the higher slope of BA denotes the expansion coefficient of the liquid phase.

Some substances are, however, not able to crystallize, for instance normal glass, as a result of a too irregular molecular structure. When such a substance is cooled down from the liquid state, and follows the line AB, then from B to D it still remains a fluid, which solidifies at D without showing a jump in volume. The line then continues as DE, with about the same slope as CF; the matter is, however, not in a crystalline condition, but in an unordered, amorphous, *glassy state*, and has, therefore, a greater volume.

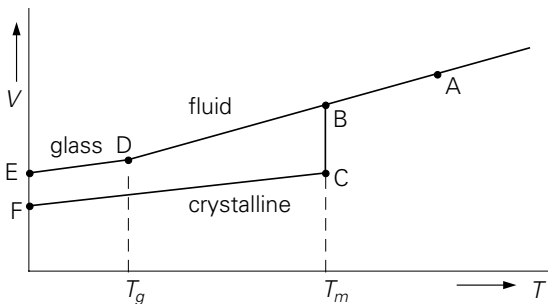


Figure 3.1. Volume as a function of temperature.

The transition at D is called the *glass transition*, occurring at the *glass transition temperature*, T_g . It follows that T_g is always lower than the melting point, T_m . It is very important to *distinguish* very carefully between T_g and T_m !!

Polymers are sometimes wholly amorphous and non-crystallizable; they then follow the line ABDE. However, when such a polymer is heated up to above its T_g it is not immediately transferred into a liquid state, but first into a rubbery state, which, upon further heating, gradually passes into a fluid. T_g is, therefore, called the *glass-rubber transition temperature*.

A more realistic representation of the phases is given by the stiffness of the material, which falls down to zero when the liquid state is reached. This is illustrated in Figure 3.2; for a low-molecular matter the E-modulus (a measure of the stiffness) decreases to zero at the glass transition temperature (though more gradually than for a crystalline substance at T_m). A polymer shows, above T_g , after a decrease in E by a factor of 1,000 to 10,000, a *rubbery region*, which, on the temperature scale, is longer as the chains are longer.

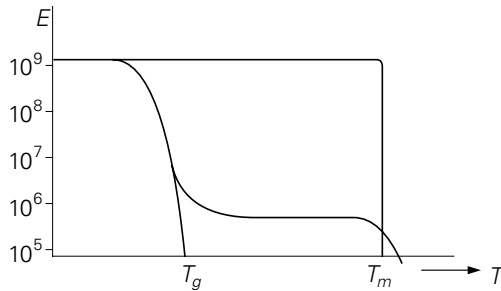


Figure 3.2. Rubbery region with polymers.

Sometimes crystallization is possible; in the solid state polymers are, however, never totally crystalline, but are still partly amorphous. The amorphous part may be above or below T_g , i.e. in the rubbery or in the glassy condition.

The nature and the properties of polymers are, therefore, governed by *two different schedules*, which are sometimes superimposed:

1. glass — rubber — liquid
2. crystalline — liquid.

First of all we shall consider the glassy condition.

In the *glassy state* the molecular structure is disorderly, and comparable to that of a liquid. This is clearly demonstrated by X-ray diffraction patterns, in which only a diffuse ring is visible, which indicates some short-distance order; in contrast to the sharp reflections found with crystals as a result of long-distance order.

The disordered state occupies a larger volume than a crystal, which explains the distance between the lines ED and FC in Figure 3.1, the so-called *free volume*.

Below T_g the free volume, V_f , is about constant; above T_g it increases strongly with increasing temperature.

The free volume in the glassy state allows some minor movements for small chain parts or for side groups. These movements are possible from a certain temperature; they are apparent from a relatively small decrease in stiffness at that temperature. Because such a decrease is much less than in the glass-rubber transition, the temperature at which it occurs is called a *secondary glass transition*. Besides the modulus, E , also the *mechanical damping* is a good criterion for the transitions. The damping is defined as the tangent of the loss angle in vibration experiments, or, also, as the rate of damping in a free vibration (see § 6.2). The damping, $\tan \delta$, shows a strong maximum at T_g , and less pronounced maxima at the secondary glass transitions T_{sec} (see Figure 3.3.).

A secondary glass transition is, in general, important for the *impact strength* of a polymer; it creates the possibility to dissipate energy in situations of shock loading, so that the polymer is less brittle.

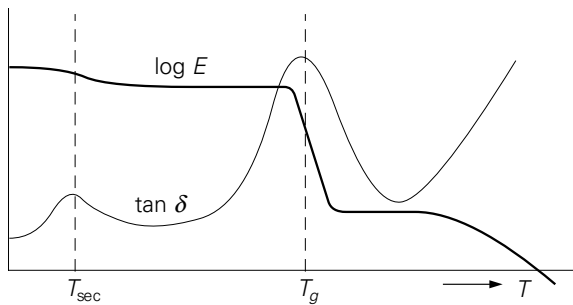


Figure 3.3. A secondary glass transition.

Besides by motions of chain parts or side groups (see § 3.4), a secondary transition can also result from the presence of a second polymer, which has been added in a small quantity by *blending*, or which has, as “tails”, be copolymerized with the main polymer. Such a second polymer then has its glass transition at T_{sec} . Both cases occur when the impact strength of a polymer has been improved, either by blending with some rubber, or by copolymerization. A similar situation is found with block copolymers. In § 3.5 these cases are dealt with in more detail.

3.2. Molecular picture

Before looking closer at the glass rubber transition, we shall try to visualize what happens on a molecular scale when a polymer is heated, starting from zero Kelvin. At $T = 0$ K the chains are at absolute rest. No thermal motions occur; everything is

completely frozen-in. The chain parts are bound together by secondary interaction forces, as discussed in § 2.6.

When the temperature is increased from $T = 0$, the thermal motion increases and, gradually, short parts of the chain or side groups may obtain some mobility, which, within the very restricted free volume, gives rise to small changes in conformation. Whether or not this occurs, is a matter of competition between the thermal energy of a group (kT) and its interaction with neighbouring groups.

The interaction can be expressed as a *potential barrier* which has to be overcome in order to realize a change in position. Since the thermal energy is statistically distributed, a fraction of the groups will be able to overcome the barrier; this fraction strongly increases when the temperature is raised. Hence, there is a characteristic transition temperature for such a specific molecular motion.

This is illustrated in Figure 3.4. The potential barrier for passing from state 1 to state 2, is ΔU ; the distribution of the thermal energy has been sketched schematically for three temperature levels. At T_1 only a small number of groups have enough energy to overcome the barrier, at T_2 much more, and at T_3 nearly all. Thus T_2 is, for that displacement, the transition temperature. For $T < T_2$ the mobility is frozen-in; for $T > T_2$ the motion is free.

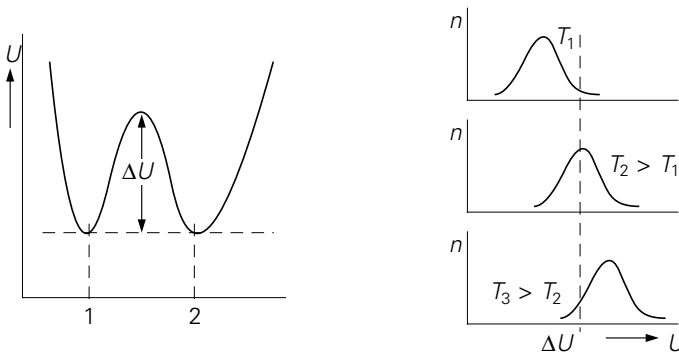


Figure 3.4. Potential barrier for changing position.

We should realize, that this is always a matter of probability, and that the time, i.e. the patience we have to wait for a change, plays an important role. Therefore, we should consider the frequency at which jumps from state 1 to state 2 occur. This frequency, ν , can be expressed by the the Arrhenius equation:

$$\nu = \nu_0 \exp(-\Delta U/kT)$$

In this equation ν_0 is the natural frequency of the vibrations about the equilibrium position. The jump frequency governs the time scale, τ , at which the transition occurs; τ is namely inversely proportional to ν :

$$\tau = A \exp(\Delta U/kT).$$

This equation provides a fundamental relationship between the effects of time and temperature on a transition mechanism. *Time* and *temperature* appear to be *equivalent* in their effect on the behaviour. At a fixed time scale, τ_1 , e.g. 1 sec, the transition temperature, T_1 , is proportional to the energy of activation, ΔU . The transition temperature can be expressed in the time scale by:

$$\ln \tau = c + \frac{\Delta U}{kT}$$

Consequently, for low-temperature transitions with a low energy of activation, such as secondary glass transitions, the transition temperature is stronger time dependent than, e.g. the main glass-rubber transition.

An example of a secondary transition is the side group rotation $-\text{CO}-\text{O}-\text{CH}_3$ with PMMA, which is set free at about 25 °C on a time scale round 1 sec. PVC shows a weak transition at -30 °C as a result of freedom of rotation for the Cl atoms. A very elegant illustration is given by polycyclohexylmethacrylate in comparison with polyphenylmethacrylate (Heijboer). The polymers are nearly identical; the difference is that the first has a saturated ring as a side group, and the second an unsaturated one:

The saturated ring is able to undergo a “flipping motion” (chair-chair transition) at -80 °C, which, in contrast to the rigid ring in PCHMA, results in a strong secondary transition (see Figure 3.5). With further increase of the temperature, bigger parts of the chain can move freely. About T_g the mobility increases drastically, so that coils can freely be transformed to other conformations, without being hindered by interactions: the polymer shows *rubbery behaviour*. This is the case for free mobility of chain parts with, on average, 20 to 70 monomeric units. Chain entanglements prevent whole chains to move relatively to each other.

3.3. Thermodynamics of the glass-rubber transition

To consider the nature of the glass rubber transition on a thermodynamic basis, we should first compare this transition with melting. The melting point is a *first-order transition*; T_g could be mentioned a *second-order transition*.

The quantity G , the (Gibbs) *free enthalpy*, plays a predominant role in the thermodynamic treatment of transitions.

$$G = U - TS + pV = H - TS = F + pV$$

in which

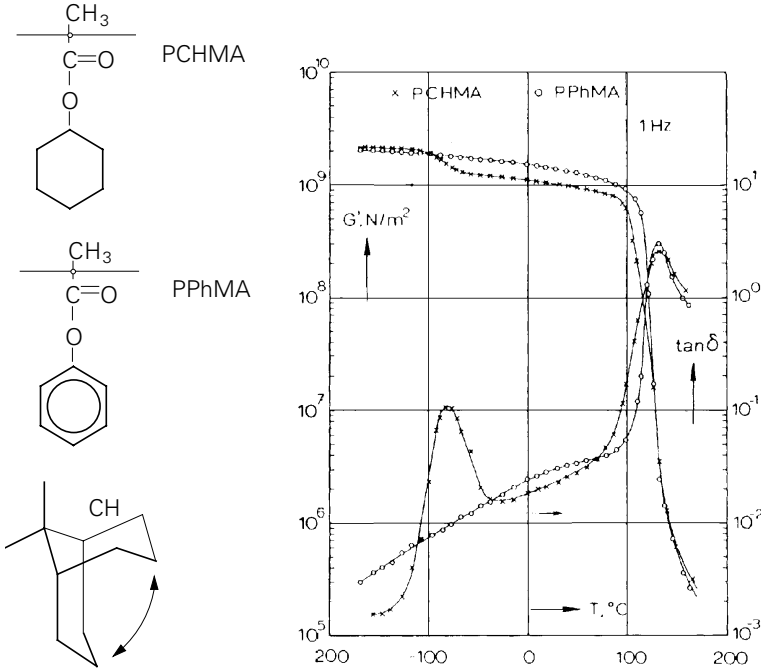


Figure 3.5. Effect of the nature of the side group on the secondary glass transition (J. Heijboer, 'Mechanical properties of glassy polymers containing saturated rings, dissertation RU-Leiden, Waltman, Delft, 1972).

U = internal energy, e.g. as a result of the attraction forces between molecules

T = absolute temperature,

S = entropy, a measure for the disorder in the system,

p = pressure,

V = volume,

$H = U + pV$ = enthalpy or heat content

= internal energy + work exerted on the environment,

$F = U - TS$ = (Helmholtz) free energy.

With each type of transition, $\Delta G = 0$, in other words: the $G(T)$ curves for both phases intersect, and slightly below and above the transition temperature the free enthalpies are equal. The various derivatives of the free enthalpy may, however show discontinuities. With a first-order transition such as melting, this is the case with the first derivatives like V and S and also with H .

$$\left[\frac{\partial G}{\partial p} \right]_T = V$$

With melting the volume differs at both sides of the melting point; a jump ΔV in volume occurs, which is a jump in the first derivative of G after p at constant T . Also a jump ΔH occurs in the enthalpy (the heat of melting), as well as a jump ΔS in entropy.

The glass-rubber transition, on the contrary, does *not show jumps in V , S and H* (no volume change, no discontinuous change in the state of order and no heat effects). However, jumps occur in the *derivatives* of these quantities, such as thermal expansion coefficient, specific heat and compressibility. Some examples:

$$\left[\frac{\partial G}{\partial p} \right]_T = V, \quad V_{\text{glas}} = V_{\text{rubber}}, \quad \Delta V = 0$$

$$\left[\frac{\partial^2 G}{\partial p \partial T} \right] = \left[\frac{\partial V}{\partial T} \right]_p = \alpha V, \quad \alpha_{\text{glass}} \neq \alpha_{\text{rubber}}$$

the coefficient of expansion shows a jump $\Delta\alpha$.

So there are jumps in the second derivatives of the free enthalpy G , and, for that reason, the glass-rubber transition might be denoted as a second-order transition. However, this appears not to be the case; the dependence of the various parameters at a real second-order transition strongly differs from what happens at T_g , which will not be further shown here.

A second argument is the time dependency: the transition from a supercooled liquid or rubber to the glassy state is clearly dependent on the rate of cooling; the line representing the liquid behaviour continues further to lower temperatures as the rate of cooling is lower; the glass transition temperature is then lower and the specific volume reaches a lower value (see Figure 3.6).

A thermodynamic equilibrium is, therefore, not reached; if such an equilibrium would exist it would be at a much lower temperature. On the basis of theoretical calculations it has been supposed that a real second-order transition could occur at a temperature which is 50 to 60 K below the observed value of T_g , and which would be reached after extremely low rates of cooling. Estimations on the basis of the empirically found relation between T_g and the rate of cooling indicate that the required cooling time would be of the order of 10^{17} years!

Experiments have also been carried out on polystyrene with various amounts of plasticizers; extrapolation to zero plasticizer content provided an insight into the course of the volume-temperature relation below T_g . Even at $(T_g - 70 \text{ K})$ no indication of a transition was found.

It thus seems that the glass transition, even with infinitely low cooling rate, is not a real thermodynamic transition, but is only governed by *kinetics*, as a *freezing-in phenomenon*.

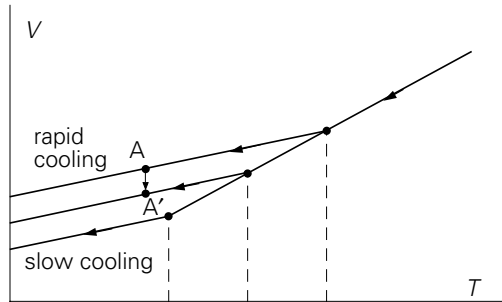


Figure 3.6. Effect of the time scale on the glass transition.

A closely related phenomenon is the *volume retardation* in the glassy condition. When, after rapid cooling, point A has been reached (Figure 3.6), the volume will, at a constant temperature, gradually decrease to e.g. A'. Possibilities for motion of chain parts, though on a very limited scale, cause the free volume to decrease gradually, though, as we now know, an equilibrium will never be reached. The rate of volume retardation is, as a matter of fact, smaller as the temperature is lower.

This phenomenon, also called *physical ageing*, is not very significant in terms of volume, but, as we shall see later on (§ 7.2.4.), it is very important for the creep behaviour of polymers.

3.4. Factors governing T_g

The height of the glass-rubber transition temperature is, in the first instance, governed by the competition between *thermal motion* and the *attraction forces* between the chains.

The thermal motion is dependent on the freedom of the chain to undergo changes in conformation. When this freedom is higher, the chain is subjected to a stronger thermal motion than a chain which, e.g. as a result of hindrance in rotation, is more rigid. The chain stiffness, as discussed in § 2.4, plays, therefore, an important role.

The primary criteria are thus:

- chain flexibility
- chain interactions.

We shall consider some examples of both criteria. In doing so, besides amorphous, also crystalline polymers will be taken into account, since the latter always contain

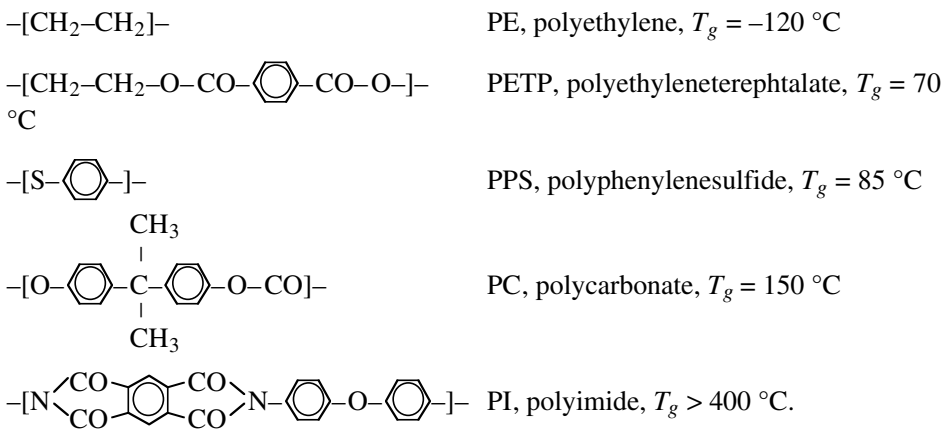
an amorphous fraction, which is subject to a glass transition.

3.4.1. Chain flexibility

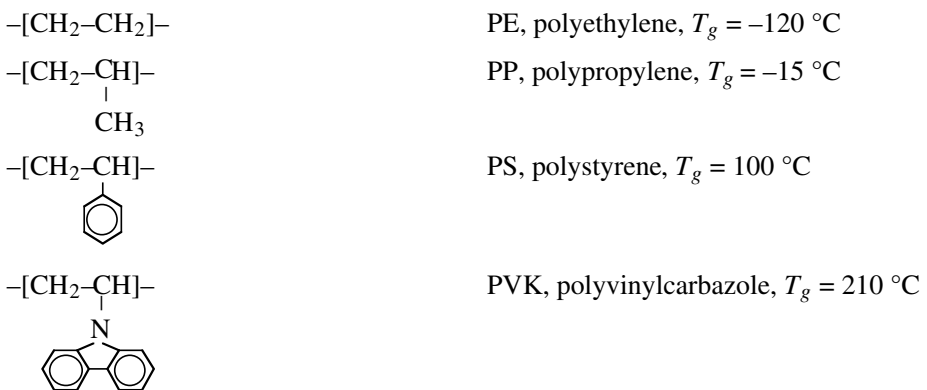
Higher chain stiffness results from a smaller number of possible chain conformations; this can be caused by:

- greater stiffness of the main chain,
- bigger side groups,
- cross links.

First a few examples of chain stiffness differences in the *main chain*; the examples are not very exact, because side groups may also play a role as to flexibility or interactions, but they represent a global trend.



Now we look at some examples of the effect of *side groups* on the chain flexibility:



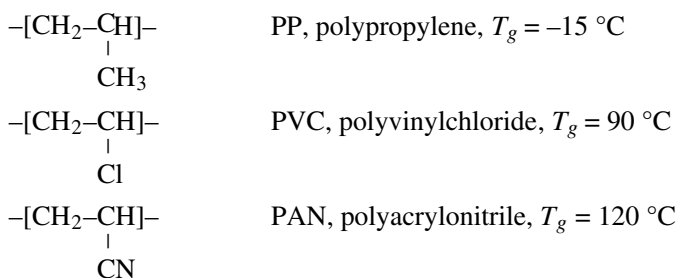
The increasing size of the side group effects a decrease of chain flexibility and an increase of T_g .

Cross-links limit the mobility of macromolecular chains, and thus give rise to an increase in T_g . With a very low concentration of cross-links this effect is hardly detectable. Experiments with the system polystyrene + divinyl benzene showed that at a concentration of 0.4 % of DVB and higher a detectable increase of T_g occurred. With rubbers, vulcanized with sulphur, the detection limit for an increase of T_g appeared to be at 1 to 2 % of sulphur, so that for a technically vulcanized rubber the level of T_g is hardly influenced by the vulcanization process.

Higher degrees of cross-linking have a significant effect; for an unsaturated polyester resin with short and stiff cross-links, T_g appeared to be increased by 21 °C when the number of atoms between cross-links amounted to 50, while with 24 atoms between cross-links the increase was 93 °C. So, with thermosets the cross-link density has a large effect on T_g , and, consequently, on the usability at higher temperatures.

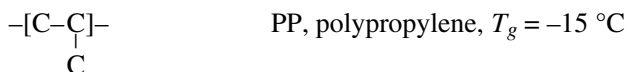
3.4.2. Chain interactions

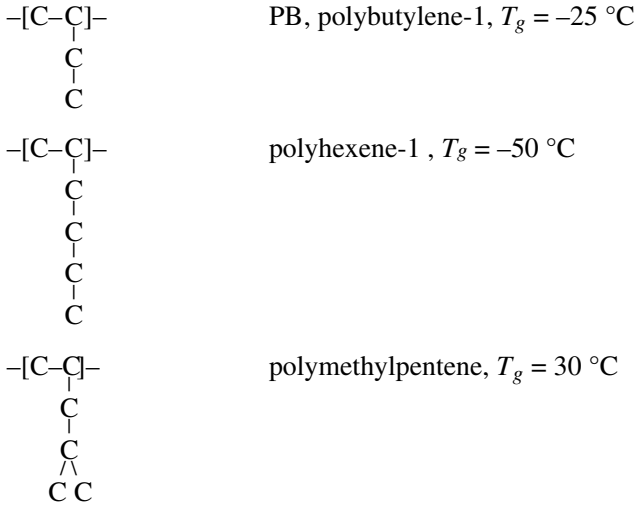
In § 2.6 we have looked at the types of interaction forces which can occur between chains. The strongest of these are the dipole forces. Their effect on T_g is illustrated by the series PP, PVC and PAN, in which the chain mobility hardly varies because the side groups are of about equal size, but in which, in the order of sequence mentioned, the dipole interactions increase.



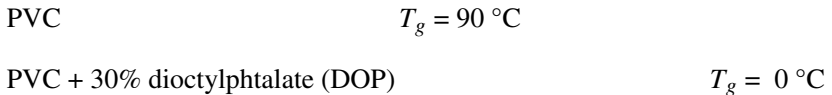
(see also Qu. 3.7).

Interactions can be decreased by increasing the *distance between the chains*, for instance with long side chains, which lower T_g . This effect appears to be greater than the increase of chain stiffness, as shown in the examples below; with PMP the more compact structure of the side group gives rise to a different balance of these counteracting effects.





Increase of the distance between chains and shielding of interactions play a very important role in plasticizing of, e.g., PVC:



3.4.3. Chain length

An empirical relation for the effect of the molar mass M on T_g is:

$$T_g = T_{g\infty} - K/M$$

in which $T_{g\infty}$ is the value of T_g for infinitely long chains and K is a constant which is, e.g., about 10^5 . Consequently, for practically used polymers T_g can, at the most, vary by a few degrees C. It can be argued that the effect of M on T_g is related to the number of chain ends. Therefore, in the above formula, M denotes the number-average molar mass, \bar{M}_n . For branched polymers we meet the complication that each chain has more than two chain ends; a large number of long branches decreases the glass transition temperature.

3.4.4. Effect of time scale

The effect of time scale on T_g has been discussed before; with very rapid cooling values can be observed which are 5° or even $10\text{ }^\circ\text{C}$ higher than with very slow cooling.

3.5. Glass-rubber transition of blends and copolymers

Polymer blends can be subdivided into two kinds: those of compatible and those of incompatible polymers. Real compatibility is an exception (see § 9.1); an example is PS with PPE (polyphenylene ether, also called PPO, polyphenylene oxide). These two polymers can be blended with each other on such a small scale that it really looks like molecular miscibility. This blend shows, therefore, only one single glass transition.

Most polymer blends are, however, composed of incompatible polymers; the blend is then a *dispersion* rather than a *real mixture*; both components retain their own individuality. In such a case, each of the two polymers shows its own glass transition.

A schematic picture of both cases is given in Figure 3.7 .

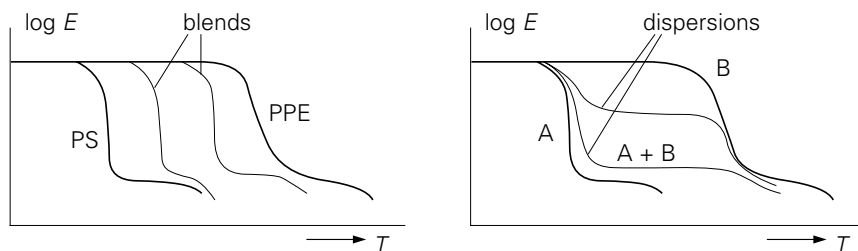


Figure 3.7. Glass-rubber transitions with real mixtures (left) and with dispersions (right).

With copolymers an analogous situation is met as with blends: Here also the components may be molecularly compatible or not. When the copolymer is “random”, i.e. the building blocks are arranged in a random sequence, then the copolymer is, as a matter of fact, homogeneous on a molecular scale, even if the components are incompatible. An example is SBR, a copolymer of styrene and butadiene. It shows a single glass transition at about $-65\text{ }^{\circ}\text{C}$, which is roughly in accordance with the styrene content (23%) and the T_g 's of polybutadiene ($-95\text{ }^{\circ}\text{C}$) and of polystyrene ($90\text{ }^{\circ}\text{C}$).

The situation is quite different with *block copolymers*. As an example we again take a copolymer of styrene and butadiene, but now as a three-block copolymer, SBS. The incompatibility of polystyrene and polybutadiene now results in a phase separation, which is enabled by the circumstance that the blocks can “live their own life”. The polystyrene chain ends clog together into PS domains, which lie embedded in a polybutadiene matrix. These glassy domains act as physical cross-links, so that the polymer has the nature of a thermoplastic rubber. The glass-rubber transitions of PS and BR both remain present; in between these two temperatures the polymer is in a, somewhat stiffened, rubbery condition (see Figure 3.8). This behaviour is dealt

with in more detail in § 9.1.4.

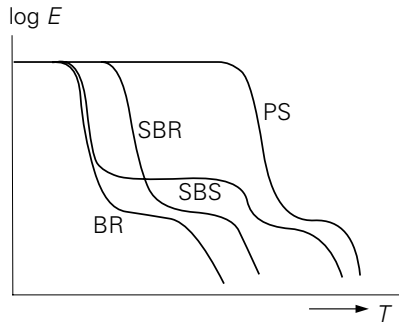


Figure 3.8. Glass-rubber transitions of two kinds of copolymer.

3.6. Methods of measuring T_g

Most methods to measure T_g are, respectively, based on the jump in specific heat and on the sharp decrease of the modulus of elasticity, accompanied by a maximum in the damping.

The *specific heat* as a function of temperature is measured by calorimetry, usually with DSC (differential scanning calorimetry). At T_g a jump to a higher level is found.

The *stiffness modulus* is, in most cases, measured in dynamical - mechanical experiments, for instance with a torsion pendulum, on a time scale of a few seconds. This experiment results in the shear modulus, G (which is related to Young's modulus, E), while the damping shows a strong maximum at T_g .

Finally, the *volume* can be measured as a function of the temperature with the aid of a dilatometer. At T_g a change in slope is detected, signifying a jump in the thermal expansion coefficient.

L.C.E. Struik, 'Physical aging in amorphous polymers and other materials', thesis TH-Delft, TNO, Delft 1977.

J. Heijboer, 'Mechanical properties of glassy polymers containing saturated rings, thesis RU-Leiden, Waltman, Delft, 1972.

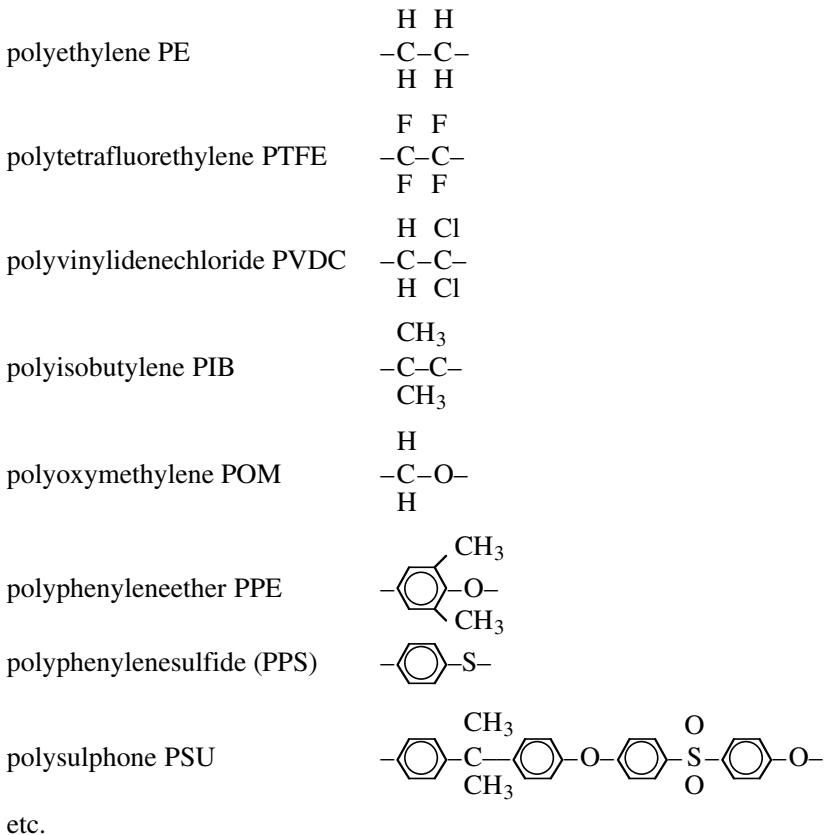
4

Crystalline polymers

4.1. Conditions for crystallization

A primary condition (although not sufficient) for crystallizability is a *regular chain* structure, which enables the formation of crystals in a lattice structure. This condition can be met in several ways:

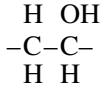
- when the side groups on both sides of an atom in the main chain are equal, so that the chain is *symmetrical*. Examples of such chains are:



- when the side groups are *small enough to be fitted* into a crystal lattice.

Examples:

polyvinylalcohol PVAL;



the OH-group is small enough, to allow, with some distortion, crystallization into a polyethylene-like crystal lattice.

polychlorotrifluoro-ethylene PCTFE;

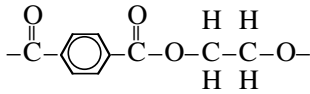


the Cl atom is not so much bigger than the F atom that it would prevent crystallization; with PVC, however, the sizes of the H and Cl atoms are too much different to allow crystallization:.

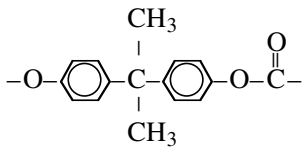


– only *one side group* to an atom in the main chain:

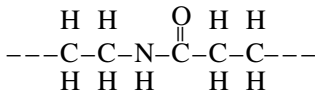
polyethyleneterephthalate PETP,



polycarbonate PC,



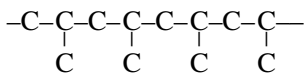
polyamides PA,



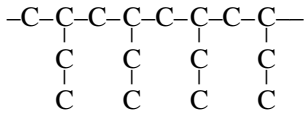
– *regular arrangement of side groups (stereospecific)*

Examples: (see also § 2.3)

polypropylene (isotactic) PP



polybutylene (isotactic) PB



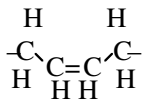
Non-stereospecific vinyl polymers may yet contain enough regular sequences, mostly syndiotactic ones, to allow a small amount of crystallization. Examples are:

polyvinylchloride PVC $-\text{CH}_2-\text{CHCl}-$ (very small), and

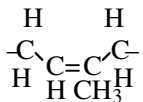
polyacrylonitrile PAN $-\text{CH}_2-\text{CHCN}-$

- With *unsaturated* main chains the configuration around a double bond is of importance. Only predominantly *cis*- or *trans*-chains are crystallizable. Here also *stereospecific* polymerization is required. Some examples (see also § 2.3):

cis-1.4-polybutadiene, BR:



cis-1.4-polyisoprene, IR, also natural rubber, NR:



- With all these examples it should be remarked, that not all polymers which are, in principle, crystallizable, actually crystallize spontaneously. The *rate of crystallization* may be too low, such as with PPE, PC, PIB, BR and IR. In particular for the rubbers (the last three mentioned) it can be said that they crystallize when strongly strained, in other words, when the chains are *highly* oriented (see also Qu. 4.1 to 4.3).

4.2. The melting point

At the melting point, T_m , the solid and the liquid phases are in thermodynamic equilibrium with each other. In § 3.3 we have, already, seen that the free enthalpies are then equal:

$$G_2 = G_1 \quad \text{of} \quad H_2 - TS_2 = H_1 - TS_1$$

This leads to the following simple expression for the melting temperature:

$$T_m = \frac{H_2 - H_1}{S_2 - S_1} = \frac{\Delta H}{\Delta S}$$

For the glass rubber transition a similar expression does not exist, since then ΔH and ΔS are both zero.

ΔH is the *enthalpy difference* between crystal and liquid, the heat of melting. ΔH is mainly governed by the difference in *interaction forces* in the solid and the liquid condition; it is the energy required to disturb the crystal lattice.

ΔS is the *entropy difference* between crystal and liquid and is related to the increase in *disorder* when a crystal melts, or with the probabilities of the chain conditions in both phases. This follows from:

$$S = k \ln W \quad (W = \text{probability})$$

so

$$\Delta S = k \ln \frac{W_2}{W_1}$$

ΔS is, therefore, controlled by the increase in the number of conformations of the chains upon melting, so, a.o. by the *chain flexibility*.

Consequently, we meet the same criteria as with the glass rubber transition, namely interactions and flexibility, but now on a quantitative thermodynamic basis. The examples which can be given for the effects of interactions and flexibility on the melting point are, therefore, similar to those for the glass transition:

Higher *interaction forces* give rise to a higher T_m :

$$\text{PP} \quad T_m = 170 \text{ }^\circ\text{C}$$

$$\text{PVC} \quad T_m = 280 \text{ }^\circ\text{C} \text{ (syndiotactic)}$$

$$\text{PAN} \quad T_m = 320 \text{ }^\circ\text{C} \quad (\text{compare with } \S 3.4)$$

Increase of *chain stiffness* results in a lower ΔS and thus in a higher T_m :

$$\text{PE} \quad T_m = 135 \text{ }^\circ\text{C}$$

$$\text{PS} \quad T_m = 240 \text{ }^\circ\text{C} \text{ (isotactic)}$$

$$\text{PTFE} \quad T_m = 325 \text{ }^\circ\text{C} \quad (\text{compare with } \S 3.4).$$

It is not always as easy to draw such conclusions. For the effect of chain flexibility

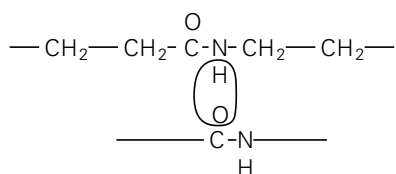
on T_m , sometimes the example is used of polyethylene oxide, PEO, $-\text{CH}_2-\text{CH}_2-\text{O}-$ ($T_m = 67\text{ }^\circ\text{C}$) in comparison with polyethylene, PE, $-\text{CH}_2-\text{CH}_2-$ ($T_m = 135\text{ }^\circ\text{C}$), with the argument that the C–O rotation is easier than C–C.

If we, however, consider a longer series of the type $-(\text{CH}_2)_n-\text{O}-$, then we are in trouble with our simple reasoning:

| | |
|-----------------------------|-----------------------------------|
| $n = 1$, polyoxymethylene, | $T_m = 181\text{ }^\circ\text{C}$ |
| 2, polyethyleneoxide, | $67\text{ }^\circ\text{C}$ |
| 3, polytrimethyleneoxide, | $35\text{ }^\circ\text{C}$ |
| 4, polytetrahydrofurane, | $37\text{ }^\circ\text{C}$ |
| ∞ , polyethylene, | $135\text{ }^\circ\text{C}$. |

There are, apparently, other effects which play a role, possibly the polarity of the $-\text{O}-$ segment in the chain and the topology of the chains in the crystal lattice; the magnitude of the *interaction* forces does not only depend on the nature of the attracting groups, but also on their *distance*. In this respect a comparison between the crystalline densities of PTHF (1.1 g/cm^3) and POM (1.5 g/cm^3) is instructive; the POM crystal is considerably denser, so that the real interactions play a much bigger role in their effect on the melting point.

A second example: when we compare the T_m 's of a polyamide, e.g. PA-6.6 ($260\text{ }^\circ\text{C}$) and polyethylene ($135\text{ }^\circ\text{C}$), then we might, superficially, conclude that the higher value for PA is caused by a higher ΔH as a result of the strong hydrogen bridges active in PA:



From experiments it appears, however, that the heat of melting, ΔH , of nylon is lower than that of PE! From $T_m = \Delta H/\Delta S$ it follows, that ΔS for PA must be considerably lower than for PE. The explanation of this discrepancy is, that in PA the *H-bridges are still existent in the melt*; they are not totally destroyed upon melting, so that ΔH is lower than expected). Moreover, the H-bridges still present in the melt, limit the chain mobility and thus the number of conformations, so that ΔS is considerably reduced.

The effects of the hydrogen bridges indeed decrease with decreasing number of $-\text{CO}-\text{NH}-$ groups in the chain, so with increasing n in PA- n . With high n -values the melting point approaches the value for PE (Figure 4.1, see also Qu. 4.16 and 4.17)).

- The melting point is slightly influenced by the *chain length* according to the equation

$$\frac{1}{T_m} = a + \frac{b}{M} \quad (\text{Figure 4.2})$$

For commonly applied polymers this effect is only small. (See also Qu. 4.6.)

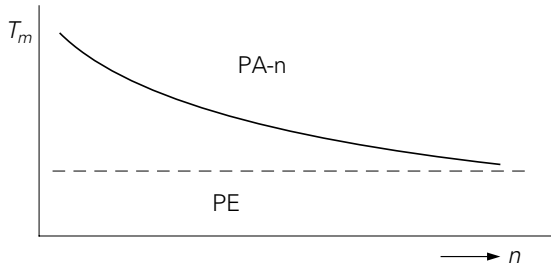


Figure 4.1. Melting points of polyamides.

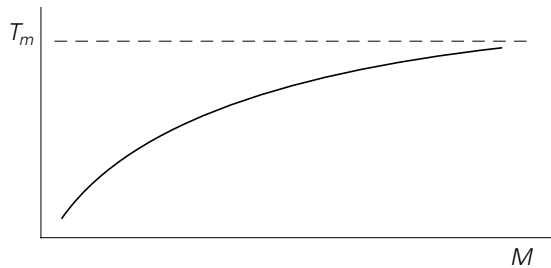


Figure 4.2. Effect of molar mass on melting point.

- *Chain orientation* influences the melting point, which is understandable from the equation $T_m = \Delta H/\Delta S$. When the polymer is stretched in the rubbery phase, its entropy is already so much decreased (see Figure 4.3 and, later on, in § 5.1), that ΔS has decreased. For natural rubber (cis-1.4-polyisoprene) a relation between T_m and the strain has been established experimentally as shown schematically in Figure 4.4.
- *Irregularities* in the chain decrease the melting point because the crystal becomes less perfect. An example is polyethylene, PE; when the chains are not branched the melting point is 135 °C; with three branches per 100 chain segments it is only 110 °C. An imperfect crystal has a lower ΔH .
- Disturbances in a crystal can be brought about by the above mentioned or by other causes. These disturbances are arbitrarily distributed over the crystallites, so that a spread in ΔH occurs, resulting in a spread in T_m , a *melting region*, which has, as an upper limit, the melting point of the “best” crystal.

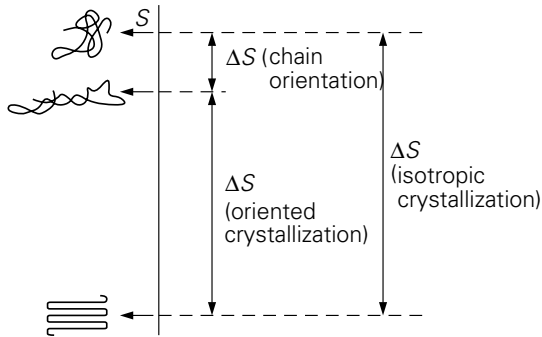


Figure 4.3. Entropy effects with straining and with melting.

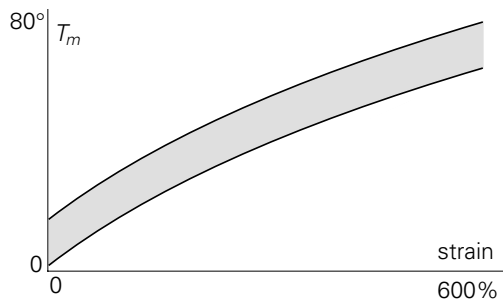


Figure 4.4. Melting point of natural rubber as a function of strain.

- The melting point is also somewhat dependent on the *crystal size*; in particular, when the crystals are very small, T_m is lower. This is, i.a., caused by the restrictions in chain conformations near the crystal surface. A spread in crystal size, therefore, also contributes to the presence of a melting region. This is clearly demonstrated by the (new) PE grades with very low density (copolymers of ethylene with e.g. 1-octene); the crystallites are so small that for a grade with $d = .86$ the melting point is only 30 °C!
- Another striking example of melting point depression is found with a new kind of isotactic polypropylene, made with the new “*metallocene*” katalyst. It is being stated that everything you wish can be made with this new technique. Such as, also, a PP with a very high degree of isotacticity, viz. 97% You would, therefore, expect a higher melting point, but, unfortunately, it appears to be only 148 °C instead of the usual value of 165 °C. What is the reason? Well, because “normal” PP, made in the Ziegler-Natta process is indeed isotactic, but it contains a number of chains which are not isotactic; these are mixed with the wholly isotactic chains and depress the melting point only slightly. With the metallocene katalyst the number of irregularities is much smaller, but they are randomly distributed over all chains. They, therefore, hinder the crystallization process much more than with the old process.

- A phenomenon related to the above mentioned factors is, that the melting point depends on the temperature at which the crystal has been formed. At a lower *temperature of crystallization* crystallization proceeds more rapidly and less regularly, while the crystal size is smaller; this results in a lower T_m .
- *Comparison T_g and T_m*

Since T_g and T_m are both primarily governed by the same chain properties, namely chain flexibility and chain interactions, some correlation between these two quantities can be expected to be present. In Figure 4.5 T_g and T_m are plotted against each other for a number of polymers. As a first approximation it appears that:

- for symmetric chains $T_g \approx \frac{1}{2} T_m$,
- for asymmetric chains $T_g \approx \frac{2}{3} T_m$,

in which T_g and T_m are, as a matter of fact, expressed in Kelvin. In reality the values are spread round this relation by 10 to 30 degrees (see also Qu. 4.5).

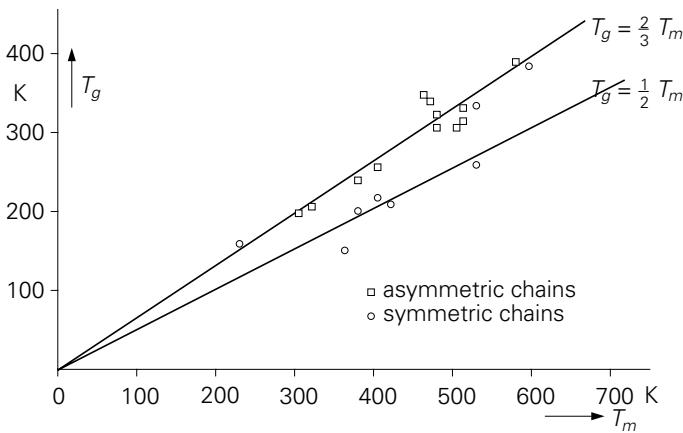


Figure 4.5. Relation between T_g and T_m .

4.3. The crystallization process

4.3.1. Nucleus formation and crystal growth

At a temperature below T_m the free enthalpy of the crystal is lower than that of the liquid; hence the polymer will tend to crystallize. A crystal can, however, only be formed from a nucleus. The process of crystallization can thus be split-up into two different processes: nucleus formation and crystal growth.

Nucleus formation. Sometimes nuclei are already present, e.g. as contaminations, additives, or as deliberately added accelerators for crystallization. Sometimes nuclei

have to be formed by the polymer itself; statistical fluctuations in density and chain conformations may form a first onset for the formation of a crystal. The first case is denoted as *heterogeneous nucleation*, the second as *homogeneous nucleation*. In both cases the nucleus size must, at a certain temperature, exceed a certain minimum to be able to grow further into a crystal. This can be understood as follows:

Suppose that a spherical nucleus with radius r is present in the liquid. We consider the difference in free enthalpy, ΔG , between this crystal and an equally large fluid sphere. ΔG is composed of two components, namely A, the decrease of free enthalpy upon crystallization, and B, the increase in free enthalpy as a result of the formation of the interface. When ΔG_v is the difference in free enthalpy per unit volume between crystal and liquid, and γ is the interfacial energy, then:

$$\Delta G = -\frac{4}{3}\pi r^3 \Delta G_v + 4\pi r^2 \gamma = \underline{A} + \underline{B}$$

Figure 4.6 shows the dependence on r for both contributions; with small values of r its square is predominant and ΔG increases with increasing r ; the nucleus will stop growing and (with homogeneous nucleation) it disappears. From a certain value of r , the *critical nucleus size*, r_k , ΔG decreases upon growth; the nucleus is then stable and continues growing. The value of r_k can be easily calculated: at r_k :

$$\frac{d\Delta G}{dr} = 0 \quad -4\pi r^2 \Delta G_v + 8\pi r \gamma = 0 \quad r_k = \frac{2\gamma}{\Delta G_v}$$

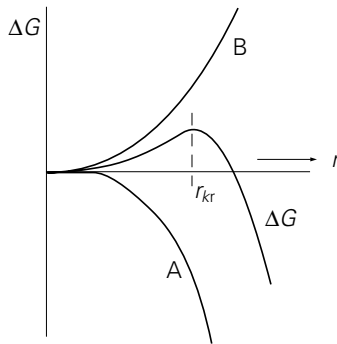


Figure 4.6 Competition between interfacial and crystallization energy.

To make this equation more accessible, we write:

$$\Delta G = \Delta H - T_m \Delta S = 0$$

At the melting point T_m is $\Delta G = 0$ and $\Delta S = \Delta H/T_m$. At a lower temperature, T ,

$$\Delta G = \Delta H - T\Delta S = \Delta H - T \frac{\Delta H}{T_m} = \Delta H \cdot \frac{T_m - T}{T_m}$$

We substitute this in the equation for r_k :

$$r_k = \frac{2\gamma}{\Delta G_v} = \frac{2\gamma T_m}{\Delta H(T_m - T)}$$

An important aspect of this equation is the factor $(T_m - T)$ in the denominator; this is the degree of undercooling. It appears that, just below T_m , very large nuclei are required; with further undercooling smaller nuclei become stable and thus able to initiate the crystallization process. A similar reasoning can be followed for heterogeneous nucleation; here also, with decreasing temperature, more and more small particles become active as nuclei.

Generally speaking, it appears that the rate of nucleation is zero at the melting point, and increases with decreasing temperature.

The *growth rate* of a crystal from a nucleus is also strongly dependent on the temperature. With low undercooling, this rate is low, because the difference in free enthalpy between liquid and crystal, which is the thermodynamic driving force for crystallization, is still low. When the temperature decreases, this driving force increases and so does the rate of crystal growth. There is, however, a counteracting effect: the growth of a crystal goes accompanied by the movement of large chain parts, and even of whole chains, with respect to each other. These movements require the loosening of chain entanglements in the same way as with the flow of a molten polymer. The chain mobility, as required for crystal growth, is thus related to the melt viscosity, and is strongly dependent on temperature and chain length.

As a result of these two counteracting effects the rate of crystal growth shows a maximum at some tens of degrees below T_m , and decreases to zero (at T_g) with further cooling.

From the rate of nucleus formation and the rate of crystal growth the *rate of crystallization* results, which can be schematically represented as the product of both, as shown in Figure 4.7. The rate of crystallization is zero at T_g and at T_m , and shows a *maximum* somewhere in between, a maximum which is lower when the chains are longer.

The maximum rate of crystallization, v_{\max} , strongly differs for different polymers; it is, e.g. very large for PE, much smaller for PETP and near zero for PC (see also Qu. 4.10 – 4.15).

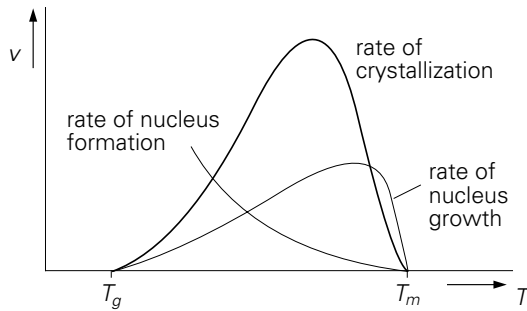


Figure 4.7. Temperature dependence of the rate of crystallization.

The degree of crystallinity, obtained after cooling down from the molten condition, depends on the ratio between rate of cooling and v_{\max} . With rapid cooling v_{\max} may be insufficient to lead to a significant crystallinity; the polymer then remains amorphous and passes, at T_g , into the glassy state. It then follows the line ABCD instead of ABEF, which holds for a crystallizing sample at a low rate of cooling (Figure 4.8). When the thus obtained amorphous sample is slowly heated up starting from D, it will be able to crystallize, and, thereafter it enters into the melting region at G (DCGBA).

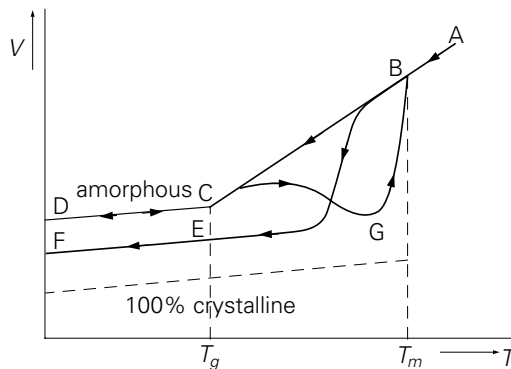


Figure 4.8. $V(T)$ relation for semi-crystalline polymers.

4.3.2. Isothermal crystallization

An analysis of the mechanism of crystallization can best be carried out at a constant temperature. A sample is rapidly cooled down from the melt to a temperature below T_m and kept constant at that level. The crystallization process can then be studied by measuring the volume as a function of time in a dilatometer. The result is a curve as shown in Figure 4.9. The volume approaches an equilibrium value at which the maximum possible crystallization is reached, and the rate of crystallization can, for example, be expressed as $1/t_{0.5}$, in which $t_{0.5}$ is the time in which half of the route is

covered. By doing so at various temperature levels between T_g and T_m , the curve for the rate of crystallization, as indicated in Figure 4.7, can be established.

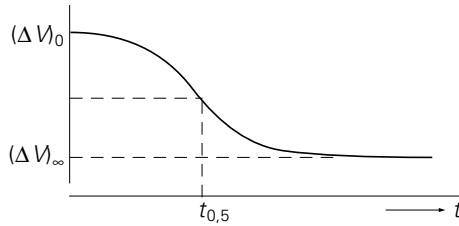


Figure 4.9. Volume change during crystallization.

Further analysis of results from isothermal experiments is based on a simple model. Suppose that we are dealing with *spherical crystallites* which grow in three dimensions. It can safely be assumed that the rate of growth is such that the radius of the sphere increases proportionally with time:

$$r = v \cdot t \quad \text{constant radial rate of growth.}$$

The volume of the sphere is then

$$V = \frac{4}{3} \pi r^3 = \frac{4}{3} \pi v^3 t^3$$

To represent the total crystalline volume V_c , V has to be multiplied by the number of spheres. With a constant number of nuclei (heterogeneous nucleation) this number is constant, so:

$$V_c(\cdot) t^3$$

With homogeneous nucleation, new nuclei are being formed continuously; the number of nuclei and thus of growing spheres is proportional to time:

$$N = vt \quad \text{so} \quad V_c(\cdot) t^3 \times t = t^4$$

If the crystals do not grow in three, but in *two dimensions*, e.g. as disks, a similar reasoning leads to:

$$\begin{aligned} V_c(\cdot) t^3 &\text{ for homogeneous nucleation,} \\ V_c(\cdot) t^2 &\text{ for heterogeneous nucleation,} \end{aligned}$$

In the same way with *one-dimensional* growth (as needles):

$$V_c(\cdot) t^2 \quad \text{respectively} \quad V_c(\cdot) t$$

In general we thus find:

$$V_c = b \cdot t^a$$

V_c cannot be measured directly but only the total volume V ; the relation between V_c and V follows from:

$$\begin{aligned} V &= V_{\text{cryst}} + V_{\text{amorphous}} = V_c + V_a = V_c + \frac{m_a}{\rho_a} \\ &= V_c + \frac{m - V_c \rho_c}{\rho_a} = \frac{m}{\rho_a} - V_c \left[\frac{\rho_c}{\rho_a} - 1 \right] \end{aligned}$$

in which m = total mass, m_a = mass of amorphous part etc, ρ_c and ρ_a the densities.

The volume decrease from the initial condition is $\Delta V = V_0 - V$, in which $V_0 = m/\rho_a$, since initially everything is amorphous.

$$\Delta V = \frac{m}{\rho_a} - \frac{m}{\rho_a} + V_c \left[\frac{\rho_c}{\rho_a} - 1 \right] = V_c \left[\frac{\rho_c}{\rho_a} - 1 \right] = \left[\frac{\rho_c}{\rho_a} - 1 \right] \cdot b t^a = c t^a$$

This is a first-order approximation, only valid for the first stage of crystallization (otherwise ΔV would increase to infinity). As soon as growing crystals touch each other, their growth is limited. A better approximation is given by the *Avrami* equation:

$$\Delta V = (\Delta V)_\infty \cdot (1 - \exp(-c t^a))$$

For small values of t this expression is equivalent to the first approximation, since then $\exp(-c t^a) \approx 1 - c t^a$.

To obtain some impression of the way in which ΔV depends on time for various values of a , Figure 4.10 gives a schematic example for three cases: $a = 1, 2$ and 4 , while in all cases a value for $t_{0.5} = 1000$ min has been chosen.

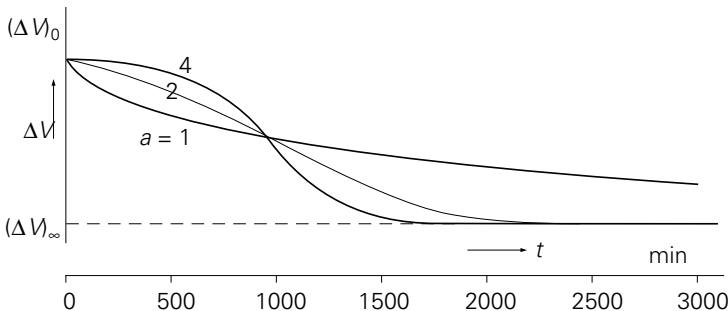


Figure 4.10. Change of volume with three different Avrami exponents.

A better impression can be obtained by rewriting the Avrami equation:

$$1 - \frac{\Delta V}{(\Delta V)_\infty} = \exp(-ct^a) \quad \ln \left(1 - \frac{\Delta V}{(\Delta V)_\infty} \right) = -ct^a$$

$$\ln \left[-\ln \left(1 - \frac{\Delta V}{(\Delta V)_\infty} \right) \right] = \ln c + a \ln t$$

From experimental data on ΔV as a function of time the proper way of plotting provides the value of a as the slope of a straight line (see also Qu. 4.22).

Finally the effect of *orientation* on the rate of crystallization should be mentioned. In a strained, oriented condition crystallization proceeds much more rapidly. By orientation the ordering is increased; the chains approach the crystalline condition more closely. As a matter of fact there is a relation to the increase in melting point, mentioned in § 4.2; under strain the amount of undercooling ΔT is increased, but this gives only a partial explanation of the increase in the rate of crystallization.

4.4. Crystalline structure

4.4.1. Crystalline fraction

Since polymers are never completely crystalline, it is of importance to know, how big, in a certain case, the crystalline fraction is. The crystalline volume fraction, φ_c , can be calculated from the specific mass, ρ , if the densities of the amorphous fraction, ρ_a , and of the crystal, ρ_c , are known, since:

$$\rho = \varphi_c \cdot \rho_c + (1 - \varphi_c) \cdot \rho_a \quad \text{of} \quad \varphi_c = \frac{\rho - \rho_a}{\rho_c - \rho_a}$$

It can be easily shown that the mass fraction, ψ_c , is given by:

$$\psi_c = \frac{\rho - \rho_a}{\rho_c - \rho_a} \cdot \frac{\rho_c}{\rho}$$

ρ_c can be determined from *X-ray diffraction* diagrams; these provide the dimensions of the unit cell of the crystalline lattice, and thus the sum of the atom masses in such a cell together with its volume (see Qu. 4.20). ρ_a can be measured at a number of temperatures above (or somewhat below) T_m ; extrapolation to room temperature gives the required value (unless T_g is passed!). The table below gives, for a number of polymers, some characteristic values, such as the range in which φ_c is mostly found, and an average value for the density.

| | ϕ_c (%) | ρ_c | ρ_a | ρ |
|--------|--------------|----------|----------|--------|
| PA 6.6 | 35–45 | 1.22 | 1.07 | 1.14 |
| POM | 70–80 | – | – | 1.41 |
| PETP | 30–40 | 1.455 | 1.335 | 1.38 |
| PBTP | 40–50 | – | – | 1.30 |
| PTFE | 60–80 | – | – | 2.1 |
| PP | 70–80 | 0.937 | 0.834 | 0.905 |
| HDPE | 70–85 | 1.00 | 0.855 | 0.95 |
| LDPE | 45–55 | 1.00 | 0.855 | 0.92 |

Another method is based on the intensity of X-ray diffraction as a function of the diffraction angle θ ; the ratio of the areas of the crystalline peaks and the amorphous background gives ϕ_c (Figure 4.11).

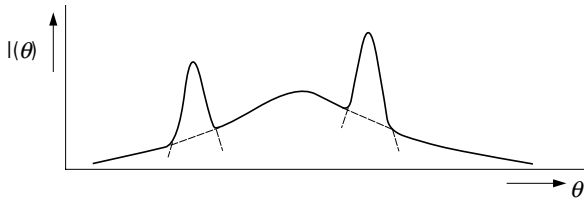


Figure 4.11. X-ray diffraction of a semi-crystalline polymer.

Finally ϕ_c can be determined from the heat of melting of a sample via calorimetry, in comparison with the melting heat of the pure crystal, known from literature.

4.4.2. Crystal morphology

An example of a polymer crystal is given in Figure 4.12, namely of PE, in which the chains should be imagined to lie in zig-zag shape perpendicular to the plane of drawing; the figure gives the projection of the C- and H-atoms. The crystal is orthorhombic with $a = 0.740$ nm, $b = 0.493$ nm; the vertical dimension of the cell, $c = 0.253$ nm. Also other polymers can crystallize with extended chains, such as PA-6 (monoclinic) and PA-6.6 (triclinic).

Isotactic vinyl polymers $-(CH_2-CHX)-$ can, because of sterical hindrance, in most cases not lie in zig-zag shape; the chain then takes, as the most regular conformation, a *helical* shape. An example is given in Figure 4.13, again as a projection on the plane of drawing, for PP, which as a helix crystallizes in a monoclinical lattice.

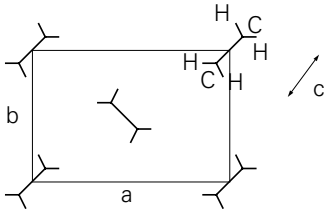


Figure 4.12 Crystal lattice of PE.

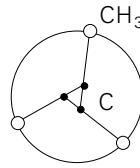


Figure 4.13. Projection of PP chain.

Because of the incomplete crystallization in polymers, crystalline and amorphous regions are spatially arranged in some way. The oldest model for this arrangement is of Hermann and Gerngross (1930), the so-called *fringed micel* structure (Figure 4.14). In this model the crystalline regions are embedded in an amorphous matrix, while the chains pass from one region into another.

In an other model, the *paracrystalline*, (Hosemann, 1936), the amorphous regions are embedded within the crystals, so the other way round (Figure 4.15). Both models are realistic, and occur in combination with each other.

A detailed model for the single crystal was introduced by Keller in 1957 for polyethylene. The chains (Figure 4.16) are more or less regularly folded in *lamellae*.

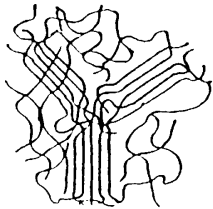


Figure 4.14. Fringed-micel model.

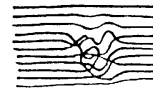


Figure 4.15. Paracrystalline model.

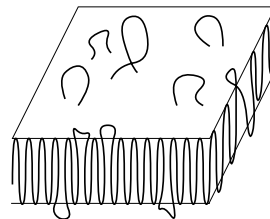
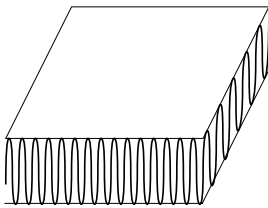


Figure 4.16. Lamellae models.

The length of folding, so the thickness of the lamella, appears to be greater as the temperature of crystallization has been higher. The most remarkable is, that the lamellae increase in thickness upon recrystallization at a temperature nearer to T_m !

Crystallization from a stirred solution of, e.g. PE, results in a strongly oriented bundle of fibres, on which, later on, transverse lamellae grow, the so-called *shish-*

kebab structure (Figure 4.17). This observation (Pennings) forms the basis for the recently by DSM developed super-strong PE-fibre.

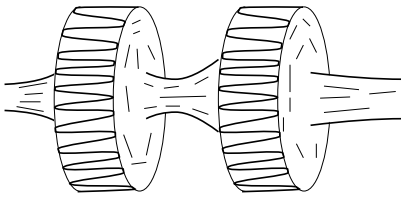


Figure 4.17. 'Shish-kebab' model.

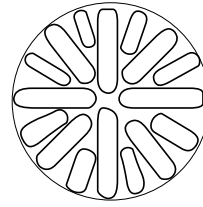


Figure 4.18. Spherulite.

In polymers crystallized from the melt, in most cases *spherulitic* structures are observed: spherical agglomerates of crystals and amorphous regions, grown from a primary nucleus via successive secondary nucleation (Figure 4.18). The dimensions of the spherulites are commonly between 5 μm and 1 mm. When spherulites grow during the crystallization process, they touch each other and are separated by planes. In a microtome slice they show a very attractive coloured appearance in polarized light.

4.5. Effect on properties

Crystallization brings about a drastic change in the pattern of properties. compared with amorphous polymers. Upon the scheme: glass - rubber - liquid now the scheme crystal - liquid is superimposed, since an amorphous phase remains always present.

This can be demonstrated easiest in the $\log E - T$ diagram. The amorphous polymer follows curve *a* in Figure 4.19; two cases have been indicated: a_1 and a_2 , for a lower and a higher molar mass, respectively.

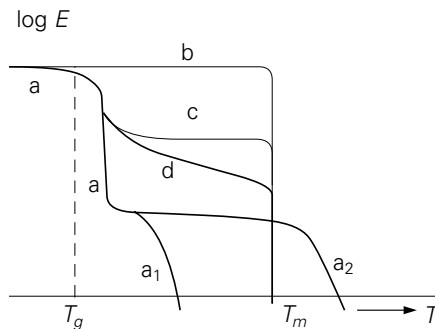


Figure 4.19. Effect of crystallization on E -modulus.

A fully crystalline polymer would follow curve *b*: no glass transition occurs and the modulus drops sharply at T_m , either to zero or to a tail of the rubbery region (a_2).

This picture is oversimplified; strictly speaking, curve *b* should be drawn at a somewhat higher level than *a* in the glassy region; the stiffness of the crystal exceeds that of the glass.

A partially crystalline polymer could follow curve *c*; at T_m the amorphous part passes into a rubber, the crystalline part is unaffected. The actual curve resembles more curve *d*, i.a. as a result of a broad *melting region*.

Some consequences of crystallization on the practical behaviour of polymers are:

- Above T_g the polymer can be used as a solid material to just below T_m , though its stiffness is lower than that of a glassy polymer, and much more *temperature dependent* (compare, e.g., E(PP) \approx 1400 MPa and E(HDPE) \approx 1000 MPa, with E(PVC) \approx 3200 MPa).
- The level of *E* between T_g and T_m strongly depends on the *degree of crystallization*. This is clearly demonstrated by PE, where the density varies between 0.91 and 0.97, the crystalline fraction between 0.40 and 0.85, and the *E*-modulus between 100 and 1200 MPa at 20 °C.
- The rubbery region is wholly or partially masked by the crystallinity; the elastic response of the melt is, therefore, much less pronounced.
- Parallel to the stronger temperature dependence of *E* for semi-crystalline polymers is the stronger dependence on time; they show a higher tendency to *creep* than amorphous, glassy polymers, (Figure 4.20), at least at temperatures above or not too far below T_g .

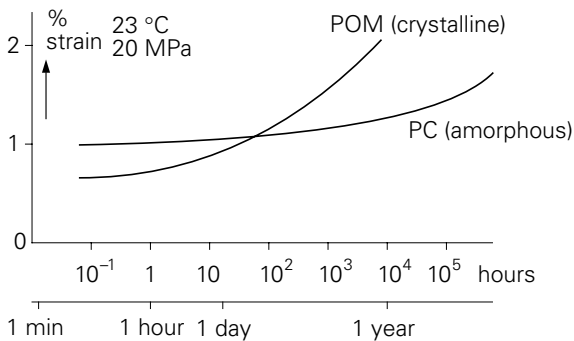


Figure 4.20. Creep of an amorphous and a semi-crystalline polymer.

- A crystalline polymer is a *two-phase* system; for $T < T_g$ it contains a glassy phase and a crystalline phase, with, in general, a low impact strength. For $T > T_g$ the amorphous phase is in the rubbery condition, which results in a much higher *impact strength*.

- Because of their to-phase nature, semi-crystalline polymers are, in most cases, *nontransparent*; the difference in refraction index is responsible for strong light scattering.
- Crystallization of *oriented chains* is, in various respects, important for the polymer properties. The fact has been mentioned before, that stereospecific rubbers such as cis-1,4 polybutadiene can crystallize when under strain. The spontaneously formed crystals contribute strongly to the strength of the vulcanizate. A vulcanized natural rubber has, without carbon black reinforcement, a tensile strength of about 40 MPa, whereas an unreinforced SBR breaks at about 3 MPa. (With SBR a high tensile strength can only be reached with carbon black.)
- Another effect of orientation and crystallization is found with *fibres*. Crystallization of oriented chains brings about a stiffness and a strength which are several times greater than those in the unoriented condition, though, as a matter of fact, only in one direction.
- To conclude with, an overall picture is given in Figure 4.21 of various polymers, ranged after T_g : the points for the crystalline polymers are connected by a vertical line to their melting points T_m . In this survey the nature of the various polymers is easily recognizable: For rubbers T_g is far below ambient temperature T_0 ; for amorphous thermoplastics T_g lies amply above T_0 . For semi-crystalline thermoplastics T_g can be below as well as above T_0 ; in the latter case the materials have an extra resistance against higher temperature.

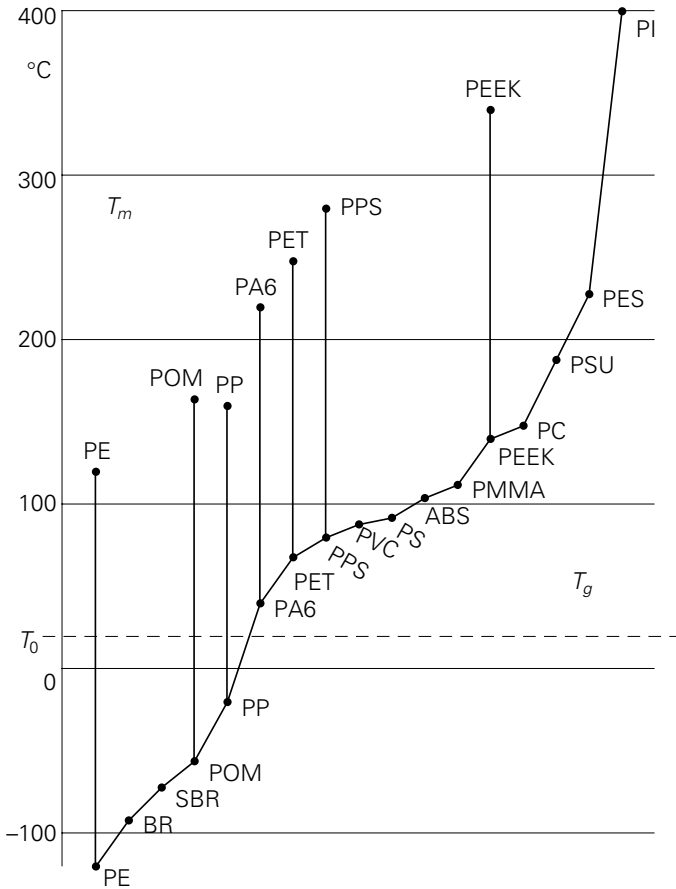


Figure 4.21. Survey of glass- and melting points.

4.6. Liquid-crystalline polymers

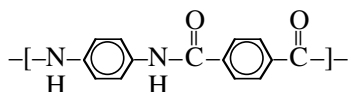
In § 4.3 we have already seen that polymers, in the rubber or fluid condition, crystallize much more rapidly when their chains are oriented. Therefore a stretched rubber, if stereospecific in its molecular structure, is able to crystallize at a temperature considerably above its equilibrium thermodynamic melting point. Also a thermoplast such as polyethylene, when in the molten state or in solution, can crystallize spontaneously when the chains are being orientated in elongational flow. The latter case is utilized when polyethylene is spun from a diluted solution (gel spinning process), resulting in fibres of super-high strength and stiffness (“Dyneema” fibres).

While with PE the chain is very flexible, a similar situation occurs with *very stiff chains*; these have, as a result of their high characteristic chain stiffness (see § 2.4), a much smaller number of conformation possibilities. Strongly exaggerated, they

behave more as *stiff rods* than as coiled chains, in particular in elongational flow, in which the “rods” are easily oriented and obtain a parallel direction. In such a flowing liquid a considerable ordering is already present, somewhat like a crystal structure, though this ordering only holds for the orientation and not for the position of the chains, as in a real crystal. For such a situation the expression “*liquid crystal*” is used. Upon solidification from the melt or the solution a material is formed which is, in the direction of orientation, extremely strong and stiff.

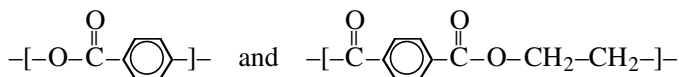
Two types of liquid crystal polymers (LCP's) can be distinguished: *lyotropic* and *thermotropic*. The first type is formed in a *solution*; this is done when the polymer has such a high melting point (low ΔS , see § 4.2), that it cannot be handled in the molten condition without being degraded. If this limitation is not present, then the orientation can be brought about in the melt; in such a case we have a thermotropic LCP.

A well-known example of a *lyotropic* LCP is the aramide fibre (Twaron or Kevlar), an aromatic polyamide with the structure:



The chain is exceptionally stiff because of the short-distance sequence of the phenyl rings. The fibre is being spun and stretched from a solution in highly concentrated sulphuric acid, and shows (in its length direction) nearly unsurpassed mechanical properties.

An example of a *thermotropic* LCP is a copolymer of polyhydroxy benzoic acid and polyethylene terephthalate:



The more flexible comonomer is introduced to reduce the melting point, so that the polymer can be processed in the molten condition, e.g. in injection moulding and extrusion. The end products show superior mechanical properties, but are, as a matter of fact, highly anisotropic.

5

Rubbery and liquid phases

5.1. Rubbery phase

Above the glass-rubber transition temperature, T_g , large parts of the chain are free to move; their thermal energy is high enough to overcome the interaction forces, and the free volume increases with increasing temperature. The polymer is, however, not yet in the liquid condition; the coiled chains are mutually entangled, in contrast to a low-molecular amorphous material above its T_g (Figure 5.1):

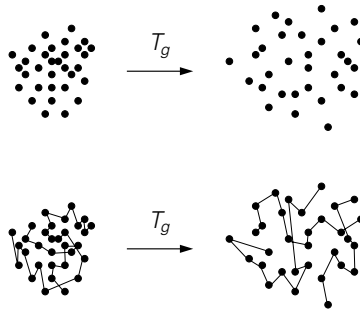


Figure 5.1. A polymer is not a liquid just above its T_g .

Dependent of the amount of entanglement, thus of the chain length, a temperature region exists in which the polymer does not flow, but is very soft, rubbery and elastic. Though the chain entanglements are not permanent, because they are being disrupted with increasing temperature and also with increased time of loading, they act as temporary, physical cross-links.

We now understand that the material is, in this condition, soft and still coherent, but the question is, for non-cross-linked polymers above T_g as well as for vulcanized rubbers: why does it show spontaneous recovery after being stretched? As a model we take a chain with freely rotating links; stretching of such a chain from a coiled state does not require any energy, while, after stretching, it retains its shape.

This model, however, is only valid for chain molecules at zero Kelvin. When $T \neq 0$ the chain parts possess thermal energy; vibration causes them to move in random directions, which always results in a contraction of the stretched chain. The chain tends to a state of higher probability, and eventually reaches a fully unoriented random conformation, as described in § 2.4 (“random walk conformation”). To

prevent this, a force is needed, which is greater with stronger vibration and thus with a higher temperature.

This implies the existence of a finite modulus of elasticity, and, also, of elastic recovery. Since it concerns a competition between order and disorder, and has nothing to do with any energy barrier, this is entropy elasticity. No change in energy is present upon stretching in the rubbery state, but the entropy changes; in the stretched condition the chains have much less conformation possibilities, and thus a lower probability, W , and a lower entropy $S = k \cdot \ln W$ (see also Figure 4.3). The system tends to increase its entropy by retracting. From this reasoning we could now try to calculate the E -modulus in the rubbery state.

Increasing the length dimension from l to $l + dl$ requires a force K and an amount of work $dF = K \cdot dl$. This work equals the increase in free energy of the system, $F = U - T \cdot S$. Since no interactions are active, U does not change, so

$$K = \frac{dF}{dl} = -T \frac{dS}{dl}$$

The next question is, how S varies with l . This can be calculated in a purely statistical way. It is possible to count, for a schematized chain, the number of conformations between two cross-links as a function of the distance between these cross-links. Assuming that the increase of this distance is proportional to the total strain, the calculation proceeds as follows:

Suppose the network is ideal, with N chain units between cross-links, while the initial dimensions are: l_x^0 , l_y^0 and l_z^0 (Figure 5.2). The network is then deformed to the dimensions l_x , l_y , l_z . Statistical calculation of the number of possible chain conformations between the cross-links results, with $S = k \cdot \ln W$, in:

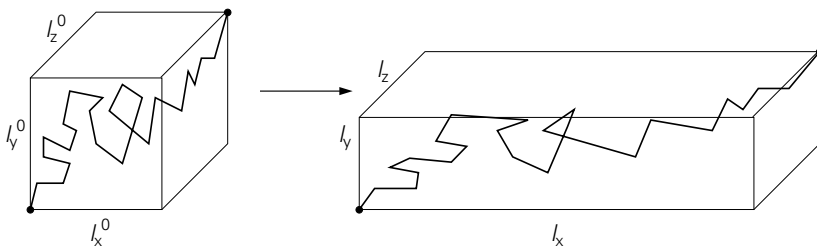


Figure 5.2. Deformation of a rubber network.

$$\Delta S = -k \cdot N \cdot [(\lambda_x^2 + \lambda_y^2 + \lambda_z^2 - 3)/2 - \ln \lambda_x \lambda_y \lambda_z]$$

in which $\lambda_x = l_x/l_x^0$ etc., the deformations in the three main directions, with $\epsilon_x = \lambda_x - 1$ etc. When the strain is unidirectional in the x -direction, then

$$\lambda_y = \lambda_z \neq \lambda_x,$$

and

$$\lambda_y^2 = \lambda_z^2 = 1/\lambda_x.$$

Since the volume

$$V = \lambda_x \lambda_y \lambda_z \cdot V_0,$$

is, for rubbers, practically independent of the strain (the Poisson ratio $\nu \approx 0.5$), is

$$\lambda_x \lambda_y \lambda_z = 1,$$

and

$$\Delta S = -k \cdot N \cdot \left[\frac{\lambda_x^2}{2} + \frac{1}{\lambda_x} - \frac{3}{2} \right]$$

The force is

$$K = -T \frac{dS}{dl} \quad \text{or} \quad K = -T \frac{d\Delta S}{dl}$$

or, with $l = l_x^0 \cdot \lambda$:

$$K = -\frac{T}{l_x^0} \frac{d\Delta S}{d\lambda_x} = \frac{NkT}{l_x^0} \left(\lambda_x - \frac{1}{\lambda_x^2} \right)$$

The stress σ is:

$$\sigma = N^* kT \cdot \left(\lambda_x^2 - \frac{1}{\lambda_x} \right)$$

in which N^* is the number of chain units per unit volume.

For small strains: $\lambda_x = 1 + \varepsilon_x$, $\lambda_x^2 \approx 1 + 2\varepsilon_x$, $1/\lambda_x \approx 1 - \varepsilon_x$, so that:

$$\sigma = N^* kT \cdot (1 + 2\varepsilon_x - 1 + \varepsilon_x) = 3N^* kT \cdot \varepsilon_x$$

and

$$E = \sigma/\varepsilon_x = 3N^* kT$$

For large strains the expression for the stress can be simplified into:

$$\sigma = N^* kT (\lambda_x)^2$$

In most cases the stress is not expressed as force per unit of the actual area of cross-section, but is, rather, based on the original area; in that case it can easily be shown that then the stress is given by:

$$\sigma = N^*kT \cdot \lambda_x$$

This relation holds for strains up to 300 or 500 % ($\lambda = 4$ to 6); with even higher strains some chain parts may approach their fully stretched conformations; moreover crystallization may occur. In both cases the slope of the stress-strain curve increases. In Figure 5.3 the resulting diagram is schematically presented.

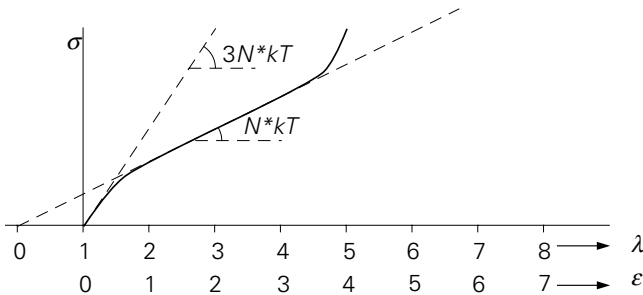


Figure 5.3. Stress - strain diagram of a rubber.

The initial modulus of elasticity, $E = 3N^*kT$, can also be written as

$$E = \frac{3\rho RT}{M_c}$$

where ρ is the density, R the gas constant and M_c the molar mass between cross-links, since:

$$N^*M_c \cdot \frac{k}{R} = \frac{N^* \cdot M_c}{N_A} = \rho$$

($N_A =$ Avogadro-number)

The initial E-modulus, and also the stresses at higher strains, appear to be proportional to the absolute temperature, as our simple model of the vibrating chain already suggested. For an ideal vulcanized rubber, showing only entropy elasticity, this can, indeed, be observed. A simple experiment on a thin tube, stretched by a dead weight to several times its initial length, through which, alternatively, water of 100 °C and of 0 °C flows, clearly shows the “negative coefficient of expansion” of strained rubber, though the theoretical ratio of the strains, 373/273, is not achieved.

Deviations from the proportionality $\sigma (\cdot) T$ result from, a.o. three complications, which have been neglected in the simplified treatment:

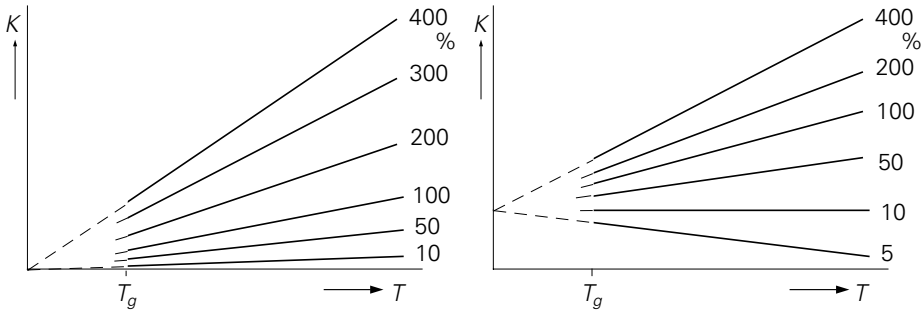


Figure 5.4. Deviations from ideal rubberelastic behaviour.

- First, some energy elasticity is always present; the lines in a plot of K against T (Figure 5.4), when extrapolated back from the glass transition temperature, do not pass through the origin; the intercept with the K -axis represents the small effect of ΔU ,
- Secondly, the coefficient of thermal expansion of the unstrained rubber has not been taken into account; its effect is evident from a decrease of the slope of the K - T curve; below a certain strain (the “thermodynamic inversion point”) this slope is even negative.
- In the third place, we have, for simplification, considered the free energy $F = U - TS$ instead of the free enthalpy $G = F + pV$; the volume, though approximately constant upon straining, still shows a minor increase.

It should also be remarked that we have supposed the existence of permanent cross-links; this may hold for vulcanized rubbers, but in unvulcanized condition the entanglements are gradually loosened under strain, to be formed again in other places. As a consequence, an increase of E with T is, for uncrosslinked polymers, hardly observable; in most cases E decreases with increasing temperature, which goes together with a gradual transition from the rubbery into the liquid state.

The E-modulus appeared to be inversely proportional to the distance between cross-links, so, approximately, proportional to the number of cross-links. If no permanent cross-links are present, i.e. in the unvulcanized condition, then E is governed by the number of physical entanglements. Light vulcanization does not contribute significantly to total number of cross-links; therefore, in lightly crosslinked vulcanizates, such as technical rubbers, the E modulus is hardly dependent on the degree of vulcanization (Qu. 5.4 en 5.5).

Strongly cross-linked systems such as thermosets, however, show in the rubbery phase a much higher modulus than a rubber, but still considerably lower than in the glassy state. Figure 5.5 schematically presents how E changes with T for systems

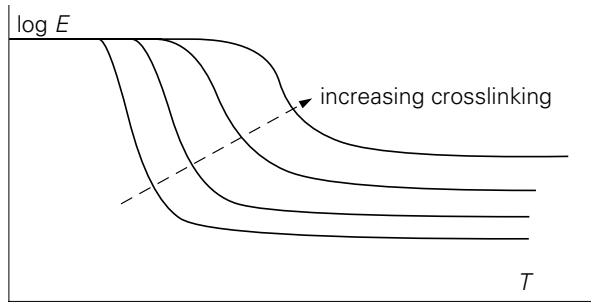


Figure 5.5. $E(T)$ for networks.

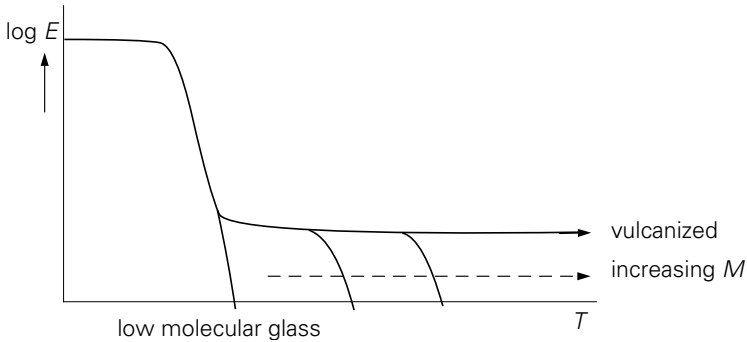


Figure 5.6. Effect of chain length on rubbery region.

with increasing degree of cross-linking; also the increase of T_g , discussed in § 3.4.1, is visible in this diagram.

5.2. Transition of rubber to fluid

With increasing temperature the rubbery phase gradually passes into a fluid state; the temperature region in which this occurs, is strongly dependent on the *chain length* (see Figure 5.6). Longer chains have a greater number of entanglements and require a higher temperature to become disentangled. Since the *longest* chains play a predominant role, higher averages such as \bar{M}_Z govern the rubber-fluid transition.

Moreover, the *time scale* is of importance, since, at a certain temperature, an entanglement can be loosened under stress after a somewhat longer time. Figure 5.7 presents, schematically, how $\log E$ varies with temperature for various loading time scales; in this figure the dependence of T_g on the time scale is indicated, and, in particular, the effect of time on the rubber- to-flow transition. On a short time scale the polymer is, at temperature T_1 , strongly rubberelastic; at a long time scale it behaves as a fluid. This dualism *visco-elastic behaviour*, has a large number of practical technological consequences, some of which will be discussed in § 5.4.

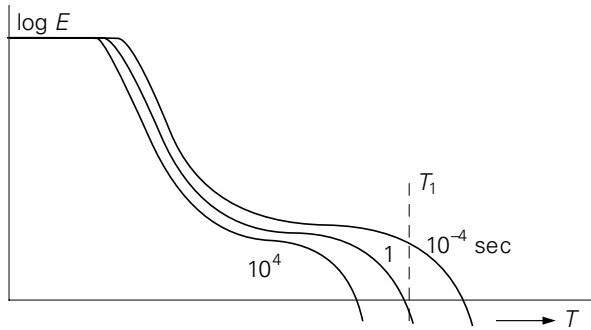


Figure 5.7. Effect of time scale on the rubber - liquid transition.

5.3. Fluid condition

5.3.1. Viscosity

In the fluid condition the chains move as a whole with respect to each other. The many entanglements have to be disrupted continuously; therefore, the viscosity of liquid polymers is very high. In the table below a comparison is given of the viscosities of various liquids, expressed in Pa·s (= N·s/m² = 10 poise) at 20 °C unless stated otherwise.

| | |
|-----------------------------|---------------|
| water | 0.001 |
| alcohol | 0.0012 |
| fluid metals | 0.001 – 0.002 |
| glycol | 0.02 |
| linseed oil | 0.05 |
| olive oil | 0.08 |
| machine oil | 0.1 - 0.5 |
| glycerol | 1.5 |
| polymers | 100 – 10.000 |
| (at processing temperature) | |

The viscosity of polymers is strongly dependent on their molar mass, namely according to $\eta \propto \bar{M}_w^{3.4}$ (weight average). The high value of the exponent, 3.4, reflects the large influence of chain entanglements on the flow behaviour; when the chains are twice as long, the number of entanglements has increased so much that the melt viscosity is more than ten times higher!

As a matter of fact, the viscosity is a very dominant property for the processing technology. A fluid polymer mass with a high viscosity requires high pressures to be transported in processing machines. How strongly the processability prevails, has already been discussed in § 2.2.3; for some thermoplasts like PE, PP and ABS,

grades differing in molar mass. are usually characterized by their melt index, which is the amount of material flowing through a standard capillary, as a first measure for their processability.

With rubbers a similar situation is met, but now with the aid of a rotation viscometer. The Mooney viscosity is measured as the torque needed to rotate two parallel plates, between which the rubber mass is present, with respect to each other. This provides a rough indication of the viscosity, and thus of the molar mass. This measurement can also be used to characterize the vulcanization behaviour; under vulcanization conditions the increase of the Mooney viscosity indicates the onset of network formation. When the network develops further, a continuous rotation can, of course, no longer be applied because the viscosity increases unlimitedly; therefore an oscillation method is mostly used with a cone-and-plate geometry. Initially, the viscosity is being measured, and later on the build-up of the *E*-modulus of the network. Another characterization of the viscosity of unvulcanized rubbers is the Hoekstra method. The rubber is present between two parallel plates, which are moved towards each other with a certain speed; the force needed to do so is an indication of the viscosity.

These simple standard methods for characterizing the viscosity only provide a first impression of the processing behaviour. In reality considerable complications occur. The first is that we are already in trouble when we try to define the viscosity properly, as a result of the non-Newtonian behaviour.

5.3.2. Non-Newtonian behaviour

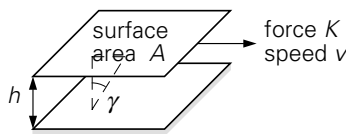


Figure 5.8. Definition of viscosity.

When using the word “viscosity” it is implicitly assumed that stress and shear rate are proportional. This means that the force *K* required to move two plates, between which a liquid is present, parallel to each other with a speed *v* (Figure 5.8), is proportional to *v*.

To eliminate the effect of the dimensions, the force is divided by the area of the plates, *A*, so as to give the shear stress:

$$\tau = K/A$$

and the speed by the plate distance, *h*, resulting in the velocity gradient *v/h*. The

latter equals the rate of shear v/t or $d\gamma/dt$ or $\dot{\gamma}$. The proportionality thus reads:

$$K(\dot{\gamma})v \quad \text{and} \quad \tau = K/A(\dot{\gamma})v/h = \dot{\gamma}$$

The proportionality constant is defined as the viscosity η :

$$\eta = \tau/\dot{\gamma}$$

When τ and $\dot{\gamma}$ are, indeed, proportional to each other, the liquid is called *Newtonian*. However, various fluids deviate from Newtonian behaviour, as indicated in Figure 5.9.

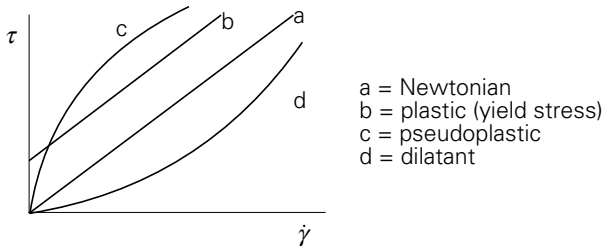


Figure 5.9. Possible deviations from Newtonian behaviour.

Fluid polymers mostly show *pseudoplastic behaviour*: the rate of flow, $\dot{\gamma}$, increases more than proportionally with increasing shear stress τ . A unique viscosity value can, therefore, not be defined; when, for instance, with a certain value of $\dot{\gamma}$, a value of τ is measured, then

$$\eta = \tau/\dot{\gamma} \text{ is nothing more than an apparent viscosity}$$

only holding for a single level of τ or of $\dot{\gamma}$.

Full characterization of the flow behaviour, therefore, requires the determination of the apparent viscosity over a broad range of τ or of $\dot{\gamma}$. For low rates of shear η can be measured with a cylindrical or a cone-plate rotation viscometer. For higher rates of shear (from about 1 sec^{-1}) capillary viscometers can be applied.

The apparent viscosity may, in the region of shear rates occurring in practice, decrease by a factor of 10 to 500 with increasing $\dot{\gamma}$. In most cases η is represented as a function of τ (or, also, of $\dot{\gamma}$) on a log-log scale. An example is given in Figure 5.10 for three grades of the same polymer.

A and B have the same viscosity at low stress: the “zero-shear viscosity”. They have, therefore, the same \bar{M}_w , since the relation given before: $\eta = \bar{M}_w^{3.4}$, is valid for this zero-shear viscosity. C has a ten times lower value; its \bar{M}_w , is thus about twice as low.

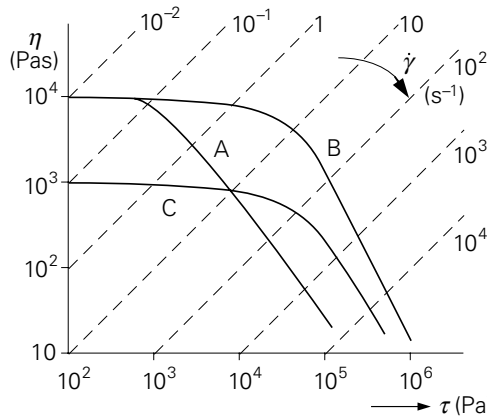


Figure 5.10. Non-Newtonian behaviour of three grades of the same polymer, differing as to molar mass and -distribution.

The difference between A and B is due to a difference in molar mass distribution MMD; for A this is broader than for B (and for C). A broader MMD causes the polymer to deviate more strongly from Newtonian behaviour. A first approximating measure of the width of the distribution is $\overline{M}_w/\overline{M}_n$; as far as the effect on the non-Newtonian behaviour is concerned, $\overline{M}_z/\overline{M}_w$ would be a better measure.

It further appears that, with higher rates of stress, the effect of the MMD may overrule the effect of \overline{M}_w on the apparent viscosity: the curves for A and C intersect. From Figure 5.10 one might conclude: there is a “Newtonian region” for A up to $\dot{\gamma} = 0.1 \text{ sec}^{-1}$ or to $\tau = 10^3 \text{ Pa}$, and for B up to $\dot{\gamma} = 1 \text{ sec}^{-1}$ or to $\tau = 10^4 \text{ Pa}$. In this “Newtonian region” the viscosity would be “constant”. In how far this is indeed true, is apparent from the linear plot in Figure 5.11. As happens more often, the use of a log-scale may lead to a distorted look on reality.

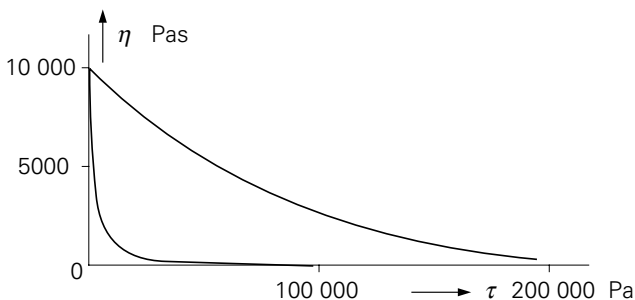


Figure 5.11. Where is the “Newtonian region”?

To represent the non-Newtonian behaviour of polymers in a formula, the “power-law” is often used

$$\tau = k \cdot (\dot{\gamma})^n$$

The exponent, n , the “power-law-index” is $n = 1$ for Newtonian behaviour, and $n < 1$ for *pseudoplasticity*. The apparent viscosity is then given by:

$$\eta = \tau / \dot{\gamma} = k \cdot (\dot{\gamma})^{n-1}$$

or by

$$\eta = k^{1/n} \cdot \tau^{(n-1)/n}$$

These expressions provide a reasonable approximation in the region where the curves, as e.g. in Figure 5.10, do not deviate too much from a straight line, so with A above 1 sec^{-1} or $\tau > 3000 \text{ Pa}$. For lower values the power-law fails, in particular because the viscosity for $\tau = 0$ or $\dot{\gamma} = 0$ would become infinitely high. Various other approximations have been proposed to meet this objection; when calculating the flow in a processing machine, one chooses the formula which gives the best fit in the relevant range of stresses.

The *temperature dependence* of viscosity is often expressed by an Arrhenius equation:

$$\eta = A \cdot \exp(E/RT)$$

In practice, most polymers vary by a factor between 1.5 and 5 over a temperature difference of $30 \text{ }^\circ\text{C}$. With non-Newtonian behaviour it is important how the temperature dependence, e.g. the value of the energy of activation E , is defined, namely for constant shear stress or for constant shear rate. Constant stress τ gives, in general, a more constant value for E , since the $\log \eta - \log \tau$ curves shifts, upon temperature change, in the vertical direction (just as with a change in M), whereas, with constant $\dot{\gamma}$ the pattern is more deformed (see Figure 5.12).

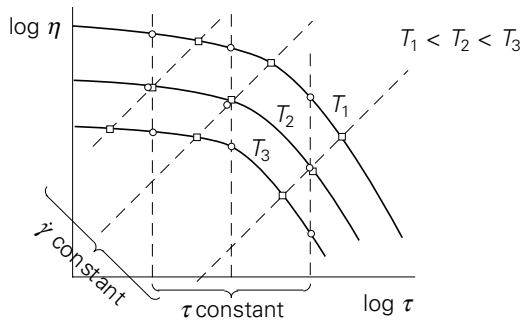


Figure 5.12. Temperature dependence of viscosity.

The deviation from Newtonian behaviour described above can also be related to the *melt elasticity* (see § 5.3.3), since this is a rubber-elasticity, which results from an

entropy decrease when the most probable, chaotic shape of the chain is transformed by orientation into a cigar-shaped one. These chains slide more easily along each other in a shear field because their mutual entanglements are decreased, which results in a lower viscosity.

When does this process start to play a significant role? When the relaxation time of such an elastic deformation exceeds the time scale at which the deformation takes place, which is the reciprocal shear rate $1/\dot{\gamma}$. We have seen before that for a number of similar polymers with the same shape of molecular mass distribution, the deviation from Newtonian behaviour starts with the same value of the shear stress, thus (according to $\dot{\gamma} = \tau/\eta$) at values of $\dot{\gamma}$ which are inversely proportional to the (zero)viscosity η . It seems plausible to suppose that (again with similar mol mass distributions) the relaxation time of the elastic deformation is proportional to the viscosity (see also next section), so that the above mentioned observation is explained.

With a broader mol mass distribution, \bar{M}_z en \bar{M}_{z+1} will increase at the same \bar{M}_w , and, therefore, the elastic response will become more pronounced. This means: a longer relaxation time and a lower value of $\dot{\gamma}$ (and of τ) at which the apparent viscosity decreases. The $\log \eta - \log \tau$ curve is then shifted to the left.

In fact, we have to speak of a spectrum of relaxation times (see, e.g. Figure 6.8), in which the value of $\dot{\gamma}$ at which the first deviation from Newtonian behaviour appears, is a (reciprocal) measure of the longest relaxation time.

5.3.3. Melt elasticity

As discussed before (§ 5.2), a molten polymer shows also elastic behaviour, particularly on a short time-scale: the fluid is visco-elastic. This can, in a simple experiment, be demonstrated in two ways. When we let a bar rotate around its axis in a viscoelastic fluid, then, after removal of the driving torque, it will rotate back over a certain angle. Moreover the fluid will, during rotation, creep upward along the bar, which indicates the existence of normal stresses next to shear stresses.

The elastic behaviour is more strongly pronounced with higher molar mass; higher averages, as \bar{M}_z and \bar{M}_{z+1} , play the most important role; the longest chains more or less tie the other chains together.

5.4. Some consequences for processing

Most processing techniques are carried out in the fluid phase. Here the melt viscosity is the most important parameter. Often this is expressed as the melt index (m.i., see §§ 2.2.3 and 5.3.1), which is a measure for the reciprocal viscosity for a given value

of shear stress. A higher m.i., so a lower viscosity, indicates a better processability. This is, e.g. evident for injection moulding, where for longer flow paths grades with a higher melt-index are being recommended, and for film extrusion, where a higher melt index enables the production of thinner films. An example of the latter case is given in Figure 5.13, derived from a list of PE-grades supplied by DSM, in which the minimum attainable film thickness is plotted against the melt-index. The grades indicated as 1 and 3 do not fit into the pattern; this will be discussed later on

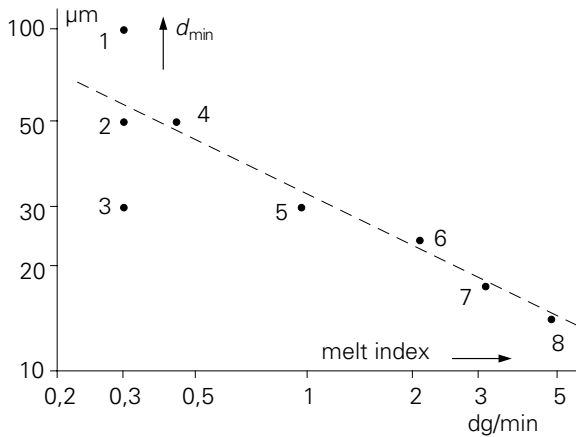


Figure 5.13. Minimum film thickness as a function of melt-index.

The melt-index is merely a one-point determination of the flow behaviour and is not a sufficient criterion in comparing grades with different molar mass distribution. This is apparent from Figure 5.10 and also from Figure 5.14, in which two grades of the same polymer with the same melt index but with different MMD are schematically represented. The curves intersect at the shear stress which is present in the melt-index measuring device ($2 \cdot 10^4$ Pa). A has a higher \bar{M}_w but a broader distribution. For injection moulding A is more attractive, since the mould filling process in injection moulding takes place at very high rates of shear. The more strongly pronounced elastic behaviour, however, increases the risk of frozen-in (rubberelastic) deformations, resulting in anisotropy, and, therefore, in poor stability of shape and dimensions, and in brittleness at the point of injection. The latter is due to the fact that the strength perpendicular to the orientation direction is lower.

Type B in Figure 5.14 is typically suited for rotational moulding. The stresses and the shear rates in this process are very low: after heating the particles flow together under the influence of their own weight and surface tension only, so that the zero-shear viscosity should be as low as possible. For a given melt index this means a narrow MMD. This also implies that, for a given \bar{M}_w (which governs the viscosity), \bar{M}_n is higher. Properties which are highly desirable for rotation moulded articles, such as a good impact strength and a high resistance against environmental stress

cracking, largely depend on the number of chain ends and thus on \bar{M}_n .

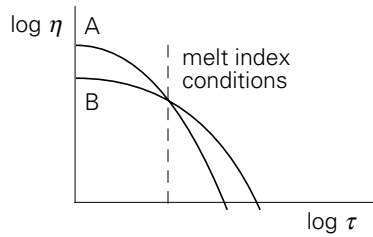


Figure 5.14. Two grades with the same melt index.

Transportation of a molten polymer through a converging channel, e.g. with extrusion, goes accompanied with elongational flow; when the rate of elongation is high, next to the viscous deformation also a considerable elastic component may be present. After the polymer leaves the channel, the elastic deformation will spontaneously recover, which is apparent as an increase in diameter of the extrudate, the so-called *die-swell*.

The rubber-elastic deformation of the liquid stream can reach such high values that the liquid breaks. Though the remaining fragments will stick together in a further part of the die channel, this “melt fracture” forms a notorious limitation in the rate of production with extrusion processes. The only remedy is to increase the time scale of deformation, so that the elastic behaviour is less outspoken.

Rapid production in e.g. injection moulding, requires a high rate of cooling from the melt; when the melt is still deformed in a rubberelastic way, these deformations are frozen-in as chain orientations and they give rise to anisotropy in the properties of the end product. On the other hand, the freezing-in of orientations is utilized in the production of fibres and oriented films; freezing-in is, in these cases, achieved by crystallization. Besides the improvement in strength and stiffness, brought about by these orientations, they may be applied in shrinkage films for packaging purposes. The lower the melt index, the better the polymer is suitable for this purpose. One of the deviating points (3) in Figure 5.13, denoting a grade with an extra low minimum film thickness, belongs to a grade with an extra broad MMD; its flow is better than would be expected from its melt-index and its elastic behaviour is more strongly pronounced; it is not surprising that this grade is specially recommended for shrinkage film. The other deviating point in Figure 5.13 (1) probably has an extra narrow MMD, as estimated from its poorer flow for a given melt index. This grade is recommended for its very high tear strength and toughness, which are, in particular, controlled by \bar{M}_n . Here again, the information provided can be joined together into a simple pattern!

Another example concerns polycarbonate PC. Here also grades of several levels of M

are available. Of actual importance is the type with the lowest M , with the lowest melt viscosity, for the manufacture of compact discs, where extremely fine reproduction of details is required. The low M is also responsible for the lowest possible frozen-in (rubberelastic) deformations; this is essential to reduce the optical anisotropy, the *birefringence*, which is catastrophic for the quality. The impact strength is certainly not promoted by the choice of a low M grade, but PC has such an exceptionally high impact strength that this does not form an objection.

A clear example of the effect of orientations during flow is the injection moulding behaviour of rubbers with a stereospecific chain structure such as NR and IR. These rubbers can, when under strain, crystallize spontaneously (which is very useful for the properties of the vulcanizate, see § 4.5). In a processing operation, such as injection moulding, this phenomenon may, however, play a negative role; orientation-induced crystallization in the converging channel may cause an intolerable increase of viscosity (Figure 5.15). With natural rubber, NR, (100% cis) injection-moulding is, therefore, much more difficult than with a synthetic isoprene rubber (IR) with, e.g., 92% cis content. In practice, for such an IR only about 40 % of the injection pressure needed for NR suffices.

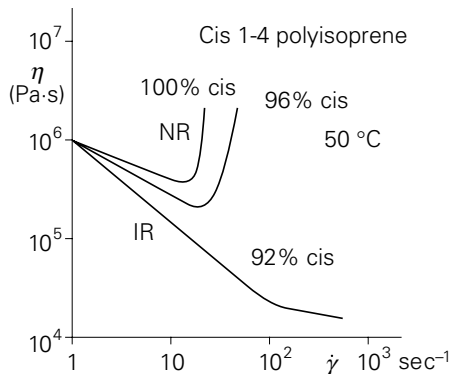


Figure 5.15. The flow behaviour is affected by crystallization.

Some processing operations are mainly carried out in the rubbery phase. With sheet forming, such as vacuum forming, the sheet should possess rubbery properties to be manageable on the machine. Consequently, the deformation is partly or wholly rubberelastic, which can be easily demonstrated by complete recovery to the initial shape after heating to above T_g (or T_m). With calendaring we have a similar situation: for taking-off the sheet from the last roll a pronounced rubberelastic behaviour is essential. The processability with these techniques, therefore, depends on the length of the rubbery region on the temperature scale. Amorphous polymers do not offer any problem; for crystalline polymers the rubbery region is partly or wholly masked by the crystallinity (see § 4.5). Only with high molar masses may such polymers,

such as PE and PP, be vacuum formed under strictly controlled temperature conditions; for polyamides and polyesters, however, the chains are not long enough.

6

Visco-elasticity

6.1. Models

The expression “*visco-elastic*” signifies the dual nature of a material: on the one hand it behaves in a viscous way, as a liquid, on the other hand elastically, as a solid.

For an *ideal solid*, *Hooke’s law* holds: the stress, σ , applied is proportional to the deformation, ε , and the proportionality constant is the *modulus of elasticity* E , so $\sigma = E \cdot \varepsilon$. Besides E also other quantities play a role, such as the shear modulus, G , in a shearing deformation or torsion, which is related to E . For the sake of simplicity we shall mainly use E as a representative quantity for the elastic stiffness in any geometry of loading.

As a model for E we take a helical spring with stiffness E . The response ε of such a spring to a stress σ is schematically indicated in Figure 6.1; the response is instantaneous, without any time dependency, and the recovery after release of the stress is also instantaneous and complete.

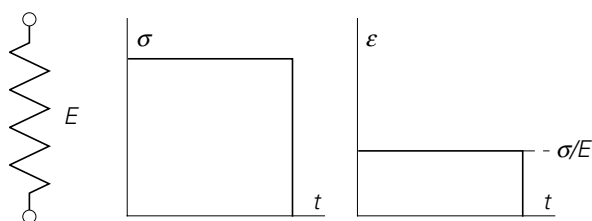


Figure 6.1. Response of an ideal spring.

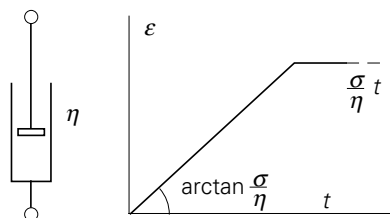


Figure 6.2. Response of an ideal liquid.

For an ideal liquid *Newton’s law* holds: the stress is proportional to the rate of

deformation $d\varepsilon/dt = \dot{\varepsilon}$; the proportionality constant is the *viscosity* η , so $\sigma = \eta \cdot \dot{\varepsilon}$. As a model we choose a *dashpot*; within a cylinder filled with a fluid a piston can move with some clearance. Figure 6.2 shows its behaviour: There is no instantaneous response; the deformation is proportional to time, and no recovery takes place. The dashpot is characterized by η .

For viscoelastic materials combinations of these two models can be used, e.g. a spring and a dashpot in series or parallel. The first combination is called the *Maxwell element*; its response under constant stress is the sum of that of its two components:

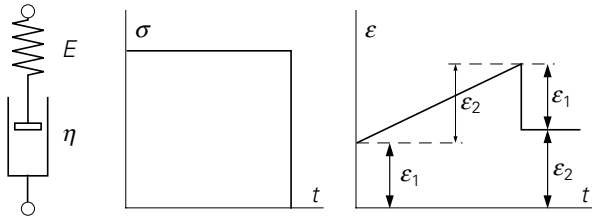


Figure 6.3. Response of a Maxwell element.

$$\varepsilon = \varepsilon_1 + \varepsilon_2 = \frac{\sigma}{E} + \frac{\sigma}{\eta} \cdot t = \sigma \left[\frac{1}{E} + \frac{t}{\eta} \right]$$

i.e. a spontaneous elastic deformation which returns when $\sigma = 0$, plus permanent flow. This element might, very roughly, represent the behaviour of a molten polymer, since we have seen that, besides the normal fluid behaviour, also an elastic component is present, which recovers upon unloading.

Next to this case of *creep* under constant loading, we also consider the *stress relaxation* which occurs when the deformation is kept constant. At $t = 0$ the model is jumpwise deformed to a strain ε . The instantaneous response is a stress $\sigma_0 = E \cdot \varepsilon$; the spring is strained, the dashpot does not yet respond. The dashpot is, at $t = 0$, subjected to the same stress, so it starts flowing, while it takes over an increasing part of the imposed strain so that the strain in the spring, and also the stress, decrease.

At time t the deformation of the spring is ε_1 and that of the dashpot ε_2 , while the stress in both $\sigma_1 = \sigma_2$. Now

$$\sigma_1 = E \cdot \varepsilon_1 = \sigma_2 = \eta \frac{d\varepsilon_2}{dt} = \eta \frac{d(\varepsilon - \varepsilon_1)}{dt} = -\eta \frac{d\varepsilon_1}{dt}$$

since

$$\varepsilon_1 + \varepsilon_2 = \varepsilon$$

$$-\eta \frac{d\varepsilon_1}{dt} = E \cdot \varepsilon_1$$

$$\frac{d\varepsilon_1}{\varepsilon_1} = -\frac{E}{\eta} dt$$

$$\ln \varepsilon_1 = -\frac{E}{\eta} \cdot t + c$$

$$\varepsilon_1 = \exp(-(E/\eta) \cdot t) \cdot c'$$

$$\sigma = E \cdot \varepsilon_1 = E \cdot \exp(-(E/\eta) \cdot t) \cdot c'$$

At $t = 0$ is $\sigma = E \cdot \varepsilon$, so $\sigma(t) = E \cdot \varepsilon \cdot \exp(-(E/\eta) \cdot t) = E \cdot \varepsilon \cdot \exp(-t/\tau)$ in which $\tau = \eta/E$, the *relaxation time*. The relaxation time, as indicated in Figure 6.4, is the time in which the stress is reduced to $1/e$ times its original value (about 37%). (See also Qu. 6.2 and 6.11).

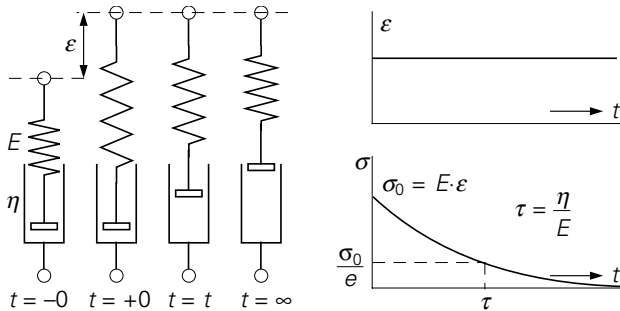


Figure 6.4. Stress relaxation of a Maxwell element.

A parallel array of E and h gives a *Kelvin-Voigt* element. This model does not allow an instantaneous deformation (the stress on the dashpot would be infinite), and it does not show stress relaxation. At a constant stress it exhibits *creep*; at time t its strain is $\varepsilon(t)$; the stress in the spring then is:

$$\sigma_1 = E \cdot \varepsilon(t)$$

in the dashpot

$$\sigma_2 = \eta \cdot \frac{d\varepsilon(t)}{dt}$$

and the total stress, $\sigma_1 + \sigma_2 = \sigma$ is constant.

$$\sigma = E \cdot \varepsilon + \eta \frac{d\varepsilon}{dt}$$

$$\eta \frac{d\varepsilon}{dt} = -E \cdot \varepsilon + \sigma$$

The solution of this differential equation is:

$$\varepsilon(t) = \frac{\sigma}{E} \left[1 - \exp(-t/\tau) \right]$$

with $\tau = \eta/E$.

At $t = 0$, $\varepsilon = 0$; at $t = \infty$, $\varepsilon = \sigma/E$; this final deformation is approached asymptotically. After taking away the stress at a new $t = 0$, while $\varepsilon = \varepsilon_1$, it follows from:

$$\sigma = 0 = E \cdot \varepsilon + \eta \frac{d\varepsilon}{dt}$$

and

$$\eta \frac{d\varepsilon}{dt} = -E \cdot \varepsilon$$

$$\varepsilon = \varepsilon_1 \exp(-t/\tau)$$

in other words: the recovery proceeds asymptotically to $\varepsilon = 0$ with the same relaxation time $\tau = \eta/E$; see Figure 6.5. (see also Qu. 6.5).

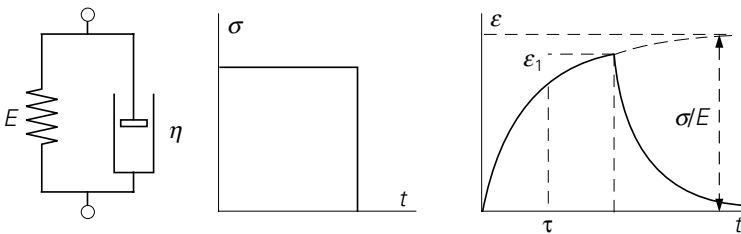


Figure 6.5. Creep of a Kelvin-Voigt element

Both models, the Maxwell element and the Kelvin-Voigt element, are limited in their representation of the actual viscoelastic behaviour; the former is able to describe stress relaxation, but only irreversible flow; the latter can represent creep, but without instantaneous deformation, and it cannot account for stress relaxation. A combination of both elements, the *Burgers* model, offers more possibilities. It is well suited for a qualitative description of creep. We can think it as composed of a spring E_1 , in series with a Kelvin-Voigt element with E_2 and η_2 , and with a dashpot, η_1

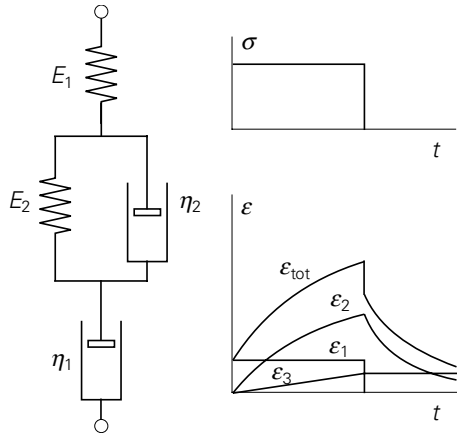


Figure 6.6. Creep of the Burgers model.

(Figure 6.6).

Under a constant load σ we can distinguish between three types of deformation:

- the spring: $\epsilon_1 = \sigma/E_1$
- the Kelvin-Voigt element: $\epsilon_2 = \sigma/E_2 \cdot [1 - \exp(-E_2 \cdot t/\eta_2)]$
- the dashpot: $\epsilon_3 = \sigma \cdot (t/\eta_1)$.

The total deformation is:

$$\epsilon = \sigma \left[\frac{1}{E_1} + \frac{1}{E_2} \left(1 - \exp(-t/\tau) \right) + \frac{t}{\eta_1} \right]$$

$$\tau = \frac{\eta_2}{E_2}$$

which means

- spontaneous elastic deformation,
- delayed elastic deformation, or reversible creep,
- irreversible creep (flow) (see also Qu. 6.7 en 6.8).

The models described so far provide a *qualitative illustration* of the viscoelastic behaviour of polymers. In that respect the Maxwell element is the most suited to represent fluid polymers: the permanent flow predominates on the longer term, while the short-term response is elastic. The Kelvin-Voigt element, with an added spring and, if necessary, a dashpot, is better suited to describe the nature of a solid polymer. With later analysis of the creep of polymers, we shall, therefore, meet the Kelvin-Voigt model again; in more detailed descriptions of the fluid state the Maxwell model is being used.

In a quantitative way, these simple models are not powerful enough to account for the behaviour of a real polymer. One of their prime shortcomings is, that they describe processes with a *single relaxation time* only. To illustrate this, we consider the stress relaxation of a Maxwell model. In a σ - $\log t$ plot (Figure 6.7) the stress relaxation curves for three different values of the relaxation time have been indicated; with this way of plotting the three curves have the same shape and are shifted with respect to the $\log t$ axis. Also a more realistic relaxation curve is drawn, which extends over a much broader region of the $\log t$ scale than a single element.

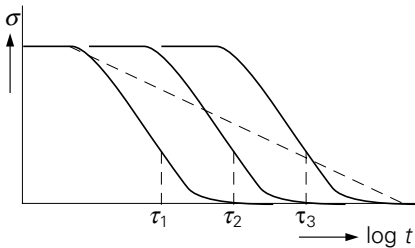


Figure 6.7. Relaxation of three single Maxwell elements compared with actual behaviour.

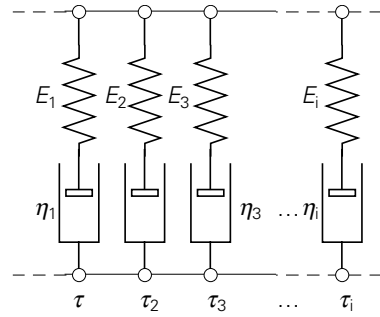


Figure 6.8 Generalized Maxwell model.

The reality is better approximated by a “generalized Maxwell model” (Figure 6.8), consisting of a large number of Maxwell elements in parallel, each with its own relaxation time, τ_i , and its own contribution, E_i , to the total stiffness. This system can be described by:

$$\sigma(t) = \varepsilon \cdot E_1 \cdot \exp(-t/\tau_1) + \varepsilon \cdot E_2 \cdot \exp(-t/\tau_2) + \dots + \varepsilon \cdot E_i \cdot \exp(-t/\tau_i)$$

or:

$$\sigma(t) = \varepsilon \cdot \sum_1^n E_i \cdot \exp(-t/\tau_i)$$

A relaxation function is now defined as

$$E(t) = \sum_1^n E_i \cdot \exp(-t/\tau_i)$$

We prefer to use a *continuous spectrum* $H(t)$, the *relaxation spectrum*:

$$E(t) = \int_0^{\infty} H(\tau) \cdot \exp(-t/\tau) \cdot d\tau$$

in which $H(\tau)d\tau$ is the contribution to the stiffness in the interval between τ and $\tau + d\tau$.

In a similar way the creep can be represented by a number of Kelvin-Voigt elements in series:

$$\varepsilon(t) = \frac{\sigma}{E_1} \cdot [1 - \exp(-t/\tau_1)] + \dots + \frac{\sigma}{E_i} \cdot [1 - \exp(-t/\tau_i)] + \dots$$

of

$$\frac{\varepsilon(t)}{\sigma} = \sum_1^n \left[\frac{1}{E_i} \cdot (1 - \exp(-t/\tau_i)) \right]$$

To express creep, use of the reciprocal modulus, the *compliance*, $D = 1/E$, is to be preferred; the creep function then reads:

$$D(t) = \frac{\varepsilon(t)}{\sigma} = \sum_1^n D_i \cdot [1 - \exp(-t/\tau_i)]$$

or, as a continuous spectrum:

$$D(t) = \int_0^{\infty} L(\tau) \cdot [1 - \exp(-t/\tau)] \cdot d\tau$$

The spectrum $L(\tau)$ is called the *retardation spectrum*. With the integration from $\tau = 0$ to $\tau = \infty$ the immediate elastic response and the irreversible flow are, respectively, automatically taken into account.

With all these models, the simple ones as well as the spectra, it has to be supposed that stress and strain are, at any time, proportional, so that the relaxation function $E(t)$ and the creep function $D(t)$ are independent of the levels of deformation and stress, respectively. When this is the case, we have *linear viscoelastic behaviour*. Then the so-called *superposition principle* holds, as formulated by Boltzmann. This describes the effect of changes in external conditions of a viscoelastic system at different points in time. Such a change may be the application of a stress or also an imposed deformation.

The superposition principle states that each change gives its own contribution to a (later) effect, independent of the other changes. This is important, since not only the magnitude of the change, but also the time elapsed to the observation of its effect, influence the magnitude of the effect.

A simple example of the superposition principle is given in Figure 6.9. At $t = t_1$ a stress σ_1 is applied, which is increased to σ_2 at $t = t_2$. The response of the system is

such that the strain from $t = t_2$ is a superposition of the strain as a result of a continuation of σ_1 and the one resulting from a stress $\sigma_2 - \sigma_1$, applied at $t = t_2$.

Expressed in a formula:

$$\varepsilon(t) = \sigma_1 \cdot D(t - t_1) + (\sigma_2 - \sigma_1) \cdot D(t - t_2)$$

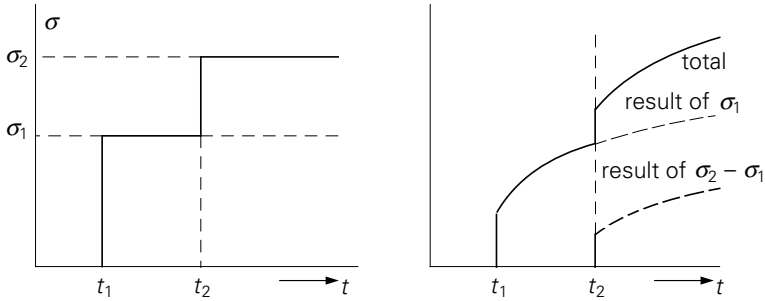


Figure 6.9. Superposition principle.

With an arbitrary, continuously changing stress $\sigma(t)$, this can be written as:

$$\varepsilon(t) = \int_{-\infty}^t D(t - t') \frac{d\sigma}{dt'} \cdot dt'$$

For each small variation in stress $(d\sigma/dt') \cdot dt'$ at $t = t'$, its contribution to the deformation is determined by the pertinent compliance $D(t - t')$.

Later on we shall see that the superposition principle is, for polymers, only seldomly obeyed; linear viscoelasticity is only met at *very small stresses and deformations*; at loading levels occurring in practice the behaviour may strongly deviate from linearity. However, the superposition principle provides a useful first-order approximation.

The functions $E(t)$ and $D(t)$ are of importance for two reasons. First, they provide a first impression of the response of a polymer under stress or strain as a function of time; they are, therefore, of interest when plastics are used in load-bearing constructions.

On the other hand knowledge of these functions and of the spectra of relaxation (or retardation) times derived from them, is very helpful for obtaining insight into the *molecular mechanisms* by which they are originated. Analysis of the time dependency of mechanical properties thus provides a powerful tool to investigate the relations between structure and properties.

Creep and relaxation experiments are carried out on time scales ranging from several

seconds up to several years. When knowledge of the viscoelastic behaviour on shorter time scales is also required, then vibration experiments (dynamic mechanical experiments) have to be carried out.

6.2. Dynamic mechanical behaviour

When a periodic deformation, $\varepsilon = \varepsilon_0 \cdot \sin \omega t$, is imposed upon a purely elastic material, the stress will also be periodic according to $\sigma = \sigma_0 \cdot \sin \omega t$ (the use of a cosine function gives the same results). With viscoelastic materials, however, a *phase shift* δ occurs:

$$\sigma = \sigma_0 \cdot \sin(\omega t + \delta)$$

This can be understood as follows: For an ideal spring $\delta = 0$; for a pure liquid:

$$\sigma = \eta \cdot (d\varepsilon/dt) = \eta \cdot \varepsilon_0 \cdot \omega \cdot \cos \omega t = \sigma_0 \cdot \sin(\omega t + \frac{\pi}{2})$$

then $\delta = \frac{\pi}{2}$ (90°); the stress proceeds in advance of the strain over a quarter of a period. For a viscoelastic material δ is in between these extremes: $0 < \delta < \frac{\pi}{2}$. The equation for σ can be worked out further:

$$\begin{aligned} \sigma &= \sigma_0 \cdot \sin(\omega t + \delta) = \sigma_0 \cdot [\sin \omega t \cdot \cos \delta + \cos \omega t \cdot \sin \delta] = \\ &= (\sigma_0 \cdot \cos \delta) \cdot \sin \omega t + (\sigma_0 \cdot \sin \delta) \cdot \cos \omega t \end{aligned}$$

This equation shows the existence of *two components of the stress*: the first one is in-phase with the deformation, with an amplitude $\sigma_0 \cdot \cos \delta$, the second one has a phase difference of 90° , with an amplitude $\sigma_0 \cdot \sin \delta$.

We can also define two moduli of elasticity σ/ε :

$$E_1 \text{ (in-phase)} = (\sigma_0/\varepsilon_0) \cdot \cos \delta$$

$$E_2 \text{ (90° out-phase)} = (\sigma_0/\varepsilon_0) \cdot \sin \delta$$

and the stress can be written as:

$$\sigma = \varepsilon_0 \cdot (E_1 \cdot \sin \omega t + E_2 \cdot \cos \omega t)$$

while

$$\tan \delta = E_2/E_1$$

Since E_1 is the elastic part of the modulus, it is called the “*storage modulus*”. It is, namely, a measure for the energy stored in a reversible way. E_2 denotes the viscous part, and is thus a measure for the energy dissipated into heat per period of vibration;

it is called “*loss modulus*”.

Periodic vibrations, mechanical as well as electrical, are often represented as a uniform motion along a circle with angular velocity ω . The projection on a horizontal axis carries out a harmonic vibration $r \cdot \cos \omega t$ (Figure 6.10). This can, mathematically, be expressed in a very elegant way by considering the rotating point as a *complex number*:

$$r^* = x + iy \quad (i = \sqrt{-1})$$

x is then the projection on the horizontal axis, varying according to $x = r \cdot \cos \omega t$, and is the real part of the complex number r^* ; iy is the imaginary part. This way of representation is based on the well-known formula:

$$e^{ix} = \cos x + i \cdot \sin x$$

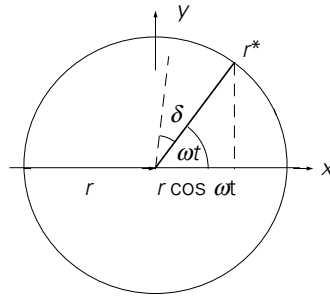


Figure 6.10. Complex representation of a harmonic vibration.

A periodic deformation with amplitude ε_0 is then given by:

$$\varepsilon = \varepsilon_0 \cdot \exp(i\omega t)$$

while we tacitly assume that we consider the real part, $\varepsilon = \varepsilon_0 \cdot \cos \omega t$, only. The expression for the stress then becomes:

$$\sigma = \sigma_0 \cdot \exp i(\omega t + \delta)$$

(by which we mean its real part:

$$\sigma = \sigma_0 \cdot \cos(\omega t + \delta))$$

The phase difference δ is, in the complex plane, the angle between the radius vectors of σ and ε . The E modulus can now easily be written as a *complex quantity*, E^* (Figure 6.11):

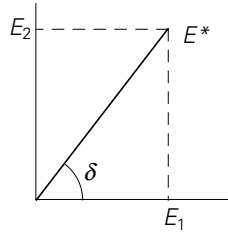


Figure 6.11. Complex modulus of elasticity.

$$E^* = \frac{\sigma}{\varepsilon} = \frac{\sigma_0 \cdot \exp i(\omega t + \delta)}{\varepsilon_0 \cdot \exp i\omega t} = \frac{\sigma_0}{\varepsilon_0} \cdot \exp(i\delta) = \frac{\sigma_0}{\varepsilon_0} \cdot (\cos \delta + i \sin \delta) =$$

$$= \frac{\sigma_0}{\varepsilon_0} \cos \delta + i \frac{\sigma_0}{\varepsilon_0} \sin \delta = E_1 + i \cdot E_2$$

In contrast to σ and ε , E^* retains its nature as a complex quantity, composed of a *storage modulus* (the real part) and a *loss modulus* (the imaginary part).

The use of complex numbers appears to offer considerable advantages in simplifying calculations on vibrating systems. A *damped vibration*, for instance, is represented by:

$$\varepsilon = \varepsilon_0 \cdot \exp(i\omega t) \cdot \exp(-\alpha t) = \varepsilon_0 \cdot \exp(i\omega - \alpha)t$$

This expression is much easier to handle in differentiation etc., since the periodic part, $\exp(i\omega t)$ (which means: $\cos \omega t$) and the damping part $\exp(-\alpha t)$ are combined into a single exponential function.

Various types of vibration experiments can be carried out to measure E_1 and E_2 at a certain frequency. An example is the *torsion pendulum*, in which the sample, connected to an auxiliary mass, is brought into a free torsional oscillation. From the frequency of the pendulum (around 1 to 10 sec) E_1 is calculated, from the rate of damping $\tan \delta$ and E_2 . Other types of dynamic mechanical measurements can be carried out at higher frequencies, such as *bending vibrations* with or without extra mass, wave propagation, etc. By combining a number of these different techniques, a time scale ranging from 10 to 10^{-8} sec can be covered.

6.3. Integration

In combination with creep and relaxation measurements a total time span of $\approx 10^{-8}$ sec to 10^8 sec (3 years) can be covered. The usual techniques to measure the response of a polymer over this time span are schematically represented in Figure 6.12.

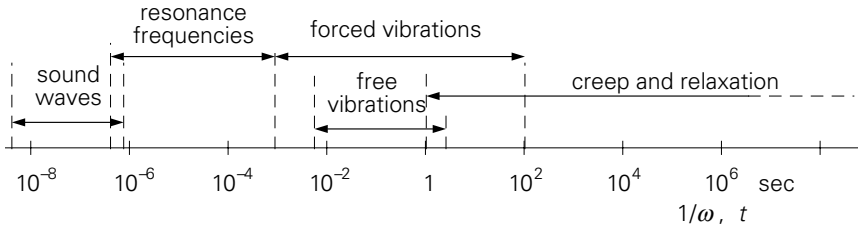


Figure 6.12. Time and frequency span for various methods.

When we try to combine the results of these various methods into a single integrated picture, we have to take into account three points:

- With some experiments a *stress is imposed*, such as with creep tests and with vibrations in which the sample is subjected to a periodic stress. With other experiments the *deformation is given* and the resulting stress is being measured, such as with stress relaxation and with vibration tests with an imposed periodic strain. The results of these two different types of methods cannot directly be translated into each other but only by complex transformations, in other words:

$$D(t) \neq \frac{1}{E(t)}$$

- In various experiments *different elastic constants* are being determined; with a torsion pendulum, for instance, the shear modulus, G , is measured, with creep or vibrations in elongation or in bending the Young's modulus, (tensile modulus), E . For an isotropic material the relation between E and G is as follows:

$$E = 2 \cdot G \cdot (1 + \nu)$$

in which ν is the Poisson ratio, or the ratio between transverse contraction and elongation in uniaxial strain. For ideal rubbers (no volume change upon elongation), $\nu = 0.5$; for glassy polymers and polymer crystals $\nu \approx 0.33$, so that E/G is in between 3 and 2.7. Complications arise when the transverse contraction in one direction is hindered, for instance with forced vibrations of a sheet; in such a case not E is measured but $E/(1 - \nu^2)$. Moreover, the Poisson ratio also depends on time or frequency.

- In the third place the question arises how the *time and frequency scales* have to be joined together to connect results of creep or relaxation to those of vibration experiments. It will be clear that here the superposition principle can be applied, since with vibrations the imposed stress (or the strain) varies continuously. Using this principle and using the complex E modulus (or the complex compliance D), it can be shown that, with a few simplifications, t and $1/\omega$ can be considered as the same parameter, while $\omega = 2\pi\nu$ (ν is the frequency in cycles/sec). It has been

shown that in this way static and dynamic experimental results can be joined together satisfactorily.

Many measurements have been carried out with a large number of, sometimes very complicated, techniques. A shorter route towards a global knowledge over such a broad range of time and frequency, is supplied by the overall *equivalence of time and temperature*. In its simplest form, this equivalence can be expressed via the assumption that the effect of temperature on a molecular process often follows Arrhenius' law:

$$\tau = c \cdot \exp(A/RT)$$

in which τ is the relaxation time of such a process. Also the frequently used model representations with springs and dashpots lead to this equation: If we suppose the spring constants, E , to be independent of temperature, and the viscosities η as $\eta = c' \exp(U/kT)$ (which is the usual behaviour of a viscosity), then the relaxation time is

$$\tau = \frac{\eta}{E} = \frac{c'}{E} \exp(U/kT) \quad (= c \cdot \exp(A/RT))$$

With an increase in temperature from T_0 to T the modulus curve will then be *shifted* along the $\log t$ axis over a distance:

$$\ln a_T = \frac{A}{R} \cdot \left(\frac{1}{T} - \frac{1}{T_0} \right)$$

in which the quantity a_T is defined as:

$$a_T = \frac{t_{\text{rel}}(T)}{t_{\text{rel}}(T_0)} \quad (\text{Figure 6.13}).$$

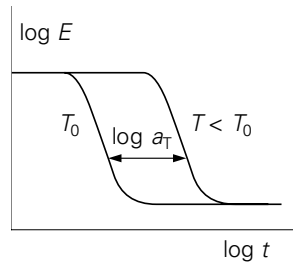


Figure 6.13. Time-temperature shift.

This offers the possibility to carry out measurements in a limited interval of $\log t$ (of $\log \omega$) at several levels of temperature, to derive the shift factor $a_T(T)$ from the results, and to construct a *master curve* over a broad range of $\log \omega$. This is

illustrated in Figure 6.14.

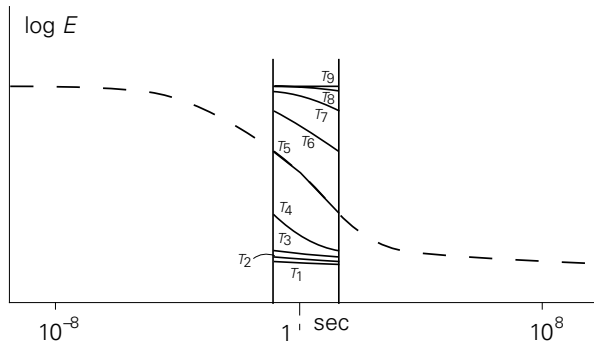


Figure 6.14. 'Mastercurve'.

Along the routes described thus far, it is possible to characterize E and its both components E_1 and E_2 , either in the complete, elaborate way or via the short-cut using the t - T relation, over a broad region of $\log t$ ($\log \omega$). A general schematic picture of E_1 and E_2 as functions of frequency or time is given in Figure 6.15. Generally speaking, *two maxima* in E_2 occur, corresponding to two transitions in E_1 . Next to these main transitions, a number of secondary transitions may be present. These are, however, not adequately represented in the resulting curve from a $\log t - T$ shift, which provides, therefore, despite of its simplicity, a very limited overall view only.

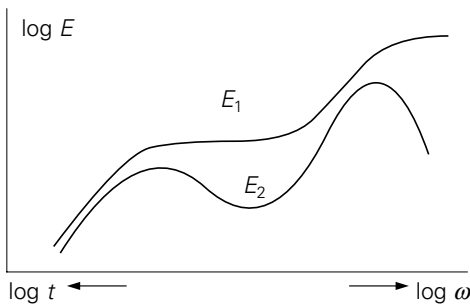


Figure 6.15. Two relaxation mechanisms.

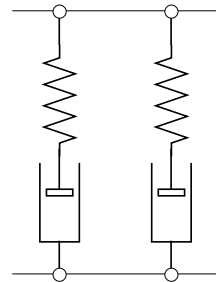


Figure 6.16. Two (broad) Maxwell elements.'

The pattern in Figure 6.15, read from the right to the left on the $\log t$ scale, resembles the relaxation behaviour, the decrease of E with increasing time under a constant strain, for two Maxwell elements in parallel (Figure 6.16), though over a much broader interval of $\log t$. It could, therefore, be considered as the behaviour of *two broad clusters of Maxwell elements*. The $\log E$ - $\log \omega$ curve thus indicates the existence of two broad relaxation mechanisms, each with a spectrum of relaxation

times. This general picture is shown by all polymers, except by *permanent networks*, where the left-hand (low ω , long t) mechanism is not present.

After what has been said about the T - t equivalence, it is not surprising that the time dependency of E_1 resembles the T -dependency, which we have considered in detail before. In $E(\log t)$ we see, indeed, the same phases and transitions as in $E(T)$ (Figure 6.17). It should be remarked that this *time-temperature equivalence* only holds for *amorphous polymers* or for the amorphous part in semi-crystalline polymers.

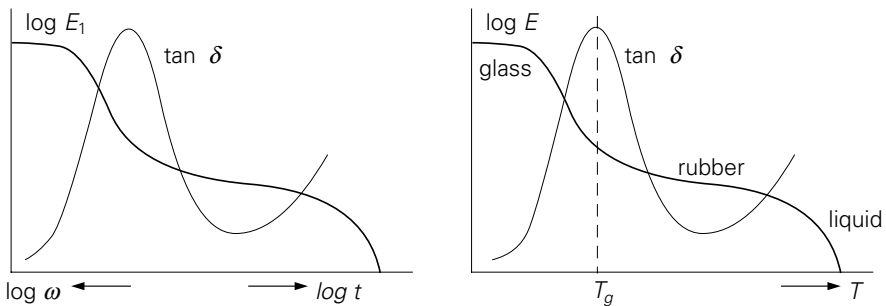


Figure 6.17. Comparison of time- and temperature scale.

In practice, $E(T)$ can be determined in a much easier way than $E(t)$; it can be done with a single device, e.g. a torsional pendulum, or its modern equivalent, DMTA, at an about constant frequency. The glass-rubber transition covers some tens of degrees on the T -scale; on the time scale it extends over many decades.

Both E_2 and $\tan \delta$ show *maxima* in the regions where E_1 strongly changes. This can be understood as follows: At very high frequencies, thus in the glassy region, the chain motions are so small that they hardly give rise to energy losses (in spring-dashpot models: the dashpot hardly moves and the whole deformation is taken up by the spring). At very low frequencies, e.g. in the rubbery region, losses also hardly occur; though the viscosity plays a role, the rates of deformation are so small that the energy dissipation is low. In between, in the transition region, these extreme situations do not exist, and the damping, the energy dissipated per cycle, shows a maximum.

7

Mechanical properties

7.1. Stress-strain diagram

A simple representation of a number of mechanical properties is given by the *stress-strain diagram*. Such a diagram can be produced in a tensile test, in which the force is recorded as a function of the elongation, which increases at a constant rate. The force is divided by the initial cross-sectional area, and the strain by the initial length, so that a stress-strain curve is obtained, which is independent of the geometry of the sample. Besides in elongation, the sample can also be deformed in bending, in compression or in torsion; this leads to different diagrams which are, as a matter of fact, related to each other.

A schematic example of a stress-strain diagram is given in Figure 7.1. From this curve the following properties can be read off: The modulus of elasticity is the slope of the first, approximately straight part of the curve. Here the relation $E = \sigma/\epsilon$ is valid, or, with an initially curved line, $E_0 = (d\sigma/d\epsilon)$ for $\epsilon = 0$. To define the modulus at a higher value of strain, ϵ_1 , the secant modulus $E_s = \sigma_1/\epsilon_1$ can be taken, or the tangent modulus $E_t = (d\sigma/d\epsilon)$ for $\epsilon = \epsilon_1$ (see Qu. 7.1).

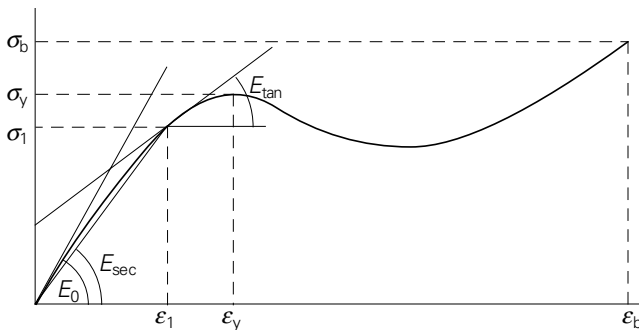


Figure 7.1. Stress-strain diagram.

Often the material shows a *yield point* at a certain stress, the yield stress σ_y ; the stress increases only slowly from this point or may even decrease. In fact the material already fails at this yield stress; actual fracture occurs at a somewhat higher stress σ_b and a considerably higher strain ϵ_b . The total area under the curve is the work required per unit volume to break the material, and is a measure for its

toughness.

We can rank the polymers according to the levels of the various properties: stiff or soft, tough or brittle, strong or weak plastics (see Figure 7.2).

The forces are expressed in newton (N), the stresses and moduli of elasticity in $\text{N/m}^2 = \text{Pa}$ (pascal), also in $\text{MPa} = 10^6 \text{ N/m}^2 = \text{N/mm}^2$ or in $\text{GPa} = 10^9 \text{ Pa}$.

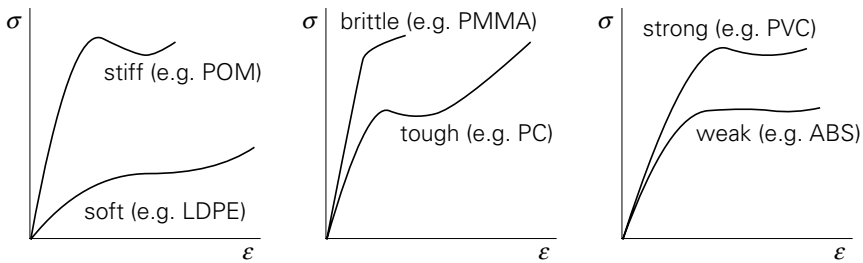


Figure 7.2 Various types of stress-strain diagrams.

7.2. Stiffness and creep

7.2.1. Modulus of elasticity

In general the stiffness of plastics is lower than that of other materials. Figure 7.3 gives (left) a schematical survey of the moduli of a number of materials. As a matter of fact, rubbers are the lowest. The thermoplastics show a broad spectrum of moduli, ranging from the softer types as PE, PP, polyamides, fluor polymers and cellulose plastics, up to a bigger group of harder ones in the region of 2 to 4 GPa. Thermosets are slightly higher in stiffness.

The gap between rubbers and the softer thermoplastics is being bridged more and more by the *thermoplastic elastomers*, TPE's (not indicated in Figure 7.3, but later, in Figure 7.27); the stiffness of these block copolymers can be adjusted by the choice of block type and block length ratio.

Plastics compare more favourably with other materials if the stiffness per unit mass is considered, or the *modulus of elasticity divided by the specific mass*. This is demonstrated by the right hand side of Figure 7.3; as a result of the lower density of polymers the values are closer to each other; an advanced composite now amply exceeds steel!

In comparing the E-values of the various polymers, the best starting point is formed by amorphous polymers in the glassy state; for this group E is mostly about 3 to 3.2 GPa (e.g. PVC, PS, PMMA), except when, below room temperature, a secondary transition occurs, such as with PC $E \approx 2.1 \text{ GPa}$).

Higher values can be reached for semi-crystalline polymers below T_g ; the crystalline phase is stiffer than the glassy amorphous phase (e.g. PEEK, $E \approx 4$ GPa). Semi-crystalline polymers above T_g have, however, a much lower E -value, such as PE (0.15 to 1.4 GPa) and PP (≈ 1.3 GPa); E is, in these cases, strongly dependent on the *degree of crystallinity* and on the distance to T_g . Sometimes a low modulus is also found for semi-crystalline polymers below T_g , due to the effect of one or more secondary transitions; a strong example is PTFE ($E \approx 0.6$ GPa!).

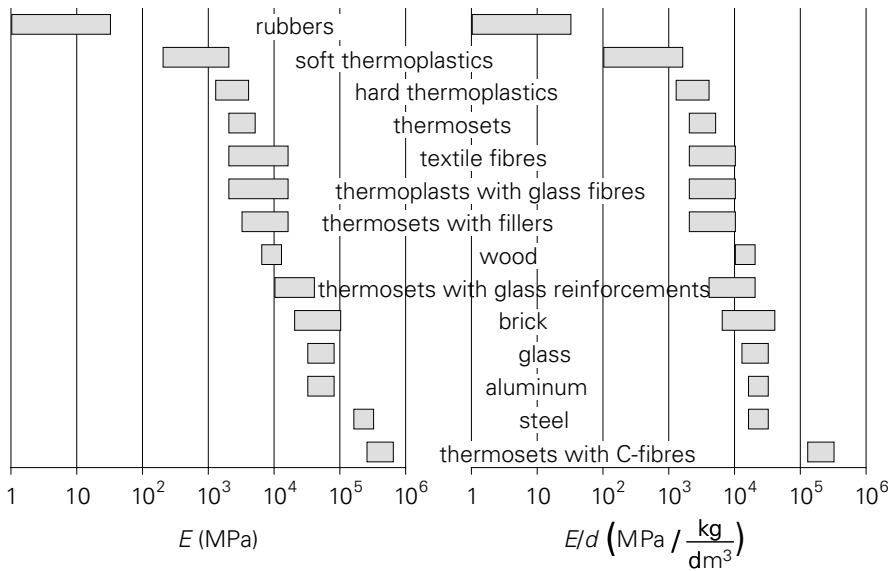


Figure 7.3. Absolute and reduced moduli of elasticity.

Higher values for E also occur with strongly *cross-linked systems* (thermosets); an example is an unfilled epoxy resin with an E -modulus higher than 4 GPa.

A special category is formed by *oriented polymers*, which have considerably higher stiffnesses. The most obvious example is the textile fibre; the orientation, frozen-in in a crystalline structure, raises E by a factor of 3 to 5. Extremely high orientations, as met in *liquid-crystal polymers (LCP's)* result in even higher E -values, namely 60 to 120 GPa!

A higher stiffness is also obtained by the incorporation of *hard particles* or *short fibres*. Particles are responsible for a 2 to 2.5 fold increase in E , while with short glass fibres a factor of 3 to 5 can be obtained. Long fibres, forming a continuous reinforcing phase, produce a much stronger effect; here the fibres practically carry the whole stress, while the matrix polymer has hardly any influence on the stiffness.

Finally, a few factors should be mentioned which do *not* influence the modulus. The

first is the *chain length* (molar mass) and its distribution. E is independent of M , unless, with semi-crystalline polymers, longer chains are responsible for a somewhat lower degree of crystallinity (e.g. with ultra-high molecular PE); in such a case E slightly decreases with increasing M .

E is also independent of *chain stiffness* and *chain interactions*; these factors play a role in the height of the glass-rubber transition temperature and the melting point. A stiffer chain, therefore, does not result in a stiffer polymer; except, sometimes, in an indirect way, namely when stiff chains enable the formation of high orientation, such as in liquid-crystalline polymers (see § 4.6).

7.2.2. Creep

We should realize that the values of the moduli of elasticity, as discussed so far, are *only applicable to short-term loading situations*. The *creep*, already mentioned several times before, renders these values unsuitable to characterize the behaviour of a polymer under stress over a longer time. In § 4.5 we already met the example of two polymers, where POM, at a certain stress, initially deforms less than PC, but, later on, its deformation exceeds that of PC.

The usual way in which the deformation changes with time, has been dealt with in § 6.1. The best representation appeared to be a Maxwell element with a Kelvin-Voigt element in series; the deformation is then composed of three components: an immediate elastic strain, which recovers spontaneously after removal of the load, a delayed elastic strain which gradually recovers, and a permanent strain. Moreover, we noticed that a single retardation time (a single Kelvin-Voigt element) is not sufficient: we need to introduce *a spectrum*:

$$D(t) = \int_0^{\infty} L(\tau) \cdot [1 - \exp(-t/\tau)] d\tau$$

Creep curves can also be represented by *empirical equations*, such as

$$D(t) = a + b \cdot t^{1/3} \quad (\text{Andrade})$$

or

$$D(t) = D_0 \cdot \exp(t/t_0)^m \quad (\text{Kohlrausch, 1866, glass})$$

The second equation appears to be applicable to a number of glassy polymers, and also to other materials; the exponent m is always about $\frac{1}{3}$, so that creep can be described by two parameters, D_0 and t_0 , while the immediate elastic deformation is also taken into account (D_0). As a matter of fact, D_0 and t_0 are temperature dependent. When the experimentally found creep curves are shifted along the horizontal axis and (slightly) along the vertical axis, they can be made to coincide

into a mastercurve, which signifies the validity of a time-temperature superposition principle (see also Qu. 7.10).

An example of such a shift is given in Figure 7.4 as creep curves of PVC, measured up to 1000 sec at temperatures ranging from 20° to 70 °C (Struik). The curves can easily be shifted into a mastercurve, shown in the figure at 20 °C. It is tempting to use this mastercurve for predicting the long-term creep; in § 7.2.4 we shall, however, see that this is not allowed!

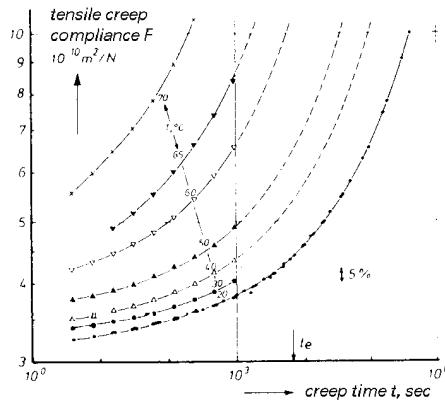


Figure 7.4 Creep of PVC as a function of temperature (both figures taken from L.C.E.Struik, thesis, Delft 1977).

The analogy in the creep behaviour of various (glassy) polymers and other substances is illustrated in Figure 7.5; on each material measurements have been carried out over a broad range of temperatures, and all results coincide, after shifting, into a *master curve* with the equation:

$$D(t) = D_0 \cdot \exp(t/t_0)^{1/3}$$

For practical use, this representation with two parameters is, however, not sufficient, due to other complications in creep behaviour, namely:

- non-linearity
- physical ageing,

In the following paragraphs these complications will be discussed.

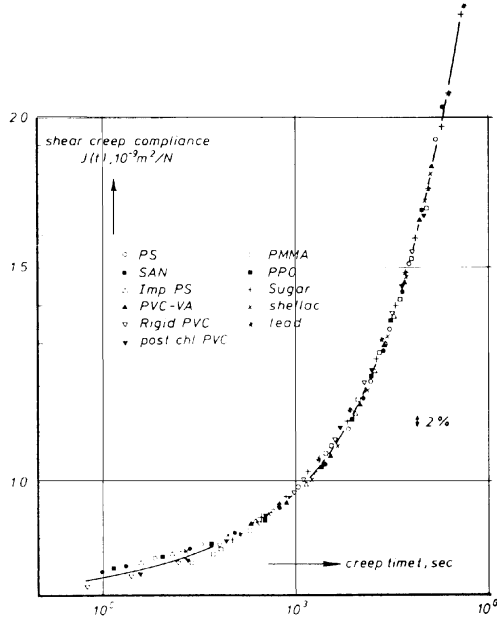


Figure 7.5. Creep mastercurve for a number of materials.

7.2.3. Non-linearity

The reduced creep curves in Figure 7.6 (ϵ/σ or $D(t)$) should coincide if Boltzmann’s superposition principle would hold; for each level of stress, $D(t)$ should be the same. However, creep behaviour is *non-linear*; linearity only occurs at very low values of σ and ϵ , as a limiting case. Therefore, $D(t)$ is $D(t, \sigma)$.

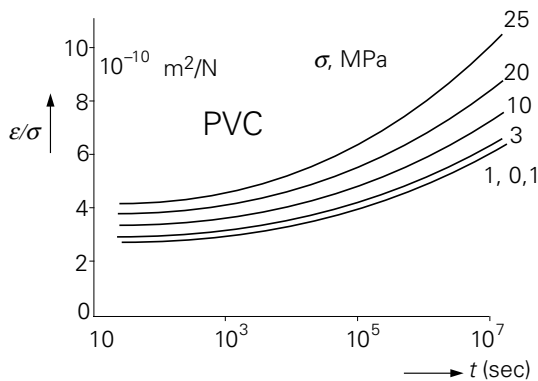


Figure 7.6. Non-linearity of creep for PVC.

Various models have been proposed to account for the non-linear creep of polymers, such as the Eyring model; this model “explains” some aspects, but fails with other ones, and will not be discussed here.

For practical applications empirically determined creep data are being used, such as $D(t)$ or, more often, $E(t)$ curves at various levels of stress and temperature. The most often used way of representing creep data is, however, the bundle of *creep isochrones*, derived from actual creep curves by intersecting them with lines of constant (log) time (see Figure 7.7). These σ - ϵ -curves should be carefully distinguished from the stress-strain diagram discussed before, as generated in a simple tensile test!

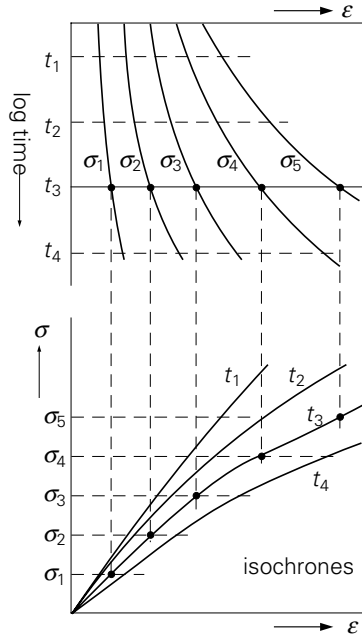


Figure 7.7. Construction of creep isochrones.

From a bundle of creep isochrones the tendency of a material to creep, can be read-off in a glance, namely from their mutual distance. Along horizontal lines of constant stress, the increase of deformation by creep can be detected. When the isochrones are straight lines, the superposition principle holds. Compliances at certain combinations of σ and t follow from the (reciprocal) slopes of connection lines to the origin.

Creep isochrones are, sometimes, used to obtain information on *stress relaxation*; the stresses are then read-off on a vertical line (constant strain). In general this is, however, not allowable, since $E(t)$ in relaxation is not equal to $1/D(t)$ in creep. In a linear region this objection is not too stringent; for want of something better, the procedure can be used as a first approximation (data on stress relaxation are very scarce!).

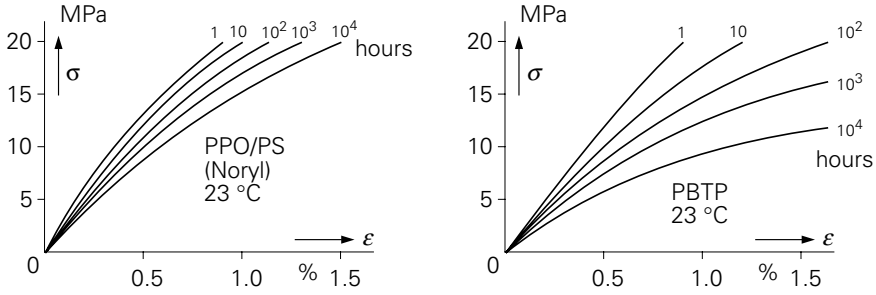


Figure 7.8. Examples of creep isochrones.

Figure 7.8 gives some bundles of isochrones as supplied by a polymer manufacturer (GE). As we saw before, when comparing POM with PC, also here the higher rate of creep of a semi-crystalline polymer (PBTP), compared with the amorphous blend of PPE with PS, is obvious.

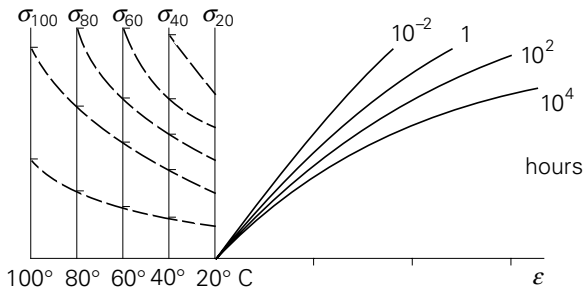


Figure 7.9. Creep isochrones at different temperatures.

Creep at different temperatures can be represented by separate bundles of isochrones. A simple time-temperature shift could mean that for higher temperatures shorter time values could be written at each curve. It is, however, easier to transform the stress scale. Sometimes this is possible with sufficient accuracy; in those cases only one bundle of isochrones is given with different stress scales for a number of temperature levels (Figure 7.9) (see also Qu. 7.13).

7.2.4. Physical ageing

In § 3.3 the effect of cooling rate on the free volume in the glassy state has been discussed. Rapidly cooled glassy polymers have a greater *free volume*, but they show *volume retardation*. This volume change, though very small, has a considerable effect on the creep behaviour: all relaxation times for creep are shifted towards higher values. This phenomenon has been studied extensively by Struik (thesis Delft 1977).

An important consequence of physical ageing is that, during a creep experiment or during creep in practice, the rate of creep is continuously reduced. Quantitative theories, supported by experimental results, give the picture as presented in Figure 7.10: the dotted lines indicate the creep as extrapolated from observations at higher temperatures; the drawn lines are experimentally determined. The differences, in a favourable sense, are enormous!

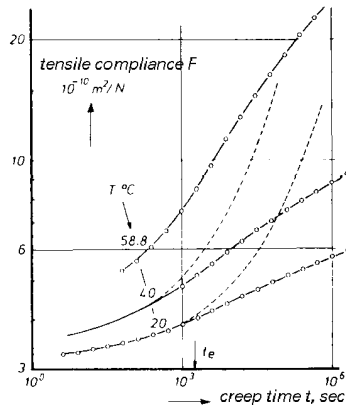


Figure 7.10. Effect of physical ageing on creep.

These large differences clearly demonstrate the impossibility to apply time-temperature extrapolations in an ageing glassy polymer. Ageing proceeds, at a temperature below $T_g - 25^\circ\text{C}$, over thousands of years, and is, therefore, an essential factor when a polymer is subjected to long-term loading. If the physical ageing would not cause a continuing increase in the resistance to creep, plastics would not be able to withstand mechanical loading over longer times: the creep would go on and on, since its upper limit is the *rubber compliance*!

Creep data should, therefore, be considered with care. In most cases the strongest ageing effects are already taken into account more or less automatically.

Summarizing: The basic idea, mentioned in chapter 6, that creep of solid polymers could be represented by a simple four-parameter model (the Burgers model), composed of a Maxwell and a Kelvin-Voigt model in series, appears to be inadequate for three reasons:

First, already mentioned in Chapter 6, a single retardation time is not sufficient to account for the real creep behaviour, which extends over many decades on the time scale; we need a *spectrum* of retardation times.

Secondly, it appears that a spectrum is also insufficient, since this is based on linear

viscoelastic behaviour; in reality creep is practically always *non-linear*. The same objection holds for other, empirical, equations, such as the one of Kohlrausch.

In the third place, it should be taken into account that the material, before and during creeping, is not constant: *physical ageing* occurs, which exerts an important influence on the creep.

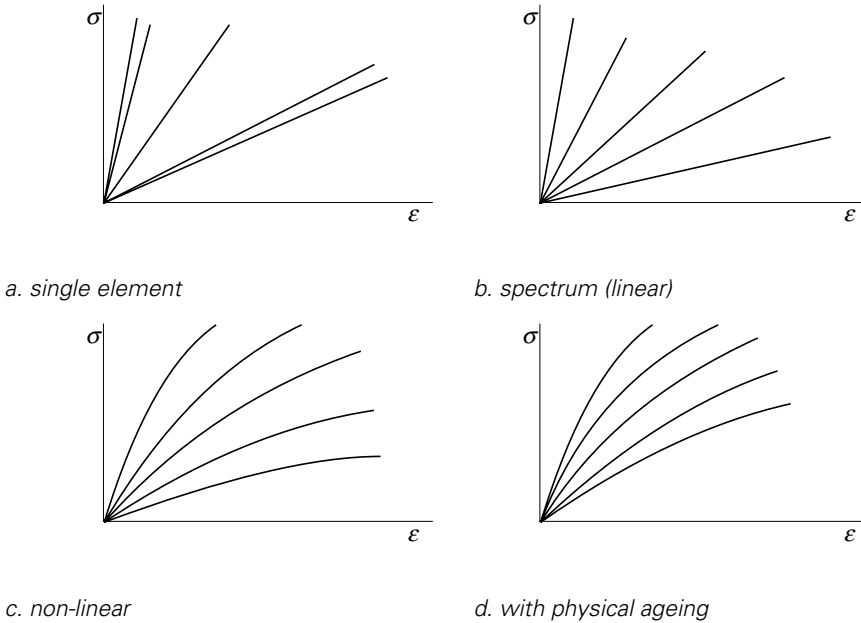


Figure 7.11. Three complications with the representation of creep by a single linear element.

These three complications are schematically shown in Figure 7.11, using creep isochrones; as a reference (a) a Kelvin-Voigt element has been chosen with a spring in series (a Burgers model without irreversible flow).

7.3. Damping

In Chapter 6 we have seen that in a strained polymer a part of the stress is used to store energy (the elastic part), while the remaining part is dissipated into heat (the viscous effect). This can, in a very simple way, be demonstrated by a stress-strain diagram with increasing and decreasing strain (Figure 7.12). The work required to strain the polymer from $\varepsilon = 0$ to $\varepsilon = \varepsilon_1$ is the area below the upper curve, while the recovered energy when ε decreases to zero is given by the area below the lower curve; these energies can, respectively, be expressed as:

$$\int_0^{\varepsilon_1} \sigma \cdot d\varepsilon \quad \text{and} \quad \int_{\varepsilon_1}^0 \sigma \cdot d\varepsilon$$

The difference between these quantities, the indicated area, is the dissipated energy, also called the *hysteresis work*.

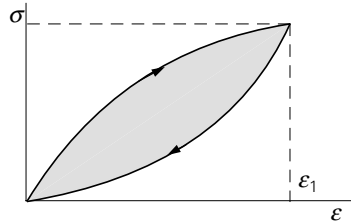


Figure 7.12. Hysteresis.

The two contributions to the deformation energy can be expressed by the quantities:

| | |
|---------------------------|-----------------------------------|
| $E^* = E_1 + i \cdot E_2$ | the complex modulus of elasticity |
| E_1 | the storage modulus |
| E_2 | the loss modulus |
| $\tan \delta = E_2/E_1$ | (see § 6.2) |

In Chapter 6 we have seen that $\tan \delta$, a measure of the relative energy dissipation, depends on temperature and frequency, and that it shows maxima at transitions. A strong maximum occurs at the glass - rubber transition, weaker maxima at secondary transitions. In general: $\tan \delta$ is higher when the $E(T)$ curve is steeper.

The loss factor, $\tan \delta$, can be measured with the aid of dynamic-mechanical experiments (such as the torsion pendulum). The deformation in such a test varies as indicated in Figure 7.13; the damping follows from the “logarithmic decrement”, Λ ; it can be easily shown that

$$\tan \delta = \frac{\Lambda}{\pi} \quad \text{with} \quad \Lambda = \ln \frac{\varepsilon_n}{\varepsilon_{n+1}}$$

An attractive simple experiment to demonstrate the damping is rotating bending: take a thin round rod, bend it, and rotate it in the bent condition without applying a torsion; then a clearly detectable resistance is met. The torque required for rotation is, according to a simple calculation, proportional to E_2 .

In several respects damping is important for practical properties:

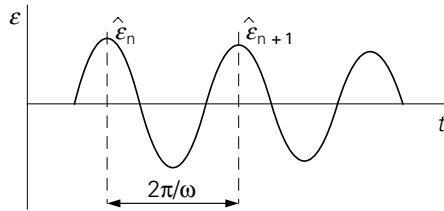


Figure 7.13. Damping factor in a free vibration.

- If it occurs at certain temperatures and frequencies it may contribute to a better *impact strength*.
- It is, of course, a predominant property in *vibration damping devices*.
- Damping is responsible for heat dissipation under *fatigue* conditions: the temperature increase may cause drastic changes in the material properties.
- The energy consumption during repeated deformation, e.g. in *tyres*, is governed by the damping.
- The *friction* of a tyre on the road is also largely dependent on the damping properties of the rubber.

Since the latter two examples lead to contradicting requirements, we shall consider the damping behaviour of a automotive tyre in more detail. For that purpose it is useful to look first at two extreme cases: butyl rubber and butadiene rubber. The former has an extremely high damping; the rebound of a falling ball is not more than 10 or 20 %, whereas with the latter 80 or 90 % is reached. A car tyre with a tread of butyl rubber would have an exceptionally good grip on the road, but it attains, in a very short time, an intolerably high temperature. A BR tread, on the contrary, is hardly heated up, but renders the car practically unmanageable. By blending with other rubbers (NR or SBR) a compromise can be reached.

Nearly always SBR is used in tyre treads for passenger cars; this rubber shows a favourable balance between *heat-build-up (h.b.u.)* and *grip*. Continuing efforts are being spent to obtain further improvements in both directions, which, on first sight, seems to imply a contradiction. The key to reach an improvement is the fact that the two damping mechanisms take place at strongly different frequencies; the heat generation is governed by the damping at the rotation frequency of the wheel, but for the friction much higher frequencies are relevant, namely those at which minute volume elements vibrate when in touch with the road surface.

The problem is, therefore, to influence the damping in these two frequency ranges independently of each other. Because time and temperature have analogous effects, we consider the diagram of $\tan \delta$ as a function of T for a vulcanized rubber (Figure 7.14). The frequencies for friction are so high that we already approach the peak at

the glass-rubber transition, T_g . T_g can be chosen at will; for a normal SBR it is about $-65\text{ }^\circ\text{C}$; an SBR with a higher styrene content shows a higher T_g and thus a higher damping and a better friction. However, the shift of the peak also results in a higher h.b.u.. The magnitude of $\tan \delta$ at temperatures considerably higher than T_g , is hardly dependent on T , but is mainly governed by the perfection of the network, in particular by the number of loose chain ends. These do not contribute to the coherence of the network, but their free mobility gives rise to damping (see also § 2.7).

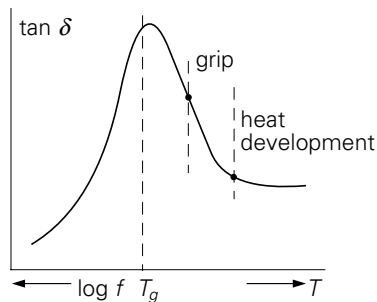


Figure 7.14. Damping curve for a rubber vulcanisate.

Both targets could thus be reached by a slight increase of T_g (by a higher styrene fraction), as well as a reduction of the number of chain ends. The latter can, in principle, be accomplished by:

- higher molar mass, if allowable for the processability;
- narrower molar mass distribution (higher \overline{M}_n);
- chains without any branching;
- end groups with some interaction with each other;
- end groups which specifically react with sulphur.

The damping curve B in Figure 7.15 then shows both improvements in comparison with A.

Recent developments are in another direction, namely in the creation of different glass-rubber transitions by the formation of blocks with different styrene content and different sterical structure of the butadiene chain parts.

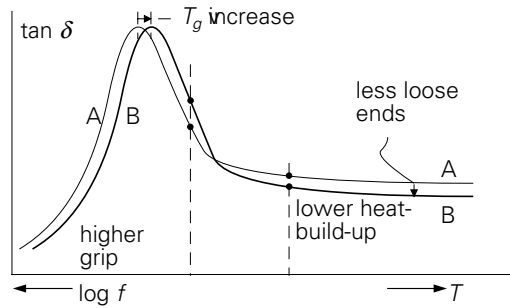


Figure 7.15. Improvement in grip and in heat-build-up.

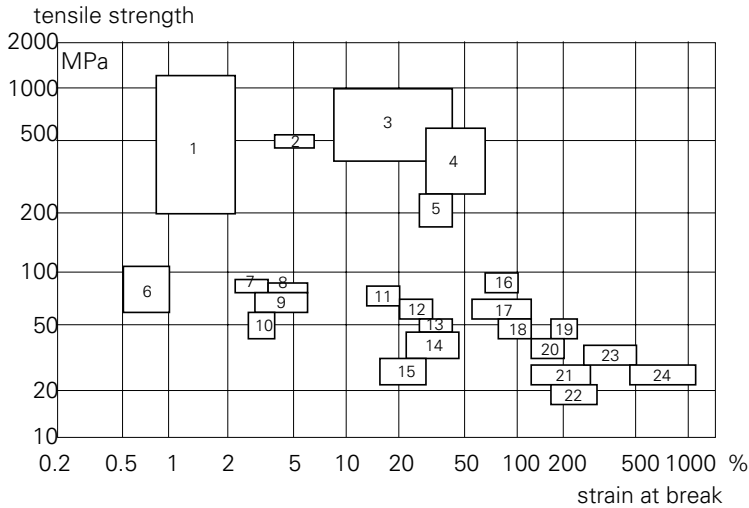
7.4. Strength

7.4.1. Tensile strength and ultimate strain

An important mechanical property is the *strength*, which is the stress at which the material breaks. Besides, the strain at break is of relevance, since this indicates whether the material is brittle or tough. Figure 7.16 gives a survey of both properties for a number of polymeric materials in comparison with other ones.

It appears that the levels of tensile strength of polymers are less widely different than the moduli of elasticity; the softer plastics are, together with the rubbers, all within the range of about 15 to 30 MPa; the harder ones are between 30 and 80 MPa. For reinforced resins the strength values are of the order of magnitude as those for fibres and metals. The diagram further shows that thermosets, PS, PVC and PMMA belong to the *brittle polymers*, while other ones, such as PA, PP, PE and PTFE are *very ductile*. It should, however, be remarked, that a shift in *temperature* or on the *time scale* may change the picture considerably; PP, for example, behaves in an impact test at 0 °C as a brittle material, despite its high strain at break under standard conditions.

Just as the stiffness, also the strength of polymers is strongly dependent on the *time scale* of loading. We distinguish two cases, namely long-term loading and impact loading, which we shall discuss in the following sections.



- | | | |
|--------------------------|---------|-------------|
| 1. reinforced thermosets | 9. PMMA | 17. PPO, PC |
| 2. cotton | 10. PS | 18. PETP |
| 3. construction metals | 11. PVC | 19. PA |
| 4. synthetic fibres | 12. POM | 20. PP |
| 5. wool | 13. CA | 21. HDPE |
| 6. thermosets | 14. TPS | 22. LDPE |
| 7. PPS | 15. ABS | 23. PTFE |
| 8. SAN | 16. PSU | 24. rubber |

Figure 7.16. Tensile strength and strain at break of various materials.

7.4.2. Long term strength

The effect of the *time of loading* on the breaking stress can be visualized in a simple way. If we carry out creep tests on a number of samples at different levels of stress, then some of these tests, at the higher stresses, will end with rupture after a minute or after a year, as indicated in Figure 7.17. From the stress levels and the times to failure, Figure 7.18 can now be constructed, in which also the times to attain a certain strain have been sketched (isometric creep curves). We are most interested in the breaking curve, which gives the relation between stress applied and the time to failure, or the dependence of tensile strength on the time of loading, for ductile failure. For practical use, this curve could be extrapolated along the log t -axis to e.g. 50 years, in order to estimate a “safe” stress level for use.

There is, however, a complication: besides ductile fracture also brittle failure may occur, which is not brought about by deformation and flow of the material, but by the initiation and propagation of *brittle cracks*. Since both processes also need time to develop, the time to brittle failure can also be represented by a curve, similar to

the one in Figure 7.18. Because the breaking mechanism is now totally different from the one in ductile failure, the position and the shape of this curve are governed by different factors; it could have the shape of the line \underline{b} in Figure 7.19, which intersects the curve \underline{a} for ductile failure at two points.

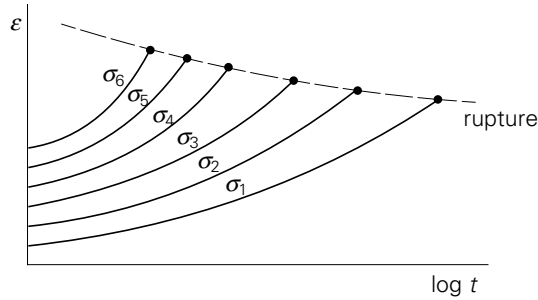


Figure 7.17. Creep to failure at various stress levels.

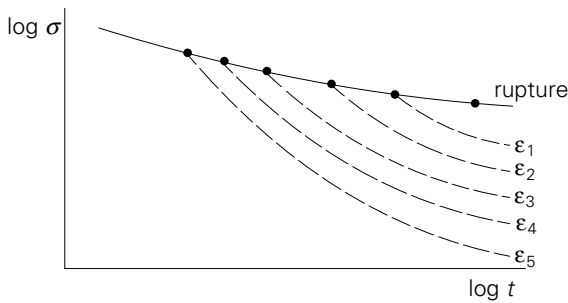


Figure 7.18. Time to failure or to a certain strain.

When a plastics material shows this picture, we can distinguish between three regions of the stress σ : In the region with the highest stress levels, A, the applied stress will result in a *brittle fracture* after a very short time. At lower stresses (B), the time to ductile failure is shorter than the time to brittle failure, so that the material breaks in a ductile manner. At even lower stresses (region C), again *brittle failure* occurs, but now after *very long* times of loading.

This situation indeed occurs frequently, for instance with PVC pipes, where high internal pressures give rise to explosive brittle fractures, while with lower pressures, after a shorter or a longer time, balloon-like fractures occur. At even lower pressures brittle hair cracks are formed, also with PE, causing the pipes to leak. This happens after very long times of use (e.g. some years), but considerably earlier than predicted from extrapolation of the curve for ductile failure.

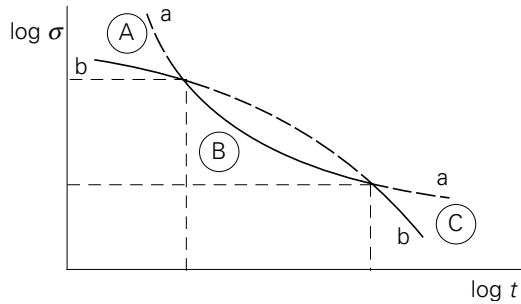


Figure 7.19. Two types of failure.

With such a complex failure behaviour, it is difficult to make a reliable estimation of the *allowable stress*, i.e. the stress at which, in the required duration of use (mostly 50 years for pipes for transportation of water), no failure will occur. Evidently, extrapolation of failure tests, even if they extend over a year, is insufficient. The transition from ductile to brittle crack failure, and the accompanying change in slope of the curve, may take place after several years! One, therefore, resorts to tests at *elevated temperatures*, on the basis of the idea that a temperature increase will accelerate both failure mechanisms, and also the transition from ductile to brittle failure.

Figure 7.20 gives an example of this procedure. From measurements of the time to failure at various levels of stress and of temperature, *two-dimensional extrapolation* allows an estimation of the position of the brittle failure curve at the temperature of use. Needless to say that this a very time-consuming procedure; especially when we realize that the scatter in measured times to failure (up to a factor of ten between the extremes) necessitates five to ten tests to be carried out at each condition (see also Qu. 7.14).

This procedure is mainly applied to plastics pipes. The reason is, that these form one of the rare (but large-scale!) examples that during a long time of loading no fracture is allowed to occur. With other applications of plastics in load-bearing constructions the ultimate strength plays hardly any role, since in most cases the strain, and thus the creep, is the limiting factor.

A further question is, how to act when the time to crack failure is too short to allow for a certain long-term application? Obviously, a grade with a *higher molar mass* should then be chosen, since the position of the curve for brittle failure is strongly dependent on the chain length (contrary to the one for ductile failure, which is largely independent of M) (see Figure 7.21). Apparently the number average molar mass, \bar{M}_n , is of importance for brittle failure, since the number of chain ends is the governing factor.

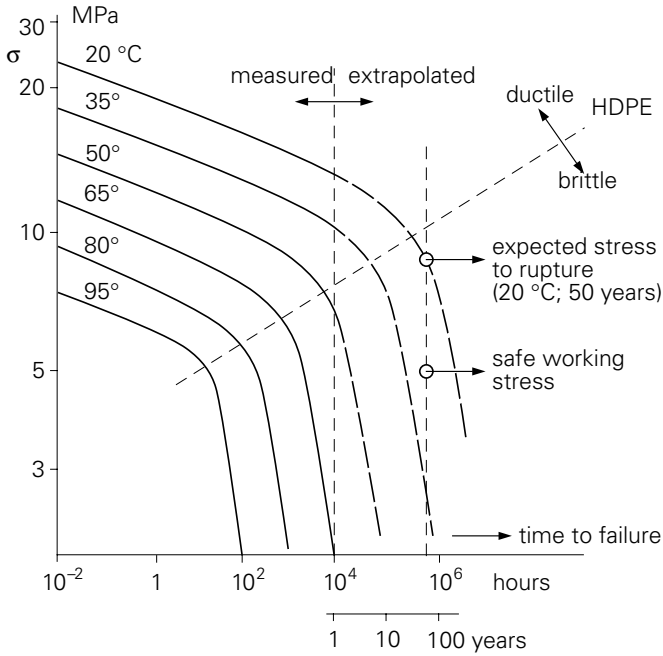


Figure 7.20. Extrapolation procedure for HDPE pipes.

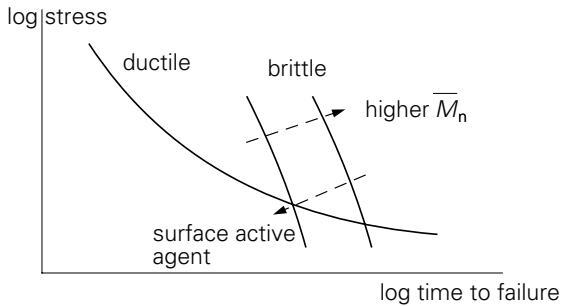


Figure 7.21. Effect of molar mass and of environment on the time to brittle failure.

The *environment* also plays a role; in some environments brittle crack failure is strongly promoted. For example, detergents such as synthetic soaps can decrease the time to brittle failure of PE by a factor between 10 and 50 (see Figure 7.21). This phenomenon is known as *stress corrosion* or *environmental stress cracking* (ESC) (see further § 8.5).

Long before a brittle hair crack has come to its complete development, it is already present as a nucleus, and the material has already undergone irreversible damage. Microscopic cracks are often partially filled with material in the form of very thin fibres, forming bridges between the fracture surfaces. These cracks are denoted as

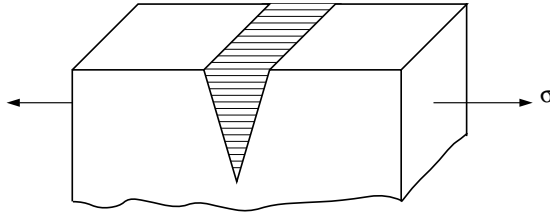


Figure 7.22. Schematic representation of a craze.

crazes; such a craze is schematically shown in Figure 7.22.

Detection of crazes is very difficult; yet craze formation should be avoided in critical applications (such as gas pipes). In order to achieve that, one uses the expression “*critical strain*”, which is based on the observation that, as long as a certain level of strain is not exceeded, no crazes are formed. It would be convenient if this critical strain would be independent of the applied stress; this is, unfortunately, not the case, as illustrated in the bundle of isochrones in Figure 7.23

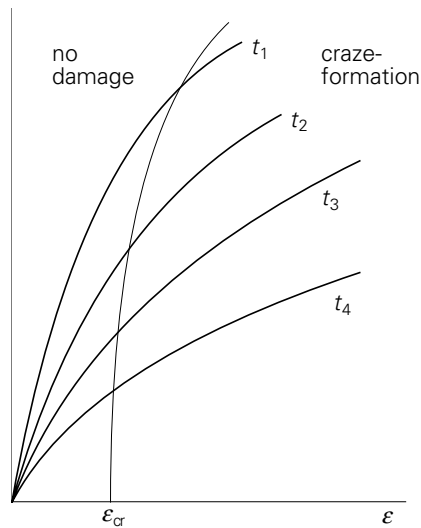


Figure 7.23. Bordering curve for the formation of craze.

For practical purposes the lower limit of the critical strain can be used as a criterion. This value appears, moreover, to be not much dependent on temperature, so that it can be considered as a material constant. It varies from $\approx 0.3\%$ for PS to $\approx 2.2\%$ for PP. From creep isochrones a stress level can now quite easily be detected at which, within a given time of usage, no damage to the material is to be expected. This stress level is, of course, much lower than the one we found from Figure 7.20.

7.4.3. Impact strength

For many applications the resistance of the material to *shock loading* is an important property. Here we find ourselves, contrary to the previous section, on the very short side of the time scale. For the impact strength the short-term tensile strength as well as the ultimate strain play a role; the impact strength is, in fact, the energy needed for rupture at a high rate of deformation, $\int \sigma \cdot d\varepsilon$. It is very difficult to characterize the impact strength accurately and uniquely.

In most cases the impact strength is determined with the aid of a standard impact test, in which a test bar is hit by a falling hammer, after which the remaining energy of the hammer is measured. Very often a *notch* has been machined in the test bar. The stress concentration round the tip of this notch causes the fracture to be initiated at a well-defined location and not at arbitrary surface cracks or inhomogenities. Moreover, the rate of deformation is, at the tip of the notch, much higher than the average value in the test bar, so that the experiment takes place at a *shorter time-scale*. On the basis of the equivalence of temperature and time, this means that the value found belongs to a lower temperature, where the material is, in general, more brittle; the notch more or less forces the material to fail in a brittle way, so that the notched impact test provides a better indication of the material behaviour under extreme conditions.

Figure 7.24 and Figure 7.25 show that the effects of the sharpness of the notch and temperature are, roughly, equivalent; polymers for which the impact strength is strongly dependent on temperature (PVC and PA), are also more notch-sensitive than, e.g. ABS.

Results of notched impact tests are found in various tables of material properties; a schematic survey of a number of plastics is presented in Figure 7.26. These values give a first impression of the ranking of the various polymers, tested under standard conditions. With other conditions, however, the order of sequence of the various materials may be quite different, as already appears from Figure 7.25. Moreover, various complications arise: Internal stresses as a result of cooling and shrinkage have a considerable effect on the impact strength. Chain orientation renders a material *anisotropic*: the impact strength in the orientation direction is increased, but is decreased in the cross direction. Reinforcing fillers in most cases bring about a decrease of impact strength, though in some cases, particularly with very brittle polymers or at low temperatures, glass fibres may effect an increase (see § 9.3).

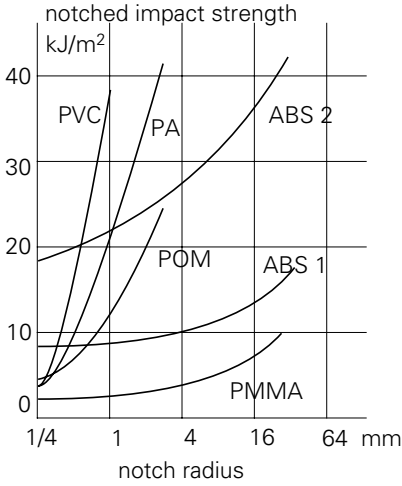


Figure 7.24. Impact strength as a function of notch tip radius.

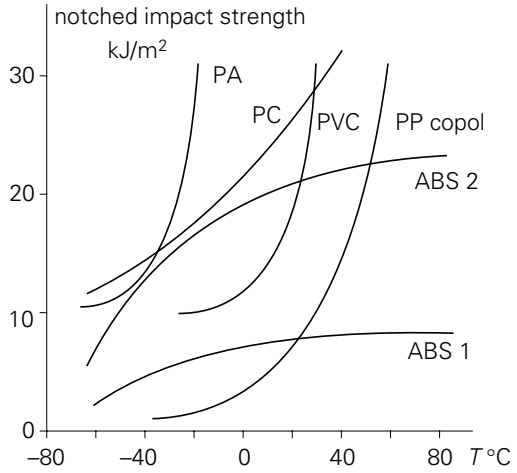


Figure 7.25. Impact strength as a function of temperature.

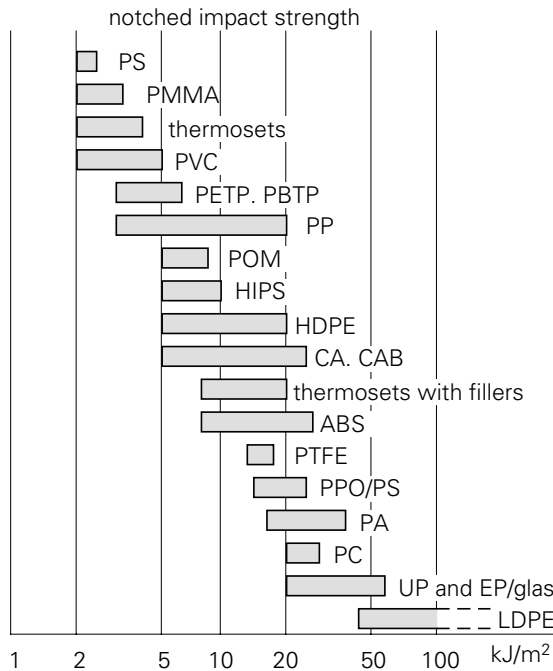


Figure 7.26. Impact strength of some plastics.

Glassy polymers are, mostly, brittle (e.g. PS), unless, below room temperature, a *secondary transition* is present; a strong example is PC, which shows a very high impact strength. Why such a transition is, below the temperature of use, still active,

can be explained by the time-temperature equivalence: the time-scale under impact conditions is very short!

Semi-crystalline polymers, such as PE and PP, are tough at temperatures above T_g , though for PP ($T_g \approx -15^\circ\text{C}$) the critical temperature limit is about room temperature; here also the time-temperature equivalence plays a role. Below T_g , semi-crystalline polymers have a low impact strength (unless secondary transitions occur).

The impact strength of brittle polymers is often improved by the incorporation of small *rubber particles*, either by blending or by copolymerization (e.g. PP copolymer).

Finally, it should be remarked that the impact strength is also dependent on the *chain length*, in particular on the number average molar mass \bar{M}_n (the number of chain ends being the governing factor).

7.5. Surface properties

7.5.1. Hardness

Hardness is the resistance of a material against penetration of a harder body. A great number of methods exist to characterize hardness; for plastics materials these methods have mostly been taken over from metal testing methods and some from rubber testing. The various methods fall apart into two, very much different, categories, namely:

- methods at which the penetration is measured *during the presence of the load* on the penetrating body,
- methods where the measurement is carried out *after removal of the load*.

To the first category belong the α -Rockwell and the Shore A, C, and D hardnesses. With α -Rockwell the penetrating body is a $\frac{1}{2}$ inch diameter sphere, loaded with 60 kg force; after 15 sec loading the penetration depth h (mm) is measured, and the hardness is defined as $R_\alpha = 150 - h/0.002$. Practical values for plastics range from $R_\alpha = 20$ to 150.

With the Shore methods the penetrating body is a cone; with A and C the tip of the cone is flattened to a circle with 0.79 mm diameter; with D it is rounded-off to a radius of curvature of 0.1 mm. The force is exerted by a spring, which for A, mainly applied to rubbers, is considerably less stiff than for C and D. Hard thermoplastics are mostly characterized by Shore D; the values found are between 50 and 90 units.

The methods suggest that these hardness values are related to the modulus of elasticity of the material. Round the penetrating body a complicated stress

distribution is present; the state of deformation is also difficult to analyse. Yet in fact a deformation is being measured at a given stress. In Figure 7.27, for a number of plastics together with some thermoplastic elastomers, the E -modulus and the Shore-D hardness, as read from material tables, are plotted against each other. The correlation appears to be satisfactory if we take into account that the deformations in the hardness test may, locally, be rather high, and that the time scales of deformation are different.

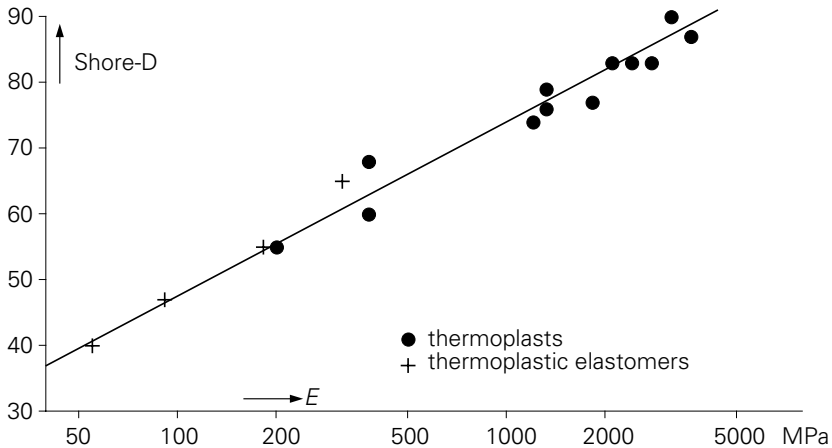


Figure 7.27. Relation between hardness and E -modulus.

With the second category of hardness tests the measurement is carried out after the load is removed. This is the case with Rockwell R, S, V, L, M and P; under a small prestress the position of the sphere is measured, so the permanent penetration depth, h (mm). The sphere diameter is $\frac{1}{4}$ or $\frac{1}{2}$ inch, the load is 60, 100 or 150 kg force, dependent on which of the six types of test is chosen. The hardness is defined as $HR = 130 - h/0.002$. This hardness value has no relation at all to the modulus of elasticity; the permanent deformation after recovery is being measured (such a type of test would result in a very high value for rubbers!).

Another criterion is used with the Vickers hardness test; after penetration of a pyramid-shaped diamond under stress, the diameter of the indent is measured after removal of the diamond. The hardness is defined as the applied force divided by the area of the indent. This is again a measure of the permanent deformation, or, possibly, of the yield stress.

7.5.2. Friction

Friction is an extremely complex phenomenon. The simplest fundamental treatment starts from the assumption that the surfaces, in touch with each other, are rough on a

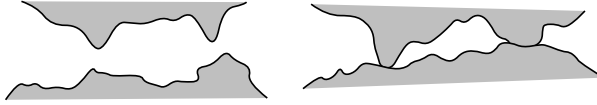


Figure 7.28. Contact between two surfaces.

micro-scale, so that the actual contact area is only very small (Figure 7.28).

The surfaces are pressed together with a force N , and they touch each other over an area A . The normal stress in the contact surface is thus N/A . This value can be considered as the yield strength of the material, σ_y , so $\sigma_y = N/A$ and $A = N/\sigma_y$.

During a sliding movement the points of contact, where the two surfaces are welded together, are continuously being broken, whereafter they reform; this requires a force $\tau_b \cdot A$, in which τ_b is the shear strength of the material. This is the friction force, $F = \tau_b \cdot A = \mu \cdot N$, where μ is the coefficient of friction. This leads to a very simple expression for μ :

$$\mu = \tau_b / \sigma_y$$

However, there are, as always, complications: both τ_b and σ_y are functions of time (viscoelasticity) and temperature. In particular the temperature effect is of importance; the continuing plastic deformation results locally in *high heat dissipation*, which, due to the low heat conduction of polymers, is not transported to the environment. An estimation of the local temperature increase can be made with:

$$\sigma_y T = T_0 + \frac{2}{\sqrt{\pi}} \cdot \frac{q' \cdot \sqrt{t}}{\sqrt{\lambda \rho c}}$$

in which

q' = heat production per unit time and area

λ = heat conduction coefficient

ρ = specific mass

c = specific heat

q' equals the heat (or work) of friction:

$$q' = \frac{W \cdot l}{F \cdot t} = \frac{W}{F} \cdot v = \frac{\mu \cdot N}{F} \cdot v = \mu \cdot \sigma_N \cdot v$$

(F = total surface area, v = sliding speed, σ_N = normal pressure), so

$$\Delta T = \frac{2}{\pi} \cdot \frac{\mu}{\sqrt{\lambda \rho c}} \cdot \sigma_N \cdot v \cdot \sqrt{t}$$

Substitution for certain polymers and conditions easily leads to values of several tens of °C.

For a semi-crystalline polymer, the coefficient of friction depends on temperature as schematically indicated in Figure 7.29:

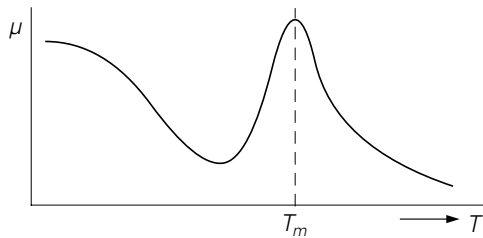


Figure 7.29. Coefficient of friction as a function of T .

After an initial decrease, a strong increase occurs as a result of the sticking together of the sliding surfaces. From the melting point, μ again strongly decreases; the surfaces are then molten.

So far we discussed friction between a pair of equal polymers. When the partners are different, e.g. a plastic against steel, the picture changes. In this case the real contact area will also be much smaller than the apparent one, but the steel “peaks” will, not flattened themselves, penetrate into the polymer, and will “plough” through the polymer when the surfaces slide over each other. It appears that, also in this case, the coefficient of friction can be expressed as $\mu = \tau_b / \sigma_y$, where τ_b en σ_y are the values for the polymer. A great difference is the much higher rate of heat transportation, which changes the whole picture. It has been observed that the friction between a metal and a polymer, after an initially high value, rapidly drops to a much lower level. Abraded polymer particles stick to the metal surface and then cause polymer-polymer friction, now, however, with a good heat transport.

A global survey of friction coefficients of various polymers is given in Figure 7.30 (all moving against steel). In general, *polymers exhibit less friction than metals*. The lowest values for the friction coefficient are found for HDPE, POM, and, in particular, PTFE.

The *surface structure* of a plastic may exert a considerable influence on the friction; an example is given by injection moulded articles of PP, which show, in touch with each other, a coefficient of 0.7, while for sand-blasted surfaces a value of only 0.3 is found. For injection-moulded nylon $\mu = 0.65$, for machined surfaces 0.47. As a matter of fact, lubrication has a strong influence: the value of 0.47 for nylon is reduced to 0.19 with water lubrication and to 0.08 with oil.

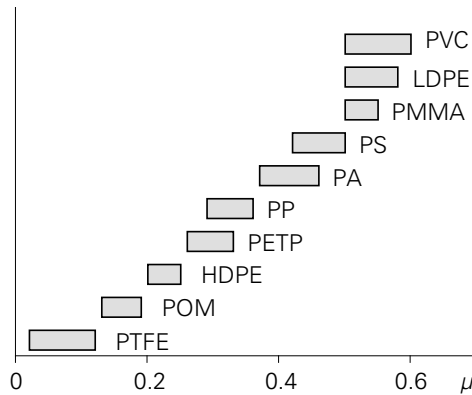


Figure 7.30. Coefficient of friction of some polymers.

7.5.3. Abrasion

Abrasion is also a complex phenomenon; it is not or hardly predictable from basic properties, and is only characterized empirically by a great variety of standard methods.

We can distinguish between, on the one hand, damage of the surface by scratches and dents, *without removal of material*, and, on the other hand, damage by *loss of material*. The first case is clearly related to the second category of hardness (permanent deformation, see § 7.5.1), while the second case depends on a combination of friction and tear strength.

The results of the numerous types of abrasion tests cannot be related to each other; the tests are only able to compare members of the same family of materials. The ranking in abrasion resistance, found for a series of materials, often depends on the method chosen. Only a few significant data will, therefore, be given here. The lowest abrasion values are found for polyamides (nylons), polyolefins (PE and PP), and polyesters (PETP and PBTP). In particular, a HDPE grade with a very high molar mass (up to 5 million) should be mentioned; this polymer has an unsurpassed resistance against abrasion. (Here again, PE, in general a simple commodity polymer, excels, just as in its electrical properties (see § 8.2.2) and as the strongest known fibre, see § 4.6).

The relation of abrasion to friction appears from Figure 7.31, in which the abrasion is given as a function of temperature for some crystalline polymers. Temperature increase causes, from a certain temperature, a drastic increase in abrasion due to sticking together of the surfaces.

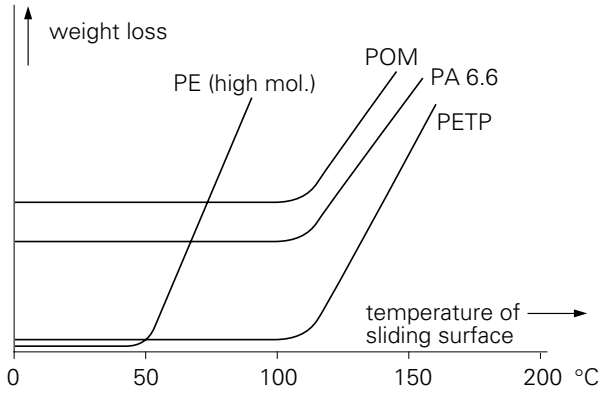


Figure 7.31. Abrasion as a function of T for some polymers.

The abrasion resistance increases considerably when *reinforcing fillers* are added to the polymer. This is, in particular, the case with rubbers: incorporation of carbon black (e.g. 40 weight parts per 100 rubber parts) increases the life of a tyre tread from 5,000 to 50,000 or even 100,000 km!

8

Further properties

8.1. Thermal properties

The temperature region in which a polymer can be used, is limited at the low as well as at the high side. The most serious limitation at low temperatures is, as a matter of fact, *the glass - rubber transition for rubbers*; below T_g they lose their rubbery nature and pass into the glassy phase. Besides, for thermoplastics, the principle limitation is that they become brittle at low temperatures, and thus lose their impact strength. The other properties are not affected, but, in most cases, (E -modulus, tensile strength), improved upon decrease of temperature. First of all we shall consider at which temperature cold-brittleness appears.

8.1.1. Brittleness temperature

Brittleness is found with semi-crystalline polymers below their glass-rubber transition T_g . An example is PP, which becomes brittle at about $T \approx -10$ °C. PE retains its ductile nature down to very low temperatures. Other polymers have a T_g of some tens of °C above room temperature, such as polyamides and thermoplastic polyesters. Various mechanisms are responsible for a reasonable impact strength at room temperature; for polyamides this is, for instance, the absorption of water; also secondary transitions in the glassy region may play a role.

Amorphous, glassy polymers, used far below their T_g , are *cold-brittle* if no other mechanisms are active; an example is PS. If a polymer has been improved in impact strength by the addition of a rubbery phase (high-impact PS or PVC, ABS etc.), then the cold-brittleness temperature is related to the T_g of the added rubber. If the polymer shows a *secondary transition* in the glassy region (such as PC), then this governs the brittleness temperature.

The tough-brittle transition temperature is hard to define; it is, of course, strongly dependent on the conditions, such as the time scale of the experiment, notch effects etc. The brittleness temperature is, in general, being determined by a series of standard impact tests, carried out at different temperatures; when 50% of the samples are broken in a brittle way, then the brittleness temperature has been reached.

8.1.2. Softening

At elevated temperatures all polymers soften, dependent on their glass-rubber transition points, T_g , and/of their melting points, T_m . These temperatures limit the practical use of plastics. To characterize the softening behaviour, in practice various types of standard tests are being carried out, resulting in values for the “softening temperature”, defined in different ways. The values mostly used are: the ISO Heat Deflection Temperature (HDT) and the Vicat Softening Temperature (VST or “Vicat”).

The *ISO-HDT* is based on a bending measurement on a standard test bar, loaded with a constant force, and gradually increased in temperature; the temperature at which a certain bending deflection is reached, is called the HDT. All conditions are normalized: sample dimensions, rate of heating ($2\text{ }^\circ\text{C}/\text{min}$), load (two cases: ISO-A with a maximum bending stress of 1.81 MPa, ISO-B with 0.45 MPa), limit of bending deflection (0.32 mm). The stress, σ , is fixed, as well as the deformation, ε , at the moment of reading-off the temperature, so also $E = \sigma/\varepsilon$. In fact, the temperature is measured at which the modulus of elasticity, E , has dropped down to a prescribed level. These levels of E are about 1000 and 250 MPa for ISO-A and ISO-B, respectively.

With the *Vicat test* a steel needle, at the end flattened to an area of 1 mm^2 , is pressed into a block of the material with a standard force (1 kgf for Vicat-A, 5 kgf for Vicat-B). The temperature is increased at a standard rate of $50\text{ }^\circ\text{C}/\text{hour}$ until the needle has penetrated 1 mm into the sample; then the Vicat softening point has been reached. As well as we have seen with the Shore hardness (§ 7.5.1), this process of penetration is, in fact, also governed by the E -modulus of the material, though in a much more complicated way. Globally, also to the Vicat test a *characteristic E-modulus* can be ascribed, which is lower than with the ISO bending test, namely about 200 MPa for Vicat-B and 40 MPa for Vicat-A.

The values of the various softening temperatures can now be related to the shape and the position of the $E(T)$ curves, discussed in Chapters 3 and 4. A satisfactory comparison is hardly possible, because the time scales of the tests differ too much; $E(T)$ curves have, in most cases, been measured by dynamical-mechanical tests at a time scale round one second, whereas the determination of softening temperatures extends over several minutes. In principle, however, the picture presented in Figure 8.1 is valid (see also Qu. 8.3).

In this picture the dependence of E on T is schematically sketched for three polymers, largely differing in softening behaviour:

1. an *amorphous polymer*, for which E drops quite steeply in the glass-rubber

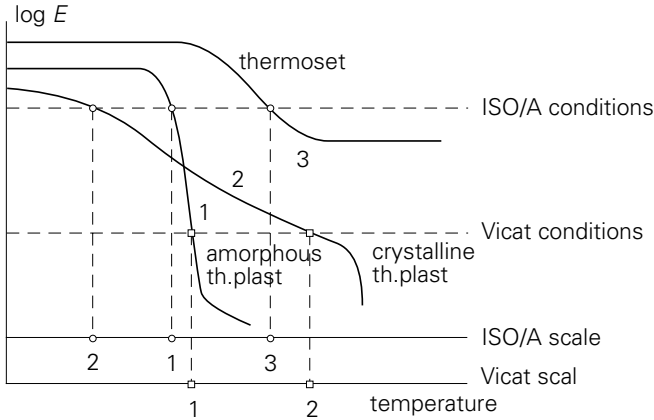


Figure 8.1. Softening temperatures and $E(T)$ curves.

transition region,

2. a *semi-crystalline polymer*, showing a gradual drop in E between T_g and T_m ,
3. a *thermoset*, for which E , also above T_g , has not dropped far enough to allow the determination of a Vicat test.

From the first two examples it appears that simple usage of an arbitrary softening temperature, taken from a table, does not provide an answer as to the temperature resistance of a polymer: the data for Vicat and ISO-HDT contradict each other!

Apparently, the Vicat point indicates the limit where the material, without being subjected to an appreciable stress, loses its solid-state nature, while the ISO-HDT gives an indication of the upper temperature which can be withstood under stress. A practical example of the discrepancy between Vicat and ISO-HDT is given in the table below.

| | VICAT | ISO-HDT |
|------|--------|---------|
| PC | 145 °C | 135 °C |
| PA-6 | 210 °C | 85 °C |

As a matter of fact, an $E(T)$ curve provides much more information than the single-point tests on softening temperatures; however, due to the time dependency of the mechanical properties, not even enough to provide a basis for construction purposes. For the use of plastics under load at elevated temperatures *creep data* are required !

Softening temperatures *increase* when reinforcing fillers are present or short fibres. T_g and T_m will, of course, not change, but the increase of stiffness causes the whole $E(T)$ curve to shift to a higher level, e.g. by a factor of 2 for various powders (quartz,

talcum etc.), and by a factor of 3 to 5 for glass fibres. The effect of reinforcement on ISO-HDT and on Vicat is, for semi-crystalline polymers, much greater than for amorphous glassy ones. This appears from Figure 8.2; it is, again, simply a matter of *slope of the curve*!

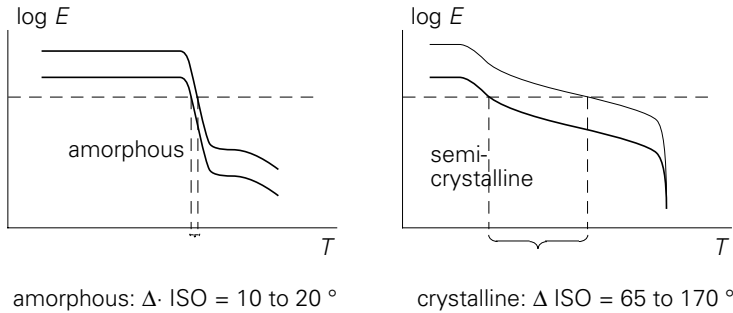


Figure 8.2. Effect of glass fibres on softening temperature.

The large effect on crystalline polymers is, on the one hand, trivial and self-evident; on the other hand it appears that reinforcing fibres bring about such an increase in the stiffness at increasing temperatures that the temperature region of application is substantially widened.

8.1.3. Thermal expansion

Polymers show, in general, a considerably *higher thermal expansion* than other materials. Figure 8.3 gives an overall survey. Roughly speaking, a relation exists between the coefficient of thermal expansion and the reciprocal stiffness.

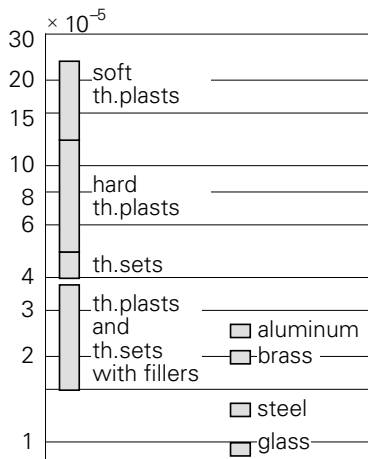


Figure 8.3. Survey of expansion coefficients.

The coefficient of expansion depends on temperature, as already discussed in

Chapter 3. In the glass-rubber transition the thermal expansion coefficient shows a discontinuous jump; with crystalline polymers the coefficient increases strongly from a few tens of °C below the melting point (Figure 8.4)

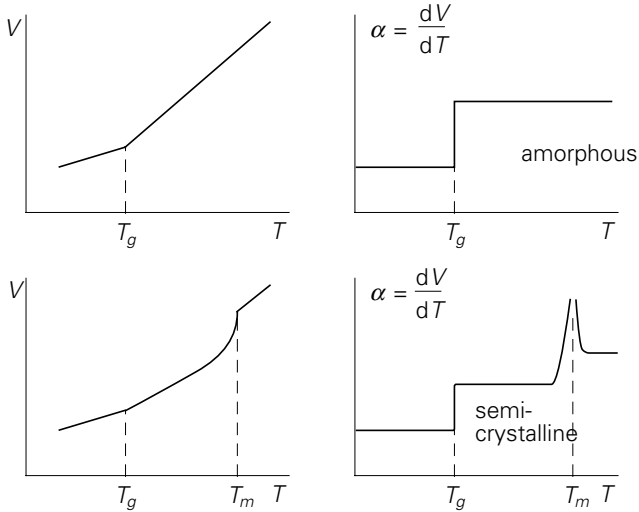


Figure 8.4. $V(T)$ and $\alpha(T)$ relations.

Fillers have a strong effect on the thermal expansion; they may reduce the coefficient by a factor of 2 to 3.

Chain orientation effects anisotropy in the expansion; in the orientation direction it is considerably lower than across. Moreover the tendency to (irreversible) shrinkage in the orientation direction upon temperature increase should be taken into account.

Fully reversible negative expansion is shown by a strained ideal rubber, as a result of the entropy-elasticity, discussed in § 5.1.

8.1.4. Thermal conduction

The coefficient of thermal conduction, λ , is defined on the basis of the formula:

$$\frac{Q}{t} = \lambda \cdot F \cdot \frac{T_1 - T_2}{d}$$

in which

Q = heat flow during time t

F = area

d = thickness of the sample,

T_1 and T_2 the temperatures of the opposing sides.

The dimension of λ is W/m·K (Watt /meter·Kelvin).

Compared to other materials such as metals, the thermal conductivity of polymers is 100 to 1000 times smaller (see Figure 8.5). Fillers increase the conduction by a factor of 3 to 4.

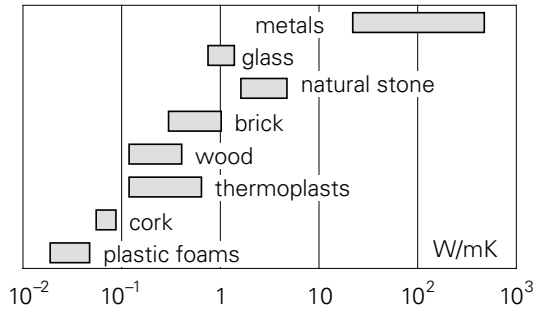


Figure 8.5. Thermal conduction of some materials

For technology the low heat conductivity is of importance as a great hinder in *processing operations*. Heating of a solid mass to reach the fluid condition takes a long time, as well as cooling down, e.g. in the mould of an injection moulding machine. The heating process can be speeded up in several ways, namely by dissipation of mechanical energy, utilizing the high viscosity, by high-frequency dielectric heating or by ultrasonic sound waves; in all these cases the heat is generated evenly throughout the whole mass (see § 11.1.1). Cooling, however, is always dependent on the heat conduction, which, therefore, largely influences the *cycle time* in processing of thermoplastics.

On the contrary, a beneficial aspect of the low heat conductivity is the possibility to apply plastics as *thermally insulating materials*, in particular as *foams*. The heat conduction of a polymer foam is composed of four components:

$$\lambda = \lambda_p + \lambda_g + \lambda_r + \lambda_c$$

λ_p = conduction of the cell walls,

λ_g = conduction of the gas in the cells,

λ_r = heat transfer by radiation,

λ_k = heat transfer by convection.

With very low foam densities λ_p is negligible, and λ is mainly governed by λ_g and by λ_r (transfer by radiation plays an increasing role with decrease in density). λ_c is, mostly, small, but may become of importance with larger cell size; within the cells convection may play a role, which increases the heat transport of the gas in the cells considerably. With increasing foam density the contribution of λ_p increases. In total, we find a minimum in the λ - d curve, (Figure 8.6), the level of which is largely

governed by the type of gas in the cells. For polyurethane foam this minimum may be very low due to the low λ_g of the blowing agent, freon, though diffusion through the cell walls will cause the thermal insulation to decrease with increasing time.

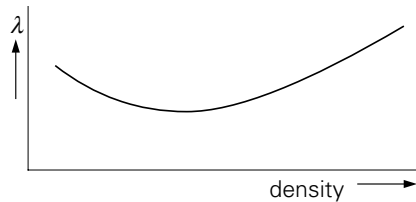


Figure 8.6, Thermal conduction through a foam as a function of density.

8.1.5. Maximum temperature of use

The most obvious limitation in the maximum temperature of use of a polymer is its *softening temperature*, as discussed in § 8.1.2. Besides, *degradation* may play a role, in particular when the material is exposed to high temperatures during a long time. In various tables of material properties maximum temperatures of use are given, often specified into short-term and long-term exposure to elevated T . An example: PC has, as far as softening is concerned, a maximum temperature of use (ISO-HDT) of 135 °C, but due to degradation, values are given ranging from 140 °C (for hours) down to 100 °C (for years). These values are, of course, also strongly dependent on the *stabilizers* which the manufacturer has added to the polymer to make it suitable for special high-temperature applications. Often a certain polymer is available in a range of grades with increasing resistance against degradation at elevated temperature.

The parameter most often used to indicate the maximum temperature of use is the “*temperature-index*”, introduced by the American Underwriters’ Laboratories Inc., and, therefore, also named the “U.L. index”. Since, for different applications, degradation affects the performance of polymers in different ways, different values of the UL index are attributed to one and the same polymer, for instance for electrical insulation and for impact strength.

8.1.6. Burning behaviour

All polymers burn when exposed to a flame (they are all organic substances), but considerable differences exist between polymers in their behaviour after removal of the flame. Some continue burning, other ones extinguish. The degree of self-extinguishing is expressed as the “*oxygen index*”, which is the oxygen concentration in the surrounding atmosphere, at which the material just extinguishes. An oxygen concentration below 21 % means that, in a normal atmosphere, the polymer burns on; if the index is higher, it stops burning.

Some values of the oxygen index are given in Figure 8.7. PTFE (teflon) appears to be highly self-extinguishing; other polymers containing chlorine or fluor also clearly belong to the self-extinguishing category.

For a number of materials the burning behaviour can be improved by the addition of bromine- or antimony compounds, mostly, however, at the cost of some mechanical or electrical properties.

Gradually, the insight is gaining ground that the heavy *smoke formation* caused by some burning polymers, involves greater risks than their flammability itself, the latter being not much different from large-scale applied materials such as wood, textiles and paper. More than ever, test methods and criteria for safe use are being developed to recognize and prevent the risks of smoke development, as regards visibility as well as toxicity.

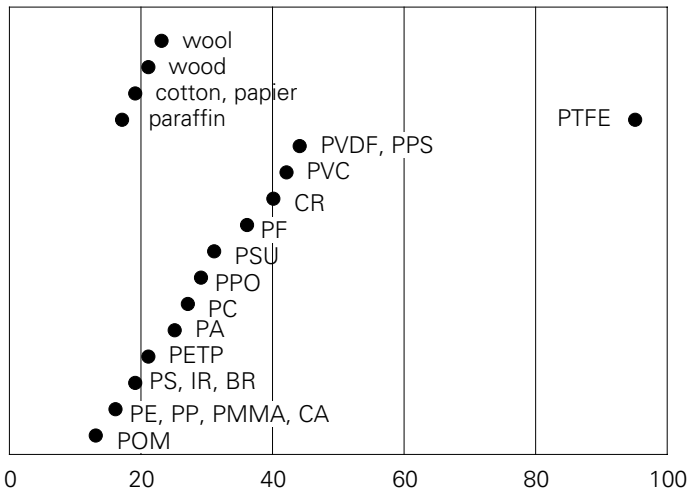


Figure 8.7. Oxygen index.

8.2. Electrical properties

8.2.1. Electric resistance

Plastics are excellent electric *insulation materials*: in their specific resistance they exceed glass and ceramics (see Figure 8.8).

It should be remarked, however, that the specific resistance of polymers cannot uniquely be defined; the electric resistance strongly depends on the electric tension applied (Ohm's law is not obeyed), and also on the time of application of the tension. Moreover, the resistance depends on temperature; it decreases drastically upon

temperature increase (by a factor of 10 or more per 50 °C). Quite often the *humidity* of the surrounding atmosphere plays a role, especially if fillers are present or with contaminated surfaces. In these cases the resistance measured is controlled by conduction along the surface rather than through the material.

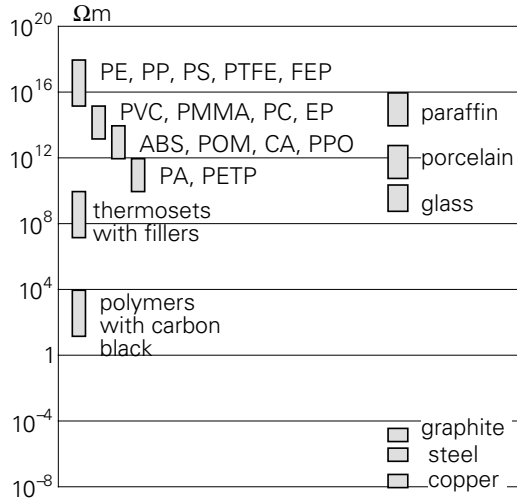


Figure 8.8. Specific resistance of some materials.

As a matter of fact, the electric resistance is of major importance for electrotechnical applications. But it also plays a role in the frequently met phenomenon of *electrostatic charging*. With all kinds of materials, charges are transferred when two bodies are brought into contact or slide against each other. A low electrical resistance causes immediate discharge, but with good insulators the charge remains present after breaking the contact. The high electric tensions which go accompanied with these charges, give rise to dust attraction, sticking together of films, or even the formation of sparks.

A rough estimation of the amount of charging can be made by considering a block of material, with thickness d and area A , as a resistance R and a capacitor C in parallel (Figure 8.9).

An initially present electric voltage V_0 will relax with time according to:

$$V = V_0 \cdot \exp(-t/RC)$$

Now:

$$R = \rho \cdot (d/A) \quad (\rho = \text{specific resistance})$$

$$C = \varepsilon \cdot (A/4\pi d)$$

(ε is the dielectric constant, the product of ε_0 , the dielectric constant in vacuum, and

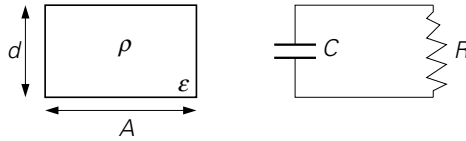


Figure 8.9. Model for electrostatic charging.

ϵ_r , the relative dielectric constant).

The relaxation time, $\tau = RC$, is then:

$$\tau = \epsilon \rho / 4\pi = \epsilon_0 \cdot \epsilon_r \cdot \rho / 4\pi$$

After converting electrostatic units to SI units, and assuming that $\epsilon_r = 2$ to 4, this leads to

$$\tau \approx 3 \cdot 10^{-11} \cdot \rho.$$

If we require, for instance, that most of the transferred charge should disappear within 1 msec ($\tau = 10^{-3}$ sec), then ρ should be smaller than $3 \cdot 10^7 \Omega\text{m}$. This seems a realistic value to prevent the formation of sparks. A much less stringent requirement is the absence of dust attraction; for that purpose τ should be lower than 100 or 1,000 sec; the maximum specific resistance would then be about $10^{13} \Omega\text{m}$, which is, indeed, the order of magnitude mentioned in technical brochures for the prevention of dust patterns on articles.

The tendency to form electrostatic charges could, therefore, be decreased by increasing the conductivity of the polymer. To obtain drastic effects in this direction, *carbon black* is added to the polymer; for less stringent requirements, *antistatic additives* are used, which, blended into the polymer in small quantities, tend to migrate to the surface and form a very thin surface layer, which considerably reduces the surface resistance, and which is continuously renewed.

An even better effect is created by blending the polymer with metal fibres, e.g. for shielding electric fields. Even a small amount of these fibres is able to form a network, which considerably increases the conductivity.

A step further leads to the *conducting polymers*, a very special class of macromolecules, which contain conjugated double bonds in the main chain (alternating single and double bonds, $-\text{C}=\text{C}-\text{C}=\text{C}-\text{C}=\text{C}-$, such as polacetylene). As such these polymers are not yet conductive; they are doped by adding or subtracting electrons (e.g. with iodine or NH_3 , resp.). The mobile charge carriers formed this way provide the conductivity, which can reach values up to those of metals! An extra advantage is that the oxydation and reduction processes are reversible. This opens

the possibility to use these polymers e.g. as the positive electrode in rechargeable batteries, together with, e.g., a lithium cathode.

8.2.2. Dielectric properties

The most important dielectric properties are the dielectric constant, ϵ , and the dielectric loss factor, $\tan \delta$. These properties are of interest for alternating currents; ϵ indicates the polarizability in an electric field, and, therefore, it governs the magnitude of the alternating current transmitted through the material when used in a capacitor. For most polymers ϵ is between 2 and 5, but it may reach values up to 10 for filled systems.

Of more importance is the *loss factor*, $\tan \delta$, denoting the fraction of the transmitted alternating current lost by dissipation in the material. Here large differences occur between polymers, as indicated in Figure 8.10. It appears that polymers with the highest specific resistance also show the lowest dielectric losses. It should be remarked, that the values given are very schematical; the losses are strongly dependent on frequency and temperature.

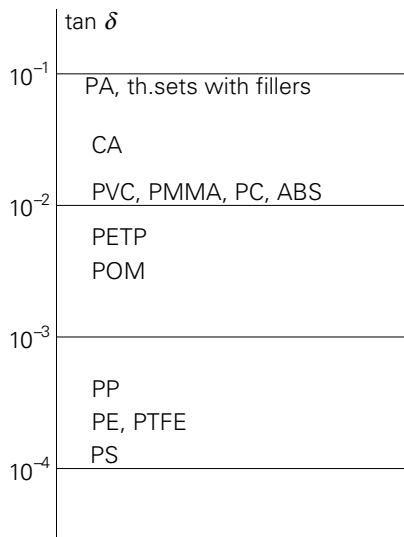


Figure 8.10. Dielectric loss factor.

As a matter of fact, these properties are highly relevant for electrotechnical applications, in particular at high frequencies (losses are proportional to the product of loss factor and frequency). The extremely low loss factor of polyethylene has enabled the use of radar in the second world war.

But also in plastics processing technology the loss factor plays a role. A not too low

value enables the *heating-up of a polymer mass* with the aid of a high-frequency alternating electric field. The heat is then generated throughout the whole material, so that the disadvantages of the low heat conductivity are evaded. Polymers with a very low loss factor are not suitable for such a process: PE and PP films cannot be welded by a high-frequency field. If such a process is explicitly required, for instance to avoid shrinkage when welding biaxially oriented film, a thin layer of a second polymer with a higher $\tan \delta$, is sometimes added by co-extrusion (see § 11.5.6).

8.2.3. Electric strength

For constructors of electrical equipment it is often of importance to know the maximum electric tension which a material can bear without showing breakdown. When studying electric failure, we notice an analogy with mechanical failure, which was discussed in § 7.4: the electric breakdown tension is also *time dependent*. So the question is, which level of stress can be applied so that within a certain period of time no breakdown will occur. When we try to find this level by extrapolation from short-term test results, we meet the same difficulties as with mechanical stresses: it appears that failure can occur by two different mechanisms. At high tensions breakdown is governed by the conductivity or the dielectric losses; the heat developed brings about a temperature increase, often resulting in higher losses. This goes on until the material softens or degrades, followed by electrical breakdown. At lower tensions a narrow conducting path may develop slowly, often branched and irregularly shaped, which eventually leads to local breakdown without overall heat development (comparable to brittle crack formation, discussed in § 7.4.2).

The temperature plays, of course, a role in both mechanisms; the electric strength decreases with increasing T . Moreover, though expressed in volts per meter thickness, it *depends on the thickness* (again: non-linearity). Thin films have a considerably higher strength than most values found in tables of properties, which are results of tests on thicker samples.

As we noticed with the resistivity, the electric strength is also largely governed by the nature of the surface. *Contaminations* may give rise to tracking currents along the surface which locally develop so much heat that the material scorches and arc-discharges occur, leading to fire risks. PVC and phenolic resins have a poor resistance against tracking, as well as thermosets filled with wood flour. A high resistance is shown by, i.a., PE, PMMA, PA and PS.

8.3. Optical properties

Most plastics transmit light, often better than glass. *Transparency*, however, is

shown by fully homogeneous systems only. When more phases are present, the components have, nearly always, a different refraction index, so that light is scattered, resulting in opacity. This is the case with rubber-modified polymers (high-impact PS, ABS etc.), with polymers containing fillers, but also with *semi-crystalline polymers*. In the latter case crystalline and amorphous regions are present, which differ in refraction index. Only if the crystallites are very small, and the scale of dispersion is small with respect to the wave length of the light, can a semi-crystalline polymer be transparent. This can be reached by quenching (e.g. thin PP film) or by the application of nucleating agents. Also *chain orientation*, uniaxial as well as biaxial, promotes the transparency; orientation creates a large number of crystallization nuclei. By exception, the refractive indices of both phases may be equal, such as in the transparent PMP.

Fully amorphous polymers may be transparent, such as PVC, PMMA, PC and PS. They can, in principle, be applied in the optical industry for spectacles, simple photographic lenses etc. For precision optics they are less suited, since because of volume retardation as well as by the fact that they are often manufactured by injection moulding, they cannot meet the requirements of narrow dimension tolerances. Moreover, their low resistance to scratching is a disadvantage in optical applications.

A special application of the high light transmittance of some polymers is the flexible light conductor, the so-called *fibre optics*. This is a bundle of PMMA fibres, in which each fibre is coated by a thin layer of another polymer, e.g. PE. Due to total reflection at the wall, light can be transported without noticeable loss of intensity along such a fibre, so that images can be transferred.

Though an amorphous glassy polymer may be perfectly transparent, it may show optical *anisotropy*, which means that the refractive index depends on the direction; the material is then birefringent. This birefringence is brought about by stresses such as external loading or internal cooling stresses, but also by frozen-in rubberelastic deformations or chain orientations. The latter are caused by the viscoelastic behaviour of a molten polymer (see § 5.3.3), and are frozen-in when the material is cooled to below its T_g before the elastic stresses are relaxed. In some critical applications, such as compact discs, birefringence is highly unwanted (see also § 5.4).

8.4. Effects of environment

Properties of plastics are affected by the *environment* in various ways, as is also the case with other materials, sometimes even to a much higher extent (wood, iron, etc.).

Factors of importance are: oxygen in the air, light, water, chemicals, bacteria, etc.

Oxygen causes, at ambient temperature, a very slow oxydative degradation; at higher temperatures the attack proceeds more rapidly. To prevent it, antioxydants are added, depending on the type of application, which protect the polymer against oxidation in a chemical way.

Light may also induce chemical breakdown; in particular the ultraviolet part of sunlight is active in this respect. Here also additives are added for protection, the *UV stabilizers*. Polymers which, by nature, are very sensitive to UV degradation, can in this way be made excellently suitable for long-term outdoors application (e.g. PP). In very demanding applications, the sunlight can be completely excluded by adding a small amount of carbon black to the polymer. The resistance against sunlight can be estimated on the basis of laboratory tests in which samples are exposed to a strong light source with about the same spectral composition as sunlight. This enables a 3 to 5-fold acceleration of the effect. Sometimes also the weather is simulated in such a test by alternating exposure to rain, radiation and temperature changes. Though these tests provide a first impression of the weathering resistance, they cannot completely replace tests in the real atmosphere. A series of results, obtained in different climates and in the “Weather-o-meter” is, as an illustration, given in Figure 8.11.

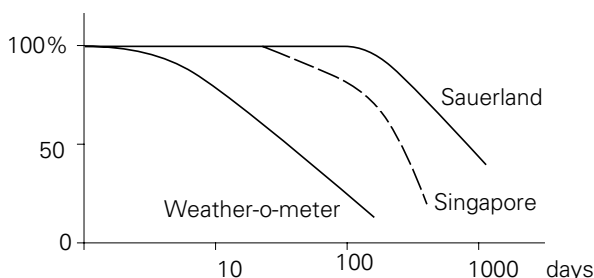


Figure 8.11. Decrease of impact strength by ageing.

The consequences of oxydative and thermal breakdown of a polymer are: discolouration, surface roughening, embrittlement, etc.; for rubbers: tackiness, followed by embrittlement. For electrical applications oxidation goes accompanied by a strong increase in the dielectric losses, and a decrease in insulation resistance and breakdown strength.

Moisture has, in itself, usually not much effect on polymer properties, though the amount of moisture which can be absorbed by polymers varies within wide limits (between zero and a few %). Logically, the electric properties such as resistivity and dielectric losses are the most sensitive to water. As to mechanical properties, nylons show the strongest dependence on water absorption. PA-6 is able to take up a

considerable amount of water, which acts as a plasticizer, in other words: it reduces the glass-rubber transition temperature by some tens of °C.

Though in general polymers are non-corrosive and resistant against chemical attack, they show, in some cases, weak spots. Ester groups are more or less sensitive to bases and acids. A global impression of the chemical resistance of some polymers is given in the following survey

Excellent *resistance to acids* as well as *bases* is shown by a.o. PTFE and PVC. Also PS, PE and PP have a very good general resistance, but they are damaged by some strong (oxidizing) acids in prolonged exposure. Polyamides, acrylates and cellulose plastics are less resistant to some acids; sensitive for bases are, a.o., cellulose plastics, polyamides, PC and some formaldehyde resins.

A different question is, whether polymers can withstand the influence of *organic liquids*. Several of these are active as solvents or swelling agents, so that the polymer, although not chemically attacked, loses its properties upon exposure. An example is PVC, which softens and swells in acetone and in aromatic hydrocarbons such as benzene. Most rubbers swell in aromatics, cellulose plastics are sensitive to alcohol and acetone. PS is soluble in aromatics; practically all thermoplastics are sensitive to chlorinated hydrocarbons, etc. A good resistance against most organic solvents is shown by PTFE, PA, POM, PP and PE, the two latter ones, however, not at elevated temperatures. Most thermosets are not affected by organic liquids.

8.5. Stress corrosion

Narrowly related to the effect of chemicals, discussed in the preceding section, is the phenomenon of *stress corrosion*. This is the formation of cracks under the simultaneous influence of a mechanical stress and a certain chemical environment; neither the stress nor the environment can, separately, cause the same mechanical damage, unless at a much longer time scale.

Typical examples of stress corrosion are: crack formation in strained rubber vulcanizates under the influence of ozone, hair cracks in PE under stress in the presence of a surface active agent (see also § 7.4.2), crack formation in PC, when exposed to e.g. CCl₄, within a few seconds after the application of a small stress.

The mechanisms of stress corrosion can be quite different: in the case first mentioned the effect can be explained by a *chemical reaction*, which leads to irreversible mechanical damage when the material is under stress. In the second case we could think of a *physical acceleration* of a process of *crack formation*, which, otherwise, would take a much longer time under stress; because of the lower interfacial tension

less work is required to create new surface in the crack region. Since, in this case, no chemical reactions take place, the expression “environmental stress-cracking” is to be preferred.

General rules for the occurrence of stress corrosion cannot be given, since the phenomenon is very specific for certain combinations of polymer and environment, and is also dependent on the processing conditions in manufacturing the article (such as the occurrence of cooling stresses and orientations). When plastics are used in articles which are subjected to mechanical stress, such as pipes, crates, bottles, screw-caps, etc., the risk of stress corrosion in the presence of fat, soap or organic liquids, should always be taken into account. Proper choice of material and dimensions can minimize the occurrence of crack formation.

8.6. Diffusion and permeability

Various low-molecular substances are more or less soluble in polymers, and are, therefore, absorbed when in contact. Within the polymer such a substance can diffuse to a place where the concentration is lower, and can leave the polymer elsewhere. This means that the polymer is permeable to the low-molecular substance. Obviously, the permeability, P , is governed by the *solubility*, S , and the *rate of diffusion*, D ; it appears that $P = S \cdot D$.

The permeability of polymers to gases and water vapour is of practical relevance. Between polymers considerable differences exist. For instance, for oxygen, polyvinylidene chloride, PVDF, is 1000 times less permeable than low-density polyethylene, LDPE. The permeability for liquids and vapours is strongly influenced by the swelling which the polymer undergoes when taking up small quantities of these substances. Even a minor degree of swelling brings about a large increase in the rate of diffusion. Therefore, water vapour permeates much more rapidly than gases; moreover the rate of permeation strongly depends on the water vapour concentration.

An impression of the order of magnitude of the permeability of some polymers for nitrogen and for water vapour is given in the table below, in which the permeability is expressed as the volume (cm^3) passing per unit of area (cm^2) when the layer thickness is 1 cm, and the pressure difference of the gas or vapour on opposing sides is 1 bar.

for nitrogen:

| | | |
|------|------------------|-------------------|
| 0.01 | $\cdot 10^{-10}$ | PVDC |
| 0.1 | | PETP, PA-6 |
| 1 | | PVC |
| 10 | | HDPE, PS, PP, IIR |
| 100 | | LDPE, SBR, IR |
| 1000 | | |

for water vapour (95% relative humidity):

| | | |
|------|-----------------|---------------------|
| 0.1 | $\cdot 10^{-7}$ | PVDC |
| 1 | | HDPE, PP, LDPE |
| 10 | | PETP, PVC, PA-6, PS |
| 100 | | PMMA, IR, PVAc |
| 1000 | | |

A few general trends can be recognized from this table, in particular as far as the effect of diffusion is concerned. Rubbers, with their high *free volume*, allow a small molecule to diffuse much faster than a glassy polymer. With semi-crystalline polymers above T_g , such as PE and PP, the rubbery phase gives rise to a higher rate of diffusion than when the amorphous phase is in the glassy state. Deviations from this simple pattern can be attributed to differences in solubility (see also Qu. 8.16 and 8.17).

Plasticizers, antioxidants etc. sometimes show the tendency to migrate to the surface, and thus to exude from the polymer. This tendency to migration is, in most cases, unwanted, since the material gradually loses the properties obtained by the presence of the additive, such as flexibility or chemical stability.

In some cases, however, the use of additives is based on their migration to the surface: antistatic additives, and also agents to reduce friction of films, perform as desired when they are present on the surface of the article, forming a thin skin.

A special problem is the migration of low-molecular substances in materials used for *food packaging*. Here very stringent limitations on food contamination by compounds which are possibly harmful for health, are necessary. This complicated area is being studied carefully over the past decades, in order to establish for each type of additive or monomer residue what its effect on the human organism could be, and how much of such a substance could, under certain conditions, be expected to migrate from the packaging into the food.

9

Polymeric compounds and composites

9.1. Polymer blends

9.1.1. General

Polymers are being blended in the fluid state. The first question is: are the polymers miscible? We can distinguish between two cases:

- *miscible*; then a real blend is formed on a molecular scale; the individual components have “disappeared”.
- *immiscible*; we have a dispersion in which both components retain their own identity.

Both types of blends are being used. Some examples:

- *real blend*: Noryl, a blend of polyphenylene ether (PPE) with polystyrene (PS). PPE has a high T_g , a high price, and is difficult to process. PS has a much lower T_g , and is cheap. The blending ratio can be adjusted; three levels are commercially available.
- *dispersion*: an example is high-impact polystyrene (TPS or HIPS), a dispersion of rubber in PS. This blend is, necessarily, a dispersion, since impact energy should be damped out in the rubber particles, which also stop developing cracks. Analogous dispersions are high-impact modifications of PP, PA and PVC, and ABS.

In most cases polymer pairs are immiscible. Dispersions occur most often, real mixtures are exceptions.

9.1.2. Miscibility of polymers

The first criterion of miscibility is of a thermodynamic nature:

$$G_{AB} < G_A + G_B \quad \text{or} \quad \Delta G_m < 0$$

(free enthalpy of mixing negative), so

$$\Delta H_m - T \cdot \Delta S_m < 0.$$

- ΔH_m is the *enthalpy of mixing*, and is governed by the interactions between the polymers

$$\Delta H = V \cdot (\delta_1 - \delta_2)^2 \cdot \phi_1 \cdot \phi_2 \quad \text{so } > 0 .$$

δ_1 and δ_2 are the solubility parameters, ϕ_1 and ϕ_2 the volume fractions of the components. With strong interactions (hydrogen bridges or polarity), H can be < 0 (exotherm); this promotes miscibility.

- ΔS_m is the *gain in entropy* upon mixing; it is always positive due to the greater number of possibilities to place chain segments (more disorder in the mixture). The entropy of mixing is strongly dependent on the chain length, or the degree of polymerization, P .

Figure 9.1 presents a simple illustration for $P = 3$ in comparison with $P = 1$ (monomer); when the monomers (o and +) are blended, there are 20 possibilities for their mutual positions in the blend (only one in the unblended condition), so:

$$\Delta S = k \cdot \ln (W_2/W_1) = k \cdot \ln 20$$

for $P = 3$ there are only six possibilities, so $\Delta S = k \cdot \ln 6$.

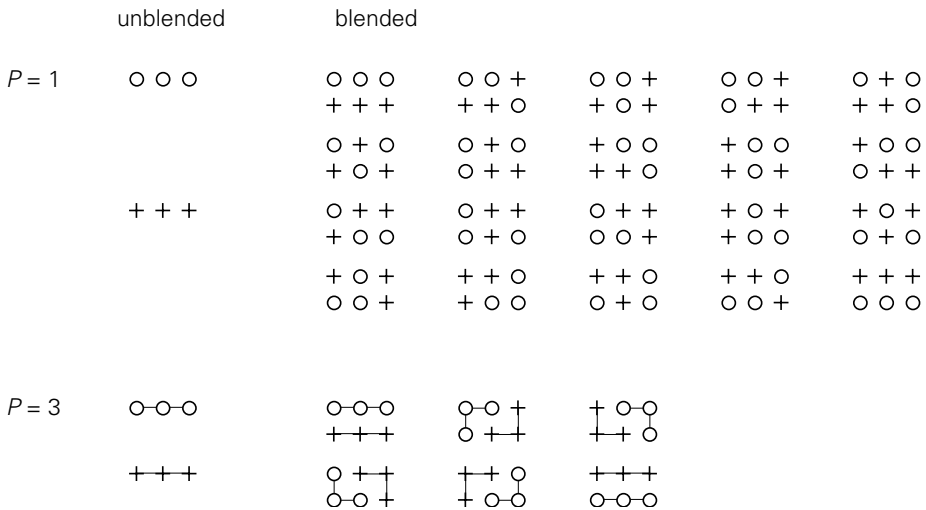


Figure 9.1. Simple illustration of entropy of mixing.

Application of conformation statistics results in a value of ΔS_m . Combination with ΔH_m gives the Flory-Huggins relation:

$$\frac{\Delta G_m}{V} = kT \cdot \left[\frac{\phi_1}{V_1} \cdot \ln \phi_1 + \frac{\phi_2}{V_2} \cdot \ln \phi_2 + \frac{\chi}{V_s} \cdot \phi_1 \cdot \phi_2 \right]$$

where ϕ_1 and ϕ_2 are the volume fractions, V_1 and V_2 the sizes of the molecules, χ the interaction parameter and V_s the interaction segment size. It appears that the first two terms, the entropy contributions, both negative, approach to zero with strongly increasing chain length.

The first condition for miscibility, $\Delta G_m < 0$, is not always sufficient for the formation of a homogeneous blend. The *kinetics of blending* also plays a role; in the blending process the domain sizes have to be sufficiently reduced before complete mixing by diffusion can take place. *Diffusion* is a slow process, so that homogeneous mixing can only be reached after a long time of mixing.

Moreover, not only the sign of ΔG_m counts, but also *the shape* of the curve of ΔG_m versus volume fraction ϕ . The simplest case is shown in Figure 9.2a, where the sign of ΔG_m is the decisive factor. The situation is more complicated with, for instance, Figure 9.2b; though ΔG_m is here negative for all blending ratios, the maximum in the curve at about $\phi = 0.5$ causes an instability.

Independent of the level of the curve (of the sign of ΔG_m), a small disturbance, caused by a local difference in concentration, will bring about an increase of ΔG_m when $\partial^2 G_m / \partial \phi_1^2 > 0$, and will, therefore, disappear; the blend is stable (Figure 9.2c). When the curve is, however, convex, with $\partial^2 G_m / \partial \phi_1^2 < 0$, a minor distortion will grow, initiating segregation; the system is not stable (Figure 9.2d).

For a situation where $\partial^2 G_m / \partial \phi_1^2 > 0$, but in the vicinity of a point of inflection ($\partial^2 G_m / \partial \phi_1^2 = 0$), a large disturbance may initiate segregation; the system is in a metastable condition (compare an upright standing pencil). The point of inflection is called the *spinodal* (Figure 9.2b and 9.2e).

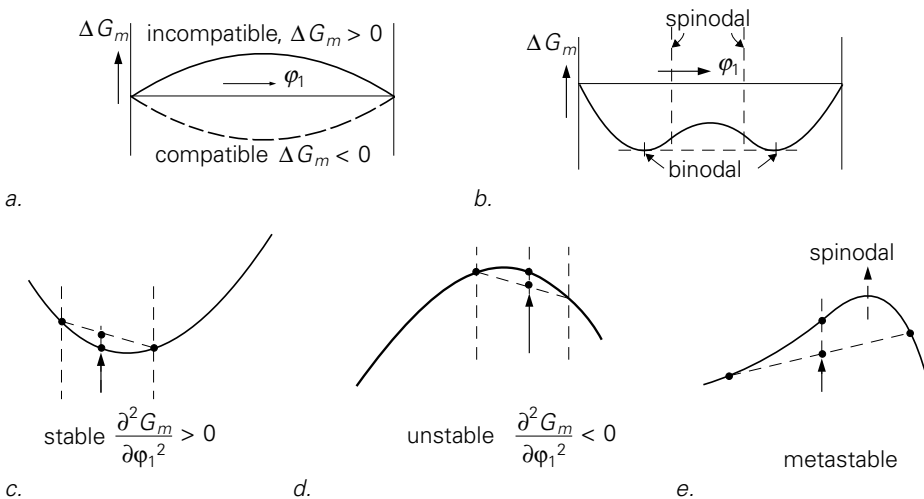


Figure 9.2. Various cases of miscibility.

With changing temperature the curves change; for spinodals and binodals (the points of contact with the common tangent), plotted as T against φ_1 , a picture as shown in Figure 9.3 may be obtained. In this case a “lower critical solution temperature”, LCST, exists, which is a maximum temperature at which, for every blending ratio, a stable homogeneous blend is possible. An “upper critical solution temperature” (UCST) may also exist; in that case the curves are upside down. Besides, more complicated cases are possible (see also Qu. 9.4 tu. 9.7).

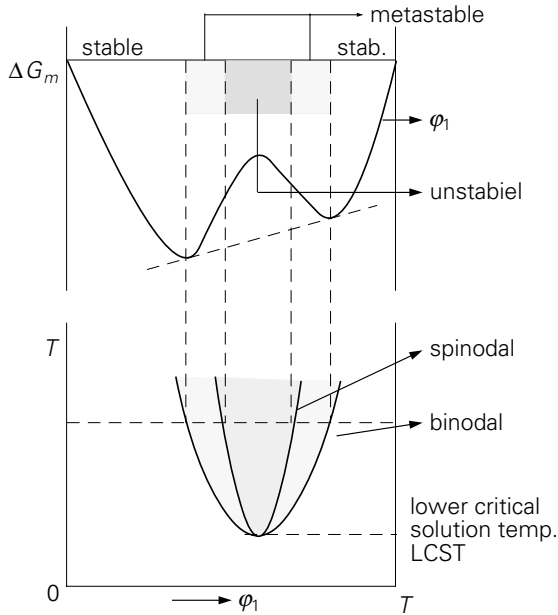


Figure 9.3. Binodals and spinodals.

9.1.3. Detection of miscibility

Microscopic or electron microscopic observations on solid blends provide information on the homogeneity or the degree of dispersion in a polymer blend. An effective method is also the analysis of the *glass-rubber transition(s)*. The presence of a single glass-rubber transition, in between the transition temperatures of the components, indicates homogeneity of the blend (see also § 3.5). However, the glass rubber transition occurs when large chain parts, of about 20 to 60 segments, acquire free mobility. A single T_g , therefore, indicates homogeneity on that scale, and not necessarily on the scale of single segments.

T_g can be determined by dynamic mechanical experiments from the $\log E-T$ diagram, but also from the maximum in the $\tan \delta - T$ curve. Another possibility is differential scanning calorimetry (DSC).

Figure 9.4 gives some possible pictures of $\log E-T$ curves (already partially

mentioned in § 3.5). Figure 9.4a refers to one extreme: a *homogeneous blend*, where the curve does not show any sign of the transition of the individual components. Figure 9.4b holds for the other extreme: it denotes the behaviour of a *pure dispersion*, in which A and B retain their own individuality.

Figure 9.4c and 9.4d represent *intermediate cases*; 9.4c indicates partial miscibility; we see a two-phase system of AB blends with different A/B ratios. This might be the result of segregation into the binodals. Figure 9.4d is called an “interphase” or a “multiphase” blend. The system is quasi-homogeneous, but it contains all A/B ratios between $\varphi_1 = 0$ and $\varphi_1 = 1$. It looks like a system with concentration gradients as a result of non-completed diffusion in a combination of well-compatible polymers.

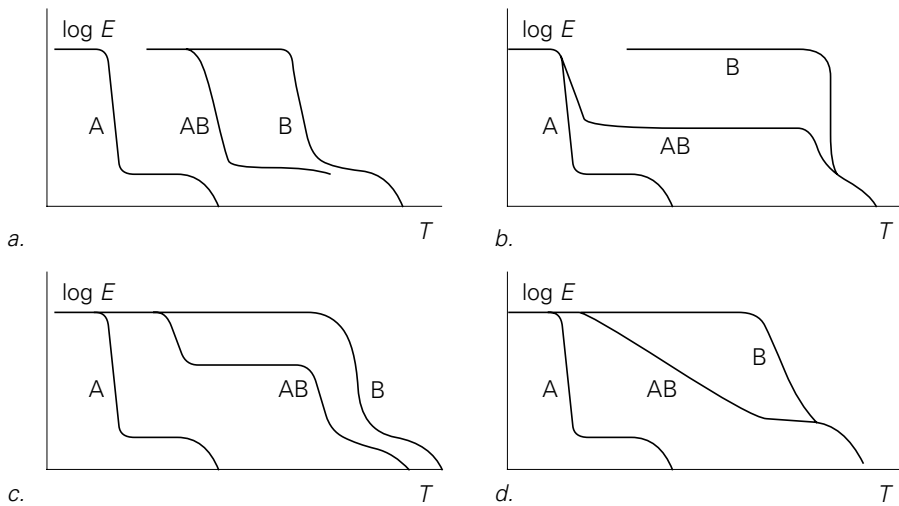
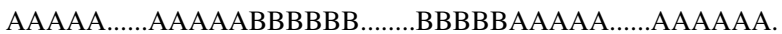


Figure 9.4. $E(T)$ for various types of blends.

9.1.4. Block copolymers

Block copolymers are a special case of two-phase systems. They are not real blends, since their components are tied together in one and the same chain. An example is: ABA:



If the homopolymers A and B are incompatible, the copolymer may show *segregation*. The A-segments and the B-segments are then located in separate *domains* (Figure 9.5).

A B A

The following questions are relevant:

- when does segregation occur?

- what is the size of the domains?
- how are the domains shaped?

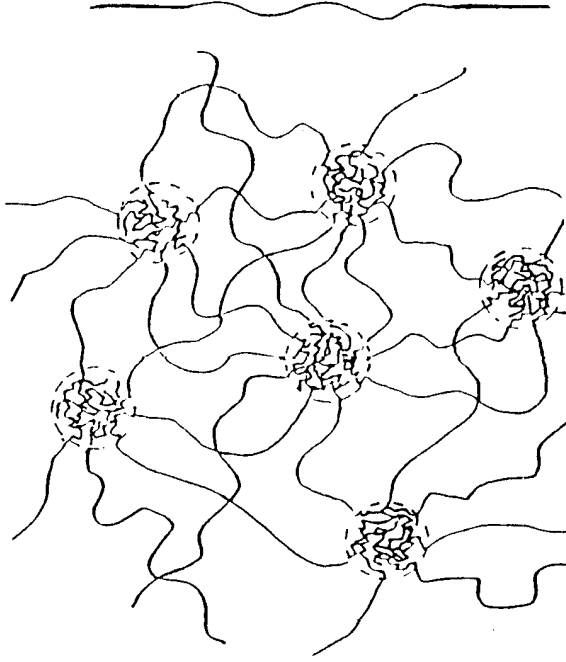


Figure 9.5. Domain formation in a block copolymer.

In some cases these questions can be answered by rigorous thermodynamical treatment, again on the basis of the formula $\Delta G = \Delta H - T \cdot \Delta S$, in which Δ now denotes the difference between between the randomly mixed and the segregated condition. The approach starts, compared with that on mixing, at the opposite side, namely not from the conformation possibilities in the mixed condition, but now in the segregated system.

The entropy difference is written as:

$$\Delta S = \Delta S_1 + \Delta S_2 + \Delta S_3$$

in which each of the terms represents one aspect of the ordering into domains, namely:

- ΔS_1 : all A-segments are present in an A-domain and all B-segments in a B-domain;
- ΔS_2 : All A-B connections are situated in the interface between A and B-domains;
- ΔS_3 : Within a domain the chain conformations are restricted in comparison with a “random flight” situation.

Moreover, an interfacial free energy term, G_s , is present, so that:

$$\Delta G = \Delta H + G_s - T(\Delta S_1 + \Delta S_2 + \Delta S_3)$$

The result of this approach for the three-block copolymer SBS (styrene-butadiene-styrene) is as follows:

- The critical molar mass, above which segregation occurs, M_{cr} , is 2.5 to 5 times greater than for equivalent blends. This means a better “miscibility” of block copolymers, as a result of the entropy restrictions in the domain structure.
- The domain size can be calculated; for a certain copolymer it amounts, e.g., to 30 nm.
- The *morphology* depends on the A/B ratio: when $A/B < 0.2$, ΔG is smallest for *spheres*, up to 0.3 for *cylinders*, and above 0.3 for *lamellae*. At $A/B \approx 0.5$ we find lamellae of A and B; at higher A/B the pattern repeats itself in the reverse direction, while the roles of A and B are exchanged (Figure 9.6). With cylinder morphology the cylinders can be oriented in elongational flow; by further *annealing* they grow into continuous “fibre reinforcement”. The properties are then strongly anisotropic: the stiffness in the direction of orientation is many times higher than across (if the cylinders are polystyrene domains). After special annealing treatment highly regular structures have been obtained with cylinders (with a diameter of 20 to 30 nm) packed in a perfect hexagonal order. But also an extruded sheet clearly exhibits *anisotropy*.

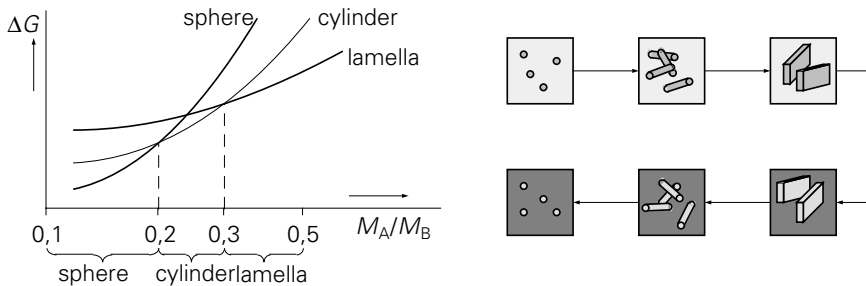


Figure 9.6. The morphology depends on the monomer ratio.

The desirability of segregation in block copolymers can be demonstrated by considering the behaviour of SBS, which is one of the oldest types. It has about the same chain composition as SBR, but, rather than SBR, it shows *two glass-rubber transitions*, namely that of polybutadiene and that of polystyrene. Between these two temperatures it behaves as a rubber, in which the PS domains act as cross-links; it is, therefore, a “*self-vulcanizing*” rubber (see also Figure 3.8; see Qu. 9.14). Moreover, the hard domains play the role of a reinforcing filler.

Above the T_g of PS, the domains soften, so that the polymer can be processed as a

thermoplast, a “thermoplastic rubber” or “*thermoplastic elastomer, TPE*” . In the fluid condition polybutadiene and polystyrene are still incompatible, so that domains are continuously being formed and disrupted. The viscosity is, therefore, higher than that of SBR with the same S/B ratio. Moreover, the domains in the fluid are responsible for the existence of a small yield stress.

Another example is even older: the thermoplastic elastomers based on polyurethane; their chains contain a number of blocks, alternatingly “hard” and “soft” PU blocks. (elastic yarns, such as “Lycra” and “Spandex”).

If the hard blocks are longer than the soft ones, such as in SBS with a high styrene content, the hard phase will be continuous, and the rubbery phase is present as domains (see Figure 9.6). In such a case SBS behaves as a high-impact PS. Another example of this type is a PP/EP block copolymer; tails of EP (random copolymer of ethylene and propylene) on the PP chains segregate into rubbery domains in the PP matrix, which improve the impact strength.

Newer developments are: polyester/polyether block copolymers (Hytrel, Arnitel), etc. By choosing various levels of block length ratio, a broad spectrum of stiffnesses (or hardnesses) can be obtained, which practically *fills the gap between rubbers and thermoplasts*. TPE’s form a rapidly growing class of materials, which find an increasing number of applications.

9.1.5. The formation of dispersions

When immiscible polymers are blended in the fluid condition, a dispersion is formed. Starting from the original dimensions (granules or powder), the size is gradually reduced down to m scale. In the mixing device the melt is subjected to shear flow and elongational flow; in both of these the domains deform and can break up. When a sphere is deformed into an ellipsoid, its surface area increases and thus its interfacial energy, until the retracting force, exerted by the interface, balances the force exerted by the flow field. Larger droplets hardly meet any counteracting force; the smaller ones attain a stable deformation.

The governing parameter in this process is the *Weber number*, $C_a = 1/k$, with

$$k = \frac{\sigma}{\dot{\gamma}\eta_c R} = \frac{\sigma/R}{\dot{\gamma}\eta_c} = \frac{\sigma/R}{\tau}$$

in which σ = interfacial stress
 $\dot{\gamma}$ = rate of shear
 η_c = viscosity of the continuous phase,
 R = initial radius of the sphere,

τ = shear stress

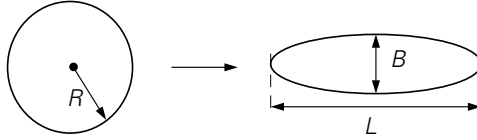


Figure 9.7. Deformation of a spherical droplet.

Cox deived:

$$D = \frac{L - B}{L + B} = \frac{5(19\lambda + 16)}{4(\lambda + 1)[(19\lambda)^2 + (20k)^2]^{1/2}}$$

with

$$\lambda = \eta_d / \eta_c = \frac{\text{viscosity droplet}}{\text{viscosity continuous phase}}$$

For $\lambda < 1$ this can be approximated by:

$$D \approx \frac{1}{k} \cdot \frac{19\lambda + 16}{16\lambda + 16} \approx \frac{1}{k} = \frac{\dot{\gamma} \eta_c R}{\sigma}$$

The droplet breaks at $D \approx 0.5$, dus $\dot{\gamma} \eta_c R \approx \sigma/2$. This is Taylor's formula for the critical shear rate at which break occurs:

$$\dot{\gamma}_b = \frac{\sigma}{2\eta_c R} \cdot \frac{16\lambda + 16}{19\lambda + 16}$$

Smaller droplets need a higher shear rate to break. At constant $\dot{\gamma}$ there is an *equilibrium drop size*:

$$R \approx \frac{\sigma}{2\eta_c \dot{\gamma}}$$

Complications may arise as a result of:

- non-Newtonian behaviour (η depends on $\dot{\gamma}$),
- elastic behaviour of molten polymers.

It is possible to take these effects into account, but the actually found scale of dispersion in practical blending operations is never properly matched by these calculations; the observed particles are much bigger (up to ten times) than according to the Taylor equation. The explanation of this discrepancy is *coalescence*: small droplets join together when they collide.

In a collision, droplets are flattened; a condition for the occurrence of coalescence is, that, within the time scale of passing each other, the layer of liquid polymer between the droplet can be squeezed out until a critical distance of approach has been reached. The rate of approach of the flattened surfaces strongly depends on the nature of the interface; this can be “rigid” or “mobile” :

- *rigid*: the interface can withstand tangential stresses without flow occurring along it.
- *mobile*: the interface is able to move.

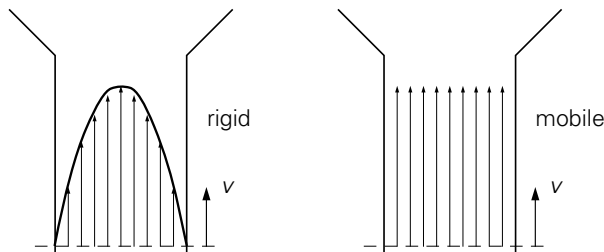


Figure 9.8. A rigid and a mobile interface.

The velocity profile in both cases is sketched in Figure 9.8; with a mobile interface the rate of approach is much higher than with a rigid one, resulting in a higher probability of coalescence. In most cases a rigid interface is met, as a result of contaminations; very low concentrations of a surface active agent (10^{-10} g/mole) are already sufficient. With polymer-polymer interfaces there are, however, indications that the interface is mobile. This means that, in a blending process, a continuous succession of break-up and coalescence occurs, so that the resulting droplet size is much greater than expected from Taylor’s formula. It has been observed that at very low concentrations ($< 0.5\%$) small droplets, approximately according to Taylor, are formed; the chance of collision is then much smaller. With increasing concentration the droplet size increases strongly.

The role of surface-active agents may, with a pair of polymers A and B, also be played by a two-block copolymer AB. It has been observed that a small addition of AB results in a considerably finer dispersion in the blend. This can be explained in two ways:

- The interfacial tension is decreased as a result of the presence of AB; the Taylor formula then predicts a smaller droplet size;
- The interface becomes rigid, so the chance of coalescence decreases.

If the interfacial tension is too small or the droplet too big, the retractive forces may be too small to counteract the droplet deformation; in such a case threads may be formed. Such a thread is, in general, not stable; a small *distortion* as a deviation from

the cylindrical shape may grow (Rayleigh, 1878). The growth of such a distortion is schematically represented in Figure 9.9.

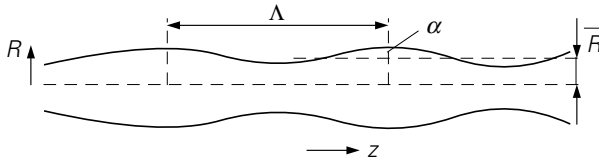


Figure 9.9. Instability of a cylindrical fluid thread.

When $R(z) = \bar{R} + \alpha \sin(2\pi z/\Lambda)$ the thread is unstable for $\Lambda > 2\pi\bar{R}$; with increasing amplitude α the total surface area will then decrease (which is, at first sight, surprising!). α then grows exponentially:

$$\alpha = \alpha_0 \cdot \exp qt$$

q is a complicated function of all variables; it shows a maximum as a function of the wave length Λ at Λ_m . Λ_m is, therefore, the “*dominant wave length*”: with an arbitrary pattern of disturbances (a broad spectrum of wave lengths) the disturbance with Λ_m will grow the fastest and will lead to a split-up of the thread into droplets.

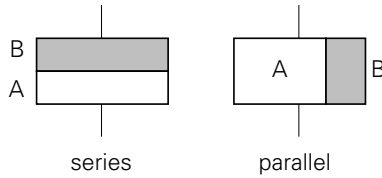
This splitting-up is driven by the interfacial tension, which causes pressure differences between parts of the thread with positive and negative curvature. Only the viscosity counteracts the growth of the distortion and limits its rate of growth.

Fluids with a small yield stress may, however, be stable, namely if this yield stress exceeds the pressure differences. An example: the three-block copolymer SBS exhibits a minor yield stress, which is hardly detectable, but sufficient to prevent the growth of distortions. As discussed in § 9.1.4, it is caused by the polystyrene domains. It has also been observed that, when blending SBS with another polymer, it shows, even at very low concentrations, a pronounced tendency to form a continuous phase, in other words: it does not break up into dispersed particles.

If the break-up time of threads is longer than the time of cooling, threads will also remain present after solidification. These are, however, not permanent; upon further processing by extrusion or injection moulding, the instabilities can grow further.

9.1.6 Properties of blends

An important question is, what the properties are of a dispersion blend of two polymers, A and B, when the properties of the components are E_A and E_B , and the volume fractions φ_A and φ_B . First we consider the two simplest cases: a series and a parallel arrangement.



Figuur 9.10 Series- and parallel arrangement.

For the parallel case, E (e.g. the modulus of elasticity, the electric or the thermal conductivity), can be expressed by :

$$E = \varphi_A \cdot E_A + \varphi_B \cdot E_B$$

and for series:

$$\frac{1}{E} = \frac{\varphi_A}{E_A} + \frac{\varphi_B}{E_B}$$

For, e.g., the electric resistance and the compliance the same formulae hold, but interchanged.

The general way to express the various quantities is:

Main phase: volume fraction $1 - \varphi$
property E_0

Additional phase: volume fraction φ
property E_1

$$\frac{E_1}{E_0} = \alpha \qquad \frac{E}{E_0} = f(\alpha, \varphi)$$

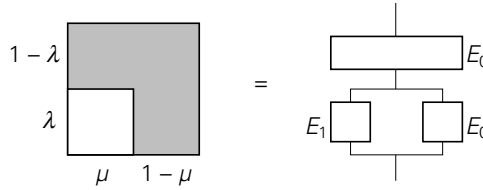
$$\text{Parallel: } \frac{E}{E_0} = 1 + \varphi(\alpha - 1)$$

$$\text{Serie: } \frac{E}{E_0} = \frac{1}{1 - \varphi(\alpha - 1)/\alpha}$$

Combinations of series and parallel provide a more realistic representation of the properties of a dispersion; instead of φ then, however, more parameters are required, e.g. (Takayanagi):

Further splitting-up necessitates the use of an increasing number of parameters, while the equations become more and more complicated.

A better theory for dispersed spheres has been given by Halpin and Tsai and by Kerner:



Figuur 9.11 Takayanagi model.

$$\frac{E}{E_0} = \frac{1 + \varphi A \frac{\alpha - 1}{\alpha + A}}{1 - \varphi \frac{\alpha - 1}{\alpha + A}} \quad \text{with } \alpha = \frac{E_1}{E_0}$$

$$\text{and } A = \frac{7 - 5\nu}{8 - 10\nu}$$

This formula is valid for the modulus of elasticity, while ν is the Poisson ratio of the matrix material. It is only valid up to $\varphi \approx 0,7$ (near the tightest packing of spheres). For higher values, from $\varphi \approx 1$ going down to $\varphi \approx 0,3$ (or lower) the structure can be reversed: the roles of the components are exchanged. We can use the same formula, but now with $1 - \varphi$ instead of φ , while α is replaced by $1/\alpha$. For $\alpha = E_1/E_0 = 100$, the curves, calculated from both formulae, are given in Figure 9.12.

Before the tightest stacking of spheres has been reached, the formula is subject to deviations, in particular if the embedded particles are not deformable, such as is the case with hard particles. The denominator of the formula is then modified as follows:

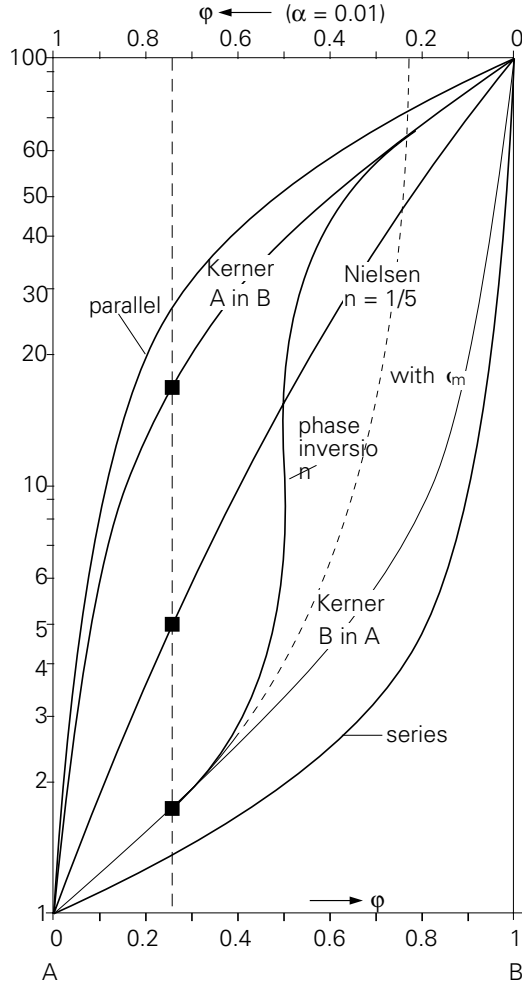
$$1 - \varphi \cdot \psi \cdot (\alpha - 1) / (\alpha + A)$$

in which

$$\psi = 1 + \varphi(1 - \varphi_m) / \varphi_m^2.$$

φ_m is the volume fraction at the tightest packing of the dispersed phase, which for equal spheres is about 0.74, so that then $\psi = 1 - 0.475 \cdot \varphi$. The curve is then steeper, as indicated in Figure 9.12. Up to $\varphi = 0.4$ the difference is negligible. With spheres of different sizes a tighter packing can be reached; the deviations are then smaller. With the inverse morphology (soft phase dispersed in a hard matrix) a similar effect occurs; the effect is, however, less pronounced, because soft spheres can more easily deform and can, therefore, attain a higher degree of filling (this is, in particular, true for foams).

At some volume fraction, mostly around $\varphi = 0.5$, phase inversion occurs; around this value, A and B are both continuous. This may, however, also happen at other values of φ , depending on the rheological behaviour of the components. Moreover, co-continuity is possible at any volume fraction (see in § 9.1.4 the remark on SBS). For the properties of a co-continuous two-phase system an expression has been derived by *Nielsen*:



Figuur 9.12 Stiffness as a function of composition.

$$E^n = (1 - \phi) \cdot E_0^n + \phi \cdot E_1^n$$

Extreme cases of this equation are:

$n = 1$ parallel arrangement

$n = -1$ arrangement in series

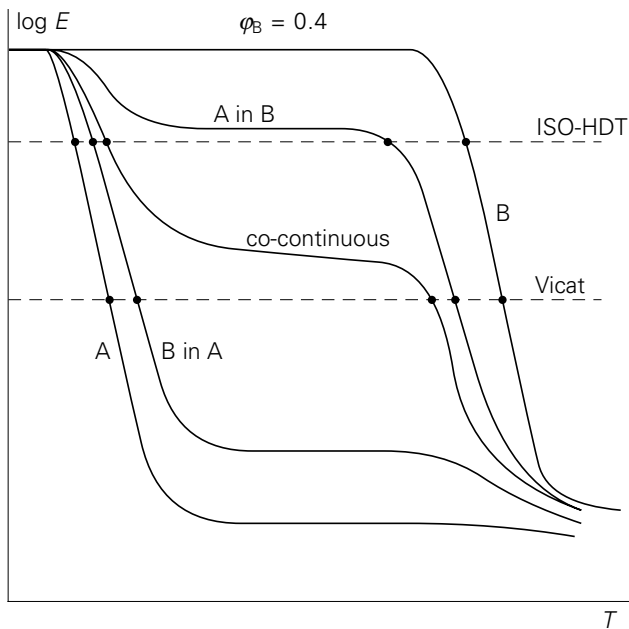
$n = 0$ $\log E = (1 - \phi) \log E_0 + \phi \log E$ (straight line on a log-log scale)

Mostly $n = \frac{1}{3}$ for heat conduction, $n = \frac{1}{5}$ for the modulus of elasticity.

Figure 9.12 shows the various possibilities. The figure demonstrates the importance of the type of dispersion with respect to the properties. When B is a stiff polymer ($E = 100$), and A a soft one ($E = 1$), we read at $\phi_B = 0.25$ the following values for E :

| | |
|------------------------|-----------|
| A dispersed in B: | $E = 16$ |
| B dispersed in A: | $E = 1.8$ |
| A and B co-continuous: | $E = 5$ |

As another example we consider two (amorphous) polymers with strongly different T_g , namely high for A and low for B. If we choose $\phi_B = 0.4$, then for each of the three types of dispersion the E -modulus can be calculated as a function of temperature from the $E(T)$ curves of the components. The result is shown in Figure 9.13, in which also the values of the ISO and Vicat softening points have been schematically indicated. It again appears that the type of dispersion has a strong effect on the properties (see also Qu. 4.24, 9.13, 9.15 and 9.23).



Figuur 9.13 Effect of morphology on softening temperatures.

Morphology control in a mixing operation is, therefore, very important for utilizing the properties of a blended-in high-performance polymer. It appears that continuity of one or both phases is often essential to obtain optimum properties. This continuity is generated in the blending process, though, unfortunately, not much is known of the ways to control it.

Continuity can also be reached by polymerizing one of the components within the other. In such a case the blend is called an IPN, an interpenetrating network; it is, in most cases formed by a thermoset in a thermoplastic polymer. An example is a compound built-up from 50% of a thermoplast (polycarbonate or polysulphone), and 50% of a cross-linked polymer on the basis of dicyanate bisphenol-A. The skeleton

of the thermoset in the thermoplastic matrix provides the material with exceptional properties. It combines the toughness and the strength of the thermoplast with the high resistance to temperature of the thermoset. When PC is used as the matrix a heat deflection temperature of 200 °C is realized (for PC: 135 °C).

9.2. Reinforcement by particles

Very often particles are blended into polymers, in thermoplasts as well as in thermosets and in synthetic rubbers. This is done for various reasons: the aim may be stiffness, strength, hardness, softening temperature, a reduction of shrinkage in processing, reduction of thermal expansion or electric resistance, or, simply, to reduce the price of the material. The fillers used are: wood flour, carbon black, glass powder, chalk, quartz powder, mica, molybdene sulphide, various metal oxides, etc. etc.

An old example of a polymer reinforced by particles is rubber with carbon black. Before 1920 this was unknown; with other, less effective fillers an automotive tyre was worn-out after 8,000 km. The much longer life (100,000 km or more) of modern tyres is, of course, due to a number of factors, but is largely brought about by the enormous effect of carbon black on the abrasion resistance. The reinforcing effect of carbon black is also demonstrated by its effect on the tensile strength of rubber vulcanizates. An unfilled, vulcanized SBR breaks at a load of 2 to 3 MPa; with carbon black the tensile strength exceeds 30 MPa. Such an enormous reinforcement is not met with any other polymer, neither with particles, nor with short fibres. Apparently something special is happening. In the first place the enormous surface area should be mentioned. Carbon black forms agglomerates, which consist of aggregates of the primary particles of a few tens of nm. In a usual formulation, for instance, 50 grammes of black are added to 100 grammes of rubber (the volume fraction of black is then 0.2), so that in a small piece of rubber thousands of m² of carbon black surface are present. Along this surface the polymer chains are tightly adsorbed, though they are able to slide along the surface in the direction of the chain; this results in a levelling of the stresses in the chain parts and thus an optimum strength.

In most cases the main effect of particles is an increase in *stiffness*, up to two or three times its original value. In the same way as with polymer blends, this increase in stiffness can be calculated theoretically, namely with the same Kerner formula as in § 9.1.6.

$$\frac{E}{E_0} = \frac{1 + \varphi A \frac{\alpha - 1}{\alpha + A}}{1 - \varphi \frac{\alpha - 1}{\alpha + A}}$$

It is interesting to consider an extreme case for very stiff spheres (α very high) at a low volume fraction. The Kerner equation can then be written as:

$$E/E_c = 1 + \varphi(A + 1) = 1 + k_E \cdot \varphi$$

With rubber as a matrix ($\nu = 0.5$), k_E has the value of 2.5, and we meet the well-known Einstein formula for the increase in viscosity as a result of the presence of spherical particles.

For non-spherical particles the relations are different; this is easiest demonstrated by the Einstein formula: the coefficient k_E increases when the particles are flattened, and even stronger upon elongation. An example of the latter case: When a sphere is extended up to a length/diameter ratio of 10, k_E increases from 2.5 to 6. Sticks and platelets, therefore, have a stronger effect; this accounts for the fact that with a volume fraction of 20 % increases in stiffness up to a factor of 3 are measured, whereas the Kerner formula would predict a much lower value.

In contrast to the stiffness, the strength of polymers is hardly influenced by “reinforcing” fillers. In most cases we observe a reduction in the ultimate strain, and often a small decrease in tensile strength and in impact strength. Here the adhesion between polymer and particle plays a substantial role; when a high shear stress induces dewetting at the interface, the chance of crack initiation is high. But also with good adhesion the particles form regions of stress concentration, which may initiate crack formation. There are exceptions in which the strength increases; the most drastic one is the effect of carbon black in rubbers, mentioned before.

9.3. Short fibres

In the foregoing we have seen the influence of the shape of particles on the increase in stiffness: longer particles have a greater effect. A logical consequence is the use of fibres. Most thermoplastics, in particular when they are intended for use as construction materials, are commercially available in formulations with short glass fibres. These formulations are manufactured as nibs, made in the usual extruder and a granulator, after a blending process in which the fibres are blended into the molten polymer. Besides glass fibres, also carbon fibres are being applied. The fibres are a few mm long, and, e.g. 10 μm thick. During blending and further processing fibres

may break, so that their final length may differ from case to case.

To get some understanding of the effect of short fibres on the properties of the composite material, we can start off with considering a single fibre, embedded in the polymer in the direction of the tensile stress (Figure 9.14). The fibre has a much higher stiffness than the polymer, but will only be able to contribute to stiffness and strength of the composite if it carries part of the load. At its extremes this is not the case; the cylindrical interface is subjected to shear loading, which, with a good adhesion, gradually decreases from the fibre end, while the tensile load in the fibre increases. The effective part of the fibre is, therefore, its total length diminished by the length of the transient parts. The fibre should, therefore, not be too short, so that its load-bearing function would be hampered.

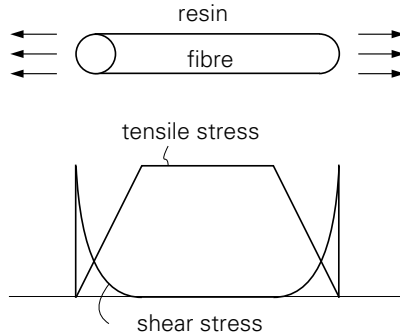


Figure 9.14 Stress distribution round a short fibre.

For the quantitative description of the stiffness of the composite, the Kerner equation of § 9.1.5. and § 9.2 can again be applied, though in a somewhat modified shape. Since a fibre brings about anisotropy of properties in its environment, we have to consider two different cases, viz. the E -modulus parallel to the fibre, E_p , and the one perpendicular to it, E_t . For both cases Kerner's equation holds, in which now A , in the parallel case, E_p , equals $2 \cdot l/d$, while for E_t , $A = \frac{1}{2}$.

A convenient approximation is found by considering a small value of φ ; then:

$$\frac{E}{E_0} = 1 + \varphi \cdot \frac{\alpha - 1}{\alpha + A} \cdot (A + 1)$$

It follows that for long fibres ($A \gg \alpha$):

$$\frac{E_p}{E_0} = 1 + \varphi(\alpha - 1)$$

or, with $E_1 = \alpha \cdot E_0$ as the modulus of the fibre:

$$E = E_0 \cdot (1 - \varphi) + E_1 \cdot \varphi$$

which, as could be expected, turns out to be a simple parallel arrangement of both components. This also appears from Figure 9.15, in which, for two values of α , the relative moduli of the composite, for $\varphi = 0.2$, are plotted as a function of l/d (upper two curves). For $\alpha = 25$, a maximum value which is representative for glass fibres in a hard polymer, of $0.8 + 25 \cdot 0.2 = 5.8$ is about reached at $l/d = 200$. For $\alpha = 125$, an average value for carbon fibres in a hard polymer, the maximum of $0.8 + 125 \cdot 0.2$ is not nearly reached at the same fibre length; with better, stiffer and more expensive fibres it is, therefore, the more important to prevent rupture of fibres during processing. It also appears that for very short fibres the nature of the fibres (cheap glass fibres or expensive carbon fibres) is of less importance.

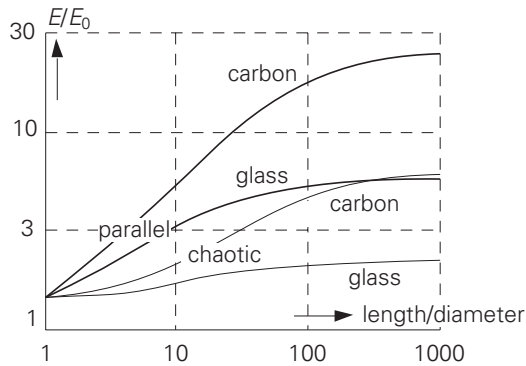


Figure 9.15 Stiffening as a function of fibre length and orientation.

These values hold for the case that the fibres are oriented in the stress direction. In reality the orientation of the fibres is at random in three dimensions; we should, therefore, not only consider E_p but also the much smaller E_t , which, even for very stiff fibres, is not higher than about $E_0(1 + 1.5 \cdot \varphi)$ or, with $\varphi = 0.2$, $1.3 \cdot E_0$. A frequently used expression for the modulus of an isotropic composite with chaotically arranged fibres, is:

$$E = 0.2 \cdot E_p + 0.8 \cdot E_t$$

For both values of α this approximation is also plotted in Figure 9.14; the effect of fibres on the stiffness is then strongly “diluted”, but is the same in three dimensions.

We can now compare these calculated values with test results. Technical brochures issued by raw material manufacturers supply an abundance of data on their products, also on the tensile moduli of the virgin polymers and on those containing a certain weight fraction of glass fibres. Combination of these data for a number of polymers (POM, PPE/PS, PC, PBTP, PET, PA-6) results in Figure 9.16. We can read from this

figure that the average stiffness ratio at 20 vol % glass is about 4. The theoretical curve for isotropic composites in Figure 9.14 yields a value of only 2.2, and for completely oriented fibres a value of 5.8. From a different theoretical approach, not to be discussed further, a ratio of only 1.9 is obtained for the isotropic case. Apparently the experimental data have been obtained on test bars in which, during their formation, the fibres were considerably oriented. These data are, therefore, not representative for the properties of an arbitrary end-product.

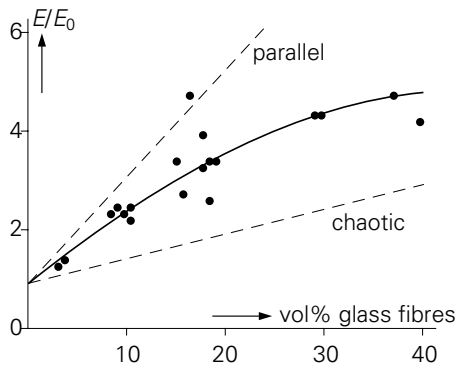


Figure 9.16 Increase in tensile modulus as a result of the presence of short glass fibres.

Contrary to particulate-filled composites, fibres induce an increase in strength. Again on the basis of data from technical brochures, it can be concluded that the tensile strength is raised by a factor between 1.5 and 3.5 at 20 vol % glass fibres. Apparently the fibres play such an important load-carrying role, that the polymer itself is considerably less stressed. The strain at break, however, strongly decreases.

The effect of short fibres on the impact strength varies; sometimes it is positive and sometimes negative. Broadly speaking, polymers with a low impact strength, and also tougher polymers at low temperatures, are improved in this respect. Also the reverse holds true: tough polymers undergo a loss in impact strength when they are filled with glass fibres. Figure 9.17 shows schematically the region in which the impact strength values for a number of polymers, containing different amounts of glass fibres, are found. Fibres appear to level out the differences in impact strength of the various polymers.

The effect of short fibres on the softening temperature has already been discussed in § 8.2.2. It appeared that their effect on amorphous polymers is minor, whereas for semi-crystalline polymers the softening points are drastically increased. Both observations are directly related to the slope of the $\log E - T$ curve.

Besides for improving mechanical properties, short fibres can also be applied for other purposes, such as electric conductivity. Metal fibres, if dispersed in such a way

that they touch each other, are suitable in this respect. Though the conductivity is not high enough to enable transport of energy, it is adequate for electromagnetic shielding.

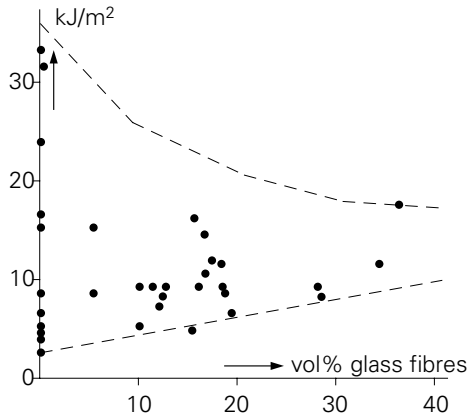


Figure 9.17 Impact strength as a function of glass fibre content.

9.4. Long fibres

For making composites of a polymer with long, continuous fibres, quite different techniques are used than for short fibres. Now it is no longer the polymer which, filled with reinforcing fibres, undergoes a formation process to produce a finished article. Now the fibre mass is formed and, thereafter, filled with the polymer. The positions are inverted, not only in the manufacturing of the composite, but also in its properties, since now its behaviour is largely governed by the fibres rather than by the polymer.

A first consequence is, that as matrices for long fibres thermosets are primarily suited. Fibre bundles or cloths can be much more easily impregnated with a low-molecular, low-viscosity resin than with highly viscous molten thermoplastics. Most of the long-fibre composites are, therefore, based on thermosets, mainly polyesters (UP) or epoxies (EP). However, during the past few years thermoplastic matrices are being used at an increasing scale; impregnating is carried out with special moulding techniques (see § 11.6.2).

Glass fibres are being used the most frequently; besides, for demanding applications, also modern fibres such as carbon and aramide, sometimes in combination with each other. The fibres can be arranged in rovings or in cloth, built-up from rovings or from twisted yarns. With rovings it is possible to achieve unidirectional orientation; with cloth the effect of the reinforcement is in two directions. Felt-lied, resulting in a three-dimensional reinforcement, though, as a matter of fact, to a lower degree than

with the anisotropic structures.

An illustration of the effect of the distribution of fibre directions is given in fig. 9.18. For glass fibre reinforcement in polyester resin some average values of tensile modulus and strength are plotted, all for 40 weight % (25 vol%) glass fibre. Moreover the properties of the pure resin and of the glass fibre are indicated. For the case of parallel fibres the test results are in good agreement with the simple rule of additivity mentioned before; also in the two other cases a reasonable agreement with theory is found.

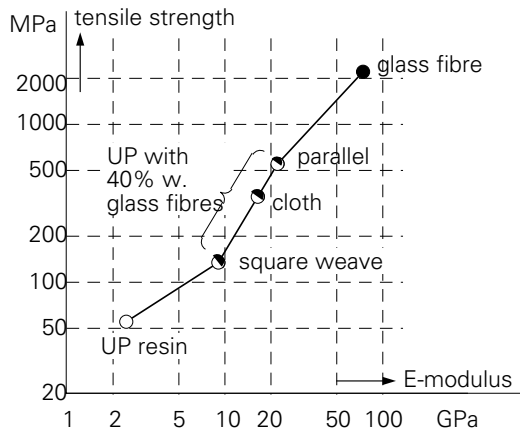


Figure 9.18 Effect of orientation distribution on properties.

Figures 9.19 and 9.20 present a survey of the mechanical properties of some (unidirectional) composites, in comparison with some other materials. In Figure 9.19 the values of modulus and strength are plotted as such, while in Figure 9.20 these values have been divided by the specific mass. From Figure 9.20 the enormous advantage of composites with respect to stiffness and strength per unit weight, in comparison to metals, is clearly visible. The modern carbon and aramide composites are superior to those based on glass fibres, for the specific stiffness even by a factor between 4 and 5.

The data in Figure 9.20 are of particular importance in applications where inertia effects and/or gravity forces should be small, e.g. in ski's, tennis rackets, motorcars, aeroplanes, space vehicles etc.

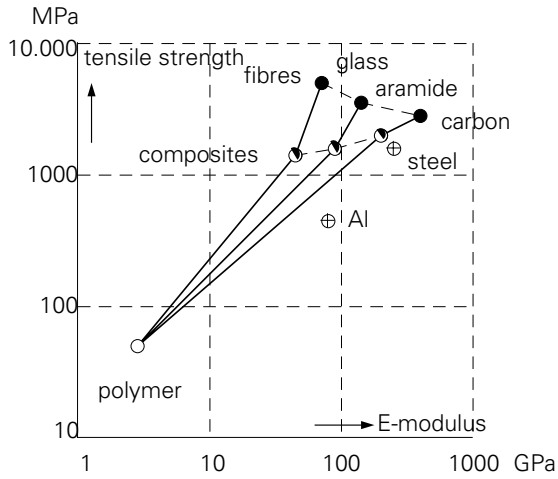


Figure 9.19. Mechanical properties for some composites.

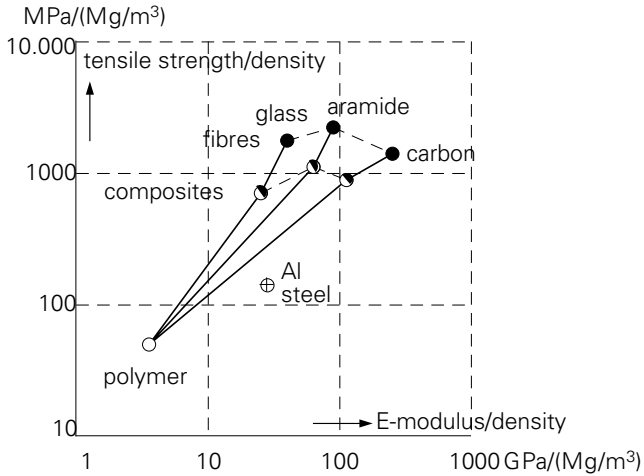


Figure 9.20. Mechanical properties for some composites, divided by density

10

Data on materials

Several properties of polymers have been dealt with schematically in the foregoing chapters.

Extensive tables of data on materials would be beyond the scope of this book; they can be found abundantly in handbooks and in the many technical brochures, issued by manufacturers.

Therefore, a few brief surveys, by no means complete, of some important properties are given on the following pages.

When using these data, it should be kept in mind that their value is, in most cases, very limited. A first reason is the strong dependence of all properties on temperature and on time, as discussed before, so that the data given can certainly not be considered as material constants.

In the second place, within a given type of polymer a *broad variety* of grades exists, as regards small variations in chain structure, differences in chain length and its distribution, and the presence of various additives for improving impact strength, fire resistance, stability etc.

Finally, it should be realized that, even with a well-defined material in a standard test method, the properties may be dependent on the way in which the test sample has been made; the *preparation conditions* may be different, and, moreover, may strongly deviate from those present in a technical processing operation. This applies, e.g. to shrinkage stresses, nature of the surface, crystalline structure, and, in particular, chain orientations.

10.1. Thermoplastics

| Abbre- viation | Name | Density kg/dm ³ | Price- class* |
|-------------------|--|-------------------------------|------------------|
| LDPE | Low density polyethene | 0.92 | 1 |
| HDPE | Highdensity polyethylene | 0.95 | 1 |
| PP | Polypropylene | 0.90 | 1 |
| PVC | Polyvinylchloride | 1.38 | 1 |
| PS | Polystyrene | 1.05 | 1 |
| TPS | High impact polystyrene | 1.05 | 1 |
| SAN | Styrene-acrylonitril copolymer | 1.08 | 2 |
| ABS | Acrylonitrile-butadiene-styrene copolymer | 1.05 | 2 |
| ASA | Acrylonitrile-styrene-acrylate copolymer | 1.07 | 3 |
| PMMA | Polymethylmethacrylate | 1.18 | 2 |
| PA 6 | Polyamide-6 (nylon-6) | 1.13 | 4 |
| PA 6.6 | Polyamide-6.6 (nylon-6.6) | 1.13 | 4 |
| PA 11 | Polyamide-11 (nylon-11) | 1.04 | 4 |
| PA 12 | Polyamide-12 (nylon-12) | 1.02 | 4 |
| POM | Polyoxymethylene | 1.42 | 3 |
| PC | Polycarbonate | 1.22 | 4 |
| PETP | Polyethylene terephthalate | 1.37 | 1 |
| PBTP | Polybutylene terephthalate | 1.29 | 3 |
| PPE/PS | Polyphenyleneether + polystyrene | 1.06 | 3 |
| PSU | Polysulfone | 1.24 | 5 |
| PPS | Polyphenylenesulfide | 1.34 | 4 |
| PI | Polyimide | 1.43 | 6 |
| PTFE | Polytetrafluoroethylene | 2.17 | 6 |
| FEP | Hexafluorpropylene-tetrafluoroethylene copolymer | 2.15 | 7 |
| PVDF | Polyvinylidene fluoride | 1.78 | 6 |
| ETFE | Tetrafluoroethylene-ethylene copolymer | 1.70 | 7 |
| CA | Celluloseacetate | 1.30 | 3 |
| CAB | Celluloseacetate-butyrate | 1.20 | 3 |
| PB | Polybutylene | 0.92 | 2 |
| PMP | Polymethylpentene | 0.83 | 4 |
| PEEK | Polyether-ether-ketone | 1.30 | 7 |
| PES | Polyethersulphone | 1.37 | 7 |
| PK | Polyketone | 1.24 | 3 |

| * price class | 1 | 2 | 3 | 4 | 5 | 6 | 7 |
|---------------|-------|-----|-----|-----|------|-------|-------|
| €/kg | 0.5–1 | 1–3 | 3–5 | 5–8 | 8–14 | 14–25 | 25–55 |

| Abbrevia- tion | E-modulus (short-term) | Tensile strength (short-term) | Strain at fracture | Notched impact strength |
|-------------------|---------------------------|-------------------------------------|-----------------------|-------------------------------|
| | MPa | MPa | % | kJ/m ² |
| LDPE | 150–250 | 20 | 300–1000 | > 40 |
| HDPE | 600–1400 | 30 | 100–1000 | 5–20 |
| PP | 1100–1600 | 30–70 | 150–700 | 3–15 |
| PVC | 2900–3400 | 50–80 | 20–40 | 2–5 |
| PS | 3000–3600 | 45–60 | 3–4 | 2 |
| TPS | 1600–2500 | 20–50 | 20–50 | 5–10 |
| SAN | 3600 | 70–80 | 5 | 3 |
| ABS | 1600–3000 | 20–50 | 15–30 | 8–30 |
| ASA | 2300–2600 | 45–60 | 15–20 | 7–14 |
| PMMA | 3300 | 50–80 | 3–7 | 2–3 |
| PA 6 | 1000–2000 | 35–50 | 150–250 | > 20 |
| PA 6.6 | 1700–2000 | 55–60 | 100–200 | 15–20 |
| PA 11 | 1100–1200 | 40–45 | 200–250 | 30–40 |
| PA 12 | 1200–1350 | 40–45 | 100–350 | 15–30 |
| POM | 3000–6000 | 65–70 | 15–60 | 5–8 |
| PC | 2000–2200 | 60–65 | 80–150 | 20–35 |
| PETP | 2800–3100 | 55–75 | 50–150 | 3–6 |
| PBTP | 2600–2800 | 50–55 | 100–200 | 3–6 |
| PPE/PS | 2200–2500 | 50–65 | 60 | > 15 |
| PSU | 2450 | 75–90 | 50–100 | 3–10 |
| PPS | 3400 | 75 | 3 | |
| PI | 3200 | 75–90 | 4–8 | 4–8 |
| PTFE | 450–750 | 20–40 | 250–500 | 14–16 |
| FEP | 360 | 18–22 | 250–330 | > 20 |
| PVDF | 800–1800 | 40–50 | 50–200 | > 20 |
| ETFE | 850–1400 | 30–55 | 200–400 | > 20 |
| CA | 1500–3000 | 50–60 | 30–40 | 5–30 |
| CAB | 500–2000 | 35–50 | 20–70 | 5–30 |
| PB | 450–600 | 22–25 | 200–350 | > 40 |
| PMP | 1500 | 25–30 | 15 | 3–10 |
| PEEK | 3700 | 90 | 50 | 55 |
| PES | 2440 | 84 | 40–80 | |
| PK | 1500 | 55 | 350 | 20 |

| Abbr. | T_g | T_m | Vicat B | ISO/A | λ | α | c |
|--------|-------|-------|---------|-------|-----------|---------------------|---------|
| | °C | °C | °C | °C | W/m·K | 10 ⁻⁵ /K | kJ/kg·K |
| LDPE | -120 | 110 | 55 | 35 | 0.35 | 23 | 2.4 |
| HDPE | -120 | 130 | 70 | 45 | 0.45 | 13 | 2.1 |
| PP | -15 | 170 | 90 | 60 | 0.24 | 18 | 1.7 |
| PVC | 87 | – | 85 | 70 | 0.16 | 8 | 0.9 |
| PS | 95 | – | 90 | 85 | 0.15 | 7 | 1.3 |
| TPS | 90 | – | 85 | 80 | 0.17 | 8 | 1.3 |
| SAN | 105 | – | 100 | 85 | 0.18 | 7 | 1.2 |
| ABS | 105 | – | 100 | 95 | 0.17 | 9 | 1.4 |
| ASA | 100 | – | 85 | 85 | 0.18 | 9 | |
| PMMA | 110 | – | 100 | 95 | 0.19 | 7 | 1.45 |
| PA 6 | 50 | 223 | 210 | 85 | 0.21 | 10 | 1.9 |
| PA 6.6 | 50 | 260 | 230 | 90 | 0.20 | 8.5 | 1.7 |
| PA 11 | 45 | 175 | 170 | 70 | 0.27 | 12 | 1.4 |
| PA 12 | | 175 | 170 | 70 | 0.23 | 9 | 1.2 |
| POM | -50 | 175 | 165 | 115 | 0.29 | 12 | 1.5 |
| PC | 150 | – | 145 | 135 | 0.21 | 6.5 | 1.3 |
| PETP | 75 | 260 | 170 | 80 | 0.24 | 7 | 1.0 |
| PBTP | 70 | 210 | 180 | 60 | 0.21 | 7 | 1.3 |
| PPO/PS | 140 | – | 130 | 125 | 0.23 | 6.5 | 1.25 |
| PSU | 190 | – | 185 | 175 | 0.22 | 5.5 | 1.0 |
| PPS | 85 | 290 | | 135 | 0.29 | 5.5 | |
| PI | > 400 | – | | > 250 | 0.52 | 5.5 | 1.15 |
| PTFE | 126 | 327 | 110 | 55 | 0.25 | 12 | 1.0 |
| FEP | | 290 | | | 0.23 | 9 | 1.15 |
| PVDF | -40 | 170 | 130 | 92 | 0.12 | 8.5 | 1.4 |
| ETFE | | 270 | | 75 | 0.24 | 7.5 | 1.95 |
| CA | 70 | 210 | 70 | 60 | 0.20 | 10 | 1.5 |
| CAB | 55 | | 65 | 60 | 0.20 | 12 | 1.5 |
| PB | -25 | 130 | 85 | 60 | 0.23 | 12 | 1.8 |
| PMP | 130 | 240 | 165 | | 0.17 | 12 | 2.2 |
| PEEK | 143 | 334 | | 160 | 0.25 | 4.7 | |
| PES | 230 | | 226 | 210 | | | |
| PK | 15 | 220 | 205 | 100 | 0.27 | 11 | 1.8 |

T_g = glass-rubber transition temperature

T_m = melting point

Vicat B = softening T at bij 10 N

ISO/A = heat deflection T at 1.85 MPa

λ = heat transmission coefficient

α = linear expansion coefficient

c = specific heat

| Abbr. | water adsorption (ASTM) | resistance against | | | | | | |
|--------|-------------------------------|--------------------|--------|-------|---------|----|------------------|----------|
| | | acids | | oxyd. | alkalis | | oils and fats | weather* |
| weak | strong | weak | strong | | | | | |
| LDPE | < 0.01 | ++ | □ | -- | ++ | ++ | + | □ |
| HDPE | < 0.01 | ++ | □ | -- | ++ | ++ | + | □ |
| PP | 0.02 | ++ | □ | -- | ++ | ++ | + | □ |
| PVC | 0.04–0.4 | ++ | ++ | □ | ++ | ++ | + | ++ |
| PS | 0.03–0.1 | ++ | + | - | + | + | + | - |
| TPS | 0.05–0.6 | ++ | □ | - | ++ | ++ | □ | □ |
| SAN | 0.2–0.3 | ++ | + | - | ++ | ++ | + | □ |
| ABS | 0.2–0.4 | ++ | □ | -- | ++ | ++ | + | □ |
| ASA | | + | □ | -- | ++ | ++ | + | ++ |
| PMMA | 0.1–0.4 | + | - | □ | ++ | ++ | ++ | ++ |
| PA 6 | 1.3–1.9 | -- | -- | -- | + | + | + | + |
| PA 6.6 | 1.5 | - | -- | -- | + | + | + | □ |
| PA 11 | 0.3 | □ | -- | -- | ++ | ++ | ++ | □ |
| PA 12 | 0.25 | -- | -- | -- | + | + | | |
| POM | 0.25 | □ | -- | -- | ++ | ++ | + | □ |
| PC | 0.16 | + | □ | - | -- | -- | + | + |
| PETP | 0.39 | ++ | + | □ | + | - | ++ | + |
| PBTP | 0.08 | □ | - | □ | ++ | ++ | ++ | + |
| PPO/PS | 0.06 | ++ | ++ | | ++ | ++ | □ | + |
| PSU | 0.02 | ++ | ++ | | ++ | ++ | + | ++ |
| PPS | 0.02 | ++ | □ | | ++ | | + | ++ |
| PI | 0.32 | ++ | ++ | ++ | - | + | □ | |
| PTFE | 0 | ++ | ++ | ++ | ++ | ++ | ++ | ++ |
| FEP | < 0.1 | ++ | ++ | ++ | ++ | ++ | ++ | ++ |
| PVDF | 0 | ++ | + | -- | ++ | ++ | + | + |
| ETFE | 0.03 | ++ | ++ | □ | ++ | ++ | | + |
| CA | 6 | □ | - | -- | □ | -- | ++ | □ |
| CAB | 1–3 | + | - | -- | + | □ | ++ | + |
| PB | < 0.02 | ++ | □ | -- | ++ | ++ | + | □ |
| PMP | 0.01 | ++ | ++ | | ++ | ++ | + | □ |
| PK | 0.5 | + | - | - | + | - | ++ | □ |

* Weather resistance can, in most cases, be improved by proper additives.

10.2. Thermosets

| | d kg/dm ³ | E GPa | tensile strength MPa | notched impact strength kJ/m ² | ISO/A °C |
|-------------------------|---------------------------|------------|----------------------------|---|-------------|
| PF phenolformaldehyde | | | | | |
| + anorg. filler | 1.8–2.1 | 6–15 | 15–25 | 2–10 | 120–170 |
| + org. filler | 1.4–1.5 | 4–8 | 25–30 | 2–10 | 120–150 |
| UF ureumformaldehyde | | | | | |
| + org. filler | 1.5 | 6–10 | 30 | 6–8 | 110–140 |
| MF melamineformaldehyde | | | | | |
| + anorg. filler | 1.8–2 | 8–13 | 25 | 2 | 150–200 |
| + org. filler | 1.5 | 6–10 | 30 | 2 | 140–180 |
| UP polyester (normal) | 1.2 | 3.5 | 30 | | 70 |
| id (high T) | 1.2 | 3.5 | 55 | | 120 |
| + short glass fibres | 2.0 | 12–15 | 30–50 | 10–20 | 100–200 |
| EP epoxy (solid) | 1.2 | 4 | 60 | 2 | 90 |
| + filler | 1.8 | 12 | 40 | 2–15 | 100–200 |
| + short glass fibres | 1.9 | 15 | 30–60 | 10–20 | 150–220 |
| (fluid resin) | 1.2 | 4 | 55 | 2 | 110–160 |
| + filler | 1.8 | 12 | 45 | 2–10 | 130–200 |
| (cold-curing) | 1.2 | 4 | 50 | 2 | 40–60 |
| + filler | 1.6 | 12 | 35 | 2 | 45–90 |

| resin | % glass | type | d kg/dm ³ | E GPa | tensile strength MPa |
|-----------|---------|------------|---------------------------|------------|----------------------------|
| polyester | 25 | cloth | 1.35 | 5 | 70 |
| polyester | 45 | cloth | 1.45 | 9 | 140 |
| polyester | 50 | cloth | 1.60 | 10 | 200 |
| polyester | 65 | cloth | 1.80 | 19 | 300 |
| polyester | 65 | unidirect. | 1.80 | 28 | 500 |
| epoxy | 50 | cloth | 1.60 | 10 | 220 |
| epoxy | 65 | cloth | 1.80 | 18 | 350 |
| epoxy | 65 | unidirect. | 1.80 | 30 | 700 |
| epoxy | 78 | unidirect. | 2.0 | 60 | 1700 |

10.3. Elastomers

| Abbr. | Name | density kg/dm ³ | price class see p. 185 | min. temp. °C | max. temp. °C | tensile strength | |
|-------|---------------------------|-------------------------------|---------------------------------|---------------------|---------------------|------------------|---------------|
| | | | | | | unfilled MPa | filled MPa |
| NR | natural rubber | 0.92 | 2 | -50 | 80 | 18-30 | 25-35 |
| SBR | styrene-butadiene rubber | 0.91 | 2 | -45 | 100 | 1-2 | 18-25 |
| BR | butadiene rubber | 0.91 | 2 | -70 | 100 | 8 | 17 |
| IR | isoprene rubber | 0.91 | 2 | -50 | 80 | 27 | 29 |
| IIR | butyl rubber | 0.92 | 3 | -45 | 150 | 18-21 | 18-21 |
| CR | chloroprene rubber | 1.23 | 3 | -40 | 115 | 21-29 | 21-29 |
| NBR | nitrile rubber | 1.00 | 3 | -40 | 130 | 4-7 | 21-32 |
| EPR | ethylene-propylene rubber | 0.86 | 3 | -50 | 120 | 2 | 14-23 |
| SI | silicone rubber | 1.10 | 6 | -75 | 270 | 2 | 10-14 |
| SBS | thermoplastic rubber | 0.95 | 3 | -70 | 60 | 20-25 | 20-25 |
| PUR | polyurethane rubber | 1.07 | 4 | -20 | 110 | 20-40 | |
| Fl.R. | fluor rubbers | 1.85 | 7 | -30 | 280 | 15-25 | 15-25 |

| Abbr. | elasti- city | tear resist- ance. | abrasion resist- ance. | gass barrier | sun | resistance against | | | |
|-------|-----------------|--------------------------|------------------------------|-----------------|-----|--------------------|------|---------------|-------|
| | | | | | | oxid. | heat | hydrocarbons. | acids |
| NR | ++ | ++ | ++ | □ | - | + | + | - | □ |
| SBR | + | □ | ++ | □ | - | + | ++ | - | □ |
| BR | +++ | □ | +++ | □ | - | □ | + | - | □ |
| IR | ++ | + | ++ | □ | - | □ | + | - | □ |
| IIR | -- | + | ++ | ++ | ++ | ++ | ++ | - | ++ |
| CR | ++ | + | ++ | + | ++ | ++ | ++ | + | ++ |
| NBR | + | + | + | + | - | + | ++ | + | + |
| EPR | + | + | ++ | □ | ++ | ++ | ++ | - | ++ |
| SI | + | - | - | □ | ++ | ++ | ++ | - | + |
| SBS | ++ | | + | □ | - | □ | □ | - | + |
| PUR | + | ++ | ++ | + | ++ | ++ | ++ | □ | - |
| Fl.R. | + | □ | + | ++ | + | ++ | ++ | + | ++ |

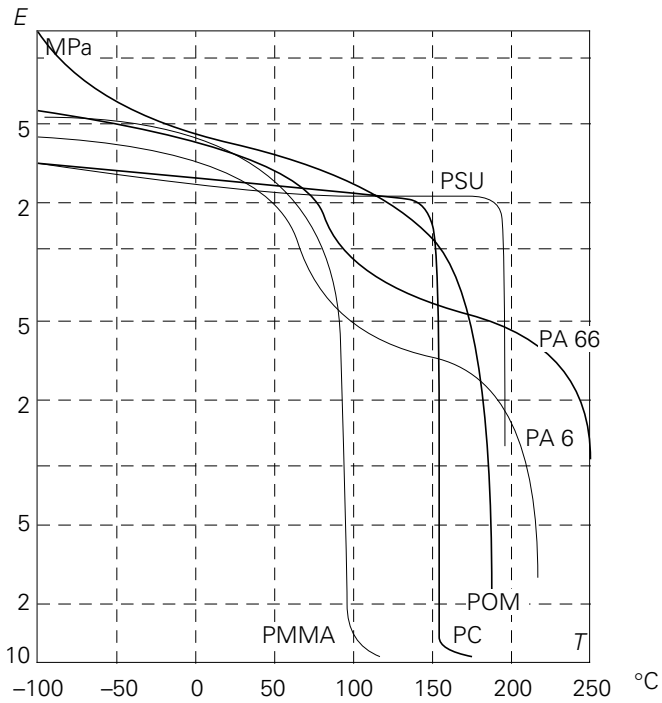
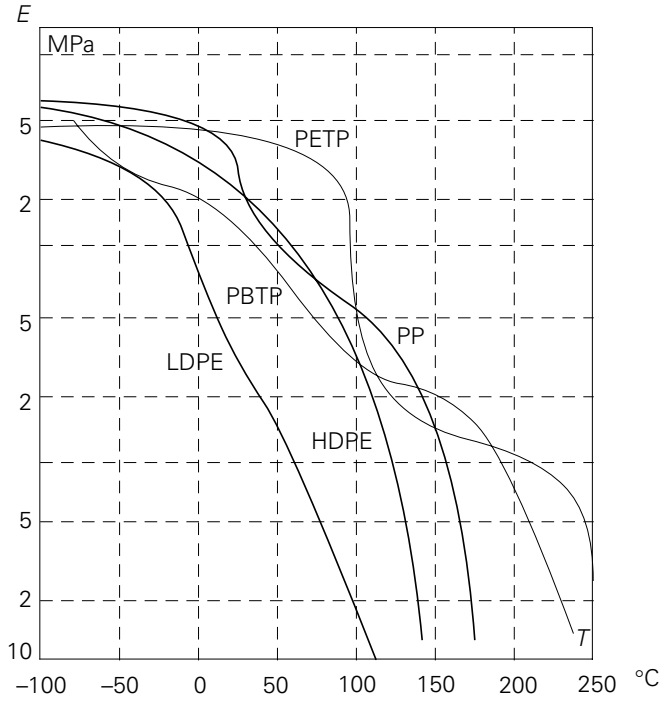


Figure 10.1. Modulus of elasticity as a function of temperature for a number of polymers.

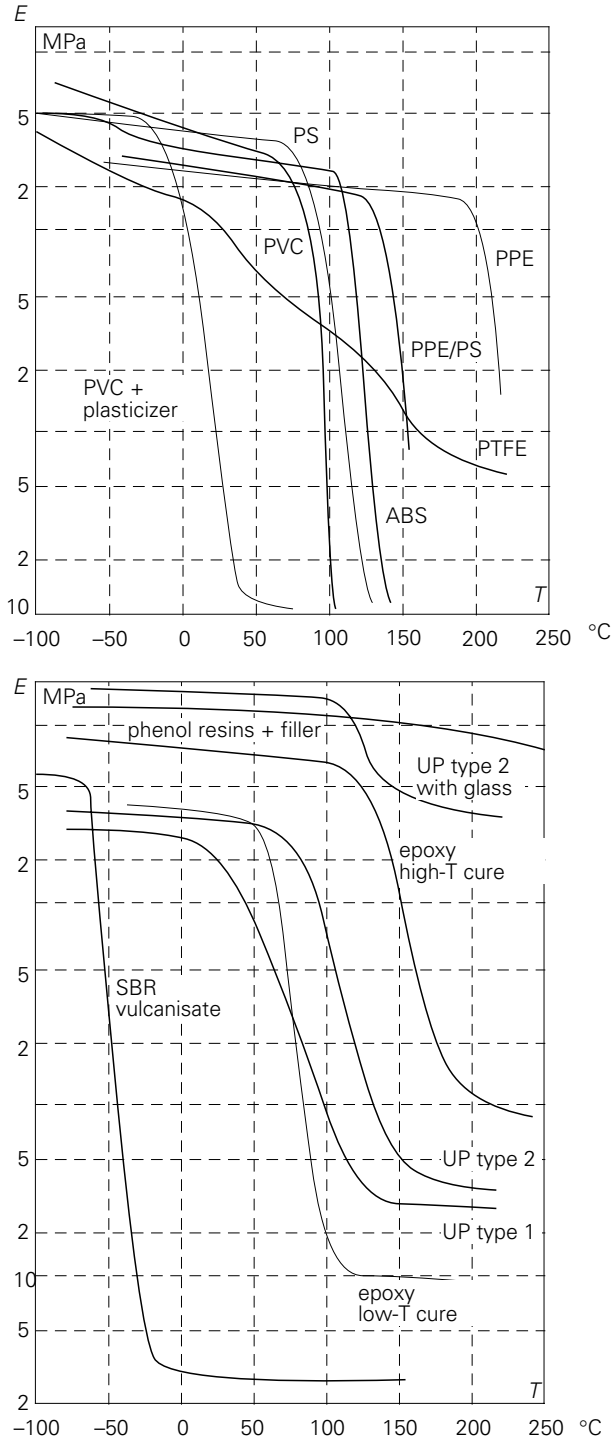


Figure 10.1. (continued) Modulus of elasticity as a function of temperature for a number of polymers.

11

Processing techniques

11.1. Principles of processing

11.1.1. General

The route from raw material to end-product proceeds in one or more steps, one of which at least takes place in the fluid condition. Most of the raw materials are available in the solid state: granules or powders of thermoplasts, moulding powders or moulding masses of thermosets, bales of rubbers.

In some cases the raw material is already in a fluid state: with thermosets as a resin for casting or impregnating, with thermoplasts, as an exception, sometimes as a monomer which is able to polymerise in the mould. In these cases the forming processes are relatively simple, since they can be carried out on low-viscous fluids which do not require high pressures to be transported.

Solid raw materials have to be transferred into a fluid or plastic state, which is, nearly always, attained by heating (in exceptional cases by solution). In the fluid state the material is shaped, after which the resulting shape is fixed by cooling (thermoplasts), or by a chemical reaction (curing of thermosets, vulcanisation of rubbers).

However, this simple schedule, solid - fluid - solid, is, in practice, less simple to be carried out. First of all the low heat conductivity of polymers plays a role: heating a polymer mass is a slow process when the heat has to be supplied from the outside. This is the case with heating by the metal case of a processing machine, or by infra-red radiation. This disadvantage is circumvented by applying *internal friction*, generated in the solid bed of granules, but even more in the highly viscous, just molten, mass during transportation. Also high-frequency *dielectric heating* can be applied to materials which, because of a not too low dielectric loss factor (see § 8.2.2), are suitable in this respect; in particular with welding of film this method is used, but also in preheating thermosetting moulding powders. A third possibility is ultrasonic heating, making use of local heat dissipation when sound waves are damped out in the material. This is a suitable method for spotwelding.

In all these cases heating-up of the polymer proceeds quicker and more homogeneously. Cooling down, however, cannot be accelerated, and, therefore, takes

the larger part of the cycle time with thicker thermoplastic end-products.

A second difficulty is the high viscosity of polymeric fluids, which we already encountered in § 5.3.1, where we also have seen that the viscosity of a molten polymer is not a constant. As a matter of fact, the viscosity decreases with increasing temperature (see Figure 11.2), but this effect is overshadowed by the influence of shear rate (see Figure 11.1). According to its definition, the viscosity should be the constant ratio between shear stress and shear rate, but with most polymers these two quantities are not at all proportional to each other. With increasing shear rate the shear stress increases considerably less than proportionally, so that the ratio, the viscosity, decreases (see § 5.3.2). As a result of this phenomenon a tenfold increase of the throughput through a channel requires an increase in pressure by a factor of only 2 to 3.

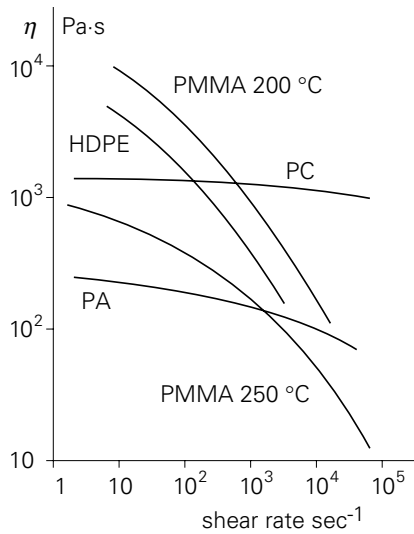


Figure 11.1. Apparent melt viscosity as a function of shear rate.

Notwithstanding this fact, high pressures are required to transport the fluid mass through the transport channels or into the mould of a processing machine with an acceptable speed. Pressure levels of 50 to 150 MPa (500 to 1500 bar) are normal, so that the machines have to be very robust.

The product, formed via the fluid state is, in some cases, *the end-product*, but may also be subject to further shaping as an *intermediate product*. Examples of the first case are injection-moulded gear-wheels, compression-moulded gramophone-records, extruded and on-line blown bottles, etc. In the second case an extruded sheet is, for instance, subjected to a heat-forming process to produce a light-dome; a gear wheel may be machined from a compression-moulded block, or an extruded tubular film is

welded to form a bag.

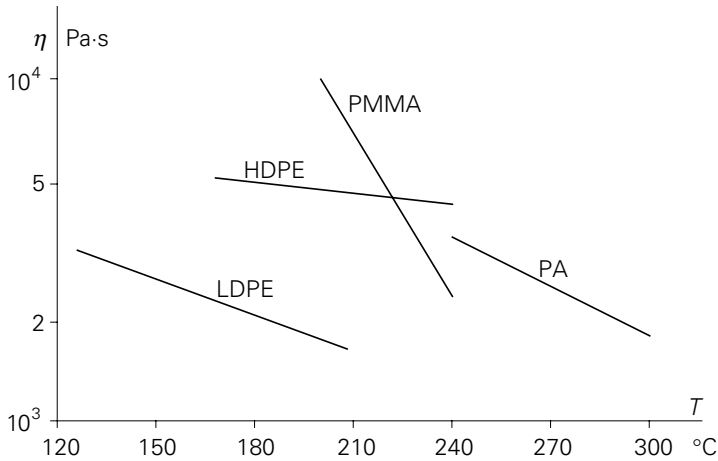


Figure 11.2 Melt viscosity as a function of temperature.

The wide variety of processing techniques enables the choice between various possibilities: a thin-walled cup can be made by injection moulding as well as by vacuum-forming of extruded sheet; a gear-wheel can be made by machining or by injection moulding or by compression moulding. The *choice of the process* depends, i.a., on the requirements set to the end-product; with injection-moulding narrower tolerances can be achieved than with heat-forming of sheets. Moreover the nature of the polymer often plays a role; it depends, for instance, on the stability of the polymer at the high temperatures in a process; the length of the rubbery region on the temperature scale governs the ease of vacuum forming; a too brittle polymer is difficult to machine, etc.

A very important factor in the choice of a process is the *economy*. The manufacturing costs of the various processing techniques are very different and are strongly dependent on the number of articles to be made. This point is discussed in the next section.

11.1.2. Production cost

The cost to produce a plastic article can be subdivided into three contributions: material cost, machine cost and the cost of the mould.

The *material costs* are composed of the price of the raw material, the dimensions of the product and the unavoidable loss of material in the shaping process.

The *machine costs* comprise the interest of the invested capital, depreciation of the equipment, energy needed, labour cost, maintenance, accommodation cost, etc. The

contribution of the machine costs to the price of the end product is governed by the cycle time, i.e. the time to produce a single article. Cycle times are strongly different: depending on the size of the product and the type of process they may vary from a few seconds up to half an hour.

The *mould cost* should be considered separately because the mould has to be made specifically for a single type of end-product. It may vary over a factor of thousand. This cost has to be apportioned over the number of articles to be made, and, therefore, it largely governs the economy of the manufacturing process.

The cost to produce a number n of a certain article, can thus be expressed by:

$$K = A + Bn$$

in which A is the cost of investment in the mould and the preparation of the production, and B the cost of material, energy, labour, depreciation etc. The cost per article is then:

$$\frac{K}{n} = \frac{A}{n} + B$$

Figure 11.3 shows how, for two different processes, this cost depends on the production volume; for the first process A is three times as high and B three times lower than for the second process. The choice is, therefore, strongly dependent on the envisaged volume of production.

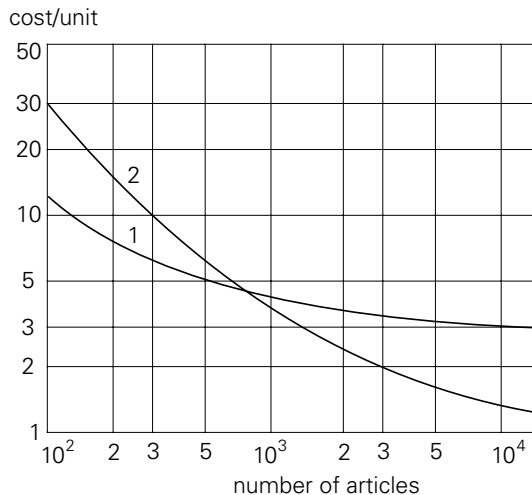


Figure 11.3. Effect of volume of production on manufacturing cost.

11.1.3. Compounding

Before the actual forming process, the raw material has often to be compounded, i.e. blended with a number of other components, as mentioned in § 1.1.

Blending can, in a first instance, be carried out in dry condition in the polymer powder or granules; the degree of blending is, however, not yet sufficient. To obtain a better dispersion, a blending process in the fluid state is necessary. To achieve this, various types of mixing devices are available, such as roll mills, internal mixers and mixing extruders.

Roll mills, in most cases, consist of two heated rolls (Figure 11.4), separated by a narrow gap, and rotating in opposite directions. The thermoplastic or rubbery material is, together with the added substances, brought onto the rolls, so that it transported through the gap by friction. By applying slight differences between the temperature and the rotation speed of the rolls, the mix is forced to adhere to one of the rolls, where is it is all the time being cut away by hand an again brought between the rolls, until a homogeneous blend has been formed. Two-roll mills come in different sizes; the biggest ones have roll diameters up to 80 cm and lengths up to 2.5 m.

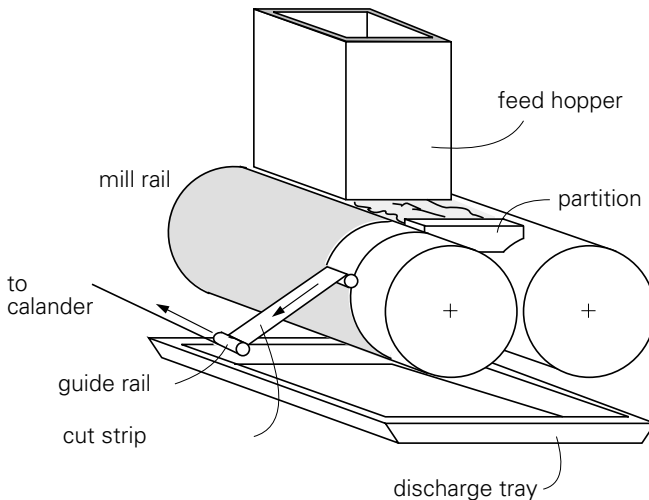


Figure 11.4. Two-roll mill.

Internal mixers, such as the *Banbury mixer* (Figure 11.5), contain two connecting chambers, in which blades rotate in opposite directions with a narrow clearance to the walls, resulting in local high rates of shear. The walls can be cooled or heated. After mixing, the pieces are removed from the chambers, milled into a sheet and cut into ribbons for storage or further processing.

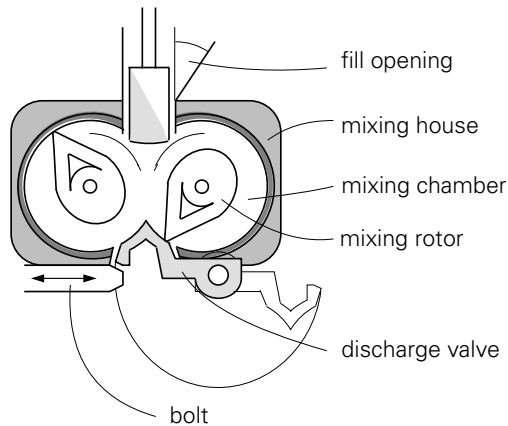


Figure 11.5. Banbury mixer.

The third type of compounding device is *the extruder*. Next to its use for fabrication (which will be dealt with in § 11.4.2), it is applied as a mixer. In essence, it is a screw pump, in which the mass to be mixed is transported in a heated cylinder by a screw, or, with twin-screw extruders, by two parallel screws. During this transport melting and intensive mixing take place. At the end of the screw the blend is pressed through a number of openings and cooled down; in most cases the strands thus obtained are on-line cut into granules.

Most manufacturers of end-products do not make the compounds themselves, but obtain them from the material supplier. In the bigger industries compounding is sometimes carried out in-house, with the advantages of economy and of flexibility to tune their products to reach the best compromise of processability on the machines available and the desired properties of the end-product.

11.2. Casting and compression moulding

11.2.1. Casting

Casting is the simplest processing technique: the mould is filled with a liquid, which, at ambient temperature, has such a low viscosity that it is able to fill the mould under its own weight. After filling, a chemical reaction should take place to form the material. With thermosets this is a reaction between the components which, prior to filling, have been mixed together, and which react into a three-dimensional network. Sometimes a catalyst is added to initiate or accelerate this reaction. Dependent on the combination chosen, curing takes place at room temperature or at an elevated temperature.

During curing heat is always being developed, which cannot escape easily due to the

low heat conductivity of polymers (see § 8.1.4). In the centre of the body the temperature may, therefore, rise unacceptably high and cause thermal degradation. With casting resins thick parts should, therefore, be avoided. By a proper choice of the type of material and the dosing of catalysts, the heat development can be controlled.

Examples used in practice are polyester and epoxy casting resins, both as two-component systems. The epoxies are more expensive than the polyester resins, but they show less shrinkage; the shrinkage, expressed as the volume difference before and after curing, amounts to 1 to 6 % for epoxies, and to 5 to 10 % for polyesters.

Epoxy casting resins are frequently applied for encapsulation of electro-technical parts such as coils and transformers. The electrical properties of epoxies are, in general, better than those of polyesters.

Casting resins may be supplemented with *fillers*, mostly with anorganic materials such as quartz powder. Sometimes this is done to lower the cost price, but also, for some applications, to improve the properties; shrinkage, for instance, is reduced and hardness is increased.

Some *thermoplastics* can also be used in casting processes; in these cases polymerisation takes place in the mould which is filled with the monomer. Examples are polystyrene, polymerised from styrene, and polymethylmethacrylate from its monomer. These reactions can take place quite easily in the presence of suitable catalysts. In this way thick sheets can be produced, but also large articles such as PA-6 ship propellers or gear wheels, as polymerisation products from caprolactam.

11.2.2. Rotational moulding

Casting of hollow articles is possible when gravity forces are replaced by centrifugal forces, brought about by rotation. A pipe can be produced by partially filling a hollow cylinder with liquid, rotating it about its axis at high speed, and heating its outside wall (Figure 11.6). Rotation about two perpendicular axes enables the formation of an arbitrarily shaped hollow article. (Figure 11.7).

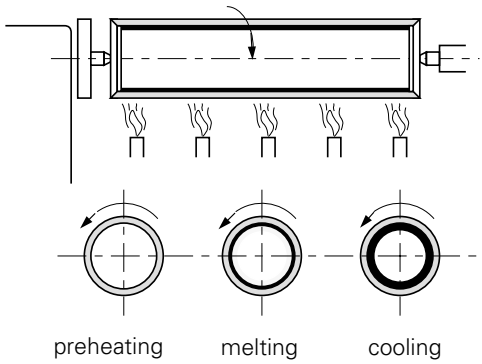


Figure 11.6. Rotational moulding.

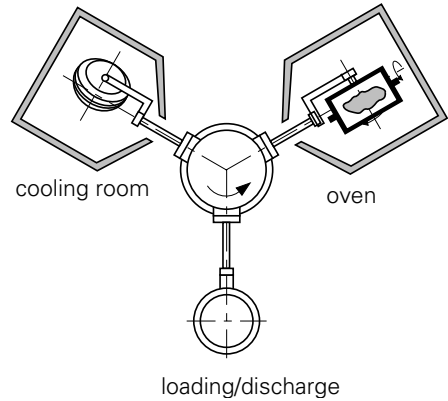


Figure 11.7. Rotational moulding with two rotating axes.

The starting material in these processes is not necessarily in the liquid state; also *pastes* of PVC with a plasticiser can be used, and even a well-flowing powder of a thermoplast. The particles will melt when in touch with the heated wall and will form a compact layer of material. In these cases the centrifugal force does not necessarily play a role; the softened powder sticks to the wall and other particles gradually complete the shaping process. Only the outer surface of an article made this way will be smooth, which is no objection for many applications.

This method is eminently suited for the manufacture of large objects such as containers of several m^3 content, and also non-closed articles such as furniture, dashboards etc. The normally applied material thickness is in between 1.5 and 15 mm, dependent on the type of article. The maximum possible thickness is about 30 mm, because with thicker parts the time needed to melt the polymer is so long that part of the material may already decompose before the whole mass is sufficiently heated. It is, sometimes, tried to circumvent this difficulty by filling the mould with pre-melted material, obtained from an extruder.

In the wall thickness fluctuations up to 5 % may occur. As a result of the uneven temperature in the molten polymer during rotation, and also by the not always exactly reproducible rate of cooling, deviations in the dimensions of the finished product may amount to 5 %. Requirements are, that the materials can be molten completely, that the melt is sufficiently low-viscous, and that the molten polymer does not degrade too rapidly. Besides plasticised PVC, HDPE and LDPE are often used, as well as copolymers of PE such as EVA (ethylene - vinyl acetate copolymer). Because the shear stresses in this process are extremely low, a *narrow molar mass distribution* is to be recommended, as discussed in § 5.4. Cycle times vary between 3 and 40 minutes, dependent on the wall thickness. Cycle times can be reduced considerably by using machines with multiple moulds, since the cycle time

is predominantly controlled by heating and cooling time. With multi-mould machines, one of the moulds is heated and filled during the cooling cycle of another mould (see Figure 11.7).

A very promising development is the combination of the *in-situ polymerisation* mentioned before, with the principle of rotational moulding. This method is, in particular, used for the manufacture of large-sized polyamide articles from the monomer caprolactam. The big advantage compared with centrifugal casting is, that one starts off with a low-viscous liquid, and ends with a solid material. During the whole process the temperature does not exceed the melting point of the polyamide formed. The article, therefore, does not need a cooling cycle before it can be taken from the mould; moreover the heating time is much shorter. An example is an oil tank of 1.200 litres with an average wall thickness of 4.5 mm, which requires 33 kg of caprolactam. The total cycle time for heating, centrifuging and simultaneous polymerisation is 13 minutes.

The moulds are mostly made of steel or aluminium. Since the forces during rotation are relatively small, thin walls of the mould suffice, viz. less than 1.5 mm.

From an economic point of view the centrifugal moulding process is characterised by the following factors: low cost of machine and mould, relatively long cycle times, suitability for thin- as well as thick-walled articles. The method is very well suited for articles made in small series.

11.2.3. Compression moulding

Compression moulding is the simplest technique to transform a raw material from the solid state into an end-product. The material is, as granules or as a powder, brought between the two heated halves of the mould, which are then being pressed together.

Thermoplasts, thermosets and rubbers can be processed by compression moulding. For *thermoplasts* this technique is an *exception*; the best known example is the manufacture of gramophone records from a copolymer of vinyl chloride and vinyl acetate (chosen to enable a very good flow into all details of the mould).

Compression moulding of thermoplastics is, in general, unattractive because the mould has to be heated and cooled in turn; the moulding has to be cooled down below its glass temperature or melting point before it can be taken from the mould. With thermosets, compression moulding is commonly applied. The starting material is a moulding powder, comprising a blend of the resin, the curing agent, and organic or anorganic fillers such as wood flour, cellulose, textile fibres, asbestos, quartz powder, glass fibres, etc. These moulding powders are prepared by intensive mixing

of the components in mixers, or via impregnation of the fillers with a resin solution, after which the solvent is evaporated. In most cases a certain amount of pre-curing takes place during this treatment, which can be adjusted by temperature and time. The pre-curing results in a reduction of cure time in the mould, and thus in a shorter cycle time and a better economy of the process. For the same reason the heating time in the mould can be reduced by preheating the material with the aid of a high-frequency electric field.

The powder is further heated in the mould; it becomes a fluid and fills the mould completely, after which the final curing reaction takes place. In this course of events *the flow process and the curing reaction are competitive*; a temperature increase reduces the viscosity but increases the reaction rate. When these effects coincide the process fails: the viscosity is not sufficiently lowered to allow complete filling of the mould. If the reaction time is much longer than the time needed for flow, then a perfect moulding is obtained, but the cycle time is too long. This is schematically shown in Figure 11.8; the level of the minimum viscosity, η_m , governs the technical aspect of the process (complete filling, required pressure), while the length of the time scale, T , is a measure of its economy. By a proper choice of resin formulation and process conditions, an optimum can be found for each article to be made.

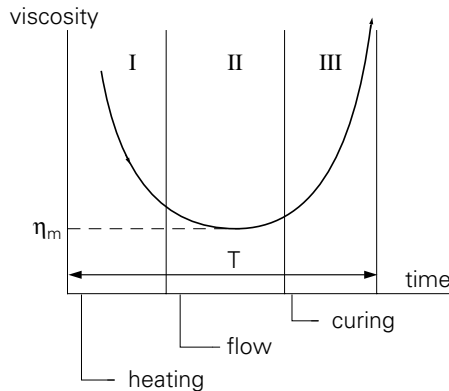


Figure 11.8. Viscosity of a resin as a function of time.

The characterisation of the flow- and curing behaviour of moulding powders is carried out with the aid of a laboratory device in which the powder is, under a constant pressure, transported from a pre-heated chamber into a narrow channel. The distance covered as a function of time is recorded, and from the so-called *flow-diagrams* the behaviour of the resin system during curing can be read off (Figure 11.9). In such a diagram the three stages of Figure 11.8 are clearly recognisable.

Moulding powders cure, in general, at temperatures between 140 and 180 °C, under pressures between 200 and 600 bars. A substantial part of the temperature increase is

provided by the reaction heat, which may raise the temperature to above the temperature of the wall. This effect will be stronger with thicker articles.

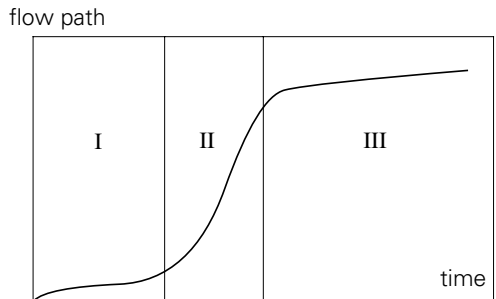


Figure 11.9. Flow diagram of a resin

Dimension tolerances are important in compression moulding. The dimensions of the finished article are smaller than those of the mould cavity, in particular because not only thermal shrinkage but also shrinkage during the reaction counts. When using resins which develop volatiles upon curing, extra shrinkage occurs due to the escape of these components.

In its simplest form a compression moulding device is sketched in Figure 11.10. A somewhat more complicated variant is *transfer moulding*, where the material is heated in a separate chamber until it is fluid, and is then rammed into the mould (Figure 11.11). The moulding time is now shorter, while curing proceeds more homogeneously. Moreover, the mould cavity is less loaded and is less sensitive to damage in its details. In fact, transfer moulding is an intermediate stage between simple compression moulding and injection moulding which will be described in the next section.

Numerous articles are made by compression moulding, such as bulb fittings, switches, wall-plugs, crockery, and many other technical and household articles. The process is very economical, since no expensive machines and moulds are required, while cycle times are short (the finished article can be taken from the mould without cooling down).

The dimensions of articles made from moulding powders are limited in two ways: wall thickness can, in general, not be less than a few mm because of the dimensions of the powder particles. On the other hand, with too thick articles (a few cm) porosity in the centre may occur as a result of thermal degradation due to the heat of reaction and the low thermal conductivity.

Compression moulding of *rubbers* is not essentially different from that of thermosets. The starting material is a blend of a rubber, vulcanisation ingredients and

fillers, which is heated to become plastically deformable, and is forced to flow into a mould, where it is kept at a high temperature until the vulcanisation reaction is completed. Also here, there is a competition between flow and curing; premature vulcanisation interferes with good processing.

Vulcanisation of rubbers can be carried out as a separate process after shaping. Shaping can take place at relatively low temperatures since the unvulcanised rubber has an outspoken plastic nature. It is still solid enough to be transferred from the mould to a separate vulcanisation chamber, in which, at a much higher temperature, e.g. by steam, the vulcanisation is achieved.

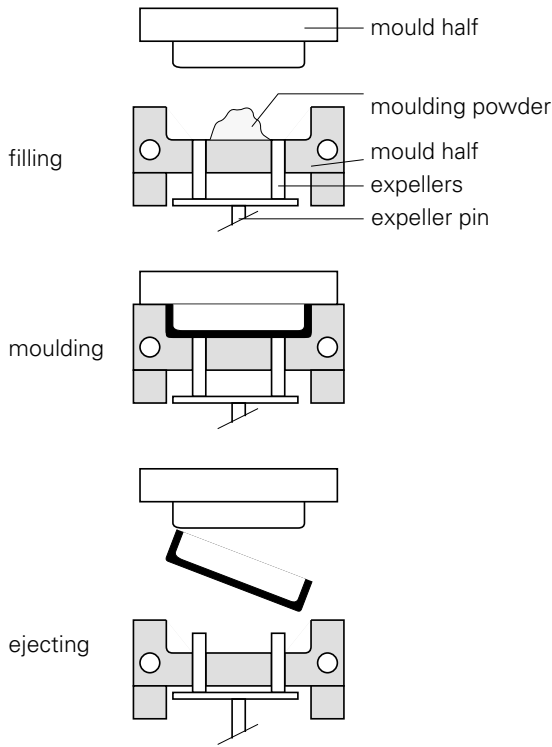


Figure 11.10. Compression mould.

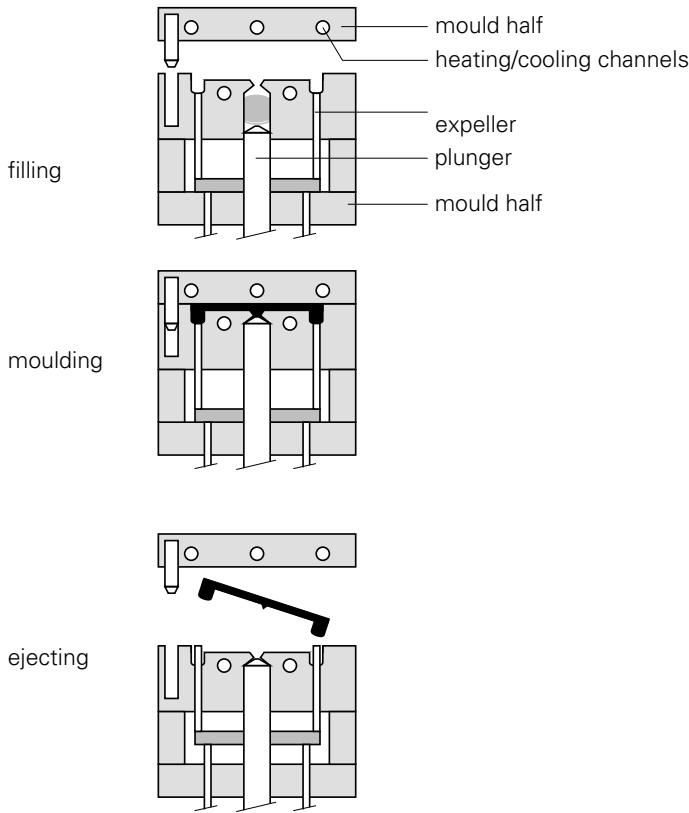


Figure 11.11. Transfer mould.

11.3. Injection moulding

11.3.1. General

Injection moulding is by far the most frequently applied technique for manufacturing end-products directly from a thermoplastic raw material. In this process articles are formed by injecting the molten polymer into a cooled mould. Also on rubbers and thermosets this method is applied, though at a smaller scale; in these cases the mould is heated rather than cooled in order to promote the vulcanisation or curing reaction.

In this section we shall mainly consider the injection moulding of *thermoplasts*.

A thermoplastic material is, usually as a granulate, brought into a cylinder, which is kept at a constant temperature by electric heating elements. With the simplest type of machine the material is molten by heat transfer from the cylinder wall. Since plastics are poor heat conductors, such a heating process takes a considerable time, so that the risk is run of degradation at the wall.

When the material is sufficiently heated, it is transported by a moving plunger under high pressure (sometimes up to 1500 bar) through a narrow channel into the mould cavity (Figure 11.12a and 11.12b). In the cooled mould the product cools down under pressure. After complete solidification the mould is opened and the product is ejected from it (Figure 11.12c).

The plunger has, in the mean time, reached its original position, so that new granulate can enter into the cylinder (Figure 11.12c). Since the cylinder acts as a storage chamber, the cold feed is being heated during the cycle. It is clear that the high injection pressure would push away the back side of the mould, if this would not be pressed against the front side by a closing force, which has to be very high, for instance, for small machines, 10 to 50 tons (100 to 500 kN), for very big machines up to 10,000 tonnes (100,000 kN).

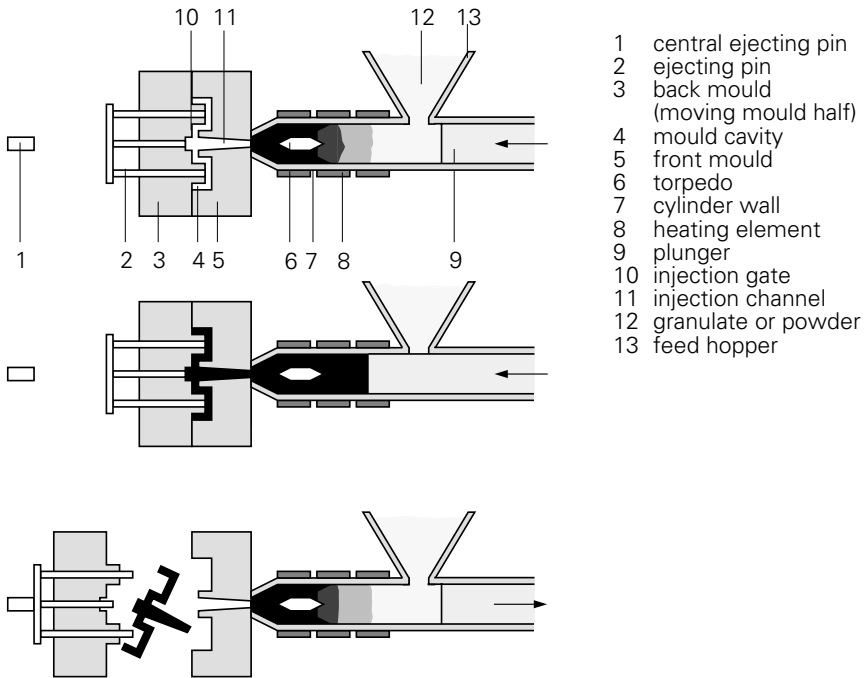


Figure 11.12. Plunger injection moulding machine.

Next to plunger machines, injection moulding machines with *screw-plastification* (reciprocating screw machines) are used at an increasing scale. Here the material is heated by heat transfer from the cylinder wall as well as by internal friction; it is transported and homogenised by an extrusion screw, and, after reaching the screw tip, it is injected into the mould by the same screw, now acting as a plunger (Figure 11.13a). After the mould is filled, the transport channel is closed; the screw continues rotating and transporting molten material to the front side, while pushing

itself backwards (Figure 11.13b). This takes place while the polymer in the mould cools down sufficiently to be demoulded (Figure 11.13c). Hereafter the mould is again closed and the cycle is repeated.

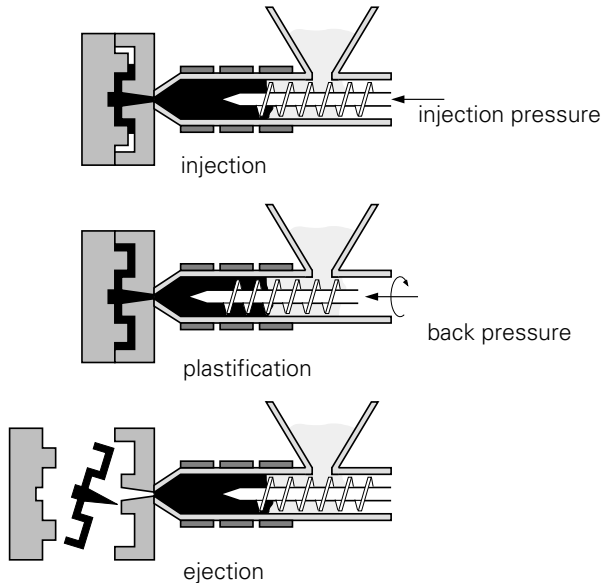


Figure 11.13. Reciprocating screw injection moulding machine.

Because of the much better temperature homogeneity of the injected material, the required injection pressure is two to three times lower than in a plunger machine, under comparable conditions; regions where the polymer is hardly molten cause a considerable increase in viscosity. Plunger machines are, therefore, only used for mass production of *very small articles*. A variant is the combination of screw and plunger, each in their own cylinder, both of which are discharged into a chamber just in front of the injection point; the screw forms and transports the melt, which is the injected into the mould by the plunger.

The *mould* is a very complicated tool. It comprises two halves: the fixed half attached to the stationary platen and the moving half attached to the moving platen. With complicated shapes, or with long flow paths, injection has to take place at several points. For the transport of the melt to these injection points channels are present, which are mostly heated (“hot runners”) in order to prevent cooling of the melt before it enters into the cavity. The mould cavity is surrounded by thick metal walls, through which cooling channels run (with rubbers and thermosets these channels are used for heating). Moreover, the mould contains an ejection mechanism to remove the moulding after opening.

The melt should be present at the appropriate temperature and pressure at each

injection point to enable the desired flow pattern into the cavity, while unwanted phenomena such as poor welding seams and frozen-in orientations or cooling stresses should be avoided.

Computer techniques have been and are still being further developed to simulate this complex mould-filling process, so that, for a given geometry and given rheological parameters and solidification behaviour, it can be predicted. This procedure results in a considerable improvement of the product quality, since it enables optimisation of the mould design.

The mould is kept closed during injection by a heavy, hydraulically controlled, *closing mechanism*. The magnitude of the required forces can be estimated as follows: With an injection pressure of, e.g. 1000 bar, the pressure in the mould may, on average, amount to 1/3 of this value, say 300 bar. When the projected area of the mould is 500 cm², the maximum closing force is 1500 kN (150 tonnes). The size of an injection moulding machine is often characterised by its closing force; for smaller machines this amounts, e.g. to 200 kN, for bigger ones e.g. 3,000 kN and even up to 100,000 kN. In the latter case the force is generated by eight hydraulic cylinders; single mouldings up to 170 kg can be made; the machine measures 30m by 13m and requires an electric power of 1000 kW.

11.3.2. *Limitations*

A first requirement for a good injection moulding process is, of course, that the mould is filled well. The pressure at which the molten polymer is injected should not only be sufficient to transport the melt through the injection channels at the desired speed, but also to continue this transport within the mould through narrow channels with cooled walls. During this transport the melt is cooled, so that the viscosity increases. Eventually, it solidifies, starting-off at the walls. If solidification has proceeded through the whole cross-section of the channel, then further flow is impossible, and an *incomplete moulding* results. The dimensions of the end-product are limited by this phenomenon; the flow-path, i.e. the ratio of the maximum distance over which the melt is able to travel and the thickness of the channel, has an upper value. A practical rule of thumb is, that for well-flowing materials this ratio should not exceed about 300. When the length/diameter ratio of the object to be formed is higher, or when the polymer flows less well, then the only solution is to increase the number of injection points.

As a matter of fact, next to the shape of the mould, the injection pressure and the temperature of the melt play an important role in the filling process. For a given raw material, at each pressure level a temperature level can be determined at which the mould is just filled. This relation is, as far as the polymer is concerned, governed by

the way in which the viscosity depends on temperature and shear rate (see § 11.1.1). In a T, p diagram these minimum values of pressure form the so-called *short-shot line*, which indicates the lower limit in the injection moulding diagram (Figure 11.14).

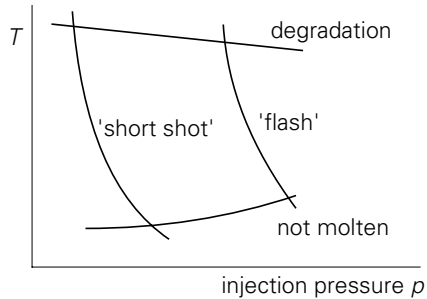


Figure 11.14. Injection moulding diagram.

The position of this curve is, of course, governed by the flow behaviour of the polymer; the fact that the melt-index does not provide sufficient information for this behaviour, has been discussed in §5.4.

Moreover, an upper limit exists to the p, T conditions, namely pressure levels which are too high to be withstood by the closing mechanism of the mould. The mould halves will then be pushed apart, allowing a small quantity of the melt to escape, which results in a filmy extension of the product (“*flash*”). At higher temperatures, so with lower viscosities, flash occurs, as a result of better pressure transfer, at lower injection pressures. The T, p relation is represented by the “*flash-curve*” (see Figure 11.14). The working area of the process is completed by a lower temperature limit which, slightly pressure dependent, represents the condition of complete melting, and an upper limit for thermal degradation.

11.3.3. Defects

Next to the primary requirement that the mould has to be adequately filled, a number of other factors, concerning the quality of the end-product, play a role. These concern, in the first place, the dimensions of the moulding, which should be within narrow specifications. *Shrinkage* during solidification always tends to reduce the dimensions to values, lower than those of the mould. The magnitude of this shrinkage, if no pressure would be applied, is shown in Figure 11.15. It appears that for amorphous polymers an average reduction in volume of about 10% occurs when the polymer is cooled down from processing temperature to ambient temperature; for crystalline polymers this reduction may even amount to 20 or 25% (Figure 11.15; see also Figure 3.1).

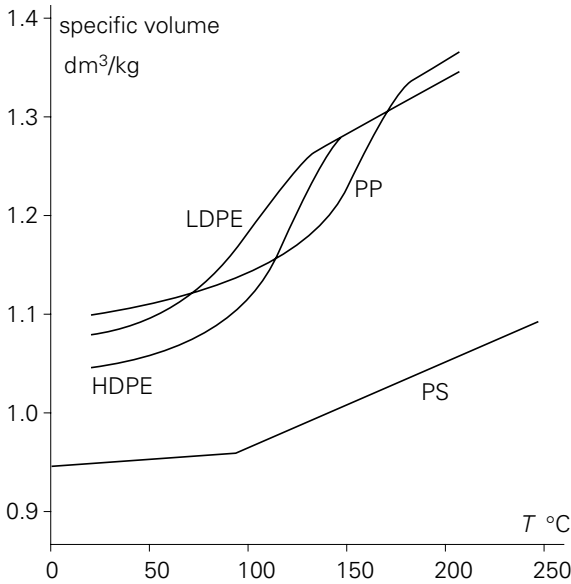


Figure 11.15. Relation between volume and temperature.

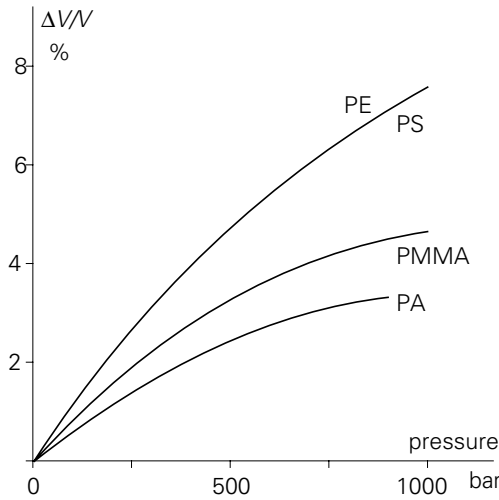


Figure 11.16. Compressibility of molten polymers.

Solidification, however, takes place under pressure; the cooling melt is compressed and has thus undergone a volume decrease as a result of its high compressibility (Figure 11.16), which is able to compensate part of the shrinkage. To demonstrate the competition between thermal shrinkage and compressibility, combined diagrams are often used, the p, V, T diagrams, giving the relation between volume and temperature at several pressure levels. Schematic examples of these diagrams are given in Figures 11.17 and 11.18, for amorphous and crystallisable polymers,

respectively. These diagrams are valid for a certain, realistic, rate of cooling. For the amorphous polymers the effect of cooling rate on the glass transition temperature is of importance, and for crystalline polymers the effect of undercooling. According to these curves, in both cases the pressure plays an important role (not dealt with in Chapters 4 and 5): higher pressures increase the glass-rubber transition temperature and increase the rate of crystallisation at a given degree of undercooling

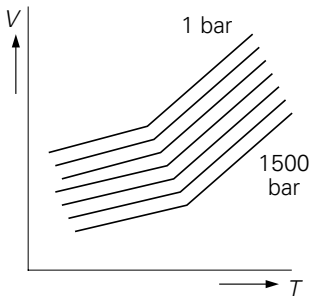


Figure 11.17. p,V,T -diagrams for an amorphous polymer.

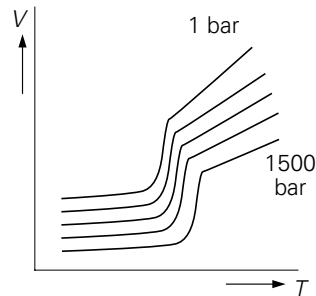


Figure 11.18. p,V,T -diagrams for a crystallising polymer.

Superficial inspection of Figures 11.15 and 11.16 shows that the compensation of shrinkage by compressibility is not complete. Further reduction of shrinkage in an injection moulding cycle is reached by maintaining the injection pressure during some time on the mould cavity, the so-called after-pressure. While the outer layers solidify and shrink, an extra amount of melt is pressed into the cavity, which further reduces the overall shrinkage. When, finally, the injection opening is closed (while a small quantity of polymer sometimes flows back), the polymer in the mould is left to itself during the final solidification process, while the pressure in the cavity decreases (Figure 11.19). A rapid pressure decrease to zero (a) indicates a considerable final shrinkage; when the end-pressure is high (b), the after-pressure has been too high or applied too long; the shrinkage is negative and the moulding is tightly clamped in the mould. The ultimate shrinkage is, for amorphous polymers, mostly between 0.3 and 0.7%, and for crystalline polymers between 1 and 3%.

Besides the total shrinkage, *shrinkage differences* are of importance. The shrinkage may vary from place to place, dependent on the time scale of solidification. The simplest example is a solid block, which solidifies rapidly at its outside; the hard skin formed this way prevents further shrinkage of the inner part. Hence the density decreases from the outside to the inside, resulting in internal stresses which may even lead to tearing and void formation.

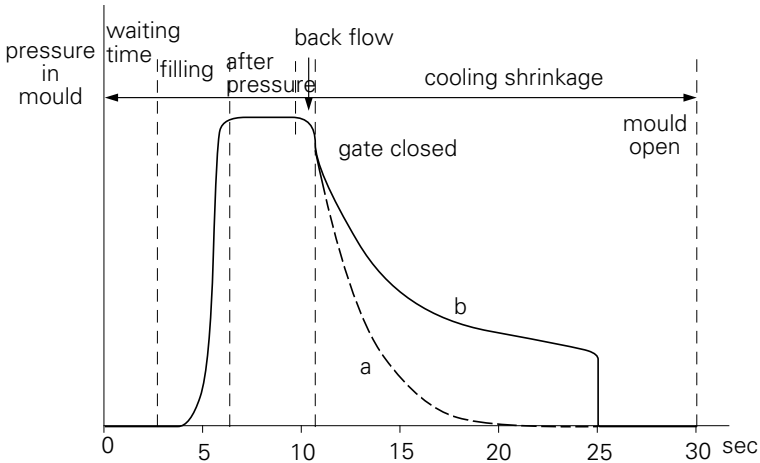


Figure 11.19. Pressure in the mould as a function of time.

Another example is the injection moulding of a pail, where the injection takes place at the bottom. The most removed part, the brim of the pail, will solidify first, thus impeding the shrinkage of the remaining part, in particular of the bottom. The bottom is, therefore, heavily stressed and may spontaneously break in shock loading. A better construction of the mould can prevent this drawback, namely by making the bottom not flat but somewhat hollow, so that the stresses easily disappear by a minor deformation of the bottom.

Another source of uneven shrinkage is a *thickness difference* in the moulding. A thicker part cools more slowly, and attains a higher density than a thin part (see Figure 3.6). These shrinkage differences may give rise to warping of the moulding, for instance when it contains reinforcing ribs or a transition from a thick to a thinner part. Also at the opposite side of a thicker part, sink marks may occur as a result of a higher local shrinkage.

Shrinkage may also be anisotropic, namely when *chain orientations* are present. As discussed in Chapter 5, these orientations result from rubber-elastic deformations in the melt; they are, therefore, found in parts where the melt has been rapidly cooled under conditions of a high rate of strain. Shrinkage is higher in the orientation direction than across, so that, for instance, a flat disk, injected from its centre, tends to deform into a saddle-like shape (warping).

Defects can also occur when two melt streams join together in a mould, forming a not properly welded interface; sharp internal angles may give rise to stress concentrations, etc.

All these defects can be avoided by taking the specific behaviour of the polymer into account when designing the product. A good mould design is also very important,

e.g. as concerns the *number and the position of injection points*, the cooling, etc. Besides, the choice of the polymer plays a role, for instance as to the chain length and -distribution in view of orientations, and the various process variables (injection pressure and -temperature, after-pressure, mould temperature).

11.3.4. Foam moulding

A special type of injection moulding is the manufacture of *foamed articles*. The foaming process takes place in the mould, so that mould filling requires considerably lower injection pressures and mould closing forces. Very large mouldings can be made in this way.

An increasingly applied process is reaction injection moulding (RIM). In fact this resembles the afore-mentioned mould-casting technique, since it starts off with low-molecular, low-viscous liquids, which in the mould react together into a solid product. The injection moulding machine is used to inject this blend into the mould at a high speed, while the pressure is relatively low. Complete filling of the mould is facilitated by the addition of a small amount of *blowing agent*, which brings about a low degree of foaming; the mould closing forces can be relatively small. Large mouldings, such as micro-porous bumpers for motorcars (e.g. of polyurethane rubber) can, in this way, be manufactured economically (see further § 11.6.3).

11.4. Calendering and extrusion

11.4.1. Calendering

Calendering is a continuous forming process, used to produce film and sheet of practically unlimited length. The whole process takes place on a number of rolls: homogenising, dosing and shaping on the heated rolls, cooling on a number of cooling rolls. Figure 11.20 presents a schematic view of the calender. The material is first heated, mixed and kneaded on a mixing mill, and is then fed into the gap between the first and the second roll, where it is further homogenised, and then transported to the third and to the fourth roll, respectively. The final shaping is carried out between the last two rolls, through which the material is squeezed. The formed sheet is then removed from the roll by a take-off roll and transferred to the cooling device, after which it is wrapped up.

The pressure difference, required to squeeze the plastic matter through the narrow gaps between the calender rolls, is generated by the calender itself according to the principle of the friction pump: When a plane moves in its own direction through a fluid by which it is wetted, then the fluid, adjacent to the plane, will have the same velocity as the plane. By transfer of impulse, the whole fluid will start moving, so

that transport can take place.

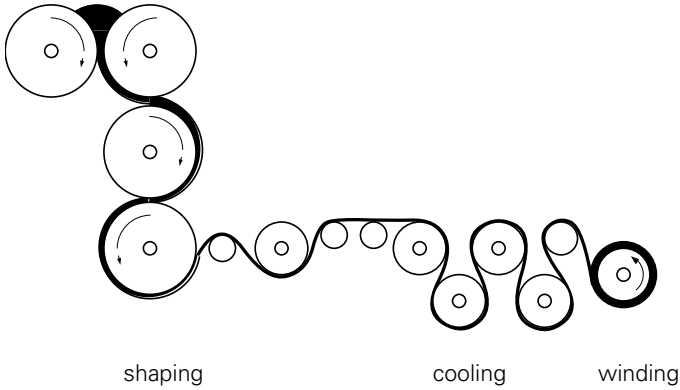


Figure 11.20. Principle of a calender.

When the cross-section of the flow channel decreases, the flow will proceed against a built-up back-pressure. This back pressure, which reaches its maximum at some distance before the narrowest part of the gap, forces the material through the gap, while it obtains a higher speed than the circumferential roll speed. A part of the material supplied by the upper roll, flows back from the location of the pressure peak, and arrives at the bank in front of the gap, in which it circulates (see Figure 11.21).

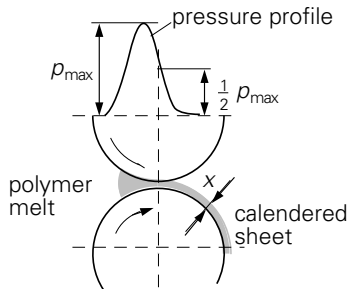


Figure 11.21. Pressure profile in the gap of calender rolls.

The generated pressures are very high as a result of the high viscosity of the polymer. When a $50 \mu\text{m}$ thick PVC film is made, the line pressure may be as high as 8 kN/cm , so that a 250 cm roll is subjected to a total force of 2000 kN (200 tonnes). This force results in a bending deformation of the roll, which increases the distance between the rolls in the middle. Though the rolls are heavily constructed (diameter about $1/3$ of the length), the deviations in film dimensions may pass the tolerance limits. An allowable thickness deviation of 5% means a maximum bending deformation of 3

μm ! A practical solution to avoid this difficulty is, to position the axes of the rolls with a small angle with respect to each other. This results in an increase of gap width from the centre to the outer parts, so that the effect of roll bending is compensated.

Another difficulty with calendering is, that the, still plastic, sheet has to be taken-off from the final shaping roll. This requires a certain force to overcome the adhesion between the sheet and the roll. The plastic material should be able to cope with this tensile stress, and, therefore, should be in a rubbery state. As a consequence, only polymers showing a pronounced rubbery region, can be processed by a calender. Possibilities are: PVC (as such or plasticized), ABS, and, as a matter of fact, rubbers. The elastic stresses generated by take-off are partly frozen-in upon cooling. In all products made by calendering, therefore, frozen-in orientations are present, resulting in anisotropy of properties (the “*calender-effect*”). Moreover these frozen-in stresses may lead to shrinkage in the length-direction, which, in particular, is a nuisance in welding operations. A measure to prevent the calender effect is the application of a strong, flat stream of heated air, which scrapes the sheet from the last roll.

11.4.2. Extrusion

With *extrusion*, also a continuous process, the material is heated, molten, pressurized, and forced through a die, all along one and the same screw. The pressure build-up again takes place according to the principle of the friction pump. In Figure 11.22 the extruder is schematically represented. Its most essential part is the screw, which fits in a cylinder, provided with heating elements and cooling channels, so that a desired temperature profile can be established and maintained. At one end of the screw the filling opening is located for the raw material supply; at the other end the molten mass leaves the machine via the shaping die to be cooled thereafter.

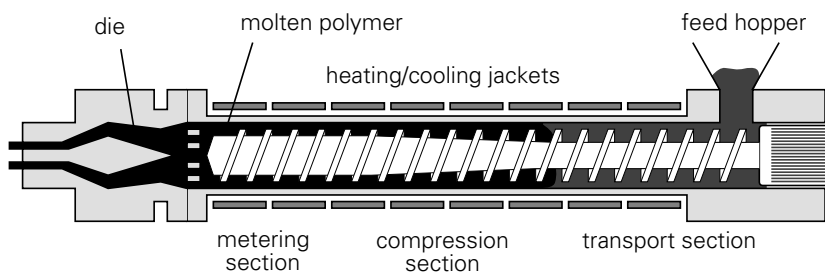


Figure 11.22. Principle of an extruder.

The screw performs the following tasks:

- transport of the granulate or powder, supplied from the hopper, to the heating zone;

- densification of the material by reduction of channel depth or pitch;
- perform work of friction on the, already plastic, mass, for homogenising and heating (an important part of the required heat is generated by friction);
- pumping the molten polymer to the die and generating the pressure required for transport through the die.

This multitude of functions makes it impossible to process a variety of polymers with one and the same screw. Each polymer has its own demands, concerning, i.a., granule size, required compression ratio, melting behaviour, risks of degradation, etc.

The final part of the screw acts as a *friction pump*. This can be visualised most easily by first imagining the screw at rest in a rotating cylinder, and then unrolling the screw channel into a straight channel with a rectangular cross-section. The cylinder wall then forms a lid on the channel, moving at a certain angle. In a cross-section through the length direction of the channel, a velocity distribution would occur as sketched in Figure 11.23a, if the end of the channel would be open, namely a linear distribution between the limits 0 (channel bottom) and v (the component of the cylinder speed in the length direction). With a flow restriction at the end of the channel (the shaping die), a back-pressure p is built up. The velocity profile as a result of this back pressure only, would look like Figure 11.23b: a parabolic distribution in the opposite direction. The combination of these two distributions is sketched in Figure 11.23c; a net flow results, which governs the throughput of the extruder. This throughput, Q , can be estimated as follows: The drag flow to the right, Q_d , is proportional to the velocity, v , and thus to the rate of rotation of the screw, n , and is also dependent on the geometry of the screw channel, but not on the viscosity of the melt, so: $Q_d = a \cdot n$. The pressure flow in the opposite direction, Q_p , is proportional to the pressure p , inversely proportional to the viscosity η , and, further, again dependent on the screw geometry, so :

$$Q_p = b \cdot \frac{p}{\eta}$$

The net flow, $Q = Q_s - Q_p$, is the flow transported through the die under the influence of the pressure, p , and is thus proportional to p/η , and, further, dependent on the flow resistance of the die. So we see:

$$Q = an - b \frac{p}{\eta} = c \frac{p}{\eta}$$

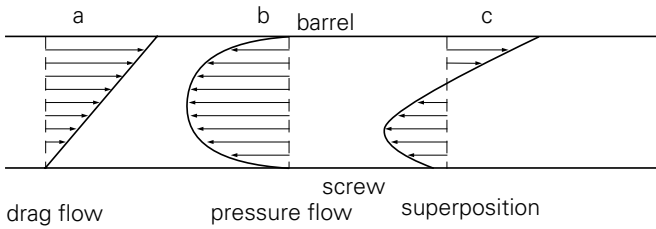


Figure 11.23. Velocity distribution in the screw channel of an extruder.

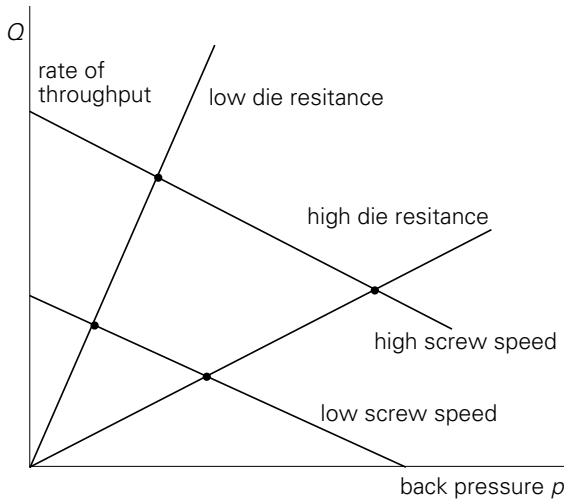


Figure 11.24. Extrusion diagram.

A plot of the throughput Q as a function of the pressure p is given in Figure 11.24. For a given screw geometry the first equation, the screw characteristic, is given for two values of the rate of rotation, n , while the second equation, the die characteristic, is shown for two levels of the flow resistance in the die, $1/c$. Each combination gives rise to an intersection of the two lines, the working point of the extruder, from which the values of Q and p can be read. Combination of the two equations results in:

$$Q = n \frac{ac}{b + c}$$

in other words: the throughput rate is, for a given screw/die combination, proportional to the rotation rate of the screw, and independent of pressure and viscosity. This treatment is only valid for a Newtonian fluid (constant viscosity). In reality, polymers deviate from this simplified picture, though the general conclusions are not affected. (see also Qu. 11.19).

Besides the single-screw extruder, also *twin-screw extruders* are being used. Two

parallel screws rotate within the same cylinder housing, either in the same or in opposite direction; in the latter case the screws intersect partially. The mechanism of transportation is much more complex than with a single screw. Twin-screw extruders are used for powders which are difficult to transport, but mainly as mixing devices in the compounding industry. Their mixing and homogenising capacity is much greater than of a single-screw extruder.

After leaving the die, the extruded strand shows an instantaneous increase in thickness. This is a consequence of the elastic elongation, in particular induced by the elongational flow in the die, which spontaneously recovers when the material leaves the die. This so-called “*die swell*” or “*extrudate swell*” has to be taken into account when designing the die; in particular, when the cross-section of the extrudate is not circular, not only a diameter increase but also a distortion in shape occurs. The distortion can be prevented by adjusting the shape of the die opening.

A second consequence of the elastic behaviour of the melt is the occurrence of *melt fracture*. At high rates of extrusion the elastic deformation of the melt may become so high that it locally breaks, resulting in an irregularly shaped extrudate or in surface roughness.

The range of products which can be made by extrusion is very large: rods, threads, pipes, hoses, sheets, films, profiles, wire coatings, etc. Threads and rods can be formed quite easily by applying a round die opening. Pipes and hoses require an annular opening; after leaving the die, the product is fed into the calibrator, a somewhat wider cylinder, in which the pipe, either by internal pressure or by vacuum suction through narrow openings, is pressed against the highly polished inside surface.

Sheet extrusion requires a broad die, in which an even distribution of the flowing polymer along its width, and an equal flow resistance at each point, has to be taken care of. Sheets are being extruded up to a width of 3 or 4 m, in thickness up to 3 cm. If desired, sheets can be produced with a wave-shape, by passing the, still plastic, extrudate between two profiled rolls. Film extrusion can be done in a similar way, as a matter of fact with a narrower die gap. After extrusion, sheets and films are cooled in a water bath or on polished cooling rolls.

An important application of extrusion is the *coating of metal wires* or profiles with a plastic layer. This is done on a large scale in the manufacturing of electrically insulated wires and cables. For this purpose a cross-head is needed (Figure 11.25). The same principle is used for plastics profiles containing a metal core. These may have a very complex shape, such as for windowframes.

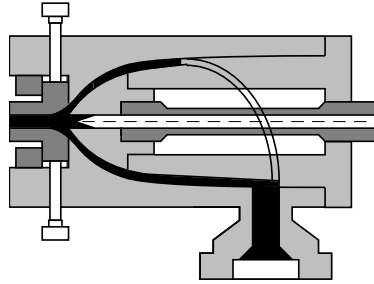


Figure 11.25. Cross-head.

Rubbers are also being extruded, in a not essentially different way from plastics. Cooling of the extrusion cylinder is necessary to prevent premature vulcanisation as a result of the heat developed by internal friction. The extruder is fed by ribbons, obtained from milled sheets. End products are: hoses, profiles, and cable mantles. On-line vulcanisation can be achieved by passing the extrudate through a steam channel, while the rate of extrusion is adjusted to the rate of curing. For this purpose high-rate vulcanisation recipes have been developed. Steam temperatures of about 200 °C are being applied (15 bars pressure). Treads for motorcar tyres are also extruded; they are wrapped round the pre-formed carcass and then formed and vulcanised in a press.

11.4.3. Film blowing

An alternative way of producing film is the *blowing process*. An annular die is used, from which the material emerges as a thin-walled tube, which is immediately blown-up by internal pressure to a much larger diameter (Figure 11.26).

The tubular film thus formed is laid flat and reeled, and can, by cutting and welding, easily be formed into plastic bags.

Multi-layer films can be produced, composed of different polymers. For each polymer a separate extruder is applied; the extruders discharge into an accumulator, in which the separate streams are guided to their own position in the film. A laminated film can thus be made, in which one of the layers provides the strength, another one acts as a gas barrier, other layers promote adhesion and weldability, etc. This laminating process is applied with flat film extrusion as well as with film blowing.

Extruded films are sometimes *bi-axially stretched*, in particular PE and PP films, which gain in strength and transparency by biaxial orientation. The stretching takes place at elevated temperatures, but below the melting point. The edges of the film are gripped by a series of clips, which diverge in the transverse direction and simultaneously accelerate in the machine direction.

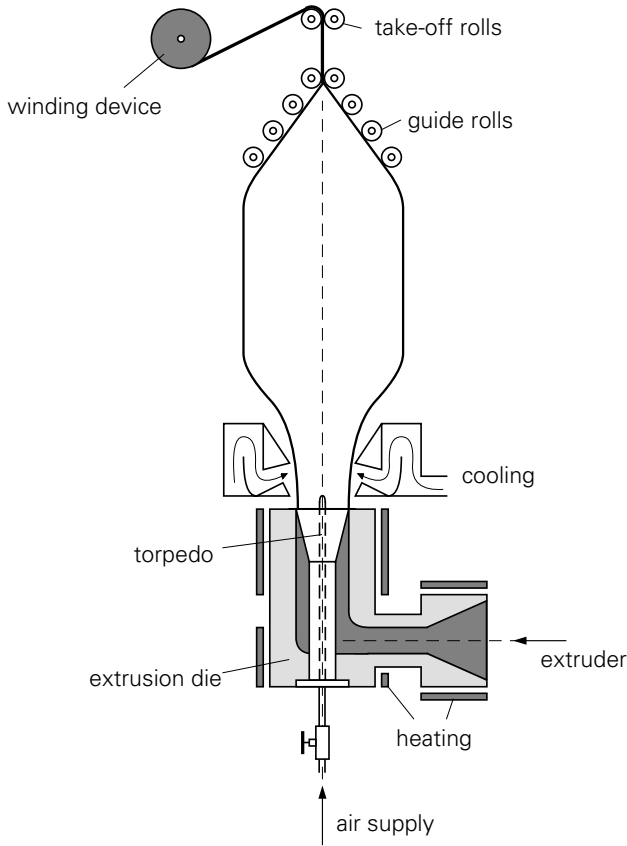


Figure 11.26. Film blowing.

11.4.3. Bottle blowing

Blowing of *hollow articles* such as bottles and containers can be carried out on-line with the extrusion process. A thermoplastic tube, emerging from the extruder die, is, in the plastic condition, blown-up against the inside of a mould comprising two halves, the walls of which are cooled. The neck of the bottle is calibrated with the aid of a mandrel; the bottom is sealed by the mould parts. The principle is indicated in Figure 11.27. Since, especially for thick-walled articles, the cooling time largely governs the cycle time, long waiting times are avoided by using a series of moving moulds. When the bottle has cooled down sufficiently, the mould is opened, and moves back to the extruder to be filled again. Since the pressures required for blowing are relatively low, the mould does not need to be heavily constructed, and is, therefore, much simpler than the mould in an injection moulding machine.

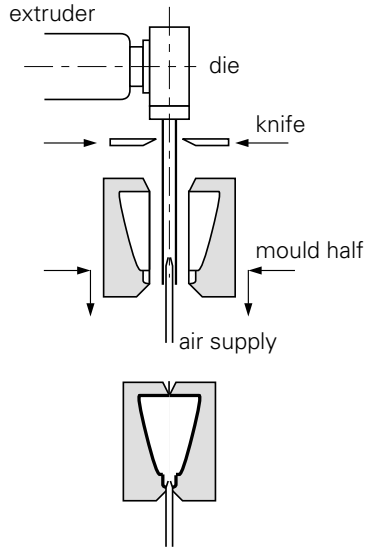


Figure 11.27. Bottle blowing.

The polymers mostly used for bottle blowing are PE, PVC, PA and PC. The size of products has gradually increased: bottles are being made up to 60 litres, containers up to 10 m³. The blowing process, though simple, has a few disadvantages: the wall thickness is uneven, pinching-off at the extremes causes a considerable loss of material, and the weld at the bottom is defacing. These drawbacks are partly taken away by a variant of the process, the injection moulding blowing process. Here a pre-form is made by injection moulding, comparable to the extruded parison, but now much more adjusted to the ultimate shape of the bottle as to shape and wall thickness distribution. This pre-form is, together with the mandrel round which it has been shaped, transported to a second part of the mould, in which it is blown-up under pressure. This process is applied for demanding articles, such as POM aerosol bottles.

A newer development is the manufacture of *bi-axially oriented* bottles, in particular for PETP. The pre-form is injection-moulded and rapidly cooled in the mould; it remains amorphous (PETP crystallises very slowly); by heating above its T_g (65°) it passes into the rubbery state, and can then be blown-up and, simultaneously, longitudinally stretched. The biaxial orientation thus obtained, accelerates the crystallisation, and, at the same time, results in a very fine crystalline texture, so that a thin-walled, strong, transparent and heat-resistant bottle is obtained.

11.5. Secondary shaping

11.5.1. Thermoforming

The processing techniques dealt with in this section are all within the category “secondary shaping”. The starting material is obtained from a primary shaping process as an intermediate, for instance as a sheet, as a film, a block or a pipe.

Sheet forming is carried out on a sheet, in most cases extruded, sometimes calendered. The sheet is first heated to above its softening temperature, then formed and thereafter cooled. The technique most frequently applied is *vacuum forming*; the force required for deformation is brought about by a vacuum below the heated sheet, which sucks the sheet onto the mould. In its simplest form, this process is sketched in Figure 11.28. Heating is mostly achieved with infra-red radiation sources, cooling with compressed air or water sprays.

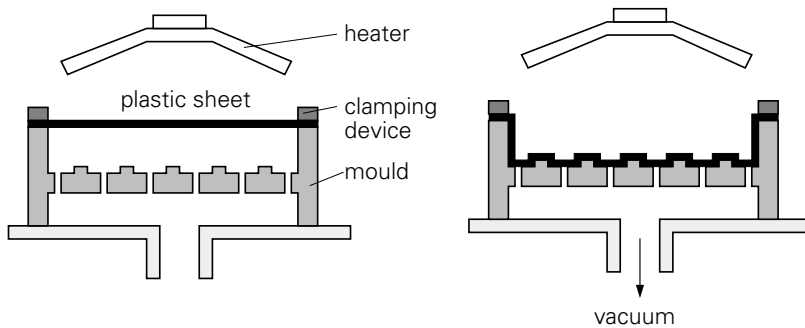


Figure 11.28. Vacuum forming.

An important factor with vacuum forming is, that the heated polymer is not too soon passing into the fluid state; the sheet would then, during transportation to the mould, be deformed too much by sagging-out. Hence, the polymer should show a pronounced *rubbery region* on the temperature scale. For this reason, amorphous polymers such as PVC, PS, PMMA, PC, ABS, etc. are eminently suited for vacuum forming. With semi-crystalline polymers the rubbery region is largely masked by the crystallinity above the glass-rubber transition (see Figure 11.29). With PE and PP, vacuum forming is, therefore, a critical operation, in which the processing conditions should be very carefully controlled. Only high-molecular grades show sufficient rubbery behaviour above their melting point to enable a sheet-forming process. PA, PETP and PBTP, however, cannot be shaped this way.

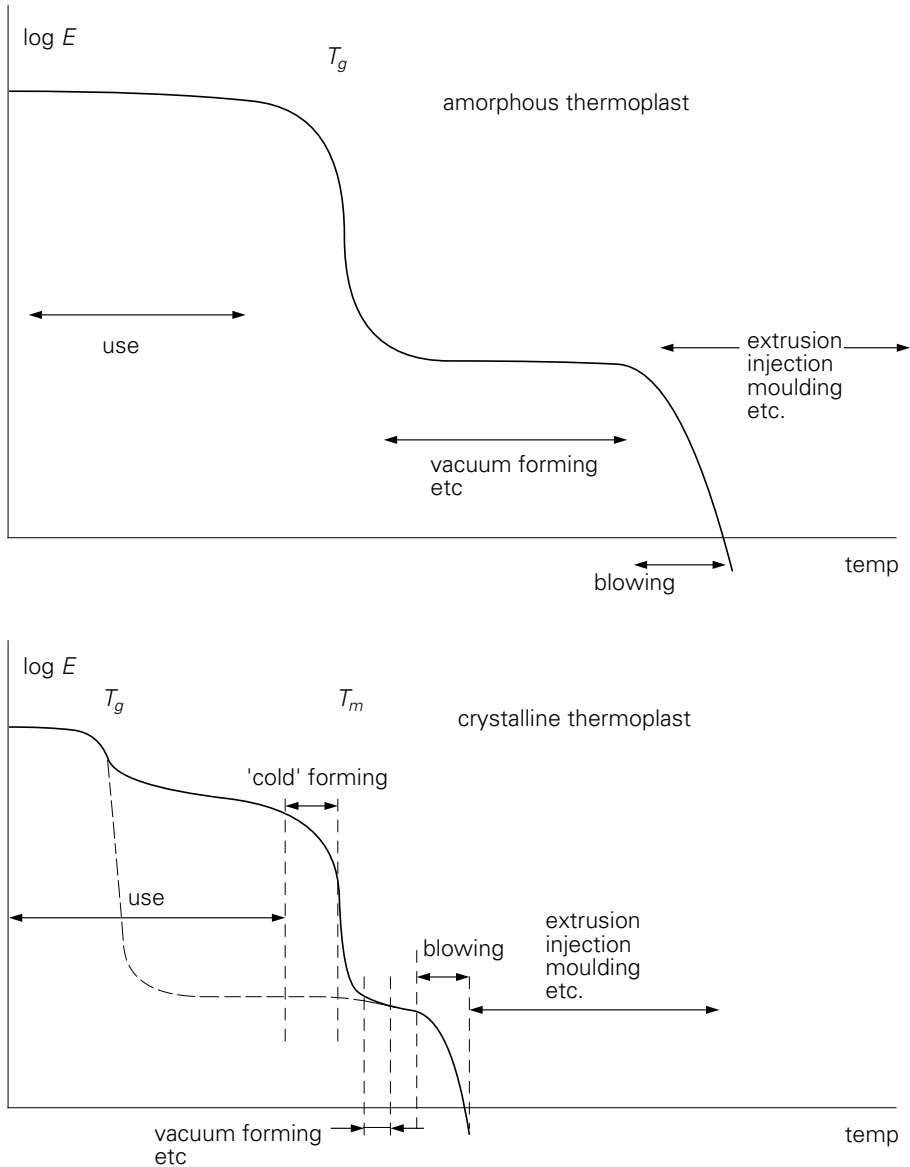


Figure 11.29. Temperature regions in which various processing techniques can be applied.

With thicker articles or with complex shapes, vacuum does not always provide a sufficiently high force to bring about the required deformation. Therefore, air pressure is sometimes applied, or plugs, either simultaneously or consecutively; various combinations are being used. Typical areas of application are: cups and trays for food packaging, articles with a larger area such as lighting ornaments, casings for apparatuses and machines, kitchen dressers, bath tubs, rowing-boats, etc. For this type of articles injection moulding is a less suitable technique, due to the

unfavourably long flow-paths and the required high mould closing forces. The moulds for sheet forming are considerably simpler and cheaper than for injection moulding because of the much lower forces required; for comparable dimensions their cost is, on average, five times lower. Cast aluminium is excellently suited for sheet forming moulds; experimental moulds can be made from timber or gypsum; for small series moulds of epoxy- or phenolic resin are suitable.

Sheet forming processes show two important drawbacks: In the first place, the pattern of deformation results in a strongly *uneven wall thickness* of the finished article. In a cup, the lower brim may, for instance, be two times thinner than the middle or the upper rim. The second drawback is associated with the fact that deformation takes place in the rubbery condition. In this condition straining goes accompanied by chain orientations, which are frozen-in upon rapid cooling. When heated to above its glass-rubber transition temperature, the article recovers to its original shape as a flat sheet, but also at lower temperatures it shows a strong tendency to shrinkage.

11.5.2. Cold sheet forming

With *cold-sheet forming* also finished products are formed from sheet, but now in the solid state, at low temperatures, so that considerably higher plug forces are required. In most cases the rim of the sheet is not clamped, so that during forming its circumference decreases: the sheet material is pulled in the inside direction. As a consequence, the differences in thickness of the finished article are much smaller than with the heat-forming process, namely not more than about 15%. A schematic picture of the deep-drawing process is given in Figure 11.30.

11.5.3. Forging

Thick-walled articles can be manufactured by forging a sheet, as shown in Figure 11.31. In this way gear wheels, pulleys, etc. can be made.

In comparison with injection moulding, forging has the disadvantage that the article is not made in a single step from the raw material, but via an extruded bar or sheet. Forging, however, offers the significant advantage of a shorter cycle time for thick articles, e.g. above 10 mm. With injection moulding the cycle time strongly increases with the material thickness, since the cooling time is proportional to the square of the thickness. This is demonstrated in Figure 11.32 for a disk-shaped PP article. Moreover, notwithstanding the higher forces required, a forging mould costs only about 30% of an equivalent mould in an injection moulding machine.

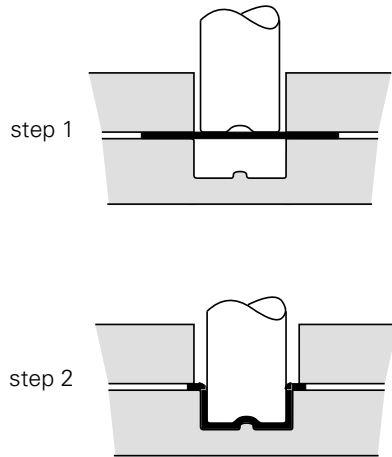


Figure 11.30. Deep-drawing.

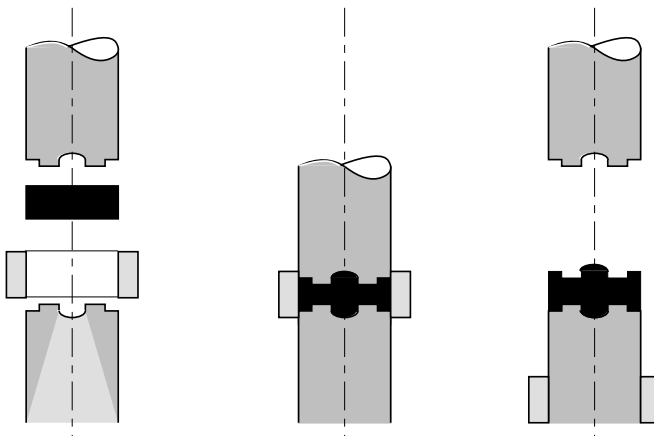


Figure 11.31. Forging.

11.5.4. Bending

Bending of a sheet or a pipe is a simple operation; in most cases the object is heated till it reaches the rubbery state. Sometimes cold bending is possible, e.g. with a thin PVC sheet to cover a wooden gutter, though at the cost of the mechanical properties. Thin-walled channels with a large cross-section are easiest made by bending of sheet; the seams are then welded.

The heating operation is hampered by the low heat conductivity of the material and by its sensitivity to heat degradation during long exposure times. Sheets up to 3 mm can be heated from one side; with thicker ones both sides should be heated. The use of a liquid bath, e.g. glycol, is, when possible, the best method.

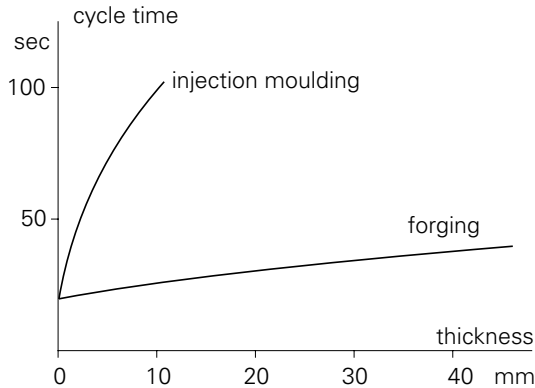


Figure 11.32. Cycle time with cold forging compared with injection moulding.

11.5.5. Machining

Plastics can be shaped by machining, though, in comparison to metals, some *special precautions* should be taken:

- The low stiffness necessitates rigid supporting and clamping devices; moreover the forces exerted should not be too high.
- Brittle plastics may present difficulties with stamping and cutting operations.
- In view of the low softening temperature, combined with low heat conductivity, very effective cooling is required as well as a low cutting speed.
- Absorption of oil or water may affect the dimension tolerances; moreover some oils and fats may cause environmental stress-cracking.
- Some polymers develop irritating or poisonous vapours upon heating, such as PVC and, in particular, fluoropolymers.
- Recoil of the material may affect the dimensions; with drilling, for instance, an over-measure of a few 0.1 mm is desirable.

Machining operations are expensive due their high cost of labour. This does not so much count if only a small number of products have to be made. For mass-production injection moulding is more economical, also with respect to the much lower material losses.

11.5.6. Welding

Welding of intermediate products such as pipes, sheets or films is mostly applied to articles in the technical sector (pipe installations, tanks etc.) and in the packaging sector (packaging film).

Since the viscosity of the molten material is always high, the weld does not flow

spontaneously together such as with metals; a good weld is only formed under pressure. Another important difference with metals is the lower specific heat of the polymer per unit volume; together with the lower melting temperatures this results in much lower required amounts of heat, namely about 10% of those for metals. Moreover, the heat is not easily removed in view of the *low conductivity*, so that the material in adjacent parts remains cold. Because of the high thermal expansion, shrinkage stresses are readily generated during cooling. These stresses may give rise to the formation of crazes around weld lines in materials which are sensitive to crazing. Crazing may also result from stresses originating from differences in crystallinity or texture, brought about by the local heat treatment.

An often used welding technique is *thread-welding*; a heated weld thread is pressed into a V-shaped groove between the sheets to be welded together. Also welds are being made without the addition of extra material; with mirror-welding a heated metal plate is used, against which the two parts are pressed at opposite sides. As soon as the material is in a sufficiently plastic state, the mirror is removed and the parts are pressed together. With socket-welding the inside of the socket and the outside of the pipe are heated and welded together. Thick-walled pipes are sometimes welded by heat of friction; both ends are brought into touch and rotated at a high speed with respect to each other; when the surfaces are sufficiently plastified, rotation is stopped and welding is finished by pressure.

Film welding requires special precautions in view of the small thickness. When the two overlapping ends are heated by an external heat source, the heat is supplied at the wrong side of the film so that the films are heavily distorted. With very short electric pulses good welds can be made, though only with thin films (up to 0.2 mm), and with special precautions to avoid sticking of the film to the clamping device.

It is much more attractive to heat the films from the inside, namely by the application of a *high-frequency electric field*. In this case the clamping device remains cold, and the highest temperature is generated at the surfaces to be welded together. Only polymers with a not too low dielectric loss factor (see § 8.2.2) are suitable for this process, such as PVC and PMMA. PE, PP and PS, on the contrary, cannot be welded in this way.

A modern method of welding is *ultrasonic welding*. High-frequency and high-intensity sound waves are passed through the material; the damping of these waves transforms the sound energy locally into the heat required for welding, while, again, the clamping device remains cold.

A special problem is met when films, possessing uniaxial or biaxial orientation, have to be welded. Heating of these films leads irrevocably to strong shrinkage. To avoid

this, PE and PP films are often coated. in a co-extrusion process, with a thin layer of a polymer which can be welded by high-frequency electric fields. The heat is then only developed in the outer layers which are welded together.

11.5.7. *Gluing*

The adhesion of a glue to a substrate can take place by three different mechanisms:

- *Mechanical anchoring* of the glue in the surface. The surface should be rough or porous and the glue should be able to penetrate into all surface details.
- *Absorption of the adhesive* into the surface. The glue should then contain a solvent which swells the plastic substrate. The glue can then penetrate into the surface, and, after evaporation of the solvent, it adheres well to the surface. As a gluing agent a solution of the same polymer is sometimes used.
- *Adsorption of the adhesive* to the surface can, also with smooth and non-swelling materials, provide a good joint; molecular attraction between both kinds of molecules effects the adhesion.

Some polymers do not swell or solve or show any adhesion with any type of adhesive, such as PE and PP, which can, therefore, not be joined by gluing. However, a very thin surface layer can be chemically modified by an electric discharge, or by strong etching chemicals, so that adhesion is enabled. Similar surface treatments are also applied to enable printing with paint or ink.

Polymers play a dominant role in the preparation of adhesives. Three groups can be distinguished: thermoplastic, thermosetting and rubbery adhesives. *Thermoplastic glues* are being applied as solutions or as suspensions in water. Mostly they are one-component systems. The presence of the solvent or water is a disadvantage, since their evaporation takes a long time, and gives rise to a considerable volume decrease. A well-known thermoplastic adhesive is polyvinylacetate, which is used as a solution or as a dispersion. Another type, polyvinylether, is in fact a highly viscous fluid, which, by its high viscosity, provides a certain adhesion, but remains sticky.

Thermosetting adhesives are, in general, two-component systems, and may be cured either at ambient or at elevated temperatures. After the components have been mixed, the glue has a limited time of application. Phenol formaldehyde, polyester resins and epoxies are being used; the latter show a very strong adhesion to practically all materials.

Adhesives on the basis of a *rubber* are applied as watery dispersions, as solvents, or as solvent-free fluids. Sometimes the rubber is vulcanised after the gluing process, sometimes it remains uncured. Polymers often used are butyl rubber, polyisobutylene, and polychloroprene. A more recent development is the use of

thermoplastic elastomers such as SBS, which is, as a hot-melt adhesive, applied in fluid condition, form a strong, elastic adhesive layer after cooling.

11.5.8. Surface coating

In some cases a *decorative or protecting layer* is brought onto a plastic article. Lacquer layers can be applied from a solution; when the lacquer has to be cured, then the curing temperature is limited by the softening point of the polymer. The formation of crazes can never be totally avoided; in most cases a decrease in impact strength to about half its initial value can be expected.

Flexible plastics and rubbers can, as a matter of fact, only be treated with rubber-elastic lacquers, mainly on the basis of polyurethane, which, moreover, should be resistant to oxidation, oils, fuel and UV light. Besides, polyurethane lacquers are often used for several other plastics, such as PVC, polyamides, ABS and glass-fibre reinforced resins.

Some polymers, such as PE and PP, should undergo a *surface treatment*, just as with gluing and printing, before a lacquer can be applied. This treatment may be a short exposure to a hot, oxidizing flame, an electric corona discharge, or a strong oxidizing agent.

Another way of surface improvement is *metallising*. Very thin metal layers (up to a few μm), are deposited by evaporating the metal under vacuum. This method can be applied to all types of plastics. Metallised films find their application in electro-technics and as reflectors for radiant heat. In an electric oven aluminium is evaporated, while the vapour is precipitated on the surface to be treated; in most cases an extra protective transparent layer is added.

Coating of polymer surfaces with thicker metal layers (10–30 μm) is a much more complicated operation. Several pre-treatment steps are required: first the polymer surface has to be modified in such a way that, by a chemical process, a layer of copper or nickel can be deposited. With ABS use is made of the circumstance that it is a two-phase system, consisting of a hard matrix in which rubber particles are dispersed. The rubber particles present at the surface, are etched away, leaving a rough, porous surface, which offers a good adhesion to the chemically deposited copper or nickel. Thereafter the application by electrolysis of further layers of other metals (e.g. chromium) is simple. Also for PP, PMMA and polyamides, methods have been developed for chemical deposition of the first metal layer.

Metal layers have a decorative function, but they also protect the plastic material against scratching, abrasion, chemical attack and UV-aging. Moreover, they contribute significantly to the bending stiffness of an article, since at the surface the

stiffening metal layer has the greatest effect on this property.

11.6. Processing of composites

11.6.1. General

For a number of composite plastic materials the processing techniques are hardly different from those for the single ones. This holds for polymer blends, polymers reinforced by particles, and polymers containing short glass fibres. Two categories, however, ask for special attention, namely the composites with continuous reinforcing fibres, and the plastic foams. The former are shaped by impregnation processes, with the latter the composite material, the foam, is also created during the forming process.

11.6.2. Impregnating

Reinforced thermosets are made by *impregnating the fibres*, present as mats, bundles or cloths, with a liquid resin system; after total impregnation the resin is cured. In most cases glass fibres are used. They can be applied as rovings, i.e. bundles of parallel elementary filaments, each 5 to 10 μm thick. These rovings offer the possibility to be positioned in various directions, so that they can match the desired distribution of strength. By applying, for example, in a cylindrical tank twice as much glass in the circumferential direction than longitudinally, the strength properties are adjusted to the various stresses brought about by the internal pressure.

Another form is the glass cloth, composed of rovings. Weaving can take place in various patterns, varying from practically unidirectional to “*square weaves*” with equal properties in the two main directions.

Another possibility is the use of *glass mats*, composed of glass felt, which is obtained by joining together pieces of fibre with a small quantity of polyester resin. The fibres are oriented at random. Glass mat is relatively cheap, and is very well suited for the construction of complex objects.

A good *adhesion* between the fibre and the resin is important. Usually, the glass fibres have already been subjected to a chemical treatment by their manufacturer in order to improve their adhesion. The most often used agents for this purpose are based on methacrylate-chromium compounds and on organic silicium compounds.

The main function of the resin is, to provide an even *stress distribution* over the fibres. The mechanical properties of the composite depend, in the first place, on the amount of glass and on its distribution over the matrix.

Fabrication can be done in various ways. The simplest method is “*hand-lay-up*”, where the resin is brought into the fibre mass by hand. The resin system can also be brought onto a mould, together with short glass fibres, by a spraying pistols. Further shaping of the impregnated fibre mass is possible by using atmospheric pressure; this is done by vacuum suction through a porous mould wall. Air pressure can also be used (the “air-bag” method). Curing can be accelerated by heating the mould.

A more streamlined form of impregnating is the continuous method, where fibre bundles are passed through an impregnation bath, filled with the resin system. The impregnated bundles are then arranged into their final position. This may be in a sheet or in a profile (*pultrusion*), but the wet roving can also be wound around a mandrel for the production of a pipe or a vessel. In this case, by proper choice of the pitch angles and, with vessels, rotation of the mandrel round various axes, the distribution of strength can be varied within wide limits. Curing of the objects thus made, is mostly carried out in hot-air ovens.

Impregnation techniques are suited to produce articles of strongly varying dimensions. With the hand-lay-up method with open moulds and with spraying techniques, the dimensions are practically unlimited. Also with the vacuum- and the air-bag methods few restrictions are being met. The minimum wall thickness is about 1.5 mm with open-mould, vacuum and air-bag techniques. With filament winding the minimum is about 1 mm. Maximum values of the thickness are, with hot-pressing and with filament winding, about 25 mm, with hand-lay-up 15 mm, with vacuum- and air-bag methods about 10 mm and with drawn profiles 8 mm.

Just as with other processing methods, *shrinkage* has to be taken into account. With polyesters shrinkage by curing may amount to 6 to 10 vol %. Glass reinforcement reduces this shrinkage by about a factor of two.

Next to glass fibres, other fibres are being used at an increasing rate, such as *carbon- and aramide* fibres. These are much more expensive than glass, but they excel in mechanical properties. For high-precision construction with these newer fibres, such as for applications in aircraft and space-craft, so-called *prepregs* are available: strips of material in which the fibres are, in perfect parallel position, embedded in the resin. The resin has undergone a partial curing reaction, so that the strips can be handled, but are still capable to deform and to be joined together in the final curing operation at a high temperature and pressure.

So far, it would seem that only thermosetting resins are suitable for reinforcement with continuous fibres. Historically, this is a logical situation, since impregnating is easiest with a not too highly viscous liquid, such as a resin, which is still a low-molecular substance during impregnation. Molten thermoplastics, on the contrary,

have such a high viscosity that simple impregnation is not possible.

Over the past few years, however, techniques have been developed to enable continuous reinforcement of thermoplastics. The simplest way is to put a cloth and a plastic sheet on top of each other in a heated press and to carry out impregnation under pressure. More difficult is the forming of an end-product from the sheet produced; with conventional sheet-forming techniques the position of the fibres will be distorted in an unacceptable way. As in nearly all processing techniques, the modern *finite-element methods* with advanced computers are able to present solutions to this problem; in principle they can predict the position of the fibres in the sheet-forming operation, so that optimum reinforcement is realised in the end product.

11.6.3. *Foaming*

A *plastic foam* is a heterogeneous blend of a polymer with a gas. The gas cells are between 1 mm and 0.1 mm. Foams are made from thermoplasts, thermosets and rubbers. In all these cases the foam structure is generated in the fluid condition; with thermoplasts it is fixed by solidification, with thermosets and rubbers by the curing or vulcanisation reaction.

Dispersion of the gas phase in the fluid polymer can be achieved in two ways, namely by mechanically *whipping* the gas into the liquid (as with eggs and cream), or by generating the gas within the liquid (as with beer).

The production of foamed rubber by whipping a latex is known for a long time. Rubber mattresses are still being made in this way. The latex is whipped into a foamy substance and then poured into a mould. The water is evaporated, and the rubber is vulcanised with the aid of vulcanization ingredients (sulphur etc.) added before to the latex. The density of a rubber latex foam for mattresses is about 70 kg/m³.

Another whipped foam is ureum formaldehyde foam. A watery solution of ureum, formaldehyde and additives, is whipped to a very light foam. When this is dried at an elevated temperature, the resin is cured into a hard foam of a few kg/m³, to be applied in packaging and as artificial snow in shop-windows etc.

The second, much more often applied, method of foam manufacture, is the generation of *gas bubbles within the liquid*. This requires the presence of blowing agents, which exist in two types: *physical and chemical ones*. To the first category belong substances which are soluble in the polymer at a high pressure or at a lower temperature, but which leave the polymer upon pressure reduction and/or temperature increase (for comparison: carbon dioxide gas escapes from beer when

the pressure is released).

One of the best-known examples of a *physical blowing agent* is pentane in polystyrene. The raw material is available as PS beads in which pentane is solved. The beads are heated by steam to 100 °C. The polymer softens and at the same time the solved pentane evaporates, forming vapour bubbles which expand the bead drastically. The foamed beads are then brought into a closed mould, in which they expand further by heating to about 120 °C, they fuse together, and fill the mould completely. In this way closed-cell foams are obtained with densities of 10 kg/m³ or higher. This PS foam is mostly used as packaging material and for thermal insulation.

Another possibility is to extrude foam into sheets; the pressure within the extruder prevents foam formation; only after leaving the die the pentane evaporates to form the foam. In most cases the extrusion process is carried out with normal PS granules; in the cylinder pentane or another blowing agent is injected, where it mixes into the polymer and brings about foam formation after leaving the die.

Besides physical blowing agents, also *chemical ones* are used. These are substances which undergo a chemical reaction upon heating, while giving off a gassy component (compare rising of dough by the reaction products in the fermentation process). Chemical blowing agents are, i.a., used in PVC, PE, PP, etc. The foaming process can take place in the usual processing machines, such as extruders and injection-moulding machines.

The development of gases may also result from the same chemical reaction which produces the polymer network, with thermosets and rubber foams. The most important examples are the polyurethane foams, of which two variants exist: the hard ones and the soft ones. Both are formed by a reaction between a liquid poly-alcohol and an isocyanate, in which CO₂ gas is formed which can act as a blowing agent. The process proceeds as follows: The fluids are mixed together and are brought into a mould, in which the reaction starts instantaneously. During the reaction carbon dioxide is developed, which foams the liquid. The heat of reaction accelerates the process, so that the substance is foamed-up and cross-linked at a high rate, and abruptly passes from the fluid into the rubbery state. The process is often carried out continuously by moving a mixing head over a conveyor belt with raised borders. The fluid mass covers the bottom and is transported by the belt. At the end of the belt foaming is complete. In this way a foam block is produced of several m² cross-section at a rate up to 10 m/min.

The blocks can be cut into mattresses, into insulating foam sheets, or into arbitrary shapes. The foam density is about 15 kg/m³, while the foam has an open structure, as

a result of the disappearance of cell walls when the cells are arranged in a tight packing in a not too highly viscous liquid. The foam consists of a skeleton of elastic bars, which is an ideal structure for mattresses; air can easily escape and re-enter.

Hard polyurethane foams are made in a similar way. Again polyols and isocyanates are used, but in a somewhat different composition, giving rise to the formation of a tighter network. Because the viscosity changes with time in a different way during curing and foaming, hard polyurethane foams contain more closed cells; the formation of a completely closed-cell structure is also attainable. The recipe is then changed in such a way that the amount of CO₂ developed is considerably lower, while a physical blowing agent is added, so far, in most cases, a freon. In view of the environmental problems (the ozone layer) other blowing agents are being tried out. The heat of reaction causes the blowing agent to evaporate at a moment when the viscosity has risen to such an extent that only closed cells can be formed. Hard polyurethane foams are mainly applied for heat insulation. They can be used as sheets, but also as in-situ formed foams, e.g. by using spraying guns to cover the outer side of a storage tank with insulating foam. With insulation of a cold tank a closed cell structure is of major importance to prevent diffusion of water vapour and ice formation within the foam. These phenomena can further be prevented by applying a layer, impermeable to water vapour, at the warm side of the foam. Cavity walls can also be filled in-situ with polyurethane foam, as well as with UF-foam.

Sheets of hard foam can be covered at both sides by a thin skin, e.g. by metal or glass-reinforced plastic, to form light and stiff sandwich panels, to be used as building panels.

A rapidly developing product is the *integral foam*, consisting of a foam core which gradually passes into a massive skin. From hard and half-hard polyurethane foams mouldings of several tens of kg are made by injecting a blend of the reacting components into a die which is rotating to achieve a proper distribution of the material. A pressure of less than 2 bar is sufficient to compress the material at the wall of the mould before solidification. The cycle times are mostly between 5 and 15 minutes. The densities vary between 200 and 900 kg/m³, depending on the application. Metal inserts can be placed in the mould to become encapsulated by the foam.

Thermoplastic structural foams are, in most cases, made in an injection moulding machine. The gas is either formed from a chemical blowing agent, or injected under pressure into the molten polymer. The melt is injected into the mould until this is filled for e.g. 60 to 80 %, after which the foaming process completes its filling. The mould has only to withstand the pressure of the expanding gas (10 to 20 bar); it can be lightly constructed and the closing forces are small.

Thermoplastic structural foam (e.g. PVC, PP, PPE/PS, PC) is applied at a large scale for furniture, apparatus casings, motorcar parts, etc. The advantages are, in the first place, the relatively simple fabrication technique, in particular for large-sized products. Moreover, the extra high stiffness is of importance. This, in itself, sounds like a paradox, since the introduction of gas bubbles in the material reduces its modulus of elasticity. In a global way, it can be stated that for a relatively high-density foam the modulus is proportional to the square of the density and, for a low-density foam, proportional to the density. When we consider, however, the bending stiffness of a foam bar, than this increases with the third power of its thickness. A foam bar has, therefore, a considerably higher stiffness in bending than a massive bar of the same weight. In most cases bars and plates are loaded in bending; hence constructions are, with the same weight, much stiffer when foam is used. For structural foam this is even more the case: the solid skin has an extra stiffening effect in bending.

Literature

Recommended for further study:

R.J. Young and P.A. Lovell, *Introduction to Polymers*, Chapman and Hall, London, 1992.

F.R. Schwarzl, *Polymer-Mechanik*, Springer, Berlin, 1990.

P.C. Hiemenz, *Polymer Chemistry*, Marcel Dekker, New York, 1984.

N.G. McCrum, C.P. Buckley and C.B. Bucknall, *Principles of Polymer Engineering*, Oxford University Press, Oxford, 1988.

H. Domininghaus, *Die Kunststoffe und ihre Eigenschaften*, VDI, Düsseldorf, 1988.

Z. Tadmor and C. Gogos, *Principles of Polymer Processing*, Wiley-Interscience, New York, 1979.

D.H. Morton-Jones, *Polymer Processing*, Chapman and Hall, London, 1989.

R.P. Sheldon, *Composite polymeric Materials*, Appl. Sci. Publ., London, 1982.

A simple introduction:

A.K. van der Vegt, *Kunststoffen in het kort*, Delta Press, 1994.

Broad survey:

A.E. Schouten en A.K. van der Vegt, *Plastics*, 9th ed., Delta Press, 1991.

Cross-sections through polymer science and technology:

A.K. van der Vegt, *Kijk op Kunststoffen*, Beaumont, 1999.

Index

- abrasion 142
- acrylonitrile-butadiene-styrene ABS 16
- additives 13
- amorphous 52
- anisotropy 98, 99, 136
- antioxydants 157
- antistatic additives 153
- aramide fibre 85
- Arrhenius equation 55, 96, 114
- atactic. 39
- averages 26
- Avrami equation 77

- Banbury mixer 197
- bending 225
- binodals 164
- birefringence 100, 156
- blending 197
- blends 20, 63
- block copolymers 63, 165
- blowing agent 213
- bottle blowing 220
- branching 40
- brittle cracks 131
- brittleness temperature 144
- Burgers 105
- burning behaviour 150
- butadiene rubber BR 19, 26, 128
- butyl rubber IIR 19, 26, 128

- calender 214
- carbochemistry 12
- carbon black 143, 176
- Carilon 26
- casting 198
- cellulose acetate CA 18
- cellulose acetate butyrate CAB 18
- chain conformations 41
- chain flexibility 47, 60, 68
- chain interactions 48, 61
- chain length and distribution 26, 31
- chain orientation 70, 83, 99, 212
- chain regularity 38
- chain structure 22
- chemical resistance 158
- chloroprene rubber CR 19, 26
- cis 100
- cis- and trans-configuration 39
- cis- or trans-chains 39, 67
- co-continuous 173
- coil density 44

- cold sheet forming 224
- complex modulus of elasticity 112, 127
- compliance 108
- composite plastics 20
- compounding 197
- compression moulding 201
- condensation 12
- conducting polymers 153
- copolymerization 40
- copolymers 26, 63
- crazes 135, 227
- creep 82, 103, 104, 108, 120
- creep isochrones 123
- cross-link density 50
- cross-links 49, 61
- crystal growth 74
- crystal morphology 79
- crystal size 71
- crystalline fraction 78
- crystalline structure 78
- crystallization of oriented chains 83

- damping 126
- dashpot 103
- degradation 150
- degree of crystallization 82, 119
- die-swell 99, 218
- dielectric heating 193
- dielectric loss factor 154
- diffusion 159
- dilatometer 75
- dipole forces 48, 61
- dispersion 63, 161, 165
- dispersion forces 49
- ductile failure 132
- dynamic mechanical behaviour 110

- effects of environment 156
- Einstein formula 45, 177
- electric conductivity 180
- electric resistance 151
- electric strength 155
- entanglements 86, 92
- enthalpy of mixing 162
- entropy 71, 97
- entropy elasticity 87
- entropy of mixing 162
- environmental stress cracking 98, 134, 159
- epoxy resin EP 19
- equivalence of time and temperature 114
- ethylene tetrafluoroethylene EFTE 17

- ethylene-propylene rubber EPR, EPDM 20
 extrusion 99, 198, 215
- fibres 83, 84, 99
 fillers 13
 film blowing 219
 film extrusion 98
 films 99
 flash 209
 Flory-Huggins 162
 fluid condition 92
 foaming 232
 foams 21, 149
 forging 224
 fractionation 37
 free enthalpy 56
 free volume 53, 160
 friction 128, 139
 fringed micel structure 80
- gel permeation chromatography 38
 glass - rubber transition 144, 164
 glass-rubber transition temperature 52, 53, 187
 glassy state 52, 53
 gluing 228
 graft copolymer 40
 grip 128
- half-synthetic polymers 11
 hand-lay-up 231
 hardness 138
 heat-build-up 128
 heterogeneity index 29, 30, 33
 heterogeneous nucleation 73
 high-density PE 40
 high-frequency electric field 227
 homogeneous blend 165
 homogeneous nucleation 73
 Hooke's law 102
 hydrogen bridges 49
 hysteresis work 127
- impact strength 54, 98, 128, 136
 impregnating 230
 in-situ polymerisation 201
 injection moulding 98, 205
 integral foam 234
 interaction forces 68
 interpenetrating network 175
 intrinsic viscosity 35
 ISO Heat Deflection Temperature (HDT) 145, 187, 189
 isoprene rubber IR 19, 26, 100
 isotactic 39, 66
- Kelvin-Voigt element 104
 Kerner 172, 176, 178
 light scattering 34
 linear viscoelastic behaviour 108, 109
 liquid-crystalline polymers 84, 119
 long fibres 181
 long-term strength 131
 loss factor 127
 loss modulus 111, 127
 low-density PE 40
 lower critical solution temperature 164
 lyotropic 85
- machining 226
 Mark-Houwink relation 36, 45
 master curve 114, 121
 maximum temperature of use 150
 Maxwell element 103
 mechanical damping 54
 melamine-formaldehyde MF 18
 melt elasticity 31, 96, 97
 melt fracture 99, 218
 melt index 37, 93, 97
 melting point 67
 melting region 70, 82
 metallising 229
 metallocene 39, 71
 miscibility of polymers 161
 modulus of elasticity 102, 117, 118, 172, 186, 189
 mol mass distribution 97
 molar mass 26
 molar mass distribution MMD 31, 37, 97, 9995
 Mooney viscosity 93
- natural polymers 11
 natural rubber NR 67, 100
 networks 14
 Nielsen 173
 nitrile rubber NBR 19
 non-linearity 122, 126
 non-Newtonian behaviour 93, 95
 nontransparent 83
 notched impact strength 136, 186, 189
 nucleus formation 72
 number average \bar{M}_n 27, 31, 33, 98, 99, 133, 138
 nylon 16, 66
- optical anisotropy 156
 orientation 78, 83, 100
 osmometry 34

- oxygen index 150
 permeability 159
 petrochemistry 12
 phenol-formaldehyde PF 18
 physical ageing 59, 124, 126
 plasticizing 62
 Poisson 113
 polyacetylene 22
 polyacrylonitrile PAN 25, 61, 67
 polyamide PA 16, 66, 69
 polybutadiene BR 19, 22, 26, 39, 67
 polybutylene PB 18, 25, 62, 67
 polybutylene terephthalate PBTP 17, 24
 polycarbonate PC 16, 23, 60, 66, 99, 118
 polychloroprene CR 26
 polyether ether ketone PEEK 18, 24
 polyether sulphone PES 18, 24
 polyethylene PE 15, 22, 60, 65, 68, 98
 polyethylene terephthalate PETP 17, 23, 60, 66, 221
 polyethyleneoxyde PEO 23
 polyethyleneterephthalate 66
 polyimide PI 17, 25, 60
 polyisobutylene PIB 25, 65
 polyisoprene IR 19, 26, 39, 67
 polyketone PK 18, 26
 polymer blends 161
 polymer synthesis 12
 polymethylene pentylene PMP 18
 polymethylmethacrylate PMMA 16, 25
 polyoxymethylene POM 16, 23, 65
 polyphenylene ether PPE 17, 24, 63, 161
 polyphenylene oxide PPO 17
 polyphenylene sulphide PPS 17, 24, 60, 65
 polyphenyleneether 65
 polyphenylenesulfide 60, 65
 polypropylene PP 15, 25, 60, 66, 68
 polypropylpene 25
 polystyrene PS 15, 25, 60, 68
 polysulphone PSU 17, 24, 65
 polytetrafluorethene 68
 polytetrafluorethylene PTFE 17, 25, 65
 polyurethane PU 19, 23, 233
 polyurethane rubber PUR 20
 polyvinylalcohol PVAL 66
 polyvinylcarbazole PVK 60
 polyvinylchloride PVC 15, 25, 61, 67
 polyvinylidene fluoride 17
 polyvinylidenechloride PVDC 25, 65
 polyvinylidene fluoride 17, 25
 power-law 95
 prepregs 231
 production cost 195
 pseudoplastic behaviour 94, 96
 pultrusion 231
 random walk 41, 86
 random-copolymer 40
 rate of crystallization 67, 74
 reciprocating screw injection moulding machine 207
 refraction index 83
 reinforcement 20
 reinforcement by particles 176
 reinforcing fillers 143
 relaxation spectrum 107
 relaxation time 97, 104
 retardation spectrum 108
 roll mills 197
 rotational moulding 98, 199
 rubber-fluid transition 91
 rubbery phase 86, 100
 rubbery region 53, 222
 SBS 20, 167
 screw-plastification 206
 secondary transition 54, 127, 137, 144
 segregation 165
 shear modulus 102
 Shore hardness 138, 145
 short fibres 177
 short-shot 209
 shrinkage 209
 silicone rubbers 20, 24
 size-exclusion chromatography 38
 softening 145
 spectrum 97, 120, 125
 spherulite 81
 spinodal 163
 stereospecific 39, 66, 67
 steric hindrance 47
 storage modulus 110, 127
 stress 103
 stress corrosion 158
 stress relaxation 107
 stress-strain diagram 117
 styrene butadiene rubber SBR 19, 167
 styrene-acrylonitrile SAN 16
 superposition principle 108, 123
 surface coating 229
 syndiotactic 39
 synthetic elastomers 14, 19
 Takayanagi 172
 Taylor equation 169
 tear strength 99
 teflon 65, 68
 temperature-index 150

- tensile strength 130, 189, 190
- tetrafluoroethylene-perfluoropropylene FEP
17
- thermal conduction 148, 187
- thermal expansion 147
- thermal properties 144
- thermoforming 222
- thermoplastic elastomers TPE 20, 63, 118, 168
- thermoplastics 14, 15, 185
- thermosets 14, 18, 189
- thermotropic 85
- theta-solvent 45
- time and temperature 56
- time scale 91
- time-temperature shift 114
- torsion pendulum 112
- transparency 155

- U.L. index 150
- UHMPE 15
- ultrasonic welding 227
- unsaturated polyesters UP 18
- upper critical solution temperature 164
- ureum-formaldehyde UF 18
- UV stabilizers 157
- vacuum forming 100, 222
- Vicat Softening Temperature (VST) 145, 187
- visco-elastic behaviour 91, 97, 102
- viscosity 92, 103, 194
- viscosity average 35
- volume retardation 59

- wateradsorption 188
- Weber number 168
- weight average 27, 34, 92
- welding 226

- yield point 117

- z-average 28, 31